Universidade de Aveiro

2023

SUSANA PATRÍCIA PINTO PEREIRA

AVALIAÇÃO DO DESTINO E EFEITOS DE NANOMATERIAIS METÁLICOS E ÓXIDO METÁLICOS EM ORGANISMOS DULÇAQUÍCOLAS

ASSESSMENT OF FATE AND EFFECTS OF METAL AND METAL OXIDE NANOMATERIALS IN FRESHWATER ORGANISMS

Universidade de Aveiro

2023

Susana Patrícia
Pinto Pereira

AVALIAÇÃO DO DESTINO E EFEITOS DE NANOMATERIAIS METÁLICOS E ÓXIDO METÁLICOS EM ORGANISMOS DULÇAQUÍCOLAS

ASSESSMENT OF FATE AND EFFECTS OF METAL AND METAL OXIDE NANOMATERIALS IN FRESHWATER ORGANISMS

Tese apresentada à Universidade de Aveiro para cumprimento dos requisitos necessários à obtenção do grau de Doutor em Biologia, realizada sob a orientação científica do Professor Doutor António Nogueira, Professor Catedrático do Departamento de Biologia da Universidade de Aveiro, do Professor Doutor James Ranville do *Department of Chemistry* da *Colorado School of Mines* no Colorado (E.U.A.) e do Professor Doutor Richard D. Handy da *School of Biological Sciences, University of Plymouth* (Reino Unido).

Thesis submitted to the *Universidade de Aveiro* for fulfillment of the necessary requirements leading to the Doctoral degree in Biology, carried out under the scientific supervision of Doctor António Nogueira, Full Professor of the Departament of Biology from the *Universidade de Aveiro*, Doctor James Ranville from the Department of Chemistry, Colorado School of Mines (U.S.A.) and Doctor Richard D. Handy from the School of Biological Sciences, University of Plymouth (United Kingdom).

Dedico esta tese as mulheres que lutam pela sua liberdade no Irão e, sei que parece totalmente desconexo, a todos os que lutam por uma educação pública em Portugal, melhor, em todo o Mundo. Infelizmente, a minha mãe e avó não tiveram as oportunidades, ou até, as liberdades para estudar até quando bem entenderam ser melhor para elas. Facilmente nos esquecemos e desconsideramos as nossas conquistas, mas comparando o efeito da educação na minha vida, na vida da minha mãe e na vida da minha avó, a diferença é colossal. Por isso, obrigada a todos que fizeram com que fosse possível eu estar aqui hoje.

o júri

Presidente   Prof. Doutor Fernando Joaquim Fernandes Tavares Rocha
Professor Catedrático, Universidade de Aveiro

Vogais   Prof. Doutor Theodore Burdick Henry
Professor Catedrático, Heriot-Watt University

Prof. Doutora Maria Teresa Henriques de Faria Fernandes
Professora Catedrática, Heriot-Watt University

Prof. Doutor António José Arsénia Nogueira
Professor Catedrático, Universidade de Aveiro

Prof. Doutora Maria Cláudia Gonçalves Cunha Pascoal
Professora Associada com Agregação, Universidade do Minho

Doutora Paula Inês Borralho Domingues
Investigadora, Universidade de Aveiro

agradecimentos

Antes de tudo, à minha família.

A Fundação para a Ciência e Tecnologia pelo apoio financeiro sob a forma de uma bolsa de Doutoramento (SFRH/BD/97877/2013).

Aos meus orientadores, António Nogueira, Richard Handy, James Ranville pela orientação científica, disponibilidade, confiança.

Ao António Nogueira pelo apoio, paciência (muiiiita!) e disponibilidade.

To Richard Handy, for all the support, insight and knowledge that he shared with me. I wouldn't be here if it weren't for you.

To James Ranville, for being a second father to all your students. Thank you for all your availability and your car. To Colorado, for being an amazing place to live despite being located in the middle of U.S.A.

To Stephen Klaine, to whom a would like to thank for all the knowledge that shared with me. No faith in after life, but hope you're happy, as usual, somewhere!

À minha avó Lurdes, que apesar de analfabeta, incitou em mim a paixão pela natureza e a curiosidade pelas pequenas coisas.

À minha mãe que apesar de não compreender conceitos, sempre se interessou pelo meu trabalho e está cá hoje a apanhar 3 horas de seca.

Ao meu pai Almerindo que apesar da quarta classe nunca questionou os rumos da minha carreira.

Aos meus irmãos, Rui e Xana, que apesar de não entenderem a regra nº1 e perguntarem "Então quando é que acabas a tese?", sempre me apoiaram. No entanto, não ponho a mão no fogo em como aturam 3 horas de defesa.

Ao meu namorado, Rui, que sempre me apoiou nas piores alturas para ambos. Obrigada pela ajuda nos esquemas, formatações, nas correções do inglês (revirar de olhos) e nas questões filosóficas da tese e da vida!

Ao A+ (Dânia, Ju, Sofia, Peeedrô), grupo com o qual partilho mais do que o grupo sanguíneo, obrigada por me aturarem com as minhas "milestones" e manias. Ah, e por alguns membros me terem visitado em Plymouth, o local que toda a gente quer visitar em Inglaterra!

Ao Jorge, Nanda, Leandra, Leonardo e Rui, obrigada por tudo.

Ao 4º Esquerdo, a família que fui arranjar em Coimbra! Até à próxima Cimeira.

palavras-chave nanomateriais sintentizados, nanoecotoxicologia, prata, óxido de cobre, metal, revestimento superficial, ecossistemas dulçaquícolas, plantas aquáticas, macrófitas, peixe-zebra, embriões de peixe, biodisponibilidade, stress osmorregulatório, stress oxidativo, distribuição de sensibilidade das espécies, avaliação de risco ecológico

Resumo Os nanomateriais de síntese (ENMs), nomeadamente de prata (Ag) e óxido de cobre (CuO), são amplamente utilizados em diversos campos, como biomedicina, sensores, embalagens de alimentos, têxteis, cosméticos, remediação ambiental, etc. Através de diferentes vias, entram nos ecossistemas dulçaquícolas e afetam a biota aquática, em particular plantas e peixes. Embora os respetivos sais metálicos tenham mecanismos de toxicidade bem conhecidos, é crucial entender se as propriedades da escala nano resultam em efeitos distintos nos organismos dulçaquícolas. Assim, o principal objetivo desta tese foi avaliar os efeitos das ENMs na biota aquática, usando ENMs de prata (Ag ENMs) e ENMs de óxido de cobre (CuO ENMs) como representantes de ENMs metálicas (Me) e ENMs de óxido metálico (MeO), respectivamente. Este trabalho focou-se no efeito de diferentes características dos ENMs (por exemplo, revestimento de superfície) na toxicidade para os organismos aquáticos *Lemna minor* e zebrafish (*Danio rerio*), como espécies modelo de plantas aquáticas e peixes. Em particular, este trabalho visou abordar as seguintes questões: os ENMs são mais tóxicos do que os respetivos sais metálicos ($AgNO_3$ e $CuSO_4$)? A toxicidade de Ag ENMs é afectada pelas suas características (por exemplo, revestimentos superficiais como citrato ou polivinilpirrolidona (PVP))? Os efeitos dos Ag ENMs sobre a *L. minor* mudam com o tempo? Os efeitos dos Ag ENMs e de CuO ENMs no organismo dos embriões de peixe-zebra são semelhantes entre si? O córion pode impedir a entrada de ENMs dentro de embriões de peixes? Os ENMs induzem stress osmorregulatório em embriões de peixe e stress oxidativo em ambos os organismos modelo? Os dados experimentais mostraram que os ENMs foram menos tóxicos do que os respetivos sais metálicos em ambas as espécies, *L. minor* e peixe-zebra. O revestimento superficial influenciou os efeitos dos ENMs de Ag na *L. minor*, pois o citrato afetou mais pronunciadamente as atividades da
(continuação) guaiacol peroxidase (GPox) e glutationa-S-transferase (GST),

(continuação)

enquanto que o PVP influenciou mais a taxa de crescimento e o número de frondes por colónia. Os efeitos dos Ag ENMs sobre a *L. minor* mudaram ao longo do tempo, pois após 14 dias (d) de exposição foi notado um efeito atenuador, comparativamente aos 7d de exposição.O córion dos embriões de peixe-zebra teve um efeito protetor contra ENMs. De fato, a biodisponibilidade de Ag ENMs e de CuO ENMs nos embriões de peixe-zebra foi muito baixa, onde a maior parte do metal total (>99% e 94%, respetivamente) foi associada ao córion; a mesma tendência que ocorreu para $AgNO_3$ (96% do metal total), mas não para $CuSO_4$, onde apenas 58% (metal total) estava associado ao córion. O stress osmorregulatório mostrou um efeito nanoespecífico (ou seja, efeitos mais significativos nos ENMs do que no sal metálico) para Ag ENMs, mas não para CuO ENMs. Além disso, os Ag ENMs e os CuO ENMs desencadearam stress oxidativo moderado, onde a depleção de glutationa (GSH) total também teve um efeito nanoespecífico. No geral, os resultados sugerem que os ENMs tendem a ser menos tóxicos do que os respetivos sais metálicos e destacam a sua capacidade de causar stress oxidativo para ambas as espécies aquáticas, mostrando ainda que alguns efeitos tóxicos são nanoespecíficos.

A menor toxicidade dos Ag ENMs em comparação com o sal metálico foi ainda confirmada usando a Distribuição da Sensibilidade das Espécies (SSD). O valor da Concentração Perigosa para 5% das Espécies (HC_5) dos Ag ENMs foi 13 vezes inferior ao do $AgNO_3$ (0,089 µg L^{-1} e 0,007 µg L^{-1}, respetivamente). As espécies mais sensíveis para ambas as formas de Ag foram os cladóceros (Daphniidae). A Concentração para a qual Não se Prevê a ocorrência de um Efeito (PNEC) foi 0,045 µg L^{-1} para os Ag ENMs e 0,007 µg L^{-1} para $AgNO_3$. O quociente de risco RQ foi de 6,3 (>1) para o $AgNO_3$ e 0,03 para os Ag ENMs (<1), sugerindo que a avaliação de risco existente para metais poderá ser extrapolada para os ENMs. No entanto, os ENMs têm um mecanismo de ação distinto dos sais metálicos. Além disso, a diversidade de características dos ENMs (por exemplo, revestimento superficial) requer mais estudos toxicológicos com o objetivo de melhorar o conhecimento sobre a toxicidade e avaliação de risco dos ENMs.

Abstract

Engineered nanomaterials (ENMs), namely silver (Ag) and copper oxide (CuO) ENMs, are widely applied in diverse fields such as biomedical, sensors, food packaging, textiles, cosmetics, environmental remediation, etc. Through different pathways, these ENMs might enter in freshwater ecosystems and affect aquatic biota, in particular plants and fish. Although their bulk counterparts (salt metals) have well known mechanisms of toxicity, it is crucial to understand if the nano scale properties result in distinct effects to freshwater organisms. Thus, the main objective of this thesis was to assess the effects of ENMs to aquatic biota, using silver (Ag) ENMs and copper oxide (CuO) ENMs as representatives of metal (Me) and (MeO) ENMs, respectively. This work focused on the effect of different characteristics of ENMs (e.g. surface coating) on their toxicity to the aquatic organisms *Lemna minor* and zebrafish (*Danio rerio*), as model species of aquatic plants and fish. In particular, this work aimed to address the following questions: Are ENMs more toxic than the respective salt metals (AgNO$_3$ and CuSO$_4$)? Is toxicity of Ag ENMs affected by their characteristics (e.g. surface coatings as citrate or polyvinylpyrrolidone (PVP))? Do the effects of Ag ENMs to *L. minor* change over time? Are the effects of both Ag ENMs and CuO ENMs similar to zebrafish embryos? Can chorion hinder the entry of ENMs inside fish embryos? Do ENMs induce osmoregulatory stress in fish embryos and oxidative stress in both model organisms? Experimental data showed that ENMs were less toxic than the respective salt metals (AgNO$_3$ and CuSO$_4$) in both species, *L. minor* and zebrafish. Surface coating influenced Ag ENMs effects in *L. minor*, as citrate affected more pronouncedly Guaiacol peroxidase (GPox) and Glutathione-*S*-transferase (GST) activities, whereas PVP influenced more the growth rate and the number of fronds per colony.

(continued)

(continued)

The effects of Ag ENMs to *L. minor* changed over time, as an ameliorative effect was noticed after 14 days (d) of exposure, compared to 7d of exposure.

In zebrafish embryos, chorion had a protective effect against ENMs. Indeed, bioavailability of both Ag ENMs and CuO ENMs to the zebrafish embryos was very low, where most of total metal (>99% and 94%, respectively) was associated to the chorion. the same trend that occurred for $AgNO_3$ (96% of total metal), but not for $CuSO_4$, where only 58% (total metal) was associated to the chorion. Osmoregulatory stress showed a nano-specific effect (i.e. more significant effects in ENMs than in the salt metal) for Ag ENMs but not for CuO ENMs. Moreover, a mild oxidative stress was triggered by both Ag and CuO ENMs, where a depletion of total glutathione (GSH) also had a nano-specific effect. Overall, results suggest that ENMs tend to be less toxic than the respective salt metals, and highlight their ability to cause oxidative stress to both aquatic species, further showing that some toxic effects are nano-specific.

The lower toxicity of Ag ENMs compared to the bulk salt was further confirmed using Species Sensitive Distributions (SSD). The hazardous concentration for 5% of species (HC_5) values was 13-fold lower for Ag NMs than for $AgNO_3$ (0.089 µg L^{-1} and 0.007 µg L^{-1}, respectively). The most sensitive species for both Ag forms were cladocerans (Daphniidae). Predicted no effect concentration (PNEC) values were 0.045 µg L^{-1} for Ag ENMs and 0.007 µg L^{-1} for $AgNO_3$. Risk quotient (RQ) was 6.3 (>1) for $AgNO_3$ and 0.03 for Ag ENMs (<1), which suggests that the existing metal risk assessment could be extrapolated to the ENMs. Nevertheless, ENMs have a distinct mechanism of action than the salt metals. Furthermore, the diversity of ENMs characteristics (e.g. surface coating) requires further toxicological studies aiming to improve the knowledge on ENMs toxicity and risk assessment.

Table of Contents

List of Figures

Figure 1-6 – Schematic model of cellular ROS generation and the cooperation of main antioxidant enzymes in animal cells. Superoxide dismutase (SOD) converts Superoxide anion ($O_2^{\bullet-}$) into hydrogen peroxide (H_2O_2). Catalase (CAT) and

List of Tables

List of Equations

List of Appendices

List of Figures

List of Tables

List of Abbreviations

Alphabetic order

ACTWW	Alachua Conservation Trust wetland water
ADaM	Aachener Daphnienmedium
AFW	Artificial freshwater
Ag	Silver
Ag$^+$	Silver ion
AGCM	Algal growth culture medium
AgNO$_3$	Silver nitrate
Ag ENMs	Silver engineered nanomaterials
Al$_2$O$_3$	Aluminium oxide
APW	Artificial pond water
ATP	Adenosine-5'-triphosphate
Au	Gold
BBM	Bold's Basal medium
BDL	Below detection limit
Ca^{2+}	Calcium ion
CAT	Catalase
CCV	Calibration control verification
CDNB	1-chloro-2,4-dinitrobenzene
CeO$_2$	Cerium oxide
CFP	Carboxy-functionalized polyacrylate
CFW	Carbon-filtered water
Cl$^-$	Chloride ion
CoO	Cobalt (II) oxide
Co$_3$O$_4$	Cobalt (II,III) oxide
CR	Continuous renewal
Cu	copper
Cu$^+$	Cuprous (I) ion
Cu^{2+}	Cupric (II) ion
Cu^{3+}	Copper (III) ion
Cu^{4+}	Copper (IV) ion
CuO	Copper oxide
CuO ENMs	Copper oxide engineered nanomaterials
CuSO$_4$	Copper sulphate
DDW	Demineralised and dechlorinated water
Dech	Dechorionated embryos
DeioW	Deionized water
DLS	Dynamic light scattering

DLVO	Derjaguin, Landau, Verwey, Overbeek
DOC	Dissolved organic carbon
DTNB	5'5'-dithiobis-2-nitrobenzoic acid
DTW	Dechlorinated tap water
EC$_{10}$	Effect concentration that affects 10% of a given population
EC$_{20}$	Effect concentration that affects 20% of a given population
EC$_{50}$	Effect concentration that affects 50% of a given population
EDTA	Ethylenediaminetetraacetic acid
EE	Eleutheroembryos
EGCG	Epigallocatechin gallate
EGP	Exponential growth phase
ELS	Early-life stages
ENMs	Engineered nanomaterials
ERM	Embryos rearing medium
EW	Embryos water
FCW	Fish culture water
FDTW	Filtered dechlorinated tap water
Fe$_3$O$_4$	Iron (II,III) oxide
FM	Fresh medium
FT	Flow through
GR	Glutathione reductase
GPx	Glutathione peroxidase
GPox	Guaiacol peroxidase
GR	Growth rate
GRI	Growth rate inhibition
GSSG	Glutathione disulphide (a.k.a. oxidized glutathione)
GSH	Reduced glutathione
GST	Glutathione *S*-transferase
H$_2$O$_2$	Hydrogen peroxide
HM	Holtfreter medium
HEPES	4-(2-hydroxyethyl)-1-piperazineethanesulfonic acid
HNO$_3$	Nitric acid
HR(NF)	Horsetooth reservoir (normal flow)
HR(HF)	Horsetooth reservoir (high flow)
ICP-AES	Inductively coupled plasma – atomic emission spectrometry
ICP-MS	Inductively coupled plasma – mass spectrometry
ICP-OES	Inductively coupled plasma – optical emission spectrometry
In	Indium
IOSSS	"Instant Ocean Synthetic Sea Salt"
Ir	Iridium
K$^+$	Potassium ion
KCl	Potassium chloride
LC$_{10}$	Lethal concentration that affects 10% of a given population

LC_{20}	Lethal concentration that affects 20% of a given population
LC_{50}	Lethal concentration that affects 50% of a given population
LDH	Lactate dehydrogenase
LOEC	Lowest observed effect concentration
LPO	Lipid peroxidation
LTW	Laboratory test water
MAPW	Modified artificial pond water
MATC	Maximum acceptable toxicant concentration
MBL	Woods Hole Marine Biological Laboratory medium
Me	Metal
MeO	Metal oxide
Mg^{2+}	Magnesium ion
$MgCl_2$	Magnesium chloride
MHW	Moderately hard water
MHRW	Moderately hard reconstituted water
MHSM	Modified high salt medium
Mn	Manganese
MnO	Manganese (II) oxide
MnO_2	Manganese (IV) oxide
Mn_3O_4	Manganese (II,III) oxide
MoA	Mechanism of action
MOPS	(3-(N-morpholino)propanesulfonic acid) buffer
MSM	Modified Steinberg medium
MTs	Metallothioneins
Na^+	Sodium ion
NaCl	Sodium chloride
$NaBH_4$	Sodium borohydride
NADH	Nicotinamide adenine dinucleotide
NADPH	β-Nicotinamide adenine dinucleotide phosphate tetrasodium salt
Na^+/K^+ - ATPase	Sodium pump
Ni	Nickel
NOEC	No observed effect concentration
NOM	Natural organic matter
NN	Nitrate-Nitrogen
NPL	Average neonate per living parent
NPs	Nanoparticles
NTA	Nanoparticle tracking analysis
O_2	Oxygen
$\cdot OH$	Hydroxyl radical
$O_2{}^{\cdot-}$	Superoxide radical
OM	Old medium
OS	Orbital shaker
PCA	Principal component analysis

PEC	Predicted environmental concentration
PEI	Polyethylenimine
PES	Polyethersulfone
PhEI	Photosynthetic efficiency inhibition
PII	Photosystem II
PMC	Production, Manufacturing and Consumption
PMS	Post-mitochondrial supernatant
PEG	Poly(ethylene glycol)
PEP	Phosphoenolpyruvate
POE	Polyoxyethylene
PVA	Poly(vinyl alcohol)
PVP	Poly(vinyl pyrrolidone)
PY	Photosynthetic yield
ROS	Reactive oxygen species
ROW	Reverse osmosis water
RTM(DSW)	Reconstituted test medium (Dutch standard water)
RW	Reconstituted water
SDBS	Sodium dodecylbenzenesulfonate
SFIR	Spring-fed Ichetucknee river
SFM	Standard freshwater medium
SFW	Synthetic fresh water
SGM	Standard growth medium
SGR	Specific growth rate
-SH	Sulfhydryl groups (a.k.a. thiol groups)
SiO$_2$	Silica dioxide
SLS	Sodium laureth sulfate
SM7	Simplified M7 medium
SOD	Superoxide dismutase
SR	Static-renewal
SR24	Static-renewal (24 hours)
SR48	Static-renewal (48 hours)
SR72	Static-renewal (72 hours)
SRW	Soft reconstituted water
SSD	Sensitive species distribution
SSF	Standard synthetic freshwater
STEM	Scanning transmission electron microscopy
STP	Sewage treatment plant
TEM	Transmission electron microscopy
TGME	Triethylene glycol monomethyl ether
TiO$_2$	Titanium dioxide
tGSH	Total glutathione
Tween 20	Polyoxyethylene sorbitan mono-laurate
Tween 65	Polyoxyethylene sorbitan tristearate polysorbate

UV	Ultraviolet
VHW	Very hard water
VSRW	Very soft reconstituted water
Wt	Weight
WWTP	Wastewater treatment plant
ZHE$_1$	Zebrafish hatching enzyme 1
ZnO	Zinc oxide

Chapter
I

GENERAL INTRODUCTION

1   Chapter I – General Introduction

1.1   Nanomaterials

In a broad sense, nanomaterials (NMs) are materials in the nanoscale dimension. The first recommended definition for NMs from the European Commission was released in 2011 and updated in an attempt to obtain a consensus with other regulatory and standardization agencies. The modified proposal declares "natural, incidental or manufactured material consisting of solid particles present, either on their own or as identifiable constituent particles in aggregates or agglomerates where 50% or more of these particles in the number-based size distribution fulfils at least one of the following conditions: 1) one or more external dimensions of the particle are in the size range 1 nm to 100 nm; 2) the particle has an elongated shape, such as a rod, fibre or tube, where two external dimensions are smaller than 1 nm and the other dimension is larger than 100 nm; 3) the particle has a plate-like shape, where one external dimension is smaller than 1 nm and the other dimensions are larger than 100 nm. In the determination of the particle number-based size distribution, particles with at least two orthogonal external dimensions larger than 100 µm need not be considered. However, a material with a specific surface area by volume of $<6m^2/cm^3$ shall not be considered a nanomaterial." (European Comission, 2022).

Nanomaterials (NMs) can be classified in function of their dimension, elemental composition, phases, crystallinity, porosity, dispersion and origin (Barhoum et al., 2022). Considering their origin, they can be categorized as natural, incidental or engineered nanomaterials (**Figure 1-1**) (Barhoum et al., 2022).

Natural NMs are nanostructures of organic (e.g. virus, natural colloids – blood or milk) or inorganic sources, formed with the action of physical forces (e.g. forest fires combustion products or volcanic ash) that occur in nature without human influence (Wigginton et al., 2007). Incidental NMs are materials unintentionally formed as by-product of direct or indirect anthropogenic influences, as mechanical or industrial processes (e.g. vehicle exhaust gases, combustion from cooking) (Wigginton et al.,

2007). Lastly, engineered NMs (ENMs) are intentionally designed with regular shapes (**Figure 1-2**) for specific applications using various techniques (Barhoum et al., 2022).
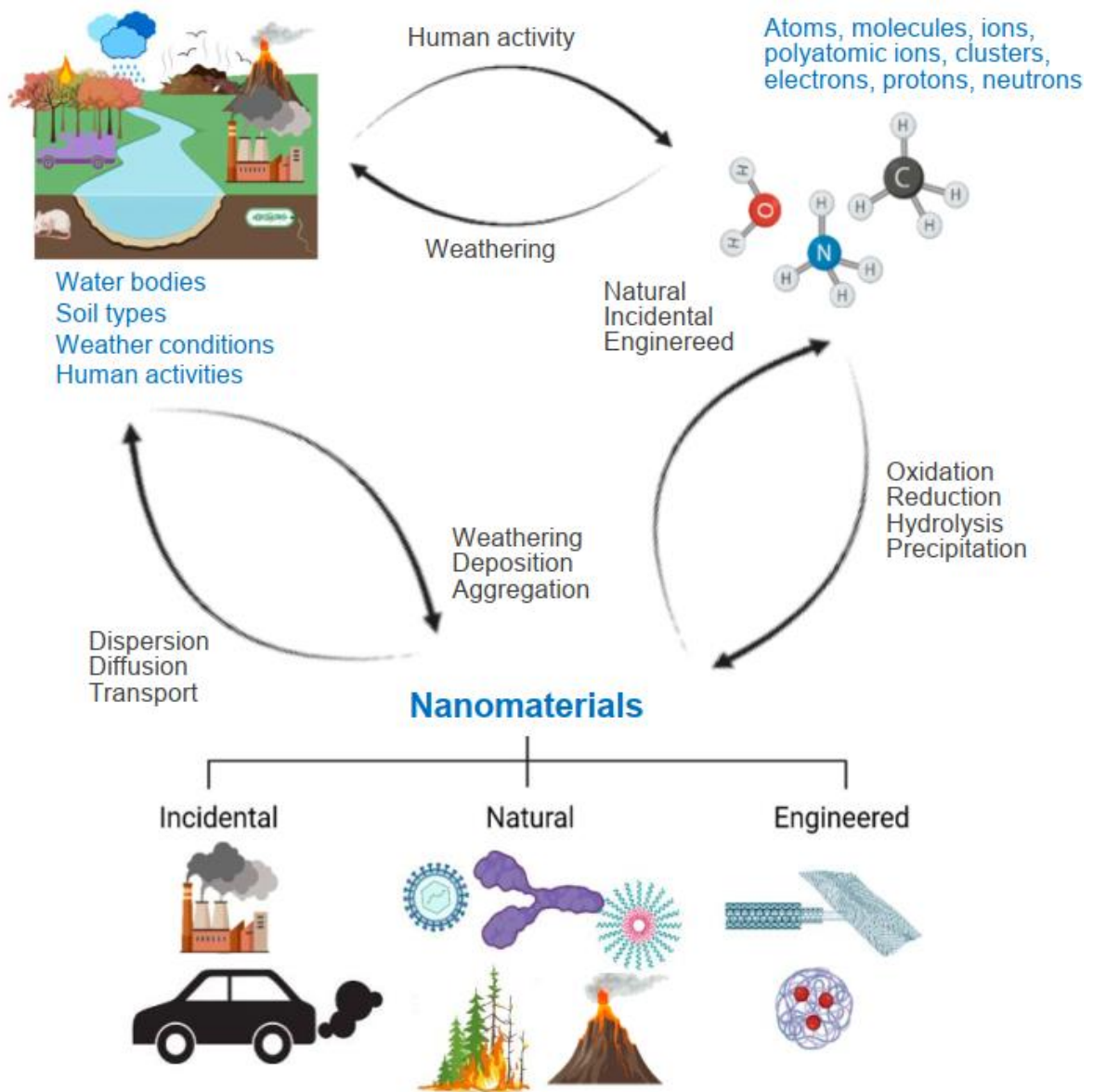
Figure 1-1 – Life cycle of different types of nanomaterials (NMs) and their classification according to the origin. Physical and chemical processes that form and transform those NMs (adapted from Barhoum et al., 2022).
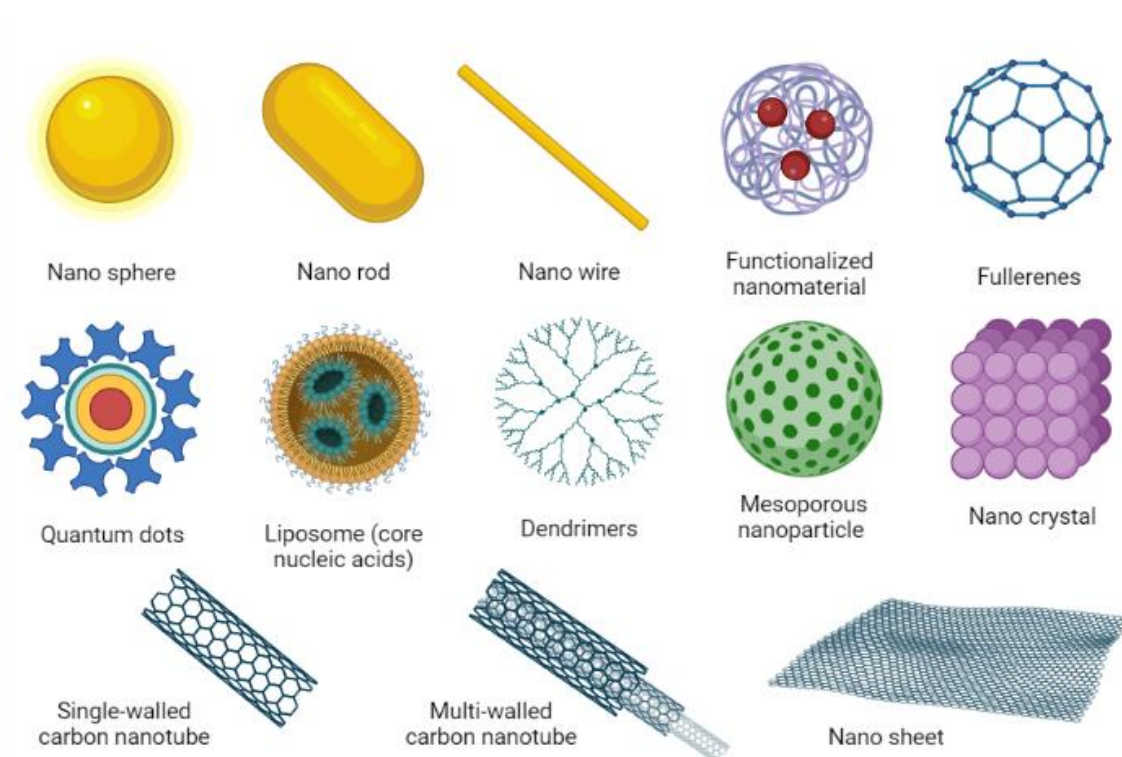
Figure 1-2 – Different shapes of engineered nanomaterials (ENMs). Figure created in BioRender.

Heterogeneous distribution that occur in the various features of the nanomaterials (e.g. size, shape, surface charge, composition and degree of dispersion) may generate significant differences between the physicochemical properties of ENMs and the respective bulk material (Delay and Frimmel, 2012).

The ratio between the surface area and the volume of the nanoparticles is a characteristic that brings out a different behaviour in comparison to the same compound at larger scale. For example, a microparticle of carbon with 60 μm diameter equals to a mass of 0.3 μg and a surface area of 0.01 mm^2. In the nanoparticulate form, the same element with 60 nm diameter would have a surface area of 11.3 mm^2, which consists of 1 billion of clustered particles. The surface-area-to-volume ratio increases with the decrease of radius of the sphere, which amplifies the rate of chemical reactions by 1000 times (Buzea et al., 2007).

In the last two decades, the market for nanotechnology-based products has been rising (2020). Among other characteristics, nanoparticles often possess unexpected optical and magnetic properties because they are small enough to confine their

electrons and produce quantum effects. In addition, nanoparticles absorb solar radiation more efficiently than bulk particles, a property that can be effectively used in sun blockers and building materials.

Products with enhanced characteristics (e.g. electro and heat conductivity, durability, self-cleaning, UV protection, fireproof, luminescence, photo catalytic ability, controlled release of active agents) become attractive to diverse industries, from textiles (Mazari et al., 2021), to medical sciences, with use in drug delivery systems, diagnostics, instrumentation and biomaterials (Maine et al., 2014).

1.2 Applications of ENMs

Among ENMs, metal [e.g. silver (Ag), copper (Cu), gold (Au)] and metal oxides [e.g., copper oxide (CuO), titanium dioxide (TiO_2), zinc oxide (ZnO)] have a high market share (Negrescu et al., 2022; Nikolova and Chavali, 2020; Shafiq et al., 2020). Owing to their unique properties, both metal ENMs (Me ENMs) and metal oxide ENMs (MeO ENMs) have diverse industrial applications, as described in detail in **Appendix A**.

The present study focused on silver (Ag) ENMs and copper oxide (CuO) ENMs. This selection was based on their representation of each class of engineered nanomaterials (Me and MeO, respectively). Silver (Ag) ENMs is the most attractive nanomaterial available in the market, being applied in diverse industries (see section **1.2.1.1**). Copper oxide (CuO) ENMs have specific properties that allow their incorporation into products from diverse industries (see section **1.2.2.1.**). Their bulk counterparts (Ag and Cu) have been thoroughly studied for at least 50 years with notorious environmental impacts (Grosell, 2011; Wood, 2011). Thus, based on the expected bioavailability and impact in the freshwater environment of bulk Ag and Cu it is important to compare the effects of both metals, at bulk and nano scales, in freshwater organisms.

Table 1-1 – Applications of the silver, representing metal engineered nanomaterials (Me ENMs), and copper oxide, representing metal oxide engineered nanomaterials (MeO ENMs), in different industries and respective characteristics/functions/application.

Metal	Industries	Characteristic/ Function/ Application	Reference
Silver (Ag)	Air and water purification	antimicrobial/ disinfectant	Deshmukh et al. (2019)
	Animal husbandry	antimicrobial	
	Antimicrobial coatings/materials	antimicrobial	Vasilev (2019)
	Biomedical	anti-tumoral	Caruso et al. (2014)
		wound healing	Deshmukh et al. (2019)
		wound dressings, tissue scaffolds, protective coatings and drug delivery	Burdusel et al. (2018)
	Cosmetics	antimicrobial	Fytianos et al. (2020)
	Food packaging	antimicrobial	Deshmukh et al. (2019)
	Printing inks	electro conductivity	Fernandes et al. (2020)
	Textiles	antimicrobial	Xu et al. (2017)
Copper oxide (CuO)	Nanofluids	electrocatalysis, photocatalysis and gas-phase catalysis	Gawande et al. (2016)
	Chemical sensor	semi-conductor	Steinhauer (2021)
	Microelectronics, Transportation, Manufacturing, Heating and cooling systems	thermal conductivity	Zhu et al. (2018)
	Water cleaning	nanoremediation	McDonald et al. (2015)

1.2.1 **Silver (Bulk)**

Silver (Ag, atomic weight 47) is a rare element from the class B of soft metals in the periodic table (Duffus, 2002). Besides its appeal as a precious metal, Ag was historically used to treat several diseases, as well as in other diverse applications such as in the photographic industry (Luoma, 2008; Wood, 2011). In rocks or soil Ag concentration averages 100 µg kg^{-1}, but in pristine freshwaters this concentration drops to 0.1-5 ng L^{-1} (Wood, 2011).

Dissolved Ag is highly reactive and considered persistent, bioaccumulative and toxic to aquatic organisms. Their mechanisms of action are well established in the literature (Ratte, 1999; Veltman et al., 2014; Veltman et al., 2008; Wood, 2011; Wood et al., 1999).

Silver (Ag) is described as a non-essential metal. However, Ag mimics Cu and sodium (Na$^+$) for cellular uptake in both respective transport pathways (Wood, 2011; Wood et al., 1999). In fish, for example, Ag inhibits the branchial sodium pump (Na$^+$/K$^+$-ATPase activity), eventually blocking the Na$^+$ and Cl$^-$ uptake (Hogstrand and Wood, 1998). Still, dissolved Ag can bind in a more direct way to sulfhydryl groups (thiol or -SH) of molecules such as, glutathione (GSH) (Leung et al., 2013; Wood, 2011). Silver has been reported to affect organisms at different levels of the biological organization from the molecular level to the population or community (Glover, 2018; Howe and S. Dobson, 2002).

1.2.1.1 **Silver (Ag) ENMs**

To increase its reactivity, Ag began to be manipulated on the nano scale so that, by increasing its surface area/volume ratio, it can display properties that do not occur in its bulk counterpart, as described in section **1.1.**

Silver (Ag) ENMs are applied in a wide range of fields (**Table 1-1**) from textiles (e.g. antimicrobial socks) to medical, cosmetics, packaging, cleaning agents, consumer electronics, optics, food and metals (Temizel-Sekeryan and Hicks, 2020). Due to its large spectrum of applications it is hard to reach a consensus about the global predicted production of Ag ENMs. To the best of our knowledge, the estimates for the global production of Ag ENMs for 2025 vary between 400 tonnes/year (sceptical

projection) and 800 tonnes/year (optimistic projection) (Pulit-Prociak and Banach, 2016). The high demand of Ag ENMs is related to the exploitation of its broad spectrum antimicrobial, antifungal, antibacterial, antifouling, stain resistance, electric conductivity properties (Hicks, 2017; Hicks et al., 2015; Hicks et al., 2016; Hicks and Temizel-Sekeryan, 2019; Hicks and Theis, 2016; Westerband and Hicks, 2018). Silver ENMs are mainly synthetized by chemical reduction methods (e.g. silver nitrate ($AgNO_3$) reduced by sodium borohydride ($NaBH_4$), but other methods are also used, as electrochemical or biological reduction (Vishwanath and Negi, 2021). Surface coating agents or stabilizers (e.g. citrate, polysaccharides, polyethylene glycol (PEG), polyvinyl alcohol (PVA), or polyvinylpyrrolidone (PVP)) are usually applied to prevent particle aggregation (Fahmy et al., 2019). Nonetheless, this feature of ENMs might affect the environmental fate and consequently the toxicity of Ag ENMs as hinted by Du et al. (2018) and Jung et al. (2018).

1.2.2 Copper (Bulk)

Copper (Cu, atomic number 29) is a trace element, present in abundance in diverse rocks and minerals (Flemming and Trevors, 1989). Typical concentrations of Cu in the earth's crust range from 2–250 mg/kg, but its presence in freshwater only occurs in the 0.2-30 µg L^{-1} range (Grosell, 2011). This metal occurs under diverse forms as the element, Cu, and different ionic states, Cu^+ (cuprous (I)), Cu^{2+} (cupric), Cu^{3+} and Cu^{4+} (Sparling, 2016b). Its applications range from the electrical industry, to building supplies, antifouling paints and under the form of copper sulphate as a pesticide (Sparling, 2016b).

Copper (Cu) is required in cellular metabolism to allow a normal growth and physiology, making it an essential metal for aerobic organisms (Grosell, 2011; Linder and Hazegh-Azam, 1996). This metal is also important in cell homeostasis and as co-factor of several enzymes involved in electron transport system (e.g. cytochrome C oxidase, Cu/Zn superoxide dismutase), oxidative phosphorylation, iron transport (ceruloplasmin), and synthesis of neurotransmitters (Ken et al., 2003; Sparling, 2016b).

Nevertheless, as any essential metal, there is an optimum dose of Cu to be assimilated by organisms, and inappropriate concentrations will cause mild or severe deficiency or toxicity to the organisms (Sparling, 2016b). The persistent nature of Cu, tendency to accumulate, toxicity to aquatic organisms and mechanisms of action are well established in the literature (Amoatey and Baawain, 2019; Donnachie et al., 2014; Eisler, 1998; Grosell, 2011; Grosell et al., 2002b; Handy, 2003; Handy et al., 2002; Nor, 1987). Its toxicity occurs via three main pathways: disruption of Na homeostasis, effects on bioenergetics and oxidative stress (Brix et al., 2022). Copper (Cu^{2+}) can bind directly to the negatively charged sulfhydryl groups (thiol or -SH) of molecules such as glutathione (GSH; section **1.5.1.2**) (Bopp et al., 2008; Sevcikova et al., 2011; Walker et al., 2016). Just like Ag, Cu affects organisms at different levels of the biological organization from the molecular level to the population or community (Brix et al., 2022).

1.2.2.1   **Copper Oxide (CuO) ENMs**

Just like Ag, Copper (Cu) also started to be manipulated in the nano scale to feature properties that do not occur in the bulk counterpart, as described in section **1.1**. Besides Cu ENMs, CuO ENMs have high reactivity and therefore have diverse applications from catalysis reactions in batteries (Gawande et al., 2016), in water purification (McDonald et al., 2015), to wood preservative and antifouling paints for boats (Ross and Knightes, 2022), to enhance electrical and thermal conductivity in sealants and coatings (Liu et al., 2011; Tran and Nguyen, 2014) and as chemical sensors (Steinhauer, 2021). Due to its myriad of applications (**Table 1-1**), CuO ENMs had a global annual production of 200 tonns in 2010, 570 tonns in 2014 and is estimated to boost up to 1600 tonnes by 2025 (Hou et al., 2017; Keller et al., 2013), to the best of our knowledge. Copper oxide ENMs are usually synthetized using mainly four chemical reactions – reduction (with chemical or biological agents), hydrolysis, condensation and oxidation (Gawande et al., 2016). Coating agents or stabilizers (e.g. aminoacids, peptides, PEG, PVA, PVP, or sodium laureth sulfate (SLS)) are usually applied to prevent particle aggregation (Gawande et al., 2016).

1.3 Route of Entry of ENMs in the Environment

The initial phase of the life cycle of ENMs (**Figure 1-3**) includes Production, Manufacturing and Consumption (PMC). After usage, products that include ENMs will move to the "Sewage Treatment Plant" (STP) and "Wastewater Treatment Plant" (WWTP), which retains a considerable % of ENMs (Sun et al., 2014). From here, further steps of ENMs treatment can occur, where recycling, incineration and landfilling are options. This waste disposable phase is named "Technosphere" (Haff, 2012) and from here, ENMs can be transferred to the "Ecosphere" that is comprised by different environmental compartments as air, soil, surface waters and, later after sinking and depositing, sediment. Further interactions and transfer between environmental compartments may happen, as leaching from soils into surface waters.

Although this is the proposed life-cycle, ENMs may follow different flows and end up in the air compartment right after the consumption phase. In most studies, the concentrations of ENMs in surface waters are predicted based on product life assessment and environmental fate. For example, concerning just the PMC phase of Ag ENMs, ≈ 6.44 % may end up in the surface waters at a ng L^{-1} range (Sun et al., 2014). Recently, the concentrations of Ag ENMs were determined in Dutch rivers (Meuse and IJssel) in a range of 0.3 to 2.5 ng L^{-1} (Peters et al., 2018). Regarding CuO ENMs, about 5.5% of manufacturing and domestic wastes were expected to reach natural water bodies (Keller et al., 2013). Nonetheless, the predicted levels of ENMs in surface waters are not consensual. Additionally, in each life cycle phase and compartment the ENMs will experience several physico-chemical transformations considering the different environmental conditions.
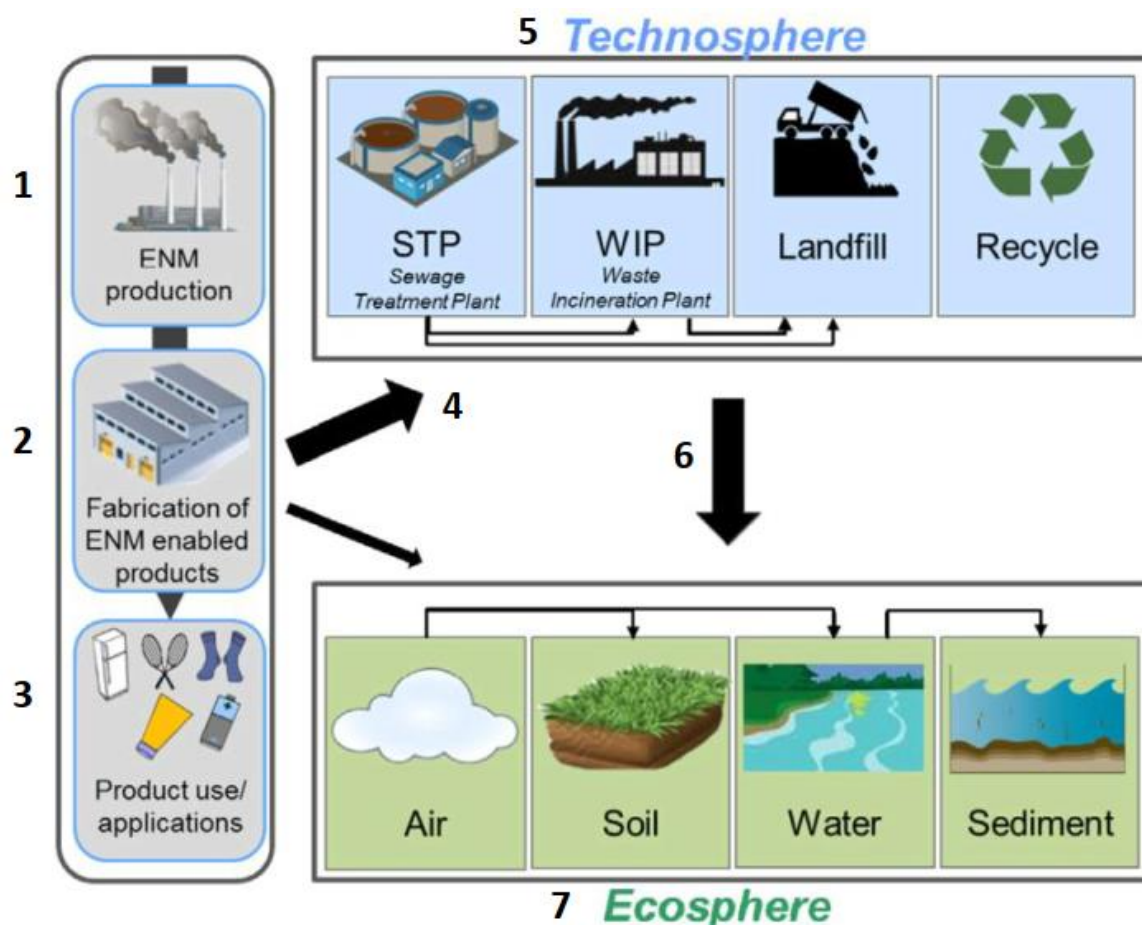
Figure 1-3 – Flow model of engineered nanomaterials (ENMs) along their whole life-cycle: 1) production, 2) manufacture; 3) consumption, 4) release from products, 5) transport and fate of between and within the technosphere, 6) transfer from technosphere to ecosphere, 7) transport between environmental compartments (adapted from Sun et al., 2014).

1.4 Environmental Fate of ENMs

The stability of ENMs is ensured by the combined effects of two opposite forces, the van der Waals attraction and the electrostatic repulsion creating an electric double layer, which is described by the DLVO theory (Wagner et al., 2014). This theory (named after Derjaguin, Landau, Verwey and Overbeek) explains the aggregation of aqueous dispersions quantitatively and describes the force between charged surfaces interacting through a liquid medium. When pristine ENMs reach the freshwater systems, the particles will integrate and interact with elements at a

colloidal scale, namely ions, natural organic matter (NOM) and microorganisms (Delay and Frimmel, 2012; Kansara et al., 2022). Hence, ENMs become susceptible to physical transformations (e.g. aggregation and/or agglomeration, adsorption, deposition/sedimentation), chemical transformations (e.g. dissolution, redox reactions, sulfidation) and interactions with macromolecules (e.g. flocculation, coating) (Amde et al., 2017; Delay and Frimmel, 2012; Ross and Knightes, 2022; Shevlin et al., 2018), as summarized in **Figure 1-4**.
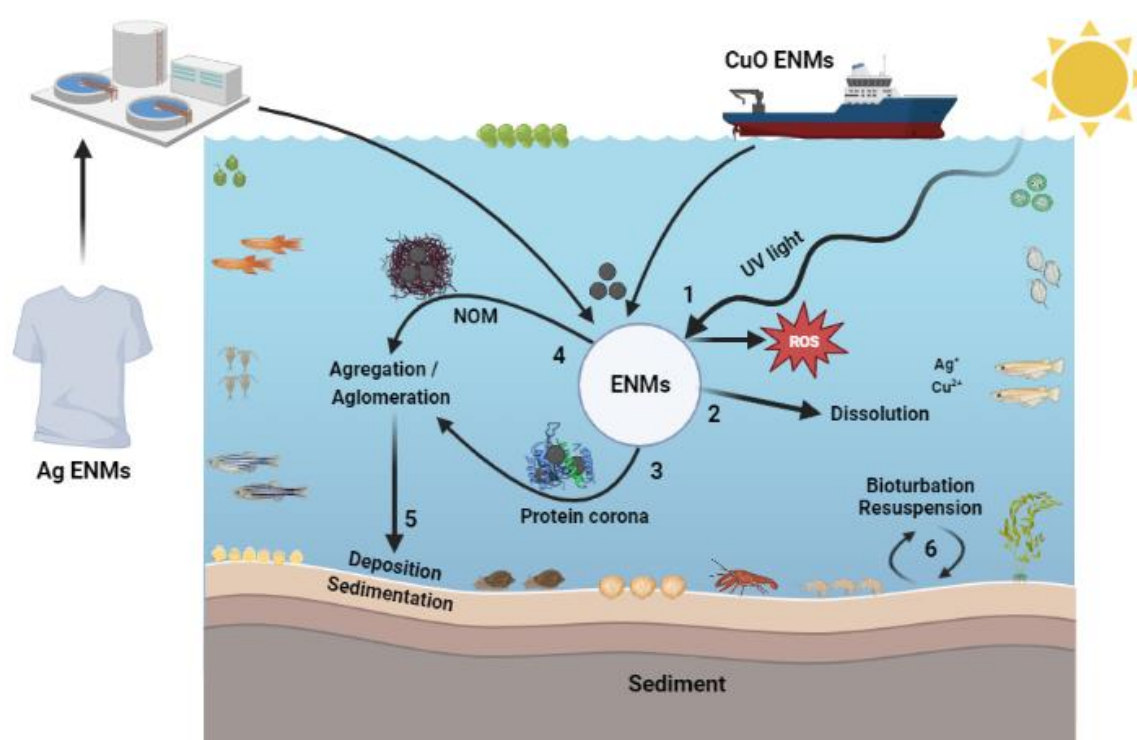
Figure 1-4 – Schematic illustration of some the transformations that Ag and CuO ENMs might undergo after being released (e.g. Ag ENMs from textiles; CuO ENMs from the hull of boats) into freshwater ecosystems: photo-oxidation (1) leading to reactive oxygen species (ROS), 2) dissolution of ENMs releasing ionic compounds, interaction with biomolecules (proteins), 3) forming coronas and 4) natural organic matter (NOM) that induce the agglomeration or aggregation (5) of ENMs and subsequent deposition in the sediment and then with the action of abiotic (streamflow) or biotic (bioturbation) will be resuspended (6). In all these scenarios, ENMs will interact with organisms from different trophic levels and possibly be uptaken by those. Figure created in BioRender.

Dissolution, one of the main transformations of Me and MeO ENMs, is defined as the molecular transference from the surface of a dissolving solid to the solution through a diffusion layer (Misra et al., 2012).

For instance, the washing of antimicrobial textiles (Ag ENMs) and the corrosion of antifouling paints (CuO ENMs) might release dissolved Ag and Cu, respectively, to the aquatic ecosystems (Mitrano et al., 2016; Mitrano et al., 2014; Ross and Knightes, 2022). The dissolution of pristine ENMs occurs due to three main causes: 1) the formation of partially soluble metal oxides, 2) the oxidation of ENMs components, and 3) complexation of the ENMs by complexants present in the water or in the ENMs embedded matrix (Vale et al., 2016). The latter, complexation of ENMs, is mainly affected by the physicochemical conditions of natural waters, as ionic components and strength, concentration of dissolved oxygen and sulphide, pH, or the presence of natural organic matter (NOM) (Stetten et al., 2022).

Furthermore, the dissolution of ENMs is also dependent on the size of the particles. As stated before, smaller particles have a larger surface-area-to-volume ratio (see section **1.1**). Dissolution rate also correlates to the surface area of the particle, that is supported by the Ostwald-Freundlich equation, hence smaller particles have higher solubility than larger ones (Ma et al., 2011; Peretyazhko et al., 2014). So, all the transformations (e.g. dissolution) that pristine ENMs can undertake in freshwater ecosystem will affect their bioavailability and, subsequently, their toxicity to the freshwater organisms.

1.4.1 Uptake Route of ENMs in Freshwater Organisms

Freshwater organisms from different trophic levels (i.e. classification based on their energy production or feeding behavior) will occupy different positions in the water depth. For example, algae and/or aquatic plants will occupy shallow parts of streams or wetlands for photosynthesis. On the other hand, pelagic fish will inhabit the water column to find food, but search for shelter in shallower waters to dispose their eggs. Thus, different organisms will present different routes of uptake of ENMs. In aquatic plants, the most likely route of entry of ENMs would be root adsorption, still ENMs can be uptaked and them translocated to other plant parts above the water

(Ebrahimbabaie et al., 2020). In fish, great part of the uptake of ENMs likely to occur through the gills (Shaw and Handy, 2011) or by ingestion (Gaiser et al., 2009). Once inside the organism, different mechanism of cellular uptake are proposed (Eddy and Handy, 2012).

1.5 Internalization of ENMs

As previously mentioned, ENMs can affect organisms at different levels of the biological organization, from the molecular level to the population or community levels. In order to produce alterations at the molecular level ENMs need to be internalized in the cell. Endocytosis by vesicle-mediated transport seems to be the the most commom mechanism, being sub-divided in five processes (**Figure 1-5**): phagocytosis, clathrin-mediated endocytosis, caveolin-mediated endocytosis, clathrin/caveolae-independent endocytosis, and micropinocytosis, as thoroughly described in (Behzadi et al., 2017). However, the physico-chemical characteristics of ENMs (e.g. surface coating) can affect their cellular uptake (Augustine et al., 2020). Once inside the cell, ENMs will induce different defence mechanisms.
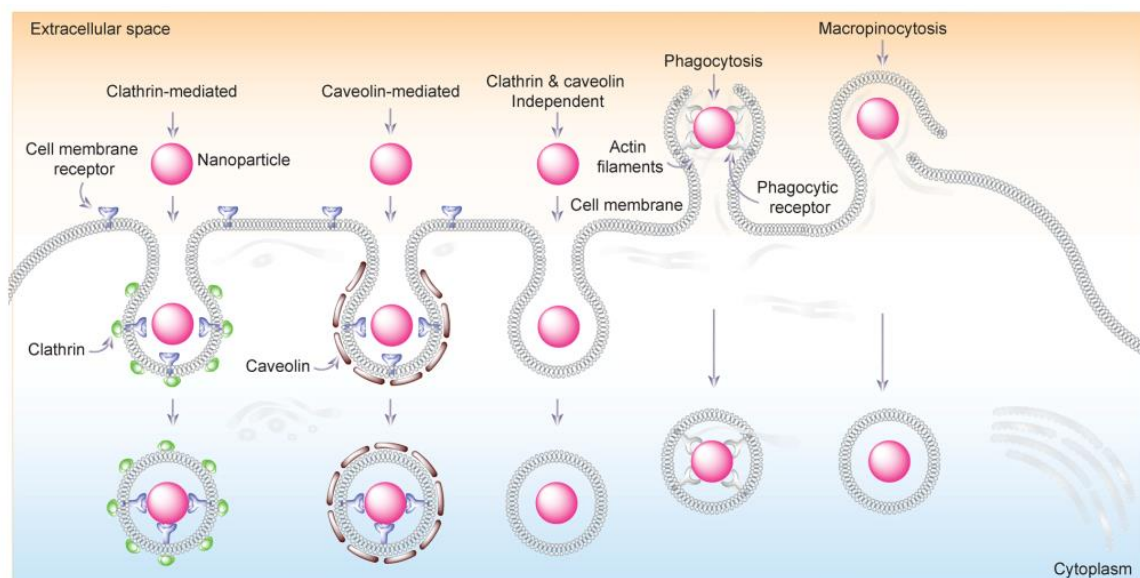
Figure 1-5 – Scheme representing the different mechanisms of cellular internalization of ENMs (from Augustine et al., 2020).

1.5.1 Antioxidant defence mechanisms

Regular oxygen (O_2) metabolism induces the generation of reactive oxygen species (ROS), by-products of O_2 reduction to produce energy (adenosine-5'-triphosphate, ATP). Although ROS are essential for cell signalling, their accumulation can be damaging to the cells and eventually to the organisms (Rudneva, 2013). This is why, antioxidant enzymes counteract the effects of ROS and try to attain cellular redox status through a balance between generation and elimination of ROS by complex mechanisms (Trachootham et al., 2008).

However, beyond the normal levels generated by aerobic cellular respiration, several biotic stressors (e.g. fungi, virus or bacteria) and abiotic stressors (e.g. UV light, ionizing radiation or metals) can trigger the overproduction of ROS, and consequently induce a redox imbalance that leads to oxidative stress (Andrés et al., 2023). Once inside the cell, Ag and Cu are likely to induce the formation of ROS, more specifically, hydroxyl radicals ($^{\bullet}OH$), through a Fenton reactions (Cortese-Krott et al., 2009). It is described that the same occurs with ENMs, with oxidative stress being described as one of the main mechanisms of nanotoxicity (Fu et al., 2014; Mendoza and Brown, 2019). Both plant and animal cells have strategies and mechanisms to deal with these stressors and some of these defence mechanisms are common as shown in **Figure 1-6** and **Figure 1-7**, respectively. Antioxidant enzymatic defences – as superoxide dismutase (SOD), catalase (CAT), guaiacol peroxidase (GPox) and glutathione-*S*-transferase (GST) – and non-enzymatic defences (e.g. glutathione, GSH) are the first line of cellular defence from ROS, as described in detail in sections **1.5.1.1** and **1.5.1.2**.
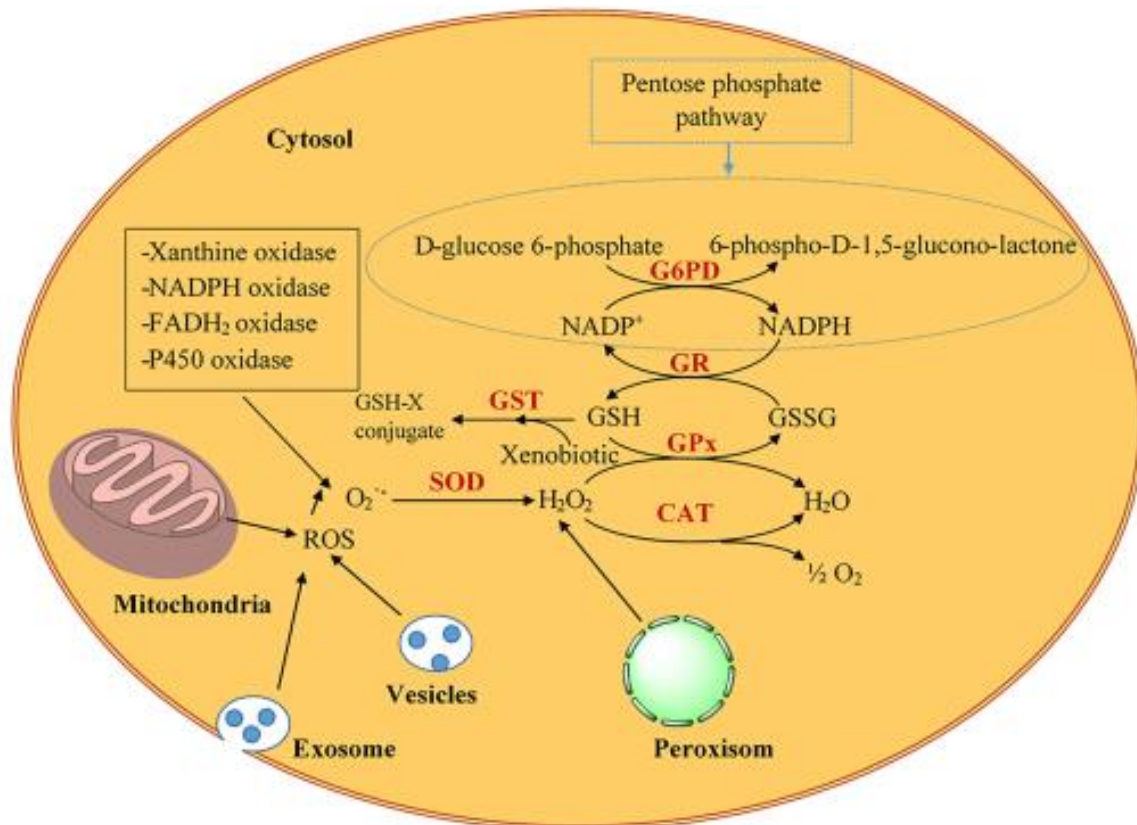
Figure 1-6 – Schematic model of cellular ROS generation and the cooperation of main antioxidant enzymes in animal cells. Superoxide dismutase (SOD) converts Superoxide anion ($O_2^{\bullet-}$) into hydrogen peroxide (H_2O_2). Catalase (CAT) and Glutathione peroxidase (GPx) are H_2O_2 detoxifying enzymes in animal cells. Glutathione reductase (GR) recycles the oxidized glutathione (GSSG) into reduced glutathione (GSH). Glutathione-*S*-transferase (GST) conjugates GSH with xenobiotics (adapted from Guller et al., 2020).
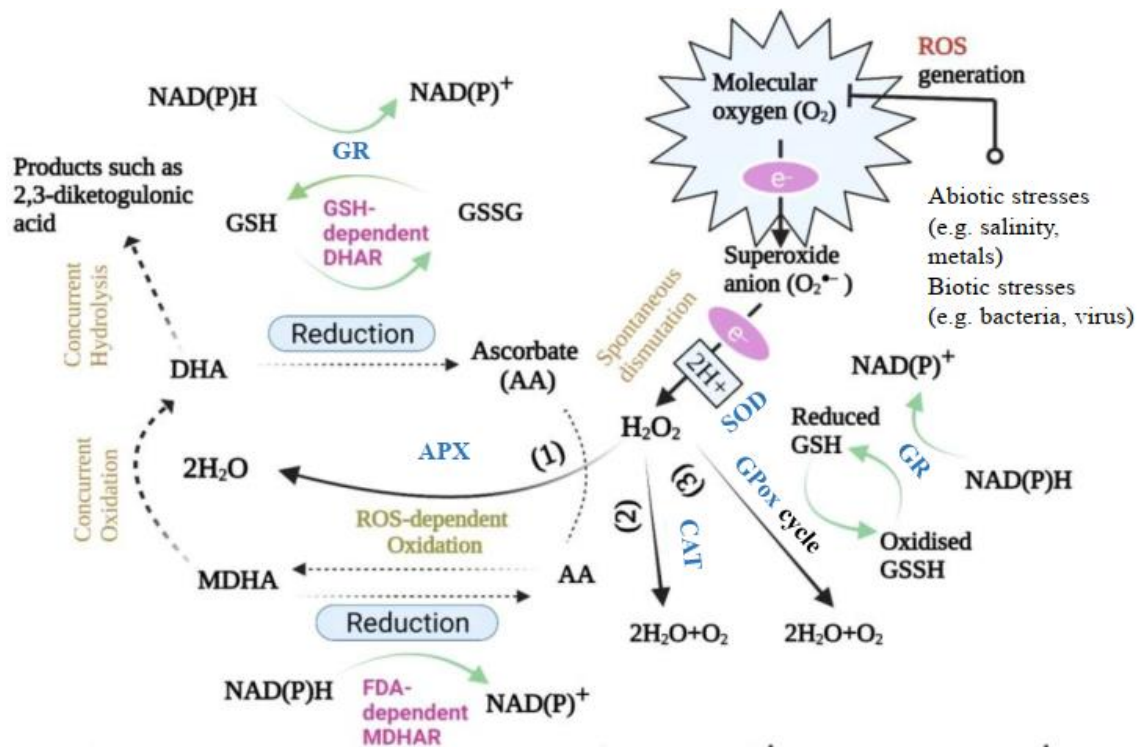
Figure 1-7 – Schematic model of oxidative stress reactions in plant cells showing the ascorbate-glutathione (AA/GSH) and guaiacol peroxidase (GPox) cycles. AA is oxidised by ROS and converted into monodehydroascorbate (MDHA). A set of three enzymes, including FAD (flavin adenine dinucleotide) - dependent monodehydroascorbate reductase (MDHAR), GSH-dependent dehydroascorbate reductase (DHAR) and glutathione reductase (GR), catalyse the recycling of ascorbate. Superoxide dismutase (SOD) converts $O_2^{\bullet-}$ into H_2O_2. Ascorbate peroxidase (APX) (1), catalase (CAT) (2), and GPox (3) act as the main H_2O_2 detoxifying enzymes. AA and GSH are antioxidants. Abbreviations: reduced glutathione (GSH), oxidized glutathione (GSSG) (adapted from Zandi and Schnug, 2022).

1.5.1.1   **Enzymatic defences**

1.5.1.1.1   **Superoxide dismutase (SOD)**

Superoxide dismutase (SOD, EC 1.15.1.1) acts as the first antioxidant defence line, is the enzyme that attacks the superoxide radical ($O_2^{\cdot-}$), a weak oxidant and highly instable ROS (Andrés et al., 2023). This enzyme catalyses the dismutation of $O_2^{\cdot-}$, into a molecule of hydrogen peroxide (H_2O_2), a more stable oxygen radical (Gagné, 2014). SOD is mostly stored in chloroplasts and peroxisomes in plant cells (Mehla et al., 2017) and in mitochondria and cytoplasm in animal cells (Gagné, 2014). This antioxidant endpoint is widely applied in ecotoxicology, including studies with ENMs (Jiang et al., 2014; Vale et al., 2016; Valerio-Garcia et al., 2017).

1.5.1.1.2   **Catalase (CAT)**

Catalase (CAT, E.C. 1.11.1.6) is a heme-containing enzyme that exists in most aerobic organisms (Yonca Yuzugullu, 2020). After SOD, CAT catalyses the breakdown of H_2O_2 into molecules of water (H_2O) and O_2. (Gagné, 2014). In both plant and animal cells, peroxisomes are the major sites of H_2O_2 generation, being the organelle where most of CAT is found (Das and Roychoudhury, 2014; Rocha et al., 2003). CAT is also widely applied in nanotoxicology (Boros and Ostafe, 2020; Gambardella and Pinsino, 2022; Jiang et al., 2014; Valerio-Garcia et al., 2017).

1.5.1.1.3   **Guaiacol peroxidase (GPox)**

Guaiacol peroxidase (GPox, E.C.1.11.1.7) is also an heme-containing enzyme usually available inside the cell, mostly in cytosol and vacuoles, but is also active outside the cell (Das and Roychoudhury, 2014). GPox is considered a key enzyme to the removal of H_2O_2, thus both CAT and GPox compete for H_2O_2 (Rico et al., 2015). GPox is an antioxidant endpoint commonly applied in plant ecotoxicology, including ENMs (Jiang et al., 2014; Majumdar et al., 2014; Srivastav et al., 2021).

1.5.1.1.4   **Glutathione-S-transferase (GST)**

Glutathione-*S*-transferases (GSTs, E.C.2.5.1.18) are a family of intracellular enzymes with the main function in detoxification processes from Phase II (Habig et

al., 1974). This enzyme catalyses the conjugation of negatively charged sulfhydryl group (–SH) of glutathione (GSH; section **1.5.1.2**) with endogenous toxic metabolites or xenobiotics (e.g. metals (Nepovím et al., 2004)), promoting their sequestration and removal from cells (Habig et al., 1974). GST is an endpoint of xenobiotic transformation widely applied in ecotoxicology, including ENMs (Bouguerra et al., 2019; Kumbhakar et al., 2019; Vale et al., 2016).

1.5.1.2   **Non-enzymatic defences (Glutathione)**

Glutathione (GSH) is the most abundant free cellular thiol (non-protein sulfhydryl) in plant (Foyer and Noctor, 2005; Hasanuzzaman et al., 2017; Noctor et al., 2011) and animal (Sparling, 2016a; Stegeman et al., 2010) cells. A tripeptide comprised of three amino acids – cysteine, glutamic acid, and glycine – present in cells around 5 milimolar (Stegeman et al., 2010). In eukaryotes cells, GSH is stored mostly in cytosol, mitochondria and endoplasmic reticulum (Lu, 2013). Glutathione is involved several aspects of cellular regulation, as in the redox signaling, antioxidant system mainly through Glutathione peroxidase (GPx), the ɣ-glutamyl cycle, growth and death regulation (Lu, 2013). As a substrate for GPx enzyme, GSH is oxidized into glutathione disulfide (GSSG), changing the GSH:GSSG ratio (Dickinson and Forman, 2002). Still, GSSG is recycled into the reduced form through the action of the Glutathione reductase enzyme (GR). This antioxidant enzyme recycles two molecules of GSSG into GSH. Additionally, GSSG in excess can also be transported to the extracellular space. Glutathione also acts as substrate of glutathione-*S*-transferase (GST; section **1.5.1.1.4**). In zebrafish, Glutathione reduced (GSH) seems to be regulated in early development of zebrafish (Timme-Laragy et al., 2013), they might be more susceptible to environmental stress in adult stage (Fish; section **1.6.2**). The measurement of the total GSH (tGSH) – analysis that accounts both states of the molecule, reduced (GSH) and oxidized (GSSG) – is used as a biomarker of oxidative stress (Domingues and Gravato, 2018) for diverse contaminants, including ENMs (Boyle et al., 2020).

1.5.2 Osmoregulation (Fish)

Freshwater fish live in hypo-osmotic environments , thus experience salt loss and water gain through their permeable bodies, most of which occurs in the gills (Eddy and Handy, 2012). Ions as sodium (Na^+) and chloride (Cl^-) are critical for osmoregulation since it accounts more than 90% of the body electrolytes (Kaneko and Hiroi, 2008). Still other electrolytes as calcium (Ca^{2+}) or magnesium (Mg^{2+}) are also osmo regulated and are essential for biological processes in fish (e.g. regulation of ion transporting cells, enzymes co-factor, muscular contraction) (Flik et al., 2009).

Sodium pump (Na^+/K^+ - ATPase, EC 3.6.1.3.) is one of the enzymes responsible for cellular homeostasis that regulate the intracellular ionic gradients (McCormick et al., 2009), thus its drift represents the active transport of ions across the membranes. Sodium pump is a highly conserved membrane-bound enzyme that releases energy from ATP to expel 3 molecules of Na^+ in exchange for 2 molecules of K^+ (Li et al., 1996). One of the main pathways of dissolved Ag and Cu toxicity is the inhibition of the sodium pump, contributing for the disruption of ionoregulation (Grosell, 2011; Wood, 2011).

Unlike adult fish that trade ions through the gills, these are not fully developed/functional in the embryonic stage. Thus, the ionic regulation is achieved by specific cells, ionocytes, currently known as mitochondria-rich cells, present in epithelial surface of embryos (Horng et al., 2022). Both the electrolytes levels and sodium pump have been used as indicators of fish osmoregulatory health for diverse environmental contaminants both in adults and embryos (e.g. metals (Handy et al., 2002)), including ENMs (Federici et al., 2007). In fact, ENMs have shown a potential for osmoregulatory stress in freshwater fishes (Boyle et al., 2020; Masouleh et al., 2017).

1.6 Model organisms to assess nanotoxicity

The choice of adequate model organisms is of paramount importance for the ecotoxicological evaluation of the ENMs to be tested. The traits of these model species should be well described and understood. Additionally, the species should

meet some criteria, as to be easy to cultivate and maintain in the laboratory, fast to grow and easy to reproduce, possess genetic tractability and availability of a broad spectrum of experimental and methodological tools (Russell et al., 2017). Standardised exposure tests are conducted with species that represent different trophic levels to test hypotheses about the impact of contaminants and eventual pollution situations (Segner and Baumann, 2015), including ENMs (Zielinska et al., 2020). Even more than that, model species should help ecotoxicologists recognise the mode of action (MoA) of chemicals, predict the toxicological and ecological outcomes of the exposure, and eventually understand which information can be extrapolated from the model species to other ecological target species, and the ecosystem as a whole (Segner and Baumann, 2015).

Model organisms include a large number of taxa, from bacteria (e.g. *Escherichia coli*), fungi (e.g. *Saccharomyces cerevisiae*), microalgae (e.g. *Raphidocelis subcapitata*), aquatic plants (e.g. *Lemna sp.*), nematodes (e.g. *Caenorhabditis elegans*), crustaceans (e.g. *Daphnia spp.*), insects (e.g. *Chironomus riparius*), amphibians (e.g. *Xenopus laevis*) to fish (e.g. *Danio rerio*, *Oryzias latipes*) (Thore et al., 2021). Most of these organisms are also being employed to study the effects of ENMs (Dumitrescu et al., 2019; Liu et al., 2022; Ong et al., 2015; Sardoiwala et al., 2017).

In this thesis two freshwater model organisms were used: the macrophyte species *Lemna minor*, and the fish species *Danio rerio*. Their selection was intended to represent not only two aquatic species from different trophic levels and with different routes of exposure to ENMs, but also some of the potentially most affected aquatic species by these contaminants.

1.6.1 **Macrophytes (*Lemna minor*)**

Macrophytes are aquatic plants, thus primary producers, that are visible to the bare eye and typically classified by growth form (i.e., rooted emergent, rooted and floating leaved, free floating, and submerged, both rooted and non-rooted) (Hanson, 2013). These plants play an important role in aquatic ecosystems because they contribute to maintain water quality (e.g. oxygen production, nutrients recycling), offer shelter

for other communities (e.g. nesting, light, wind buffer), provide biomass for herbivorous and detritivorous and among other functions (Hanson, 2013; Mohammad et al., 2010; Thomaz, 2021). Macrophytes reproduce vegetatively, so each plant is a clone, reducing the inter-individual variability. *Lemna* sp. (**Figure 1-8**) is a genus of free-floating aquatic plants, commonly known as duckweed, that belongs to the family Lemnaceae and can be found in temperate climates on the surface of fresh and brackish waters rich in nutrients such as lakes, ponds and streams (Leblebici and Aksoy, 2011; Mohammad et al., 2006).

For decades, duckweed toxicity testing has been part of the requirements for the risk assessment and registration of metals, pesticides and other contaminants (Wang, 1990; Ziegler et al., 2016). The popularity of *Lemna sp.* arose from its easy cultivation and handling in the laboratory, small size, rapid growth and reproduction (vegetative), test conductance, statistical and toxicological sensitivity and replicability of results (Rentz and Hanson, 2009; Wang et al., 2010).

Figure 1-8 – *Lemna minor*

Duckweed, more specifically *Lemna sp.*, have been widely used as a model organism in ecotoxicology with established protocols of 7-day assays that evaluate endpoints as biomass (wet and dry), frond numbers, chlorophyll-a concentrations, and growth rate (Brain and Solomon, 2007; ISO 20079, 2005; OECD, 2006). In the last two decades, studies been published focused on the monitoring of the water quality for diverse pollutants (Drost et al., 2007; Hou et al., 2007; Mohammad et al., 2010; Radic et al., 2011). Recently, studies have been performed to evaluate the

effects of ENMs to different duckweed species (Boros and Ostafe, 2020), specifically in *Lemna minor* (Kalcikova et al., 2018; Yue et al., 2018).

1.6.2 Fish (*Danio rerio*)

The term "fish" is used to describe a wide-ranging array of organisms that live in a diversity of habitats, ecological niches and trophic levels, comprising about 32,000 species (Nagel and Isberner, 1998; Nelson et al., 2016). Such a diversity of morphological and physiological characteristics among so many species poses a challenge into choosing a suitable model organism among fishes. Zebrafish (Danio rerio, Figure 1-9) is a small tropical freshwater fish from the Cyprinidae family, native from Southeast Asia (Eaton and Farley, 1974).
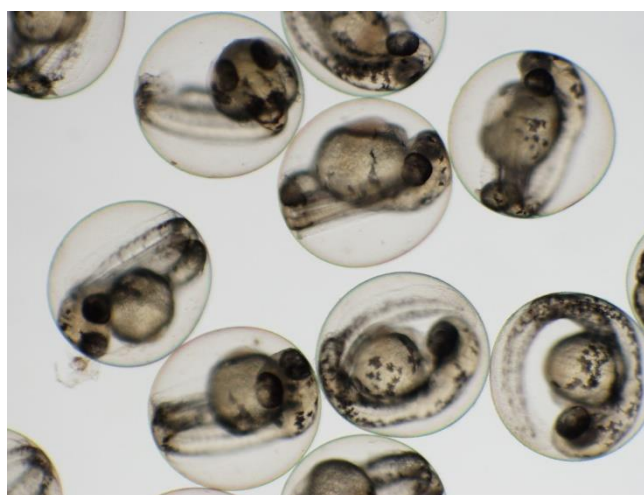
Figure 1-9 – Embryos of zebrafish (*Danio rerio*) at 48 hours post fertilization. Source: https://news.ucr.edu/media/image/zebrafish-embryos

This species share 70% of orthologous genes (i.e. evolved from a common ancestral gene) with human protein-coding genes, including disease-associated genes, in the brain, innate immune system, digestive tract, etc. (Khan and Sulaiman Alhewairini, 2019; Segner and Baumann, 2015). For these reasons, zebrafish is an established model organism since the 1990s (Khan and Sulaiman Alhewairini, 2019), being reputable in drug discovery toxicology (Cassar et al., 2020). Only recently, this species started to be applied to ecotoxicology and regulatory studies

with diverse environmental contaminants (Bambino and Chu, 2017; Fako and Furgeson, 2009; Segner, 2009; Truong et al., 2011). The initial guidelines of exposure to chemicals by OECD were designed to expose adults to acute test (OECD, 2019), later juveniles (OECD, 2000) and ten years ago, embryos (OECD, 2013b) and early-life stages (OECD, 2013a).
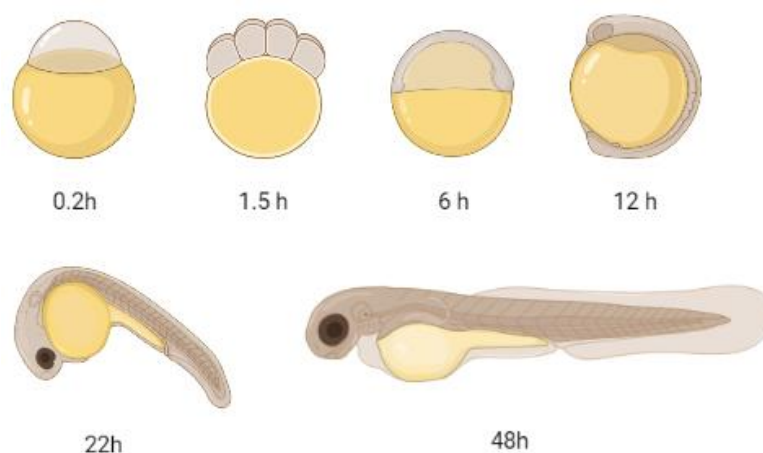
Figure 1-10 – Stages of development of zebrafish (*Danio rerio*) embryos. Adapted from Braunbeck et al. (2005) and Kimmel et al. (1995). Stages do not obey the same scale and the sketch of the embryo at 22h represents a dechorionated embryo for easier perception. Figure created in BioRender.

This shift to earlier life stages occurred mainly due to the European Directive 2010/63/EU on the animal welfare legislation for scientific purposes that demanded the 3Rs principle (replacement, reduction, refinement) (Braunbeck et al., 2005; Busquet et al., 2014). The embryonic development of zebrafish (**Figure 1-10**) is considered a resourceful tool to establish associations with diverse vertebrates (Truong et al., 2011). Other characteristics of embryos of zebrafish are also sought after, such as high fecundity of females, external development, transparent chorion, small size (millimetres), easy collection and manipulation – individual assessment in multiwell plates – and rapid development (i.e. hatching after ≈ 72 hours post fertilization), which allows to assess a wide array of parameters (e.g. hatching rate, movement impairment, heart beat) (Brundo and Salvaggio, 2018; Richendrfer et al., 2014). Additionally, the acute toxicity in zebrafish embryos has shown a good

correlation with the acute toxicity in zebrafish adults for diverse contaminants (Busquet et al., 2014; Rawlings et al., 2019), including ENMs (Kovrižnych et al., 2013).

Chorion, an acellular out layer, provides a physical barrier for external threats (Pelster and Bagatto, 2010). Embryos are sheltered not only by the chorion, but also by the inner perivitelline membrane. Passive diffusion of nutrients and oxygen to the inner mass of the embryo and elimination of wastes is promoted by chorionic pores – size was determined as 0.17 μm^2 (Cheng et al., 2007). Chorionic pores act as sievers for the uptake of exogenous substances (e.g. chemicals) by size-dependent restriction (Scholz et al., 2008). So, in theory, ENMs only small particles would pass through these pores. Nevertheless, transformations of ENMs (e.g. agglomeration) would create clusters of particles covering the chorion of the embryos that could block its pores, thus affecting the passive diffusion of oxygen and nutrients and jeopardizing their survival. In normal conditions, the proteolysis of chorion occurs by the action of hatching enzymes (particularly ZHE1) that are released in the perivitelline space (Muller et al., 2015); then, hatching occurs when chorion is thin enough for larvae to release themselves (Ong et al., 2014). Thus, without the protection of the "egg", larvae are often more vulnerable to waterborne chemicals than embryos (Zimmer et al., 2014), being also the case of some ENMs (Shaw et al., 2016).

1.7 Aims of the Thesis

The effects of metal and metal oxide nanomaterials in freshwater ecosystems are not fully understood. The sensitivity of aquatic plants and fish make them suitable to study the effects of ENMs, here represented by one metal ENMs and one metal oxide ENMs. Therefore, this thesis aimed to evaluate the effects of silver (Ag) and copper oxide (CuO) ENMs in two model organisms, *Lemna minor* and *Danio rerio*. Additionally, comparisons were made on the effects of both ENMs with their bulk counterparts, silver, a non-essential element, and copper, an essential trace element, respectively. This thesis focused on different characteristics of ENMs and on how these characteristics might affect their toxicity. Thus, the aims were:

1. Compare the physiological responses of *L. minor* exposed to Ag ENMs with two surface coatings (citrate vs PVP) to assess if their characteristics affected the toxicity of Ag ENMs, but also if these effects depend on the duration of the exposure period (7 vs 14 days; **Chapter II**).

2. Evaluate if the effects of Ag ENMs and silver nitrate (AgNO$_3$) on *L. minor* depended on the duration of the exposure period (7 vs. 14 days) (**Chapter II**).

3. Compare the response of selected antioxidant enzymes to citrate-Ag ENMs and PVP-Ag ENMs exposed plants (*L. minor*) (**Chapter II**).

4. Determine the most sensitive and vulnerable time and stages of embryonic development that affect the survival, hatching, osmoregulation and antioxidant status by exposing the embryos to waterborne Ag ENMs and AgNO$_3$ (**Chapter III**).

5. Evaluate the effects of waterborne CuO ENMs and copper sulphate (CuSO$_4$) exposure to zebrafish embryos (**Chapters IV**), using the same experimental design as point 4.

6. Understand if the chorion could hinder the entry of Ag and CuO ENMs inside the embryos or if the ENMs could pass through the chorionic pores. For this, the bioavailability of Ag and CuO ENMs was assessed through metal quantification with the presence or absence of the chorion, in comparison to the respective salt metals (**Chapters III** and **IV**, respectively).

7. Determine the embryonic electrolyte levels as well as the sodium pump activity that might help to understand the mechanisms of action of Ag ENMs and CuO ENMs in comparison to the respective salt metals (**Chapters III** and **IV**, respectively).

8. Understand the role glutathione as a scavenger and detoxifying agent of both Ag and Cu metals through the assessment of this non-enzymatic defence mechanism in both Ag and CuO ENMs, in comparison to the respective salt metals (**Chapters III** and **IV**, respectively).

Overall, these studies aim to contribute to understand the toxicity of Ag ENMs and CuO ENMs to freshwater environments, via the waterborne exposure of *Lemna minor* and *Danio rerio* embryos. Thus, this thesis fit in the United Nations 2030

Agenda for Sustainable Development, in particular the goal 15 "Protect, restore and promote sustainable use of terrestrial ecosystems, sustainably manage forests, combat desertification, and halt and reverse land degradation and halt biodiversity loss". Indeed, a deeper knowledge of the toxicity caused ENMs might ultimately lead to decrease their release to the aquatic environment, reducing aquatic pollution. Thus contributing "to reduce the degradation of natural habitats, halt the loss of biodiversity and protect and prevent the extinction of threatened species" (goal 15.5) and "ensure the conservation and sustainable use of inland freshwater ecosystems" (goal 15.1).

1.8 **Thesis Structure and Overview**

The present thesis is organized in five main chapters. The first chapter (I) provides a general introduction to the theme of the present thesis, highlighting the relevance of studying the effects of Ag ENMs and CuO ENMs in freshwater species. Chapters II to IV describe the results obtained during this study and are structured as scientific papers. These manuscripts were published or submitted to peer reviewed journals. The last chapter (V) provides a general discussion and conclusion.

Chapter I provides a brief theoretical introduction regarding the impacts of ENMs, in particular Ag and CuO, to freshwater model organisms that represent aquatic plants and fish.

Chapter II is entitled "Phytotoxicity of silver nanomaterials to *Lemna minor*: surface coating and exposure period-related effects". In this chapter was studied the effects of Ag ENMs in *Lemna minor* at individual and sub-individual levels, focusing on three variables: Ag form (ENMs versus salt metal), surface coating (citrate versus PVP) and exposure period (7 versus 14 days). **aims 1, 2, 3**

Chapter III is entitled "Comparison of toxicity of silver nanomaterials and silver nitrate on developing zebrafish embryos: bioavailability, osmoregulatory and oxidative stress". This chapter describes the experimental results conducted to evaluate the lethal and sub-lethal effects of Ag ENMs in zebrafish embryos in comparison to the salt metal. **aims 4, 6, 7, 8**

Chapter IV is entitled "Differences in toxicity and accumulation of metal from copper oxide nanomaterials compared to copper sulphate in zebrafish embryos: Delayed hatching, the chorion barrier and physiological effects". This chapter describes the experimental results conducted to evaluate the lethal and sub-lethal effects of CuO in zebrafish embryos in comparison to the salt metal. **aims 5, 6, 7, 8**

Chapter V provides a general discussion on the results obtained in Chapter II to IV. As each of these chapters includes its own discussion, only a concise and integrative discussion of results is presented in this chapter. In order to highlight global trends and synergies among the results of these chapters and demonstrate the coherence of the work. Also, a comprehensive overview of the present results, and their ecological implications, is presented.

1.9 **References**

2020. Allied market research – nanomaterials market [Internet]. Retrived on 25 Jan 2023 from: https://www.alliedmarketresearch.com/nano-materials-market

Amde, M., et al., 2017. Transformation and bioavailability of metal oxide nanoparticles in aquatic and terrestrial environments. A review. Environ Pollut 230, 250-267. https://doi.org/10.1016/j.envpol.2017.06.064

Amoatey, P., Baawain, M. S., 2019. Effects of pollution on freshwater aquatic organisms. Water Environ Res. 91, 1272-1287. https://doi.org/10.1002/wer.1221

Andrés, C. M. C., et al., 2023. Superoxide Anion Chemistry—Its Role at the Core of the Innate Immunity. Int J Mol Sci. 24, 1841. https://doi.org/10.3390/ijms24031841

Augustine, R., et al., 2020. Cellular uptake and retention of nanoparticles: Insights on particle properties and interaction with cellular components. Mater Today Commun. 25, https://doi.org/10.1016/j.mtcomm.2020.101692

Bambino, K., Chu, J., 2017. Zebrafish in Toxicology and Environmental Health. Curr Top Dev Biol. 124, 331-367. https://doi.org/10.1016/bs.ctdb.2016.10.007

Barhoum, A., et al., 2022. Review on Natural, Incidental, Bioinspired, and Engineered Nanomaterials: History, Definitions, Classifications, Synthesis, Properties, Market, Toxicities, Risks, and Regulations. Nanomaterials. 12, 77. https://doi.org/10.3390/nano12020177

Behzadi, S., et al., 2017. Cellular uptake of nanoparticles: journey inside the cell. Chem Soc Rev. 46, 4218-4244. https://doi.org/10.1039/c6cs00636a

Bopp, S. K., et al., 2008. Copper-induced oxidative stress in rainbow trout gill cells. Aquat Toxicol. 86, 197-204. https://doi.org/10.1016/j.aquatox.2007.10.014

Boros, B. V., Ostafe, V., 2020. Evaluation of Ecotoxicology Assessment Methods of Nanomaterials and Their Effects. Nanomaterials. 10, 610. https://doi.org/10.3390/nano10040610

Bouguerra, S., et al., 2019. Effects of cobalt oxide nanomaterial on plants and soil invertebrates at different levels of biological organization. J Soils Sediments. 19, 3018-3034. https://doi.org/10.1007/s11368-019-02285-8

Boyle, D., et al., 2020. Toxicities of copper oxide nanomaterial and copper sulphate in early life stage zebrafish: Effects of pH and intermittent pulse exposure. Ecotoxicol Environ Saf. 190, 109985. https://doi.org/10.1016/j.ecoenv.2019.109985

Brain, R. A., Solomon, K. R., 2007. A protocol for conducting 7-day daily renewal tests with *Lemna gibba*. Nat Protoc. 2, 979-987. https://doi.org/10.1038/nprot.2007.146

Braunbeck, T., et al., 2005. Towards an alternative for the acute fish LC_{50} test in chemical assessment: The fish embryo toxicity test goes multi-species - an update. ALTEX. 22, 87-102.

Brix, K. V., et al., 2022. Adverse Outcome Pathways for Chronic Copper Toxicity to Fish and Amphibians. Environ Toxicol Chem. 41, 2911-2927. https://doi.org/10.1002/etc.5483

Brundo, M. V., Salvaggio, A., 2018. Zebrafish or *Danio rerio*: A New Model in Nanotoxicology Study, in: Y. Bozkurt (Ed.), Recent Advances in Zebrafish Researches. IntechOpen, London, pp. 121-133. https://doi.org/10.5772/intechopen.74834

Burdusel, A. C., et al., 2018. Biomedical Applications of Silver Nanoparticles: An Up-to-Date Overview. Nanomaterials. 8, 681. https://doi.org/10.3390/Nano8090681

Busquet, F., et al., 2014. OECD validation study to assess intra- and inter-laboratory reproducibility of the zebrafish embryo toxicity test for acute aquatic toxicity testing. Regul Toxicol Pharmacol. 69, 496-511. https://doi.org/10.1016/j.yrtph.2014.05.018

Buzea, C., et al., 2007. Nanomaterials and nanoparticles: sources and toxicity. Biointerphases. 2, 17-71. https://doi.org/10.1116/1.2815690

Caruso, G., et al., 2014. Nanoparticles potential: types, mechanisms of action, actual in vitro and animal studies, recent patents, in: G. Caruso, et al. (Eds.), Innovative Brain Tumor Therapy. Woodhead Publishing, Sawston, pp. 53-150. https://doi.org/10.1533/9781908818744.53

Cassar, S., et al., 2020. Use of Zebrafish in Drug Discovery Toxicology. Chem Res Toxicol. 33, 95-118. https://doi.org/10.1021/acs.chemrestox.9b00335

Cheng, J., et al., 2007. Effect of carbon nanotubes on developing zebrafish (*Danio Rerio*) embryos. Environ Toxicol Chem. 26, 708-716. https://doi.org/10.1897/06-272R.1

Cortese-Krott, M. M., et al., 2009. Silver ions induce oxidative stress and intracellular zinc release in human skin fibroblasts. Free Radic Biol Med. 47, 1570-7. https://doi.org/10.1016/j.freeradbiomed.2009.08.023

Das, K., Roychoudhury, A., 2014. Reactive oxygen species (ROS) and response of antioxidants as ROS-scavengers during environmental stress in plants. Front Environ Sci. 2, 1-13. https://doi.org/10.3389/fenvs.2014.00053

Delay, M., Frimmel, F., 2012. Nanoparticles in aquatic systems. Anal Bioanal Chem. 402, 583-592. https://doi.org/10.1007/s00216-011-5443-z

Deshmukh, S. P., et al., 2019. Silver nanoparticles as an effective disinfectant: A review. Mater Sci Eng C. 97, 954-965. https://doi.org/10.1016/j.msec.2018.12.102

Dickinson, D. A., Forman, H. J., 2002. Cellular glutathione and thiols metabolism. Biochemical pharmacology. 64, 1019-1026. https://doi.org/10.1016/S0006-2952(02)01172-3

Domingues, I., Gravato, C., 2018. Oxidative Stress Assessment in Zebrafish Larvae, in: L. Félix (Ed.), Teratogenicity Testing: Methods and Protocols. Humana, New York, pp. 477-486. https://doi.org/10.1007/978-1-4939-7883-0_26

Donnachie, R. L., et al., 2014. Using risk-ranking of metals to identify which poses the greatest threat to freshwater organisms in the UK. Environ Pollut. 194, 17-23. https://doi.org/10.1016/j.envpol.2014.07.008

Drost, W., et al., 2007. Heavy metal toxicity to *Lemna minor*: studies on the time dependence of growth inhibition and the recovery after exposure. Chemosphere. 67, 36-43. https://doi.org/10.1016/j.chemosphere.2006.10.018

Du, J., et al., 2018. A review on silver nanoparticles-induced ecotoxicity and the underlying toxicity mechanisms. Regul Toxicol Pharmacol. 98, 231-239. 10.1016/j.yrtph.2018.08.003

Duffus, J. H., 2002. "Heavy metals" a meaningless term? (IUPAC Technical Report). Pure and Applied Chemistry. 74, 793-807. https://doi.org/10.1351/pac200274050793

Dumitrescu, E., et al., 2019. Nanotoxicity Assessment Using Embryonic Zebrafish, in: Q. Zhang (Ed.), Nanotoxicity: Methods and Protocols. Springer New York, New York, NY, pp. 331-343. https://doi.org/10.1007/978-1-4939-8916-4_20

Eaton, R. C., Farley, R. D., 1974. Spawning cycle and egg production of zebrafish, *Brachydanio rerio*, in the laboratory. Copeia. 195-204.

29

Ebrahimbabaie, P., et al., 2020. Phytoremediation of engineered nanoparticles using aquatic plants: Mechanisms and practical feasibility. J Environ Sci. 93, 151-163. https://doi.org/10.1016/j.jes.2020.03.034

Eddy, F. B., Handy, R. D., 2012. Ecological and Environmental Physiology of Fishes, first ed. Oxford University Press, Oxford. https://doi.org/10.1093/acprof:oso/9780199540945.001.0001

Eisler, R., 1998. Copper hazards to fish, wildlife and invertebrates: A Synoptic Review. U.S. Geological Survey. Biological Resources Division, Biological Science, Lafayette.

European Comission, 2022. Commission Recommendation of 10.06.2022 on the definition of nanomaterial. Retrived on 15/02/2023 from: https://ec.europa.eu/environment/chemicals/nanotech/pdf/C_2022_3689_1_EN_ACT_part1_v6.pdf

Fahmy, H. M., et al., 2019. Coated silver nanoparticles: synthesis, cytotoxicity, and optical properties. RSC Adv. 9, 20118-20136. https://doi.org/10.1039/c9ra02907a

Fako, V. E., Furgeson, D. Y., 2009. Zebrafish as a correlative and predictive model for assessing biomaterial nanotoxicity. Adv Drug Deliv Rev. 61, 478-486. https://doi.org/10.1016/j.addr.2009.03.008

Federici, G., et al., 2007. Toxicity of titanium dioxide nanoparticles to rainbow trout (*Oncorhynchus mykiss*): Gill injury, oxidative stress, and other physiological effects. Aquat Toxicol. 84, 415-430. https://doi.org/10.1016/j.aquatox.2007.07.009

Fernandes, I. J., et al., 2020. Silver nanoparticle conductive inks: synthesis, characterization, and fabrication of inkjet-printed flexible electrodes. Sci Rep. 10, 8878. https://doi.org/10.1038/s41598-020-65698-3

Flemming, C. A., Trevors, J. T., 1989. Copper toxicity and chemistry in the environment: a review. Water Air Soil Pollut. 44, 143-158. https://doi.org/10.1007/BF00228784

Flik, G., et al., 2009. Regulation of calcium and magnesium handling in fishes, in: R. D. Handy, et al. (Eds.), Osmoregulation and ion transport: integrating physiological, molecular and environmental aspects. SEB, London, pp. 151-181

Foyer, C. H., Noctor, G., 2005. Oxidant and antioxidant signalling in plants: a re-evaluation of the concept of oxidative stress in a physiological context. Plant Cell Environ. 28, 1056-1071. https://doi.org/10.1111/j.1365-3040.2005.01327.x

Fu, P. P., et al., 2014. Mechanisms of nanotoxicity: generation of reactive oxygen species. J Food Drug Anal. 22, 64-75. https://doi.org/10.1016/j.jfda.2014.01.005

Fytianos, G., et al., 2020. Nanomaterials in Cosmetics: Recent Updates. Nanomaterials. 10, 979. https://doi.org/10.3390/nano10050979

Gagné, F., 2014. Oxidative Stress, in: F. Gagné (Ed.), Biochemical Ecotoxicology. Academic Press, Oxford, pp. 103-115. https://doi.org/10.1016/B978-0-12-411604-7.00006-4

Gaiser, B. K., et al., 2009. Assessing exposure, uptake and toxicity of silver and cerium dioxide nanoparticles from contaminated environments. Environmental Health. 8, S2. https://doi.org/10.1186/1476-069X-8-S1-S2

Gambardella, C., Pinsino, A., 2022. Nanomaterial Ecotoxicology in the Terrestrial and Aquatic Environment: A Systematic Review. Toxics. 10, 393. https://doi.org/10.3390/toxics10070393

Gawande, M. B., et al., 2016. Cu and Cu-Based Nanoparticles: Synthesis and Applications in Catalysis. Chem Rev. 116, 3722-811. https://doi.org/10.1021/acs.chemrev.5b00482

Glover, C. N., 2018. Defence mechanisms: the role of physiology in current and future environmental protection paradigms. Conserv Physiol. 6, 1-12. https://doi.org/10.1093/conphys/coy012

Grosell, M., 2011. Copper, in: C. M. Wood, et al. (Eds.), Homeostasis and Toxicology of Essential Metals. Academic Press, San Diego, pp. 53-133. https://doi.org/10.1016/s1546-5098(11)31002-3

Grosell, M., et al., 2002. Sodium turnover rate determines sensitivity to acute copper and silver exposure in freshwater animals. Comp Biochem Physiol C Toxicol Pharmacol. 133, 287-303. https://doi.org/10.1016/S1532-0456(02)00085-6

Guller, U., et al., 2020. Effects of different LED light spectra on rainbow trout (*Oncorhynchus mykiss*): in vivo evaluation of the antioxidant status. Fish Physiol Biochem. 46, 2169-2180. https://doi.org/10.1007/s10695-020-00865-x

Habig, W. H., et al., 1974. Glutathione S-transferases. The first enzymatic step in mercapturic acid formation. J Biol Chem. 249, 7130-7139. https://doi.org/10.1016/S0021-9258(19)42083-8

Haff, P. K., 2012. Technology and human purpose: the problem of solids transport on the Earth's surface. Earth Syst Dynam. 3, 149-156. https://doi.org/10.5194/esd-3-149-2012

Handy, R. D., 2003. Chronic effects of copper exposure versus endocrine toxicity: two sides of the same toxicological process? Comp Biochem Physiol A 135, 25-38. https://doi.org/10.1016/s1095-6433(03)00018-7

Handy, R. D., et al., 2002. Sodium-dependent copper uptake across epithelia: a review of rationale with experimental evidence from gill and intestine. Biochim Biophys Acta. 1566, 104-115. https://doi.org/10.1016/s0005-2736(02)00590-4

Hanson, M. L., 2013. Aquatic Macrophytes in Ecotoxicology, in: J.-F. Férard, C. Blaise (Eds.), Encyclopedia of Aquatic Ecotoxicology. Springer, Dordrecht, pp. 89-98. https://doi.org/10.1007/978-94-007-5704-2_9

Hasanuzzaman, M., et al., 2017. Glutathione in plants: biosynthesis and physiological role in environmental stress tolerance. Physiol Mol Biol Plants. 23, 249-268. https://doi.org/10.1007/s12298-017-0422-2

Hicks, A. L., 2017. Using multi criteria decision analysis to evaluate nanotechnology: nAg enabled textiles as a case study. Environ Sci Nano. 4, 1647-1655.

https://doi.org/10.1039/C7EN00429J

Hicks, A. L., et al., 2015. Life Cycle Payback Estimates of Nanosilver Enabled Textiles under Different Silver Loading, Release, And Laundering Scenarios Informed by Literature Review. Environ Sci Technol. 49, 7529-7542. https://doi.org/10.1021/acs.est.5b01176

Hicks, A. L., et al., 2016. Environmental impacts of reusable nanoscale silver-coated hospital gowns compared to single-use, disposable gowns. Environ Sci Nano. 3, 1124-1132. https://doi.org/10.1039/C6EN00168H

Hicks, A. L., Temizel-Sekeryan, S., 2019. Understanding the potential environmental benefits of nanosilver enabled consumer products. NanoImpact. 16, 100183. https://doi.org/10.1016/j.impact.2019.100183

Hicks, A. L., Theis, T. L., 2016. A comparative life cycle assessment of commercially available household silver-enabled polyester textiles. Int J Life Cycle Assess. 22, 256-265. https://doi.org/10.1007/s11367-016-1145-2

Hogstrand, C., Wood, C. M., 1998. Toward a better understanding of the bioavailability, physiology, and toxicity of silver in fish: implications for water quality criteria. Environ Toxicol Chem. 17, 547-561. https://doi.org/10.1002/etc.5620170405

Horng, J. L., et al., 2022. Differential effects of silver nanoparticles on two types of mitochondrion-rich ionocytes in zebrafish embryos. Comp Biochem Physiol C Toxicol Pharmacol. 252, 109244. https://doi.org/10.1016/j.cbpc.2021.109244

Hou, J., et al., 2017. Ecotoxicological effects and mechanism of CuO nanoparticles to individual organisms. Environ Pollut. 221, 209-217. https://doi.org/10.1016/j.envpol.2016.11.066

Hou, W., et al., 2007. Effects of copper and cadmium on heavy metal polluted waterbody restoration by duckweed (*Lemna minor*). Plant Physiol Biochem. 45, 62-9. https://doi.org/10.1016/j.plaphy.2006.12.005

Howe, P. D., S. Dobson, S., 2002. Silver and silver compounds: environmental aspects. Concise international chemical assessment document. World Health Organization, Geneva. pp. 1-44

ISO 20079, I. D., Water quality — Determination of the toxic effect of water constituents and waste water on duckweed (*Lemna minor*) — Duckweed growth inhibition test 2005.

Jiang, H. S., et al., 2014. Silver nanoparticles induced accumulation of reactive oxygen species and alteration of antioxidant systems in the aquatic plant *Spirodela polyrhiza*. Environ Toxicol Chem. 33, 1398-405. https://doi.org/10.1002/etc.2577

Jung, Y., et al., 2018. Implications of Pony Lake Fulvic Acid for the Aggregation and Dissolution of Oppositely Charged Surface-Coated Silver Nanoparticles and Their Ecotoxicological Effects on Daphnia magna. Environ Sci Technol. 52, 436-445. https://doi.org/10.1021/acs.est.7b04635

Kalcikova, G., et al., 2018. The use of multiwell culture plates in the duckweed toxicity test-A case study on Zn nanoparticles. N Biotechnol. 47, 67-72. https://doi.org/10.1016/j.nbt.2018.06.002

Kaneko, T., Hiroi, J., 2008. Osmo- and Ionoregulation, in: R. N. Finn (Ed.), Fish larval physiology. CRC Press, Boca Raton. https://doi.org/10.1201/9780429061608

Kansara, K., et al., 2022. A critical review on the role of abiotic factors on the transformation, environmental identity and toxicity of engineered nanomaterials in aquatic environment. Environ Pollut. 296, 118726. https://doi.org/10.1016/j.envpol.2021.118726

Keller, A. A., et al., 2013. Global life cycle releases of engineered nanomaterials. J Nanopart Res. 15, 1692. https://doi.org/10.1007/s11051-013-1692-4

Ken, C. F., et al., 2003. Characterization of fish Cu/Zn-superoxide dismutase and its protection from oxidative stress. Mar Biotechnol. 5, 167-73. https://doi.org/10.1007/s10126-002-0058-1

Khan, F. R., Sulaiman Alhewairini, S., 2019. Zebrafish (*Danio rerio*) as a Model Organism, in: L. Streba, et al. (Eds.), Current Trends in Cancer Management. IntechOpen, London, pp. 1-16. https://doi.org/10.5772/intechopen.81517

Kimmel, C. B., et al., 1995. Stages of embryonic development of the zebrafish. Dev Dyn. 203, 253-310. https://doi.org/10.1002/aja.1002030302

Kovrižnych, J. A., et al., 2013. Acute toxicity of 31 different nanoparticles to zebrafish (*Danio rerio*) tested in adulthood and in early life stages - comparative study. Interdiscip Toxicol. 6, 67-73. https://doi.org/10.2478/intox-2013-0012

Kumbhakar, D. V., et al., 2019. Assessment of oxidative stress, antioxidant enzyme activity and cellular apoptosis in a plant based system (*Nigella sativa* L.; black

cumin) induced by copper and cadmium sulphide nanomaterials. Environ Nanotechnol Monit Manag. 11, 100196. https://doi.org/10.1016/j.enmm.2018.100196

Leblebici, Z., Aksoy, A., 2011. Growth and Lead Accumulation Capacity of *Lemna minor* and *Spirodela polyrhiza* (Lemnaceae): Interactions with Nutrient Enrichment. Water Air Soil Pollut. 214, 175-184. https://doi.org/10.1007/s11270-010-0413-1

Leung, B. O., et al., 2013. Silver(I) complex formation with cysteine, penicillamine, and glutathione. Inorg Chem. 52, 4593-4602. https://doi.org/10.1021/ic400192c

Li, J., et al., 1996. Kinetics of Cu^{2+} inhibition of $Na^+/K(^+)$-ATPase. Toxicol Lett. 87, 31-38. https://doi.org/10.1016/0378-4274(96)03696-x

Linder, M. C., Hazegh-Azam, M., 1996. Copper biochemistry and molecular biology. Am J Clin Nutr. 63, 797S-811S. https://doi.org/10.1093/ajcn/63.5.797

Liu, M., et al., 2011. Enhancements of thermal conductivities with Cu, CuO, and carbon nanotube nanofluids and application of MWNT/water nanofluid on a water chiller system. Nanoscale Res Lett. 6, 297. https://doi.org/10.1186/1556-276X-6-297

Liu, Z., et al., 2022. Emerging trends in nanoparticle toxicity and the significance of using Daphnia as a model organism. Chemosphere. 291, 132941. https://doi.org/10.1016/j.chemosphere.2021.132941

Lu, S. C., 2013. Glutathione synthesis. Biochim Biophys Acta. 1830, 3143-53. https://doi.org/10.1016/j.bbagen.2012.09.008

Luoma, S. N., 2008. Silver nanotechnologies and the environment: Old problems or new challenges. Project on Emerging Nanotechnologies Woodrow Wilson International Center for Scholars & The Pew Charitable Trusts, Washingtion, D.C. pp. 1-72

Ma, R., et al., 2011. Size-Controlled Dissolution of Organic-Coated Silver Nanoparticles. Environ Sci Technol. 46, 752-759. https://doi.org/10.1021/es201686j

Maine, E., et al., 2014. The emergence of the nanobiotechnology industry. Nat Nanotechnol. 9, 2-5. https://doi.org/10.1038/nnano.2013.288

Majumdar, S., et al., 2014. Exposure of cerium oxide nanoparticles to kidney bean shows disturbance in the plant defense mechanisms. J Hazard Mater. 278, 279-87. https://doi.org/10.1016/j.jhazmat.2014.06.009

Masouleh, F. F., et al., 2017. Silver nanoparticles cause osmoregulatory impairment and oxidative stress in Caspian kutum (*Rutilus kutum*, Kamensky 1901). Environ Monit Assess. 189, 448. https://doi.org/10.1007/s10661-017-6156-3

Mazari, S. A., et al., 2021. Environmental impact of using nanomaterials in textiles, in: A. Ehrmann, et al. (Eds.), Nanosensors and Nanodevices for Smart Multifunctional Textiles. Elsevier, Amsterdam, pp. 321-342. https://doi.org/10.1016/B978-0-12-820777-2.00018-2

McCormick, S. D., et al., 2009. Distinct freshwater and seawater isoforms of Na^+/K^+-ATPase in gill chloride cells of Atlantic salmon. J Exp Biol. 212, 3994-4001. https://doi.org/10.1242/jeb.037275

McDonald, K. J., et al., 2015. Intrinsic properties of cupric oxide nanoparticles enable effective filtration of arsenic from water. Sci Rep. 5, 11110. https://doi.org/10.1038/srep11110

Mehla, N., et al., 2017. An Introduction to Antioxidants and Their Roles in Plant Stress Tolerance, in: M. I. R. Khan, N. A. Khan (Eds.), Reactive Oxygen Species and Antioxidant Systems in Plants: Role and Regulation under Abiotic Stress. Springer, Singapore, pp. 1-23. https://doi.org/10.1007/978-981-10-5254-5_1

Mendoza, R. P., Brown, J. M., 2019. Engineered nanomaterials and oxidative stress: current understanding and future challenges. Curr Opin Toxicol. 13, 74-80. https://doi.org/10.1016/j.cotox.2018.09.001

Misra, S. K., et al., 2012. The complexity of nanoparticle dissolution and its importance in nanotoxicological studies. Sci Total Environ. 438, 225-232. https://doi.org/10.1016/j.scitotenv.2012.08.066

Mitrano, D. M., et al., 2016. Unraveling the Complexity in the Aging of Nanoenhanced Textiles: A Comprehensive Sequential Study on the Effects of Sunlight and Washing on Silver Nanoparticles. Environ Sci Technol. 50, 5790-5799. https://doi.org/10.1021/acs.est.6b01478

Mitrano, D. M., et al., 2014. Presence of Nanoparticles in Wash Water from Conventional Silver and Nano-silver Textiles. ACS Nano. 8, 7208-7219. https://doi.org/10.1021/nn502228w

Mohammad, M., et al., 2010. Effects of herbicides on *Lemna gibba* and recovery from damage after prolonged exposure. Arch Environ Contam Toxicol. 58, 605-612. https://doi.org/10.1007/s00244-010-9466-9

Mohammad, M., et al., 2006. Recovery of *Lemna sp.* after exposure to sulfonylurea herbicides. Bull Environ Contam Toxicol. 76, 256-263. https://doi.org/10.1007/s00128-006-0915-0

Muller, E. B., et al., 2015. Quantitative adverse outcome pathway analysis of hatching in zebrafish with CuO nanoparticles. Environ Sci Technol. 49, 11817-11824. https://doi.org/10.1021/acs.est.5b01837

Nagel, R., Isberner, K., 1998. Testing of chemicals with fish — a critical evaluation of tests with special regard to zebrafish, in: T. Braunbeck, et al. (Eds.), Fish Ecotoxicology. Birkhäuser Basel, Basel, pp. 337-352. https://doi.org/10.1007/978-3-0348-8853-0_11

Negrescu, A. M., et al., 2022. Metal Oxide Nanoparticles: Review of Synthesis, Characterization and Biological Effects. J Funct Biomater. 13, 274. https://doi.org/10.3390/jfb13040274

Nelson, J., et al., 2016. Fishes of the World, 5th ed. Wiley, Hoboken. https://doi.org/10.1002/9781119174844

Nepovím, A., et al., 2004. Effects of heavy metals and nitroaromatic compounds on horseradish glutathione S-transferase and peroxidase. Chemosphere. 57, 1007-1015. https://doi.org/10.1016/j.chemosphere.2004.08.030

Nikolova, M. P., Chavali, M. S., 2020. Metal Oxide Nanoparticles as Biomedical Materials. Biomimetics. 5, 27. https://doi.org/10.3390/biomimetics5020027

Noctor, G., et al., 2011. Glutathione. Arabidopsis Book. 9, e0142. https://doi.org/10.1199/tab.0142

Nor, Y. M., 1987. Ecotoxicity of copper to aquatic biota: A review. Environ Res. 43, 274-282. https://doi.org/10.1016/S0013-9351(87)80078-6

OECD, Test No. 215: Fish, Juvenile Growth Test. Section 2. Organization for Economic Co-Operation and Development, Paris, 2000. pp. 16. https://doi.org/10.1787/9789264070202-en

OECD, Test No. 221: *Lemna sp.* Growth Inhibition Test, OECD Guidelines for the Testing of Chemicals. Section 2. OECD Publishing, Paris, 2006. pp. 22. https://doi.org/10.1787/9789264016194-en

OECD, Test No. 210: Fish, Early-life Stage Toxicity Test. Section 2. Organization for Economic Co-Operation and Development, Paris, 2013a. pp. 24. https://doi.org/10.1787/9789264203785-en

OECD, Test No. 236: Fish Embryo Acute Toxicity (FET) Test. Section 2. Organization for Economic Co-Operation and Development, Paris, 2013b. pp. 22. https://doi.org/10.1787/9789264203709-en

OECD, Test No. 203: Fish Acute Toxicity Test. Section 2. Organization for Economic Co-Operation and Development, Paris, 2019. pp. 24. https://doi.org/10.1787/9789264069961-en

Ong, C., et al., 2015. Drosophila melanogaster as a model organism to study nanotoxicity. Nanotoxicology. 9, 396-403. https://doi.org/10.3109/17435390.2014.940405

Ong, K. J., et al., 2014. Mechanistic insights into the effect of nanoparticles on zebrafish hatch. Nanotoxicology. 8**,** 295-304. https://doi.org/10.3109/17435390.2013.778345

Pelster, B., Bagatto, B., 2010. Respiration, in: S. F. Perry, et al. (Eds.), Zebrafish. Academic Press, London, pp. 289-309. https://doi.org/10.1016/s1546-5098(10)02907-9

Peretyazhko, T. S., et al., 2014. Size-controlled dissolution of silver nanoparticles at neutral and acidic pH conditions: kinetics and size changes. Environ Sci Technol. 48**,** 11954-11961. https://doi.org/10.1021/es5023202

Peters, R. J. B., et al., 2018. Detection of nanoparticles in Dutch surface waters. Sci Total Environ. 621**,** 210-218. https://doi.org/10.1016/j.scitotenv.2017.11.238

Pulit-Prociak, J., Banach, M., 2016. Silver nanoparticles – a material of the future…? Open Chem. 14**,** 76-91. https://doi.org/10.1515/chem-2016-0005

Radic, S., et al., 2011. Duckweed *Lemna minor* as a tool for testing toxicity and genotoxicity of surface waters. Ecotoxicol Environ Saf. 74**,** 182-187. https://doi.org/10.1016/j.ecoenv.2010.06.011

Ratte, H. T., 1999. Bioaccumulation and toxicity of silver compounds: A review. Environ Toxicol Chem. 18**,** 89-108. https://doi.org/10.1002/etc.5620180112

Rawlings, J. M., et al., 2019. Fish embryo tests and acute fish toxicity tests are interchangeable in the application of the threshold approach. Environ Toxicol Chem. 38**,** 671-681. https://doi.org/10.1002/etc.4351

Rentz, N., Hanson, M., 2009. Duckweed toxicity tests are appropriate for ERA. Integr Environ Assess Manag. 5**,** 350-351. https://doi.org/10.1897/1551-3793-5.3.350

Richendrfer, H., et al., 2014. The embryonic zebrafish as a model system to study the effects of environmental toxicants on behavior, in: C. A. Lessman, E. A. Carver (Eds.), Zebrafish: Topics in Reproduction, Toxicology and Development. Nova Science, New York, pp. 245-264

Rico, C., et al., 2015. Chemistry, biochemistry of nanoparticles, and their role in antioxidant defense system in plants, in: M. H. Siddiqui, et al. (Eds.), Nanotechnology and plant sciences: nanoparticles and their impact on plants. Springer, Cham, pp. 1-17. https://doi.org/10.1007/978-3-319-14502-0

Rocha, M. J., et al., 2003. Measurement of peroxisomal enzyme activities in the liver of brown trout (*Salmo trutta*), using spectrophotometric methods. BMC Biochem. 4**,** 2. https://doi.org/10.1186/1471-2091-4-2

Ross, B. N., Knightes, C. D., 2022. Simulation of the Environmental Fate and Transformation of Nano Copper Oxide in a Freshwater Environment. ACS EST Water. 2, 1532-1543.
https://doi.org/10.1021/acsestwater.2c00157

Rudneva, I., 2013. Biomarkers for stress in fish embryos and larvae, 1st ed. CRC Press, Boca Raton. https://doi.org/10.1201/b15378

Russell, J. J., et al., 2017. Non-model model organisms. BMC Biol. 15, 55.
https://doi.org/10.1186/s12915-017-0391-5

Sardoiwala, M. N., et al., 2017. Toxic impact of nanomaterials on microbes, plants and animals. Environ Chem Lett. 16, 147-160.
https://doi.org/10.1007/s10311-017-0672-9

Scholz, S., et al., 2008. The zebrafish embryo model in environmental risk assessment - applications beyond acute toxicity testing. Environ Sci Pollut Res. 15, 394-404. https://doi.org/10.1007/s11356-008-0018-z

Segner, H., 2009. Zebrafish (*Danio rerio*) as a model organism for investigating endocrine disruption. Comp Biochem Physiol C Toxicol Pharmacol. 149, 187-195.
https://doi.org/10.1016/j.cbpc.2008.10.099

Segner, H., Baumann, L., 2015. What constitutes a model organism in ecotoxicology? Integr Environ Assess Manag. 12, 195–205.
https://doi.org/10.1002/ieam.1727

Sevcikova, M., et al., 2011. Metals as a cause of oxidative stress in fish: a review. Vet Med. 56, 537-546. https://doi.org/10.17221/4272-VETMED

Shafiq, M., et al., 2020. An Overview of the Applications of Nanomaterials and Nanodevices in the Food Industry. Foods. 9, 148.
https://doi.org/10.3390/foods9020148

Shaw, B. J., Handy, R. D., 2011. Physiological effects of nanoparticles on fish: a comparison of nanometals versus metal ions. Environ Int. 37, 1083-1097.
https://doi.org/10.1016/j.envint.2011.03.009

Shaw, B. J., et al., 2016. A critical evaluation of the fish early-life stage toxicity test for engineered nanomaterials: experimental modifications and recommendations. Arch Toxicol. 90, 2077-2107. https://doi.org/10.1007/s00204-016-1734-7

Shevlin, D., et al., 2018. Silver engineered nanoparticles in freshwater systems – Likely fate and behaviour through natural attenuation processes. Sci Total Environ. 621, 1033-1046. https://doi.org/10.1016/j.scitotenv.2017.10.123

Sparling, D. W., 2016a. Bioindicators of Contaminant Exposure, in: D. W. Sparling (Ed.), Ecotoxicology Essentials. Academic Press, San Diego, pp. 45-66.
https://doi.org/10.1016/B978-0-12-801947-4.00003-2

Sparling, D. W., 2016b. Metals, in: D. W. Sparling (Ed.), Ecotoxicology Essentials. Academic Press, San Diego, pp. 225-275. https://doi.org/10.1016/B978-0-12-801947-4.00003-2

Srivastav, A., et al., 2021. Effect of ZnO Nanoparticles on Growth and Biochemical Responses of Wheat and Maize. Plants. 10, 2556. https://doi.org/10.3390/plants10122556

Stegeman, J. J., et al., 2010. Perspectives on zebrafish as a model in environmental toxicology, in: S. F. Perry, et al. (Eds.), Zebrafish. Academic Press, San Diego, pp. 367-439. https://doi.org/10.1016/S1546-5098(10)02910-9

Steinhauer, S., 2021. Gas Sensors Based on Copper Oxide Nanomaterials: A Review. Chemosensors. 9, 51. https://doi.org/10.3390/chemosensors9030051

Stetten, L., et al., 2022. Towards Standardization for Determining Dissolution Kinetics of Nanomaterials in Natural Aquatic Environments: Continuous Flow Dissolution of Ag Nanoparticles. Nanomaterials. 12, 519. https://doi.org/10.3390/nano12030519

Sun, T. Y., et al., 2014. Comprehensive probabilistic modelling of environmental emissions of engineered nanomaterials. Environ Pollut. 185, 69-76. https://doi.org/10.1016/j.envpol.2013.10.004

Temizel-Sekeryan, S., Hicks, A. L., 2020. Global environmental impacts of silver nanoparticle production methods supported by life cycle assessment. Resour Conserv Recycl. 156, 104676. https://doi.org/10.1016/j.resconrec.2019.104676

Thore, E. S. J., et al., 2021. Towards improved fish tests in ecotoxicology - Efficient chronic and multi-generational testing with the killifish *Nothobranchius furzeri*. Chemosphere. 273, 129697. https://doi.org/10.1016/j.chemosphere.2021.129697

Thomaz, S. M., 2021. Ecosystem services provided by freshwater macrophytes. Hydrobiologia. https://doi.org/10.1007/s10750-021-04739-y

Timme-Laragy, A. R., et al., 2013. Glutathione redox dynamics and expression of glutathione-related genes in the developing embryo. Free Radic Biol Med. 65, 89-101. https://doi.org/10.1016/j.freeradbiomed.2013.06.011

Trachootham, D., et al., 2008. Redox regulation of cell survival. Antioxid Redox Signal. 10, 1343-1374. https://doi.org/10.1089/ars.2007.1957

Tran, T. H., Nguyen, V. T., 2014. Copper Oxide Nanomaterials Prepared by Solution Methods, Some Properties, and Potential Applications: A Brief Review. Int Sch Res Notices. 2014, 856592. https://doi.org/10.1155/2014/856592

Truong, L., et al., 2011. Evaluation of embryotoxicity using the zebrafish model. Methods Mol Biol. 691, 271-279. https://doi.org/10.1007/978-1-60761-849-2_16

Vale, G., et al., 2016. Manufactured nanoparticles in the aquatic environment-biochemical responses on freshwater organisms: A critical overview. Aquat Toxicol. 170, 162-174.https://doi.org/10.1016/j.aquatox.2015.11.019

Valerio-Garcia, R. C., et al., 2017. Exposure to silver nanoparticles produces oxidative stress and affects macromolecular and metabolic biomarkers in the goodeid fish *Chapalichthys pardalis*. Sci Total Environ. 583, 308-318. https://doi.org/10.1016/j.scitotenv.2017.01.070

Vasilev, K., 2019. Nanoengineered Antibacterial Coatings and Materials: A Perspective. Coatings. 9, 654. https://doi.org/10.3390/coatings9100654

Veltman, K., et al., 2014. Toxicokinetic Toxicodynamic (TKTD) Modeling of Ag Toxicity in Freshwater Organisms: Whole-Body Sodium Loss Predicts Acute Mortality Across Aquatic Species. Environ Sci Technol. 48, 14481-14489. https://doi.org/10.1021/es504604w

Veltman, K., et al., 2008. Metal Bioaccumulation in Aquatic Species: Quantification of Uptake and Elimination Rate Constants Using Physicochemical Properties of Metals and Physiological Characteristics of Species. Environ Sci Technol. 42, 852-858. https://doi.org/10.1021/es071331f

Vishwanath, R., Negi, B., 2021. Conventional and green methods of synthesis of silver nanoparticles and their antimicrobial properties. Curr Opin Green Sustain Chem. 4, 100205. https://doi.org/10.1016/j.crgsc.2021.100205

Wagner, S., et al., 2014. Spot the difference: engineered and natural nanoparticles in the environment -release, behavior, and fate. Angew Chem Int Ed Engl. 53, 12398-12419. https://doi.org/10.1002/anie.201405050

Walker, C. H., et al., 2016. Principles of Ecotoxicology, 4th ed. CRC Press, Boca Raton. https://doi.org/10.1201/b11767

Wang, W., 1990. Literature review on duckweed toxicity testing. Environ Res. 52, 7-22. https://doi.org/10.1016/S0013-9351(05)80147-1

Wang, W., et al., 2010. DNA barcoding of the Lemnaceae, a family of aquatic monocots. BMC Plant Biol. 10, 205. https://doi.org/10.1186/1471-2229-10-205

Westerband, E. I., Hicks, A. L., 2018. Nanosilver-Enabled Food Storage Container Tradeoffs: Environmental Impacts Versus Food Savings Benefit, Informed by Literature. Integr Environ Assess Manag. 14, 769-776. https://doi.org/10.1002/ieam.4093

Wigginton, N. S., et al., 2007. Aquatic environmental nanoparticles. J Environ Monit. 9, 1306-1316. https://doi.org/10.1039/b712709j

Wood, C. M., 2011. Silver, in: C. M. Wood, et al. (Eds.), Homeostasis and Toxicology of Non-Essential Metals. Academic Press, San Diego, pp. 1-65.

https://doi.org/10.1016/S1546-5098(11)31023-0

Wood, C. M., et al., 1999. Physiology and modeling of mechanisms of silver uptake and toxicity in fish. Environ Toxicol Chem. 18, 71-83. https://doi.org/10.1002/etc.5620180110

Xu, Q., et al., 2017. Antibacterial cotton fabric with enhanced durability prepared using silver nanoparticles and carboxymethyl chitosan. Carbohydr Polym. 177, 187-193. https://doi.org/10.1016/j.carbpol.2017.08.129

Yonca Yuzugullu, K., 2020. Typical Catalases: Function and Structure, in: B. Margarete Dulce (Ed.), Glutathione System and Oxidative Stress in Health and Disease. IntechOpen, Rijeka, pp. 1-16. https://doi.org/10.5772/intechopen.90048

Yue, L., et al., 2018. Interaction of CuO nanoparticles with duckweed (*Lemna minor* L.): Uptake, distribution and ROS production sites. Environ Pollut. 243, 543-552. https://doi.org/10.1016/j.envpol.2018.09.013

Zandi, P., Schnug, E., 2022. Reactive Oxygen Species, Antioxidant Responses and Implications from a Microbial Modulation Perspective. Biology. 11, 55. https://doi.org/10.3390/biology11020155

Zhu, D., et al., 2018. Intriguingly high thermal conductivity increment for CuO nanowires contained nanofluids with low viscosity. Sci Rep. 8, 5282. https://doi.org/10.1038/s41598-018-23174-z

Ziegler, P., et al., 2016. Duckweeds for water remediation and toxicity testing. Toxicol Environ Chem. 98, 1127-1154. https://doi.org/10.1080/02772248.2015.1094701

Zielinska, A., et al., 2020. Nanotoxicology and Nanosafety: Safety-By-Design and Testing at a Glance. Int J Environ Res Public Health. 17, 4657. https://doi.org/10.3390/ijerph17134657

Zimmer, A. M., et al., 2014. Exposure to waterborne Cu inhibits cutaneous Na^+ uptake in post-hatch larval rainbow trout (*Oncorhynchus mykiss*). Aquat Toxicol. 150, 151-158. https://doi.org/10.1016/j.aquatox.2014.03.001

Chapter II

**PHYTOTOXICITY OF SILVER NANOMATERIALS TO
LEMNA MINOR: SURFACE COATING AND EXPOSURE
PERIOD-RELATED EFFECTS**

2   Chapter II – Phytotoxicity of silver nanomaterials to *Lemna minor*: surface coating and exposure period-related effects

2.1 **Highlights**

- Ag ENMs and $AgNO_3$ reduced plants growth rate, more noticeably $AgNO_3$.

- Citrate- Ag ENMs effects were more pronounced on GPox and GST activities.

- PVP-Ag ENMs affected more distinctively the growth rate and fronds per colony.

- GPox and GST were induced by citrate and PVP-Ag ENMs, but CAT remained unaffected.

- 14 days exposure alleviated chlorosis in Ag ENMs, but the opposite occurred in $AgNO_3$.

2.2 **Abstract**

Silver engineered nanomaterials (Ag ENMs) exponential production raises concern about their environmental impact. The effects of Ag ENMs to aquatic plants remain scarcely studied, especially in extended exposures. This paper aims to evaluate Ag ENMs effects in *Lemna minor* at physiological and oxidative stress endpoints, focusing on three variables: Ag form (ENMs versus salt metal– silver nitrate, AgNO$_3$), ENMs surface coating (citrate vs polyvinylpyrrolidone – PVP) and exposure period (7 vs 14 days (d)). In this study were assessed physiological endpoints (specific growth rate (SGR), chlorosis incidence and number of fronds per colony) and oxidative stress endpoints (enzymatic activities of catalase (CAT), guaiacol peroxidase (GPox) and glutathione-S-transferase (GST)). Generally, plants exposed to all Ag forms underwent decays on growth rate and fronds per colony, and increases on chlorosis, GPoX and GST, but no effects on CAT. The most sensitive endpoints were specific growth rate and GPox activity, showing significant effects down to 0.05 mg L^{-1} for Ag ENMs and 3 µg Ag L^{-1} for salt metal, after 14d. The salt metal showed higher toxicity with a 14d-EC$_{50}$ of 0.0037 mg Ag L^{-1}. Concerning surface coating, PVP-Ag ENMs were more deleterious on growth rate and fronds per colony, whereas citrate-Ag ENMs affected more the chlorosis incidence and GPox and GST activities. The exposure period significantly affected chlorosis: 14d triggered a chlorosis increase in the salt metal and a decrease in Ag ENMs when compared to 7d. Ag ENMs induced an oxidative stress status in cells, thus ensuing upregulated enzymatic activity as a self-defence mechanism. Since Ag ENMs dissolution might occur on a steady and continuous mode along time, and the average longevity of fronds, we propose longer exposures periods than the recommended by the OECD guideline. This approach would provide more relevant and holistic evidences on the overall response of freshwater plants to Ag ENMs in an ecological relevant scenario.

Keywords

2.3 Introduction

The manufacture of silver engineered nanomaterials (Ag ENMs) increased exponentially in recent years, with a worldwide estimated production of 55 tons/year (Piccinno et al., 2012). Their inherent antibacterial and antifungal properties led to a ubiquitous incorporation, from textiles and biocides to personal care products (Woodrow Wilson International Centre of Scholars, 2005). At the end of their life cycle Ag ENMs are expected to flow into environmental compartments as surface waters (e.g. lakes, streams and rivers) (Sun et al., 2014). Moreover, Ag ENMs-containing products may leach dissolved Ag, which are persistent, bioaccumulative and highly toxic to aquatic organisms (Ratte, 1999). Thus, the intensifying production of Ag ENMs combined with dissolved Ag toxicity raises concern about their environmental impact.

Predicted environmental concentration (PEC) of Ag ENMs in European surface waters was reported to be between 0.002 ng L^{-1} (Dumont et al., 2015) and 0.66 ng L^{-1} (Sun et al., 2014). Even these low concentrations can induce deleterious effects in prokaryotes, plants, invertebrates and fish (Arruda et al., 2015; Fabrega et al., 2011; Klaine et al., 2008). Additionally, the predictable industrial proliferation of Ag ENMs and follow-on residues should generate significant and proportional increases of PECs in surface waters in a near future and, thus, increased environmental risk (Fabrega et al., 2011; Massarsky et al., 2014).

Nanomaterials are commonly stabilized to prevent aggregation through surface coating, using organic (e.g. citrate and PVP) or inorganic molecules (Levard et al., 2012). Citrate-coated silver nanomaterials (citrate-Ag ENMs) and PVP-coated Ag ENMs (PVP-Ag ENMs) are respectively stabilized by electrostatic and steric repulsive forces between Ag ENMs (Li et al., 2013). Surface coating may also affect properties of particles such as optical properties (UV-Vis absorption spectra), dispersion and shape (Tejamaya et al., 2012). However, ENMs stability might be modified under environmental conditions (Badawy et al., 2010; Levard et al., 2012). Eventual modifications will influence dissolution (Angel et al., 2013), size and aggregation status (Tejamaya et al., 2012; Topuz et al., 2014) and, consequently, toxicity (Cupi et al., 2016; El Badawy et al., 2011) of Ag ENMs. For instance, citrate-

Ag ENMs were reported to be more unstable than PVP-Ag ENMs (Badawy et al., 2010; Tejamaya et al., 2012) and, thus, more toxic to aquatic bacteria (El Badawy et al., 2011) and microalgae (Angel et al., 2013). Furthermore, the physicochemical changes mentioned above might occur on a steady and continuous mode along time. Thus, the exposure period might also be relevant to assess the effects of Ag ENMs on aquatic organisms.

Effects of Ag ENMs to plants have been studied in a broad spectrum of species (Reddy et al., 2016; Tolaymat et al., 2017). However, less attention has been given to the uptake and toxicity of Ag ENMs in aquatic plants (Jiang et al., 2014; Kim et al., 2011a; Oukarroum et al., 2013; Van Koetsem et al., 2016). Few studies addressed extended exposure-related effects, as standard protocol recommends a 7 days (d) test period (OECD, 2006). In aquatic systems, Ag ENMs might be released and persist over large periods (Furtado et al., 2015), with consequent Ag ENMs-plant interactions. Thus, the assessment of Ag ENMs effects during an extended exposure period would be pertinent from an ecological perspective, as sustained by Gubbins et al. (2011), who reported severe Ag ENMs-related effects on *Lemna sp.* prompted by 14d of exposure down to 5 µg L^{-1}.

The toxicity of ENMs has been linked to a reactive oxygen species (ROS)-mediated mechanism, as suggested by several studies in algae (Oukarroum et al., 2012a; Perreault et al., 2012) and plants – duckweed (Hu et al., 2013; Oukarroum et al., 2013; Perreault et al., 2013; Song et al., 2012), potatoes (Bagherzadeh Homaee and Ehsanpour, 2016), rice (Mirzajani et al., 2013; Mirzajani et al., 2014), tomatoes (Song et al., 2013), water hyssop (Krishnaraj et al., 2012) and wheat (Dimkpa et al., 2012; Dimkpa et al., 2013). Nanomaterials induce excessive ROS generation that might impair the cell structure (e.g. chloroplasts), damaging lipids, carbohydrates, proteins and DNA (Rico et al., 2015). In fact, chloroplasts accumulate ROS that lead to photoinhibition and photooxidation of their constituents, then distressing photosynthesis (Brain and Cedergreen, 2009). ROS are efficiently scavenged by antioxidant enzymes, as catalase (CAT, EC 1.11.1.6) and guaiacol peroxidase (GPox, EC 1.11.1.7) that counteract the imbalances and, thus, contribute for plants detoxification (Ma et al., 2015). Glutathione-*S*-transferase (GST, EC 2.5.1.18) mediates detoxification processes (phase II) conjugating xenobiotics with

glutathione (GSH) and improving their sequestration and removal (Gill and Tuteja, 2010). However, for Ag ENMs few studies address the biochemical responses of plants, either aquatic or terrestrial (Bagherzadeh Homaee and Ehsanpour, 2016; Jiang et al., 2014; Krishnaraj et al., 2012; Song et al., 2013; Zou et al., 2016). Metallic ENMs toxicity has also been linked to chlorosis (Tripathi et al., 2017; Wang et al., 2013), a morphological alteration that suggests changes on the photosynthetic machinery.

This work aims to contribute towards a better comprehension of the physiological and biochemical responses of aquatic plants exposed to Ag ENMs with different surface coatings and extended exposure, using *Lemna minor* as a representative species. Summarily, this study aims to answer the following questions: Which are the effects of Ag ENMs and salt metal to *L. minor*? Do Ag ENMs and salt metal have similar effects to *L. minor*? Do the effects of Ag ENMs to *L. minor* depend on the respective surface coating? Do the effects of Ag ENMs and salt metal depend on the extent of the exposure period? Hence, this study evaluated the physiological and oxidative stress response of *L. minor* to Ag ENMs focusing on three variables: Ag form (ENMs versus salt metal), surface coating (citrate versus PVP-Ag ENMs) and exposure period (7d versus 14d). The physiological endpoints were the growth rate, chlorosis incidence and number of fronds per colony, whereas the oxidative stress endpoints were the enzymatic activities of CAT, GPox and GST.

2.4 Materials and Methods

2.4.1 Chemicals

Suspensions of silver nanomaterials (20 mg L^{-1}, NanoXact) with distinct organic surface coatings (citrate and PVP) were bought from NanoComposix (U.S.A.). According to the manufacture, both suspensions had spherical particles with a diameter of 79.0 (S.D. = ± 8.0) nm (Transmission electron microscopy (TEM) measurement) and 99.99% purity. Citrate and PVP-Ag ENMs suspensions are commercialized in aqueous 2 mM citrate. Salt metal ($AgNO_3$) was bought from Sigma-Aldrich (U.S.A.) with 99.99% of purity (CAS: 7761-88-8). Nitric acid (HNO_3,

≥69.0% TraceSELECT) was bought from Sigma-Aldrich (U.S.A.) and used for acid digestion.

2.4.2 **Preparation, characterization and quantification of Ag ENMs**

Citrate and PVP-Ag ENMs were used as bought. Stock solutions of $AgNO_3$ were prepared in Milli-Q water and kept refrigerated in dark. Dilutions for all treatments solutions were performed in Steinberg medium (ISO/DIS 20079, 2005; OECD, 2006). Suspensions of Ag ENMs (2 mg L^{-1}) in Steinberg medium were analyzed by Scanning Transmission Electron Microscopy (STEM; Hitachi SU-70, at 4.0 kV). In addition, Ag ENMs-Steinberg suspensions of lowest and highest concentrations (0.05 and 2 mg L^{-1}) were characterized by Dynamic Light Scattering (DLS, Malvern Instruments, Zetasizer Nano ZS). Zeta potential and conductivity were measured in both fresh (0d) and aged (7d) suspensions through micro electrophoresis measurements using a disposable electrophoretic flow through cell. Standard deviation for all measurements was lower than 1.5 mV.

Samples from aged (7d) exposure medium were collected from wells (independent replicates) (see section 2.4), representing total Ag in suspension. Then, these samples were digested overnight in HNO_3 (1:1 molar ratio) in teflon tubes at 60ºC and then diluted up to 5 mL. Total Ag concentration (Ag wavelength = 328 nm) was quantified by Inductively Coupled Plasma – Atomic Emission Spectrometry (ICP-AES; Optima 5300 DV, PerkinElmer). Instrument was calibrated with an internal standard of scandium. A mixed metal standard (calibration control verification (CCV) metals diluted to 25 µgL^{-1}) was run every 15 samples. Detection limit for Ag was 0.0022 µg L^{-1}.

2.4.3 **Maintenance of Lemna minor cultures**

L. minor cultures were kept in sterile Steinberg medium (ISO/DIS 20079, 2005; OECD, 2006). This culture initial specimens were collected in a pond (Vidal et al., 2012) near Tondela, Viseu (Portugal) in 2010 and, since then, have been kept under laboratorial conditions: 21 ± 1 °C, 16h:8h (dark: light) photoperiod and under 18.9 µmol m^{-2} s^{-1} (photosynthetic photon flux) of continuous cool-white fluorescent light.

Best fitted-specimens were washed in distilled water and transferred to fresh medium twice a week. Material was properly sterilized to maintain, handle and expose the specimens.

2.4.4 Experimental design

Growth inhibition tests followed OECD guideline N221 (OECD, 2006) with an extension of the exposure period to 14 days. Tests were carried out in covered plastic well plates. Each plate contained all treatments of a single Ag form (citrate-Ag ENMs, PVP-Ag ENMs and $AgNO_3$), including controls. Plants were exposed to concentrations of citrate and PVP-Ag ENMs (0.05-2 mg L^{-1}), $AgNO_3$ (3-300 µg Ag L^{-1}) and controls in triplicates. Replicates consisted in 10 fronds (3 colonies) per well in 15 mL of solution. Each well was considered as an independent replicate. After 7d, plants were transferred to a new plate with Steinberg medium freshly contaminated with respective concentration from stock solution. Test conditions were identical to the culture ones and all material was previously sterilized and acid washed (15% HNO_3).

2.4.5 Physiological endpoints

Physiological endpoints were assessed after 7d and 14d of exposure, through photographic records (stereo microscope Nikon SMZ1500, 7.5x magnification) of all plants (independent replicates). Based on these records, total number of fronds, number of colonies and number of chlorotic fronds were determined. A colony was considered an aggregate of fronds attached to each other. A frond was considered chlorotic when displayed yellowish regions next to the border or signs of necrosis including dark regions or spots (OECD, 2006). At 14d, plants were weighted (fresh weight) and snap-frozen in microtubes for posterior enzymatic analysis.

The following physiological endpoints were calculated for each replicate, to assess the health status of plants:

1)

$$\mu_{i-j} = \frac{\ln(N_j) - \ln(N_i)}{t}$$

Equation 2-1– Specific growth rate (**d^{-1}**): where μ_{i-j} is the average specific growth rate from time i to j; N_i is the number of fronds at time i; N_j is the number of fronds at time j; t is the time period from i to j.

2)

$$\varsigma = \left(\frac{C}{f}\right) x\ 100\ (\%)$$

Equation 2-2 – Chlorosis (**%**): where ς is the chlorosis percentage; C is the number of chlorotic fronds; f is the total number of fronds.

3)

$$F = f/c$$

Equation 2-3 – Fronds per colony (**n**): where F is the number of fronds per colony; f is the total number of fronds; c is the number of colonies.

2.4.6 **Oxidative stress endpoints**

Oxidative stress endpoints of citrate and PVP-Ag ENMs were assessed based on GPox, GST and CAT (redox-stress enzymes) activities. Plants exposed to AgNO$_3$ and to 0.8 mg L^{-1} of PVP-Ag ENMs lacked enough biomass to perform enzymatic analysis. Plants (independent replicates) were ice-defrosted, homogenized (sonicator KIKA Labortechnik U2005 ControlTM) and centrifuged (11500 rpm, 20 min) to isolate the post-mitochondrial supernatant (PMS) (Howcroft et al., 2011). Enzymatic activities were spectrophotometrically measured (Thermo Scientific Multiskan® Spectrum) in 96-well microplates. GPox activity was determined by mixing 10 µL of PMS, 160 µL of 96 mM guaiacol, 30 µL of 12 mM H$_2$O$_2$ and 100 µL in K-phosphate buffer (0.01 M, pH 6.1); and then recording the increase of absorbance (each 20s during 5 min) at 470 nm as described by Castillo et al. (1984).

GST activity was determined by mixing 100 µL of PMS, 100 µL of reaction mixture (20 mM reduced GSH) and 120 mM 1-chloro-2,4-dinitrobenzene (CDNB) in K-phosphate buffer (0.1 M, pH 6.5); and then measuring the increase of absorbance (each 20s during 5 min) at 340 nm, as described by Habig and Jakoby (1981)) and modified by Frasco and Guilhermino (2002). CAT activity was quantified by mixing 15 µL of PMS and 185 µL of reaction solution (hydrogen peroxide = H_2O_2), 30 mM in K-phosphate buffer (K-phosphate = 0.05 M, pH 6.5); and then measuring the decrease of absorbance, i.e. degradation of H_2O_2 (each 10s during 1:30 min), at 240 nm as described by Clairborne (1985). Enzymatic activities were determined in triplicate, expressed as nanomoles of substrate hydrolyzed per minute per mg of protein and then normalized to control percentage (basal level equal to 100%). Protein concentration was quantified ($\lambda = 595$ nm) in quadruplicate by Bradford method (Bradford, 1976), using albumin as standard.

2.4.7 Statistical analyses

All data were statistically analyzed with SigmaPlot v14 and SPSS software v22. A priori all data were tested for normality (Kolmogorov-Smirnov test) and homogeneity of variance (Levene's test). For each Ag compound, comparisons against control were performed with ANOVA followed by Dunnett's test (parametric) or Kruskal-Wallis test (non-parametric); multiple comparisons between treatments of citrate-Ag ENMs versus PVP-Ag ENMs and 7 days versus 14 days were performed with post-hoc Holm-Sidak test. Two significance levels ($p<0.01$ and $p<0.05$) were employed for statistical analyses. Two-way ANOVA was used to assess the significance of independent variables concentration and surface coating on the endpoints specific growth rate, percentage of chlorosis, number of colonies and enzymatic activities (**Appendix B**). Effect concentrations (EC_{50}) were calculated using a non-linear allosteric decay function. Relationships between individual and sub-individual endpoints were evaluated through Pearson correlations. Principal Component Analysis (PCA) with orthogonal rotation (varimax) was executed with two types of variables: individual (growth rate, chlorosis and fronds per colony) and sub-individual (CAT, GPox, GST) endpoints for 14 days' exposure to both Ag ENMs.

Only eigenvalues over 1 and component values over 0.30 were considered; all variables were standardized by Z score method (mean=0 and standard deviation=1).

2.5 **Results**

2.5.1 **Characterization of silver nanomaterials (Ag ENMs)**

Both Ag ENMs (citrate and PVP) suspensions in Steinberg medium displayed particles with a quasi-spherical shape and small-sized agglomerates (**Figure 2-1**). STEM analysis showed that citrate and PVP-Ag ENMs exhibited sizes of 80.8 ± 7.5 nm and 91.8 ± 7.1 nm (mean ± S.D.*, n=20*), respectively.

Zeta potential values are shown in **Table 2-1**. Ag ENMs-Steinberg suspensions had low zeta potential for both surface coatings (absolute values between 7.25 and 13.7 under a stable pH), representing incipient instability (Elzey and Grassian, 2010). Still, zeta potential and, thus, suspensions stability, differed significantly considering surface coating and suspensions age **(Table 6 III, Appendix B)**. In fresh suspensions, citrate-Ag ENMs were more stable than the PVP-ones. However, in aged suspensions, stability was not affected by surface coating **(Table 6 III, Appendix B)**. Suspensions stability decayed with aging, except for 2 mg L^{-1} of PVP-Ag ENMs. These results suggest that Ag ENMs suspensions in Steinberg medium tend to form agglomerates, which agrees with STEM images. Conductivity varied slightly among treatments **(Table 6 IV, Appendix B)**. After 7d aging in exposure medium, total Ag concentration in Ag ENMs suspensions was only 12.7 ± 6.6 % (citrate) and 9.4 ± 7.2 % (PVP) from the initial concentration (**Figure 2-2**). These low values agree with Ag ENMs low stability in the exposure medium. Higher values were found for citrate-Ag ENMs than PVP-ones. For instance, for nominal concentration 2 mg L^{-1}, the measured total Ag concentration in citrate-Ag ENMs suspensions was 3-fold higher than for PVP-ones. Comparing both Ag ENMs, similar values were found for 2 mg L^{-1} of PVP-Ag ENMs and 0.8 mg L^{-1} of citrate-Ag ENMs (87 and 89 µg L^{-1}, respectively). Measured total Ag concentration in AgNO$_3$ suspension was 97 ± 17 % from the initial concentration (nominal concentration 300 µg Ag L^{-1}).
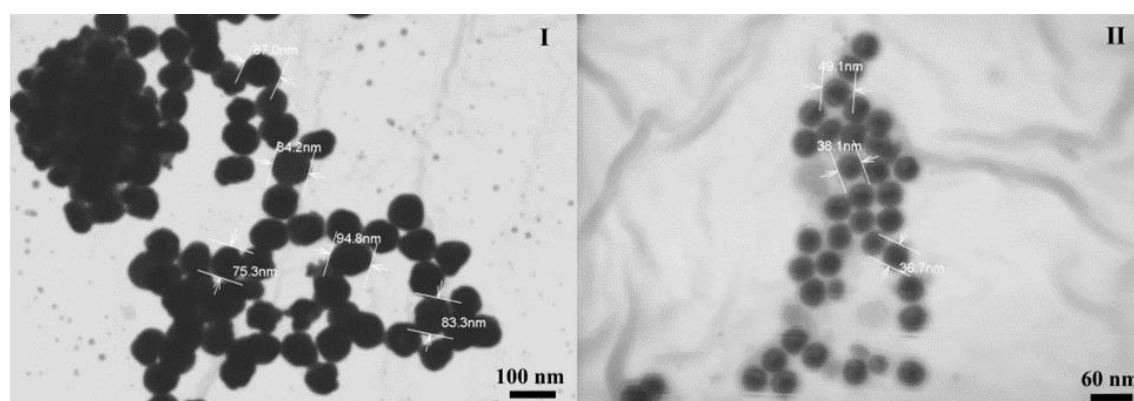
Figure 2-1 – High resolution transmission electron microscopic image of silver nanomaterials (Ag ENMs): citrate-Ag ENMs (**I**) and PVP-Ag ENMs (**II**) suspensions in Steinberg medium. The size of Ag ENMs was 80.78 ± 7.46 nm for citrate (range of the agglomerates: 66 – 99 nm) and 91.81 ± 7.07 nm for PVP (range of the agglomerates: 74 – 101 nm) (mean ± standard deviation, $n=20$).

Table 2-1 – Zeta potential (mV) of citrate and PVP-Ag ENMs suspensions (capital letters to denote differences between coatings) in Steinberg medium at day 0 and day 7 (small-case letters to denote differences between days) for the lowest and highest nominal test concentrations (mean ± standard deviation, $n=3$); pH is also showed at day 7.

Surface coating	Concentration (mg L^{-1})	pH	Zeta potential (mV)	
		Day 7	Day 0	Day 7
citrate	0.05	6.15 ± 0.02^{A}	- 11.7 ± 0.17^{aA}	- 7.0± 0.39^{bA}
	2	6.15 ± 0.005^{A}	- 13.7± 0.1^{aB}	- 9.8 ± 0.47^{aB}
PVP	0.05	6.1 ± 0.03^{A}	- 8.5 ± 0.84^{aA}	- 8.3 ± 1.38^{bA}
	2	6.04 ± 0.01^{B}	- 7.25 ± 0.23^{aB}	- 9.11 ± 0.55^{aB}
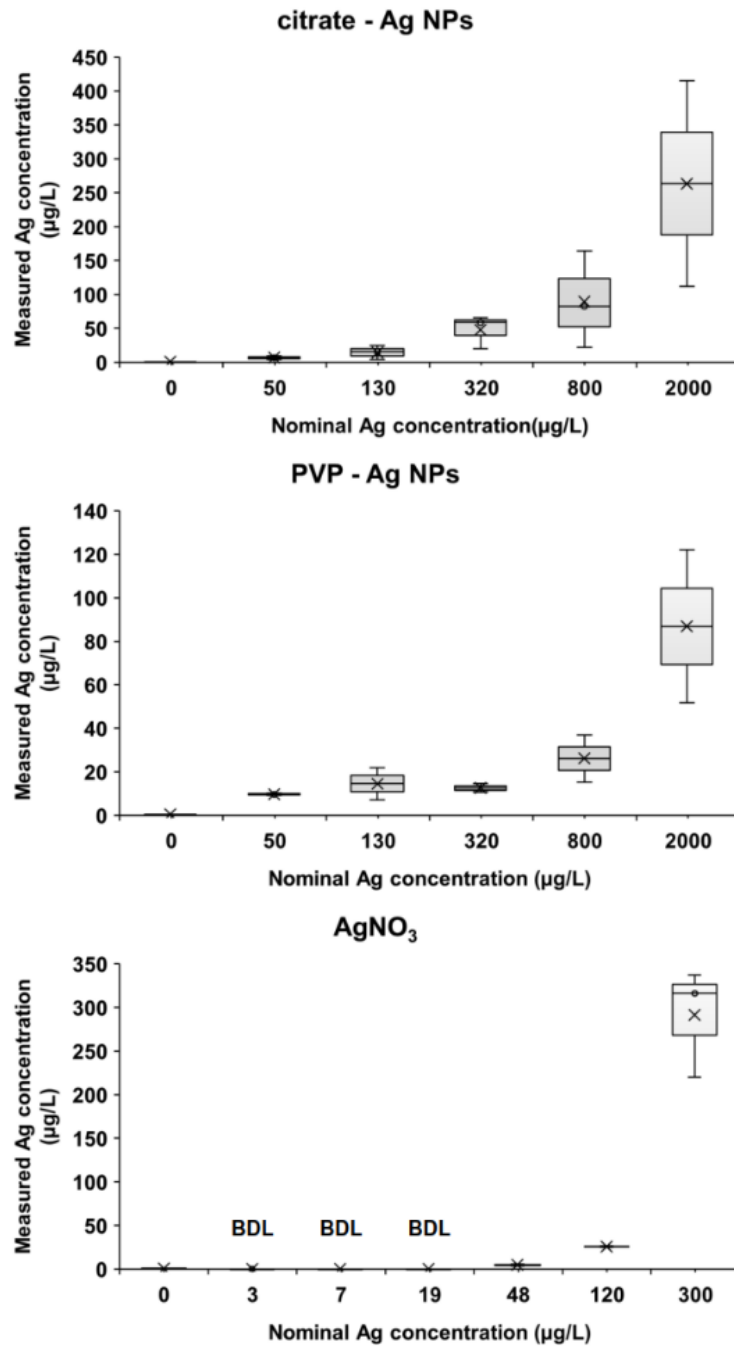
Figure 2-2 – Total Ag concentration measured (average ± standard deviation, *n*=3) in aged (7 days) suspensions of Ag ENMs and salt metal (AgNO₃) in Steinberg medium. "BDL" stands for below detection limits.

2.5.2 **Physiological endpoints**

Among physiological endpoints, the specific growth rate was the most sensitive with significant differences relative to the control down to 0.05 mg L^{-1} for Ag ENMs and 3 µg Ag L^{-1} for AgNO$_3$ after 14d of exposure. The specific growth rate of *L. minor* declined after 7d and 14d of exposure to all Ag forms, being the ionic form the most toxic **(Figure 2-3).**

Plants exposed to salt metal exhibited significant growth delays in concentrations equal and above 3 µg Ag L^{-1} (7d) and 8 µg Ag L^{-1} (14d). After 14d of exposure, plants exposed to 120 µg AgL^{-1} (AgNO$_3$) exhibited 92% reduction in growth rate, whereas those exposed to 300 µg Ag L^{-1} died. EC$_{50}$ values were similar for both exposure periods: 30 (± 7) µg Ag L^{-1} after 7 days and 37 (± 8) µg Ag L^{-1} after 14d (95% confidence interval values between brackets). Plants exposed to Ag ENMs lacked dose-response curves: significant differences against control were observed for low concentrations (0.05 or 0.13 mg L^{-1}) and the highest concentration (2 mg L^{-1}) in both Ag ENMs, but not for in-between concentrations. Effects of PVP-Ag ENMs were more pronounced than effects of citrate-Ag ENMs: at 2 mg L^{-1}, PVP-Ag ENMs reduced the growth rate of plants 1.5-fold more than citrate-ones (14 days of exposure). Additionally, this ratio increases to 4.6-fold for 2 mg L^{-1} PVP-Ag ENMs and 0.8 mg L^{-1} citrate-Ag ENMs that showed similar Ag concentration in suspension. Plants exposed to both ENMs and salt metal lacked significant growth rate differences between both exposure periods (7d versus 14d) **(Table 6 V, Appendix B).**

Phenotype of plants exposed to each Ag form displayed physical alterations as chlorosis, aggregation and dissociation of fronds (**Table 2-2**). However, these endpoints were not sensitive compared to growth rate, since significant effects relative to the control were only found at high concentrations. The incidence of chlorotic fronds followed a dose-response, only significant at high concentrations of citrate-Ag ENMs and $AgNO_3$ (**Figure 2-3** and **Table 6 VI, Appendix B)**. Salt metal induced the most pronounced effects: plants exposed to 300 µg Ag L^{-1} showed 78% of chlorosis after 7d and died after 14d **(Figure 2-3).**

Among ENMs, the highest chlorosis incidence was observed in 2 mg L^{-1} PVP-Ag ENMs, but for lower concentrations the effects in citrate-Ag ENMs were higher than the PVP-ones **(Figure 2-3)**. Chlorosis was significantly affected by the exposure period, mainly at high concentrations. Between 7d and 14d, chlorosis incidence decreased for the Ag ENMs-exposed plants, but increased for the salt metal. These opposite trends are related to plants growth between 7d and 14d: new fronds were healthy for Ag ENMs and fewer and chlorotic for salt metal. Chlorosis correlated negatively with growth rate (r=-0.421, *p<0.05*).

Number of fronds per colony was only affected at high concentrations of PVP-Ag ENMs and $AgNO_3$, more pronouncedly for the later **(Figure 2-3** and **Table 6-VII, Appendix B)**. In fact, plants exposed to 120 µg Ag L^{-1} of salt metal had about 1.4 fronds per colony, 4-fold less than the control, after both 7d and 14d of exposure. Plants exposed to the highest concentration (300 µg Ag L^{-1}) also showed small colonies after 7d (1.2 fronds per colony) that died one week later **(Figure 2-3** and **Table 6-VII, Appendix B)**.
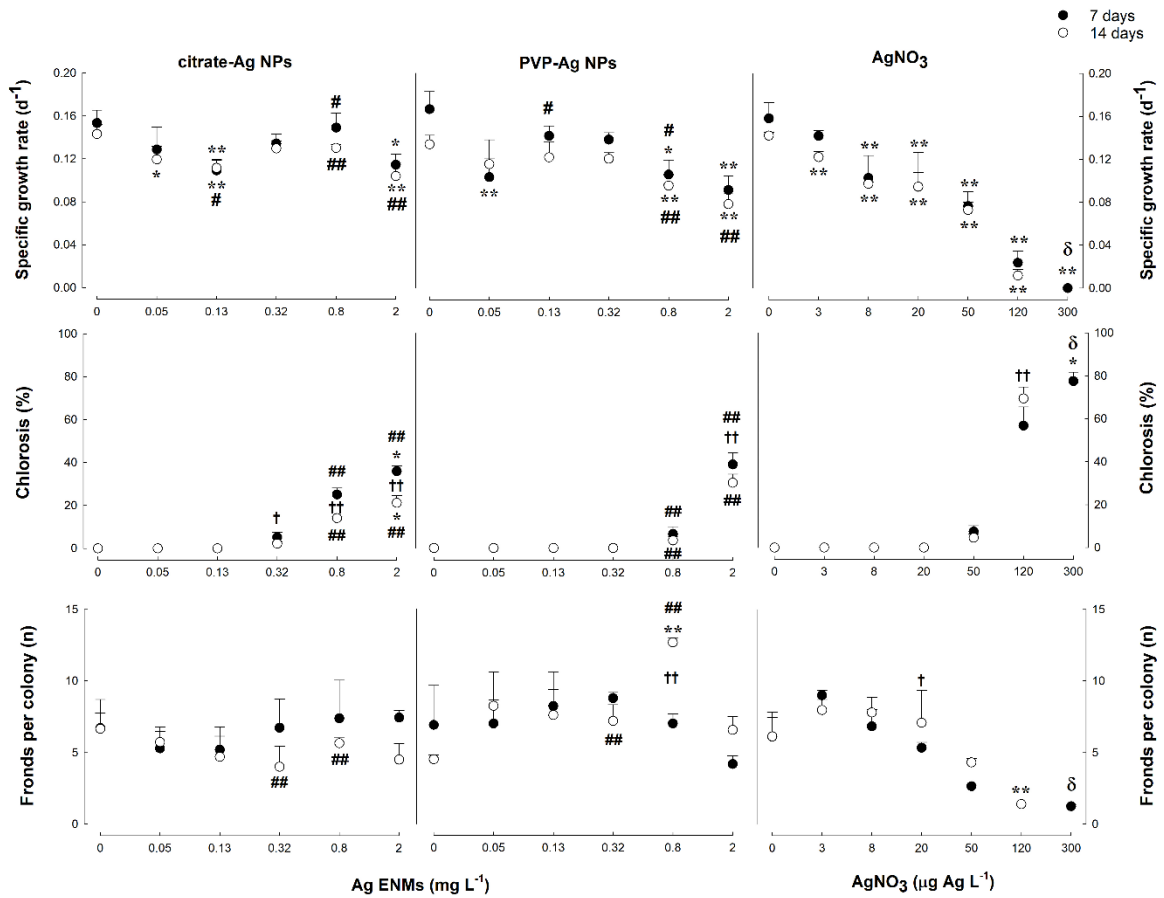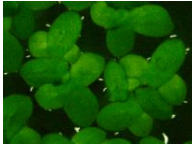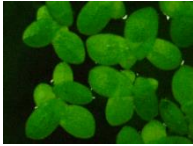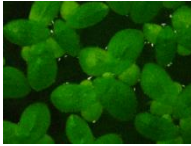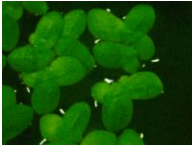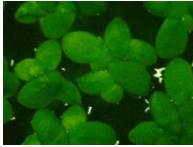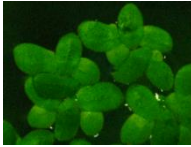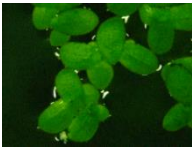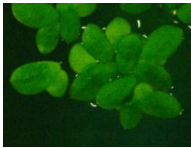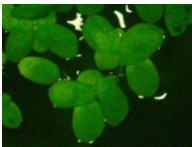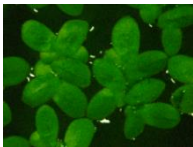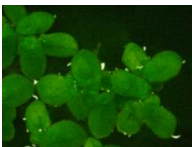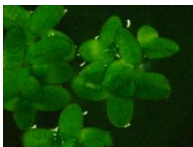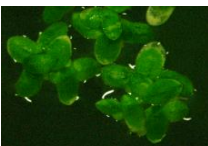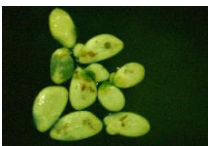
Figure 2-3 – Individual level endpoints (specific growth rate, percentage of chlorosis and number of fronds per colony) (mean ± S.D., *n=3*) of *L. minor* exposed to Ag ENMs (citrate and PVP) and $AgNO_3$ for 7d (black dots) and 14d (white dots). "*, **" stands for statistical differences against the control groups (*Dunnet's or Dunn's test with p<0.05 and p<0.01, respectively*). "#, ##" stands for statistical differences between citrate-Ag ENMs and PVP-Ag ENMs (*Holm-Sidak test with p<0.05 and p<0.01, respectively*). "†, ††" stands for statistical differences between 7d and 14d of exposure (*Holm-Sidak test with p<0.05 and p<0.01, respectively*). "δ" indicates lack of survival in the treatment.

Table 2-2 – Phenotype of *Lemna minor* after 14d of exposure to citrate and PVP-Ag ENMs and salt metal (AgNO$_3$).

citrate-Ag ENMs	PVP-Ag ENMs	AgNO$_3$
0 mg L^{-1}	0 mg L^{-1}	0 µg Ag L^{-1}
0.05 mg L^{-1}	0.05 mg L^{-1}	3 µg Ag L^{-1}
0.13 mg L^{-1}	0.13 mg L^{-1}	8 µg Ag L^{-1}
0.32 mg L^{-1}	0.32 mg L^{-1}	20 µg Ag L^{-1}
0.8 mg L^{-1}	0.8 mg L^{-1}	50 µg Ag L^{-1}
2 mg L^{-1}	2 mg L^{-1}	120 µg Ag L^{-1}

2.5.3 **Oxidative stress endpoints**

Oxidative stress endpoints were measured after 14d in Ag ENMs-exposed plants (**Figure 2-4**). GPox activity was the most sensitive, with significant differences against the control down to 0.05 mg L^{-1} for both Ag ENMs. This enzyme showed a pronounced induction. For instance, in plants exposed to 0.8 mg L^{-1} of citrate-Ag ENMs, GPox activity was almost 6-fold higher compared to control. Despite GPox activity was significantly induced by both Ag ENMs ($p<0.001$; **Table 6-VIII, Appendix B**), more pronounced variations were found for the citrate ones. In fact, at 0.32 mg L^{-1} GPox was 2-fold higher for citrate-Ag ENMs compared to PVP-ones ($p<0.001$; **Table 6-VIII, Appendix B**). Effects on GST activity were less pronounced: only significant for plants exposed to 0.8 mg Ag L^{-1} of citrate-Ag ENMs, showing a 2-fold increase compared to control ($p=0.009$; **Table 6-VIII, Appendix B**). CAT activity lacked significant differences, being constant for all concentrations of both Ag ENMs. Whereas GPox (*r=0.754, p<0.05*) and GST (*r=0.847, p<0.01*) correlates positively with chlorosis, GPox correlates positively with GST (*r=0.913, p<0.01*) and CAT (*r=0.710, p<0.05*).
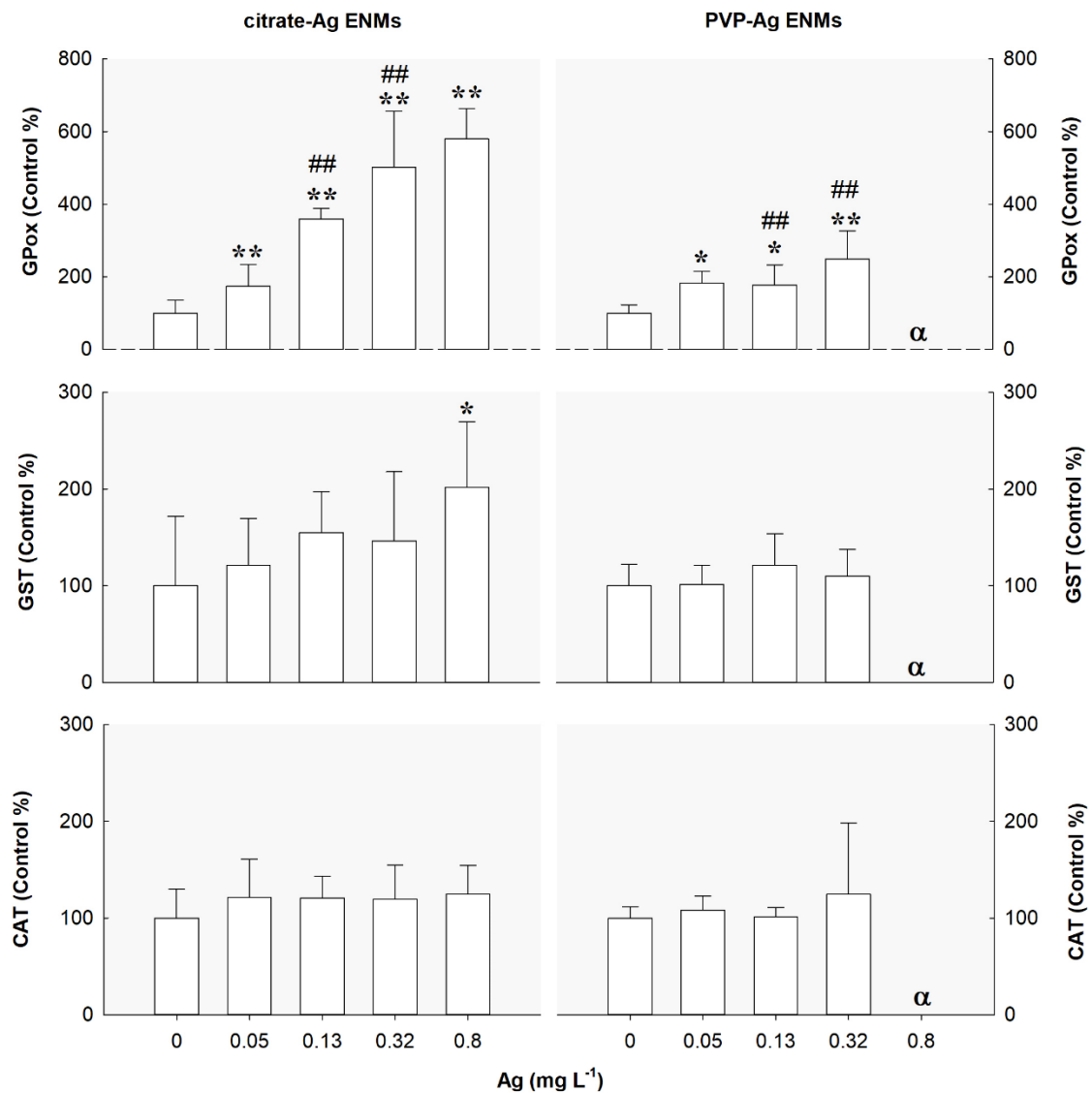
Figure 2-4 – Enzymatic activities of GPox, GST and CAT (mean ± standard deviation, *n*=3) of *Lemna minor* exposed to Ag ENMs (citrate and PVP) for 14d. "*,**" stand for significant differences against control (Dunnet's or Dunn's test with $p<0.05$ and $p<0.01$, respectively). "#,##" stands for statistical differences between citrate and PVP-Ag ENMs (Holm-Sidak test with $p<0.05$ and $p<0.01$, respectively). "α" indicates lack of biomass in the treatment.

2.5.4 Relationship between endpoints (Principal Components Analysis)

Principal Components Analysis (PCA) results (**Figure 2-5a**) propose 2 principal components to explain the variables (physiological and oxidative stress endpoints), accounting for 78.77% of total variance **(Table 2-3).** Principal Component 1 (PC1) took credit for 55.85% of the original variance and experienced positive (GPox, GST, chlorosis, CAT) and negative (fronds per colony) influences. PC2 accounted for 22.92% of total variance: positive values only associated to growth rate and negative values to CAT and fronds per colony.

Plot of scores for PC1 and PC2 from different concentrations of Ag ENMs and two surface coatings (citrate and PVP) (**Figure 2-5b**) shows distinct trends. Responses of plants show a surface coating-dependency: concentrations of citrate and PVP-Ag ENMs formed two separated clusters, except for control and 0.05 mg L^{-1} citrate-Ag ENMs grouped with the PVP-ones. Whereas the outcome of GPox, GST and CAT activities is more influenced by citrate-Ag ENMs (0.13 – 0.8 mg L^{-1}) (**Figure 2-5b**), growth rate (positively) and chlorosis and fronds per colony (negatively) are more influenced by PVP-Ag ENMs.

Table 2-3 – Component loadings of the variables for the two principal components (PCA) from 14d of exposure of *Lemna minor* to Ag ENMs (citrate and PVP).

Variables	Component 1	Component 2
Eigen values	3.351	1.375
% of variance	55.85	22.92
GPox	0.958	-
GST	0.952	-
Chlorosis	0.847	-
CAT	0.707	-0.551
Fronds per colony	-0.530	-0.361
Growth rate	-	0.958
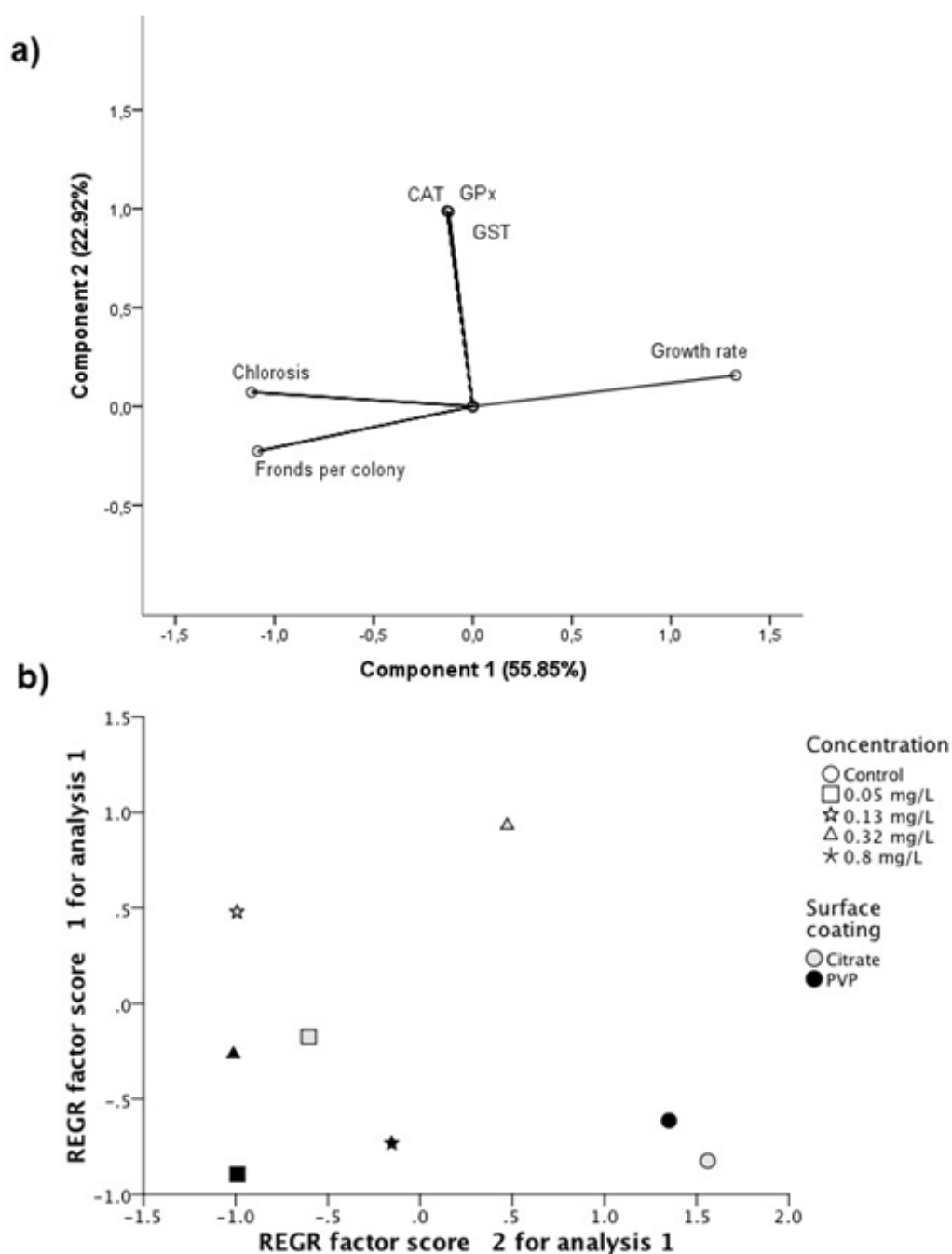
Figure 2-5 – **a**) Plot of variable vectors for the two dominant components produced by the individual (growth rate, chlorosis and fronds per colony) and sub-individual (CAT, GPox, GST) endpoints of *Lemna minor* exposed to Ag ENMs (citrate and PVP) for 14d. **b**) The distribution diagram of the different groups of concentrations of Ag ENMs (mg L^{-1}) for two different surface coatings as a function of the two principal component axes. Principal component loading and total variance associated with each axis are provided in **Table 2-3.**

2.6 **Discussion**

In this study, the effects of Ag ENMs to *L. minor* were assessed using physiological and oxidative stress endpoints for 14d, exploring additional experimental features: silver form (Ag ENMs versus salt metal), surface coating (citrate versus PVP-Ag ENMs) and exposure period (7d versus 14d). A dose-dependent effect occurred in most endpoints: decay in growth rate and fronds per colony; increase in the chlorosis incidence, GPox and GST activities. The reduced growth rate of plants agrees with the findings of previous studies in *Elodea canadensis* (Van Koetsem et al., 2016), *Lemna gibba* (Oukarroum et al., 2013), *L. minor* (Gubbins et al., 2011; Ucuncu et al., 2014) and *Spirodela polyrhiza* (Jiang et al., 2012). Specific growth rate (SGR) and GPox were the most sensitive physiological and oxidative stress endpoints, respectively. Thus, the use of these endpoints is supported in future phytotoxicity studies addressing the effects of Ag ENMs to aquatic plants.

Considering silver form, Ag ENMs caused less pronounced effects than the salt metal at similar concentrations. These findings are coherent with previous studies for a wide range of aquatic species (Fabrega et al., 2011), including algae, for which $AgNO_3$ reported to be 3 to 18-fold more toxic than Ag ENMs (Angel et al., 2013; Navarro et al., 2008b). The lower Ag ENMs toxicity might be related to the mode of action of ENMs, as discussed below.

Surface coating caused distinct and significant effects in the plants. The few studies that address the effects of citrate and PVP-Ag ENMs are focused on other aquatic species, namely algae (Angel et al., 2013). Thus, this paper originally reports a comparison between the effects of citrate and PVP-Ag ENMs to the aquatic plant *L. minor*. Both Ag ENMs affected physiological and oxidative stress endpoints distinctively: citrate-Ag ENMs affected more the GPox and GST activities and PVP-Ag ENMs affected more the growth rate. Chlorosis was affected by both ENMs, being unclear which one was more damaging. The distinct effects of both Ag ENMs, allied to differences in their stability and total Ag concentration in suspension suggest that citrate and PVP-Ag ENMs have different chemical dynamics and modes of action. Previous studies also found distinct aggregation and dissolution of both Ag ENMs; where PVP were found to be more stable than the citrate-ones, as

those aggregated less (Badawy et al., 2010; Tejamaya et al., 2012) and are likely driven by steric repulsion (Huynh and Chen, 2011). The conflicting results might be related to the exposure medium; Steinberg in the present study versus water or *Daphnia* culture medium in the above mentioned studies. Still, differences in zeta potential for both surface coatings were only found in fresh suspensions and were minor. Without further research, it remains unclear if these variances are enough to elicit distinct effects of both Ag ENMs. Li et al. (2013) noticed that under irradiation conditions, PVP-Ag ENMs had higher concentrations of dissolved Ag in suspension than citrate-ones, supporting a different chemical dynamics of both Ag ENMs. The same study found that citrate-Ag ENMs generated significant levels of ROS, in contrast with the PVP-ones that did not generate detectable levels of ROS. These findings match the results in the oxidative stress endpoints, since GPox and GST activities increased more pronouncedly in citrate-Ag ENMs than the PVP-ones. Distinct effects of both Ag ENMs were also reported for the algae *Raphidocelis subcapitata*; citrate was more deleterious (6.5-fold on the growth rate) than the PVP-ones, being attributed to the higher dissolution rates of the citrate-Ag ENMs (Angel et al., 2013). In the present study, the total Ag in suspension was higher for citrate than PVP-Ag ENMs in aged suspensions, but PVP were more deleterious than the citrate-ones. Other factors might explain the conflicting results, namely the experimental conditions (e.g. chloride (Cl^-) concentration and specific defence mechanisms of both species. In Angel et al. (2013), the Cl^- concentration was 36-fold higher than in this study (50 vs. 1.4 µM Cl^-, respectively). Chloride (Cl^-) ions form complexes with dissolved Ag (e.g. $AgCl^{(0)}$), thus Cl^- concentration will regulate the availability of dissolved Ag (Ag^+) in suspension (Behra et al., 2013) ultimately influencing the Ag ENMS toxicity. Another hypothesis could be the distinct defence mechanisms of each group of organisms (algae vs. aquatic plants). Aquatic plants are able to shed parts, a well described metal translocation mechanism that allows plants to allocate excessive metal in old fronds before detachment (Shaw et al., 2005; Weis and Weis, 2004), counteracting the Ag effects. This mechanism might explain the reduced number of fronds per colony in plants exposed to high concentrations of salt metal.

Concerning exposure period effects, these were mainly significant on chlorosis, particularly at higher concentrations. From 7d to 14d, chlorosis incidence enhanced in plants exposed to the salt metal, but declined for the Ag ENMs-ones. This suggests that the photosynthetic machinery of plants exposed to Ag ENMs recovered faster than the ones exposed to the salt metal, due to lower stress conditions. This suggests that over time chlorosis tends to tends to decrease in plants exposed to low Ag ENMs concentrations, but it aggravates under exposure to high concentrations. This apparent recovery is relevant in natural aquatic systems, since it might suggest that plants facing low-stress conditions could exhibit decreasing chlorosis incidence over time. However, further studies are required to confirm this hypothesis. The exposure period did not influence the growth rate, which disagrees with Gubbins et al. (2011) that reported a more severe response in the growth rate of *L. minor* after 14d than 7d for citrate-Ag ENMs. The contrasting results of both studies might be associated with the experimental conditions or the properties of Ag ENMs (synthetized by Gubbins et al. (2011) vs. NanoComposix). In the present study, the effects of exposure period were more pronounced for citrate-Ag ENMs than for the PVP-ones. These results match the total Ag concentration in suspension and agree with the higher and faster dissolution rates of citrate-Ag ENMs compared to PVP-ones, as reported by Angel et al. (2013).

Effects observed in physiological endpoints agree with the oxidative stress endpoints. Higher GPox activity matches the moderate inhibition of growth rate in plants exposed to citrate-Ag ENMs when compared to the PVP-ones. GPox plays an important role on growth, development, senescence and self-defence of plants (Hiraga et al., 2001; Song et al., 2012). GPox induction in plants exposed to citrate-Ag ENMs might be linked to enhanced self-defence mechanisms and, thus, endure less severe effects on the growth rate of plants when compared to PVP-ones. CAT, as well as GPox, takes part in the degradation pathway of H_2O_2 (ROS), yet typically it exhibits a higher specificity and energy-efficiency than GPox (Sharma et al., 2012). However, the higher activity of GPox than CAT in this study suggests higher affinity for the GPox pathway, agreeing with Krishnaraj et al. (2012), where GPox activity was higher than CAT in water hyssop exposed for 15d.

The modes of action of Ag ENMs in aquatic plants remain unclear. The dissolution of Ag ENMs with the subsequent release of dissolved Ag is referred as the major responsible for Ag ENMs toxicity. Dissolved Ag can enter the cells by passive diffusion (Fortin and Campbell, 2000), being later translocated from root-to-shoot (Stegemeier et al., 2015). However, recent studies show that Ag ENMs toxicity cannot be explained solely by dissolved Ag uptake, as reported for algae by Wang et al. (2016). Thus, other mechanisms may contribute to Ag ENMs effects, namely uptake. Stegemeier et al. (2015) reported the internal presence of Ag ENMs ($\approx$ 10-20 nm) and dissolved Ag (in similar doses) in root cells of *Medicago sativa*, suggesting Ag ENMs uptake. However, the intracellular presence of Ag ENMs could be caused only by dissolved Ag bioreduction and not by Ag ENMs uptake, as pointed out by Kadukova (2016). In fact, given the typical pore size (5-10 nm) of the cell walls of plants (Ma et al., 2015), the uptake of Ag ENMs would only be expected in ENMs smaller than 10 nm. However, increased walls plasticity during cell reproduction might boost their permeability to ENMs (> 10 nm) (Navarro et al., 2008a). Moreover, Liu et al. (2009) suggested endocytosis-mediated ENMs uptake by indirect interference: carbon nanotubes penetrated the cell walls of tobacco cell lines by vesicle-mediated transport. Although cellular internalization of Ag ENMs lacks enough evidence and is supported by contradictory results (Skjolding et al., 2016), this assumption cannot be discarded.

Another possible mechanism of action of ENMs in aquatic photosynthetic organisms is light shading, as suggested for algae by Sørensen et al. (2016). ENMs agglomerates adsorbed to leaves surface could obstruct light (physical shading), causing decays in light absorption and consequently inhibiting the growth of plants. Besides, ENMs-induced ROS might also disrupt photosynthesis. Thus, both light shading and ROS-mediated mechanisms might lead to chlorosis, which could explain the positive correlation between chlorosis and both GPox and GST. Whereas chlorosis only occurred in plants exposed to high Ag concentration (ENMs and AgNO$_3$), GPox and GST activities were induced in plants exposed to low concentrations of Ag ENMs – suggesting ENMs-related damage of the photosynthetic machinery (Siddiqui et al., 2015; Tripathi et al., 2017). Decays of chlorophyll content and photosynthetic yield were also found in *C. reinhardtii*,

Chlorella vulgaris, and *L. gibba* (Dewez and Oukarroum, 2012; Melegari et al., 2013; Navarro et al., 2008b; Oukarroum et al., 2012b; Perreault et al., 2012; Perreault et al., 2013; Perreault et al., 2014), leading to potential morphological alterations as chlorosis (Begovic et al., 2016). Although Oukarroum et al. (2013) observed a direct association between intracellular ROS formation and cell viability in *L. gibba* exposed to Ag ENMs, the role of oxidative stress enzymes on Ag ENMs-induced effects remains unclear.

Ag ENMs can accumulate in aquatic environments. The low PEC of Ag ENMs in surface waters, between 0.002 ngL^{-1} (Dumont et al., 2015) and 0.66 ngL^{-1} (Sun et al., 2014), allied to their low toxicity would suggest a reduced risk for aquatic organisms. However, Ag ENMs also accumulate in the sediments (PEC = 2.3 $\mu g/kg^{-1}$ $year^{-1}$) and, over time, stored Ag ENMs might release dissolved Ag to water, due to their intricate solubility dynamics. In fact, dissolution and/or aggregation of Ag ENMs, and consequently their toxicity, is deeply influenced not only by Ag ENMs properties (e.g. size and surface coating) but also by the water physicochemical properties, such as pH, ionic strength, Cl^- concentrations and natural organic matter (Badawy et al., 2010; Behra et al., 2013; Levard et al., 2012). Moreover, dissolution might occur on a steady and continuous mode along time. Considering that and the fact that individual fronds can last for 6 weeks (Leng, 1999), long-term exposures would provide more relevant and holistic evidences involving the overall phytotoxicity of Ag ENMs of plants in an ecological relevant scenario.

2.7 **Conclusions**

The main results of the present study can be summarized by answering the questions mentioned in the introduction. Which are the effects of Ag ENMs and the salt metal to *L. minor* in different organizational levels? In general, growth rate and fronds per colony decayed; chlorosis, GPox and GST increased, but CAT remained unaffected. Moreover, the most sensitive physiological and oxidative stress endpoints were the growth rate and GPox activity, respectively. Do Ag ENMs and the salt metal have similar effects to *L. minor*? The effects of both Ag ENMs and the salt metal follow a similar trend, but they are less pronounced for Ag ENMs than

AgNO$_3$. Do the effects of Ag ENMs to *L. minor* depend on the respective surface coating? Whereas PVP-Ag ENMs were more deleterious for growth rate of plants and fronds per colony, citrate-Ag ENMs were more deleterious for GPox and GST activities. Do the effects of Ag ENMs and the salt metal depend on the extent of the exposure period? The extended exposure (14d) when compared to the standard one (7d) affected mainly chlorosis: whereas an ameliorative effect was observed for citrate-Ag ENMs (high concentrations), an aggravation effect was observed for the salt metal. Thus, in aquatic systems, plants exposed to low concentrations of citrate-Ag ENMs might possibly show an ameliorative effect in chlorosis over time. Effects in oxidative stress denote that Ag ENMs induced an oxidative stress status in cells, thus resulting on the upregulated enzymatic activity, negatively affecting PVP-exposed plants but improving the health status of citrate-exposed ones. Longer exposure periods than the recommended by the OECD guideline should be considered due to 1) the solubility dynamics of Ag ENMs, 2) the possible steady and continuous dissolution along time, and 3) the mean longevity of fronds. This approach would provide more relevant and holistic evidences about the overall response of freshwater plants to Ag ENMs in an ecological relevant scenario.

2.8 Acknowledgments

2.9 **References**

Angel, B. M., et al., 2013. The impact of size on the fate and toxicity of nanoparticulate silver in aquatic systems. Chemosphere. 93, 359-65. https://doi.org/10.1016/j.chemosphere.2013.04.096

Arruda, S. C., et al., 2015. Nanoparticles applied to plant science: a review. Talanta. 131, 693-705. https://doi.org/10.1016/j.talanta.2014.08.050

Badawy, A. M. E., et al., 2010. Impact of Environmental Conditions (pH, Ionic Strength, and Electrolyte Type) on the Surface Charge and Aggregation of Silver Nanoparticles Suspensions. Environ Sci Technol. 44, 1260-1266. https://doi.org/10.1021/es902240k

Bagherzadeh Homaee, M., Ehsanpour, A. A., 2016. Silver nanoparticles and silver ions: Oxidative stress responses and toxicity in potato (*Solanum tuberosum* L.) grown in vitro. Hortic Environ Biotechnol. 57, 544-553. https://doi.org/10.1007/s13580-016-0083-z

Begovic, L., et al., 2016. Response of *Lemna minor* L. to short-term cobalt exposure: The effect on photosynthetic electron transport chain and induction of oxidative damage. Aquat Toxicol. 175, 117-26. https://doi.org/10.1016/j.aquatox.2016.03.009

Behra, R., et al., 2013. Bioavailability of silver nanoparticles and ions: from a chemical and biochemical perspective. J R Soc Interface. 10, 20130396. https://doi.org/10.1098/rsif.2013.0396

Bradford, M. M., 1976. A rapid and sensitive method for the quantitation of microgram quantities of protein utilizing the principle of protein-dye binding. Anal Biochem. 72, 248-254. https://doi.org/10.1016/0003-2697(76)90527-3

Brain, R., Cedergreen, N., 2009. Biomarkers in Aquatic Plants: Selection and Utility, in: D. Whitacre (Ed.), Reviews of Environmental Contamination and Toxicology. Springer New York, pp. 49-109. https://doi.org/10.1007/978-0-387-09647-6_2

Castillo, F. J., et al., 1984. Peroxidase Release Induced by Ozone in *Sedum album* Leaves Involvement of Ca^{2+}. Plant Physiol. 74, 846-851. https://doi.org/10.1104/pp.74.4.846

Clairborne, A., 1985. Catalase activity, in: R. A. Greenwald (Ed.), Handbook of Methods in Oxygen Radical Research. CRC Press, Boca Raton, pp. 283–284. https://doi.org/10.1201/9781351072922

Cupi, D., et al., 2016. Influence of pH and media composition on suspension stability of silver, zinc oxide, and titanium dioxide nanoparticles and immobilization of *Daphnia magna* under guideline testing conditions. Ecotoxicol Environ Saf. 127, 144-152. https://doi.org/10.1016/j.ecoenv.2015.12.028

Dewez, D., Oukarroum, A., 2012. Silver nanoparticles toxicity effect on photosystem II photochemistry of the green alga *Chlamydomonas reinhardtii* treated in light and dark conditions. Toxicol Environ Chem. 94, 1536-1546. https://doi.org/10.1080/02772248.2012.712124

Dimkpa, C. O., et al., 2012. CuO and ZnO nanoparticles: phytotoxicity, metal speciation, and induction of oxidative stress in sand-grown wheat. J Nanopart Res. 14. https://doi.org/10.1007/s11051-012-1125-9

Dimkpa, C. O., et al., 2013. Silver nanoparticles disrupt wheat (*Triticum aestivum* L.) growth in a sand matrix. Environ Sci Technol. 47, 1082-90. https://doi.org/10.1021/es302973y

Dumont, E., et al., 2015. Nano silver and nano zinc-oxide in surface waters – Exposure estimation for Europe at high spatial and temporal resolution. Environ Pollut. 196, 341-349. https://doi.org/10.1016/j.envpol.2014.10.022

El Badawy, A. M., et al., 2011. Surface charge-dependent toxicity of silver nanoparticles. Environ Sci Technol. 45, 283-7. https://doi.org/10.1021/es1034188

Elzey, S., Grassian, V. H., 2010. Agglomeration, isolation and dissolution of commercially manufactured silver nanoparticles in aqueous environments. J Nanopart Res. 12, 1945-1958. https://doi.org/10.1007/s11051-009-9783-y

Fabrega, J., et al., 2011. Silver nanoparticles: Behaviour and effects in the aquatic environment. Environ Int. 37, 517-531. https://doi.org/10.1016/j.envint.2010.10.012

Fortin, C., Campbell, P. G. C., 2000. Silver uptake by the green alga *Chlamydomonas reinhardtii* in relation to chemical speciation: Influence of chloride. Environ Toxicol Chem. 19, 2769-2778. https://doi.org/10.1002/etc.5620191123

Frasco, M. F., Guilhermino, L., 2002. Effects of dimethoate and beta-naphthoflavone on selected biomarkers of *Poecilia reticulata*. Fish Physiol Biochem. 26, 149-156. https://doi.org/10.1023/a:1025457831923

Furtado, L. M., et al., 2015. Environmental Fate of Silver Nanoparticles in Boreal Lake Ecosystems. Environ Sci Technol. 49, 8441-50. https://doi.org/10.1021/acs.est.5b01116

Gill, S. S., Tuteja, N., 2010. Reactive oxygen species and antioxidant machinery in abiotic stress tolerance in crop plants. Plant Physiol Biochem. 48, 909-30. https://doi.org/10.1016/j.plaphy.2010.08.016

Gubbins, E. J., et al., 2011. Phytotoxicity of silver nanoparticles to *Lemna minor* L. Environ Pollut. 159, 1551-1559. https://doi.org/10.1016/j.envpol.2011.03.002

Habig, W. H., Jakoby, W. B., 1981. Assays for differentiation of glutathione S-transferases, in: B. J. William (Ed.), Methods in Enzymology. Academic Press, San Diego, pp. 398-405. https://doi.org/10.1016/S0076-6879(81)77053-8

Hiraga, S., et al., 2001. A Large Family of Class III Plant Peroxidases. Plant Cell Physiol. 42, 462-468. https://doi.org/10.1093/pcp/pce061

Howcroft, C. F., et al., 2011. Biochemical characterization of cholinesterases in *Enchytraeus albidus* and assessment of in vivo and in vitro effects of different soil properties, copper and phenmedipham. Ecotoxicology. 20, 119-30. https://doi.org/10.1007/s10646-010-0562-4

Hu, C., et al., 2013. Biochemical responses of duckweed (*Spirodela polyrhiza*) to zinc oxide nanoparticles. Arch Environ Contam Toxicol. 64, 643-51. https://doi.org/10.1007/s00244-012-9859-z

Huynh, K. A., Chen, K. L., 2011. Aggregation kinetics of citrate and polyvinylpyrrolidone coated silver nanoparticles in monovalent and divalent electrolyte solutions. Environ Sci Technol. 45, 5564-71. https://doi.org/10.1021/es200157h

ISO/DIS 20079, Water quality — Determination of the toxic effect of water constituents and waste water to duckweed (*Lemna minor*) – Duckweed growth inhibition test. ISO, 2005. pp. 23

Jiang, H.-S., et al., 2012. Physiological analysis of silver nanoparticles and AgNO$_3$ toxicity to *Spirodela polyrhiza*. Environ Toxicol Chem. 31, 1880-1886. https://doi.org/10.1002/etc.1899

Jiang, H. S., et al., 2014. Silver nanoparticles induced accumulation of reactive oxygen species and alteration of antioxidant systems in the aquatic plant *Spirodela polyrhiza*. Environ Toxicol Chem. 33, 1398-405. https://doi.org/10.1002/etc.2577

Kadukova, J., 2016. Surface sorption and nanoparticle production as a silver detoxification mechanism of the freshwater alga *Parachlorella kessleri*. Bioresour Technol. 216, 406-413. https://doi.org/10.1016/j.biortech.2016.05.104

Kim, E., et al., 2011. Growth inhibition of aquatic plant caused by silver and titanium oxide nanoparticles. Toxicol Environ Health Sci. 3, 1-6. https://doi.org/10.1007/s13530-011-0071-8

Klaine, S. J., et al., 2008. Nanomaterials in the environment: Behavior, fate, bioavailability, and effects. Environ Toxicol Chem. 27, 1825-1851. https://doi.org/10.1897/08-090.1

Krishnaraj, C., et al., 2012. Effect of biologically synthesized silver nanoparticles on *Bacopa monnieri* (Linn.) Wettst. plant growth metabolism. Process Biochem. 47, 651-658. https://doi.org/10.1016/j.procbio.2012.01.006

Leng, R. A., 1999. Duckweed: A tiny aquatic plant with enormous potential for agriculture and environment. FAO, Rome (Italy). Animal Production and Health Div.; University of Tropical Agriculture Foundation, Phnom Penh (Cambodia). pp. 108 p.

Levard, C., et al., 2012. Environmental Transformations of Silver Nanoparticles: Impact on Stability and Toxicity. Environ Sci Technol. 46, 6900-6914. https://doi.org/10.1021/es2037405

Li, Y., et al., 2013. Surface-Coating-Dependent Dissolution, Aggregation, and Reactive Oxygen Species (ROS) Generation of Silver Nanoparticles under Different Irradiation Conditions. Environ Sci Technol. 47, 10293-10301. https://doi.org/10.1021/es400945v

Liu, Q., et al., 2009. Carbon Nanotubes as Molecular Transporters for Walled Plant Cells. Nano Lett. 9, 1007-1010. https://doi.org/10.1021/nl803083u

Ma, C., et al., 2015. Metal-based nanotoxicity and detoxification pathways in higher plants. Environ Sci Technol. 49, 7109-22. https://doi.org/10.1021/acs.est.5b00685

Massarsky, A., et al., 2014. Predicting the environmental impact of nanosilver. Environ Toxicol Pharmacol. 38, 861-873. https://doi.org/10.1016/j.etap.2014.10.006

Melegari, S. P., et al., 2013. Evaluation of toxicity and oxidative stress induced by copper oxide nanoparticles in the green alga *Chlamydomonas reinhardtii*. Aquat Toxicol. 142-143, 431-40. https://doi.org/10.1016/j.aquatox.2013.09.015

Mirzajani, F., et al., 2013. Effect of silver nanoparticles on *Oryza sativa* L. and its rhizosphere bacteria. Ecotoxicol Environ Saf. 88, 48-54. https://doi.org/10.1016/j.ecoenv.2012.10.018

Mirzajani, F., et al., 2014. Proteomics study of silver nanoparticles toxicity on *Oryza sativa* L. Ecotoxicol Environ Saf. 108, 335-339. https://doi.org/10.1016/j.ecoenv.2014.07.013

Navarro, E., et al., 2008a. Environmental behavior and ecotoxicity of engineered nanoparticles to algae, plants, and fungi. Ecotoxicology. 17, 372-386. https://doi.org/10.1007/s10646-008-0214-0

Navarro, E., et al., 2008b. Toxicity of Silver Nanoparticles to *Chlamydomonas reinhardtii*. Environ Sci Technol. 42, 8959-8964. https://doi.org/10.1021/es801785m

OECD, Test No. 221: Lemna sp. Growth Inhibition Test, OECD Guidelines for the Testing of Chemicals. Section 2. OECD Publishing, Paris, 2006. https://doi.org/10.1787/9789264016194-en

Oukarroum, A., et al., 2013. Silver nanoparticle toxicity effect on growth and cellular viability of the aquatic plant *Lemna gibba*. Environ Toxicol Chem. 32, 902-7. https://doi.org/10.1002/etc.2131

Oukarroum, A., et al., 2012a. Inhibitory effects of silver nanoparticles in two green algae, *Chlorella vulgaris* and *Dunaliella tertiolecta*. Ecotoxicol Environ Saf. 78, 80-5. https://doi.org/10.1016/j.ecoenv.2011.11.012

Oukarroum, A., et al., 2012b. Temperature influence on silver nanoparticles inhibitory effect on photosystem II photochemistry in two green algae, *Chlorella vulgaris* and *Dunaliella tertiolecta*. Environ Sci Pollut Res. 19, 1755-1762. https://doi.org/10.1007/s11356-011-0689-8

Perreault, F., et al., 2012. Polymer coating of copper oxide nanoparticles increases nanoparticles uptake and toxicity in the green alga *Chlamydomonas reinhardtii*. Chemosphere. 87, 1388-1394. https://doi.org/10.1016/j.chemosphere.2012.02.046

Perreault, F., et al., 2013. Different toxicity mechanisms between bare and polymer-coated copper oxide nanoparticles in *Lemna gibba*. Environ Pollut. 185C, 219-227. https://doi.org/10.1016/j.envpol.2013.10.027

Perreault, F., et al., 2014. Effect of soluble copper released from copper oxide nanoparticles solubilisation on growth and photosynthetic processes of *Lemna gibba* L. Nanotoxicology. 8, 374-82. https://doi.org/10.3109/17435390.2013.789936

Ratte, H. T., 1999. Bioaccumulation and toxicity of silver compounds: A review. Environ Toxicol Chem. 18, 89-108. https://doi.org/10.1002/etc.5620180112

Reddy, P. V. L., et al., 2016. Lessons learned: Are engineered nanomaterials toxic to terrestrial plants? Sci Total Environ. 568, 470-479. https://doi.org/10.1016/j.scitotenv.2016.06.042

Rico, C., et al., 2015. Chemistry, biochemistry of nanoparticles, and their role in antioxidant defense system in plants, in: M. H. Siddiqui, et al. (Eds.), Nanotechnology and plant sciences: nanoparticles and their impact on plants. Springer, Cham, pp. 1-17. https://doi.org/10.1007/978-3-319-14502-0

Sharma, P., et al., 2012. Reactive oxygen species, oxidative damage, and antioxidative defense mechanism in plants under stressful conditions. J Bot. 2012, 26. https://doi.org/10.1155/2012/217037

Shaw, B., et al., 2005. Detoxification/Defense Mechanisms in Metal-Exposed Plants, in: M. N. V. Prasad, et al. (Eds.), Trace Elements in the Environment: Biogeochemistry, Biotechnology, and Bioremediation. CRC Press, Boca Raton, pp. 291-305. https://doi.org/10.1201/9781420032048

Siddiqui, M. H., et al., 2015. Nanotechnology and plant sciences: nanoparticles and their impact on plants, 1st ed. Springer, Cham. https://doi.org/10.1007/978-3-319-14502-0

Skjolding, L. M., et al., 2016. Aquatic Ecotoxicity Testing of Nanoparticles—The Quest To Disclose Nanoparticle Effects. Angew Chem Int Ed. 55, 15224-15239. https://doi.org/10.1002/anie.201604964

Song, G., et al., 2012. Physiological effect of anatase TiO_2 nanoparticles on *Lemna minor*. Environ Toxicol Chem. 31, 2147-52. https://doi.org/10.1002/etc.1933

Song, U., et al., 2013. Functional analyses of nanoparticle toxicity: A comparative study of the effects of TiO_2 and Ag on tomatoes (*Lycopersicon esculentum*). Ecotoxicol Environ Saf. 93. https://doi.org/10.1016/j.ecoenv.2013.03.033

Sørensen, S. N., et al., 2016. A Multimethod Approach for Investigating Algal Toxicity of Platinum Nanoparticles. Environ Sci Technol. 50, 10635-10643. https://doi.org/10.1021/acs.est.6b01072

Stegemeier, J. P., et al., 2015. Speciation Matters: Bioavailability of Silver and Silver Sulfide Nanoparticles to Alfalfa (*Medicago sativa*). Environ Sci Technol. 49, 8451-60. https://doi.org/10.1021/acs.est.5b01147

Sun, T. Y., et al., 2014. Comprehensive probabilistic modelling of environmental emissions of engineered nanomaterials. Environ Pollut. 185, 69-76. https://doi.org/10.1016/j.envpol.2013.10.004

Tejamaya, M., et al., 2012. Stability of Citrate, PVP, and PEG Coated Silver Nanoparticles in Ecotoxicology Media. Environ Sci Technol. 46, 7011-7017. https://doi.org/10.1021/es2038596

Tolaymat, T., et al., 2017. The effects of metallic engineered nanoparticles upon plant systems: An analytic examination of scientific evidence. Sci Total Environ. 579, 93-106. https://doi.org/10.1016/j.scitotenv.2016.10.229

Topuz, E., et al., 2014. A systematic evaluation of agglomeration of Ag and TiO_2 nanoparticles under freshwater relevant conditions. Environ Pollut. 193, 37-44. https://doi.org/10.1016/j.envpol.2014.05.029

Tripathi, D. K., et al., 2017. An overview on manufactured nanoparticles in plants: Uptake, translocation, accumulation and phytotoxicity. Plant Physiol Biochem. 110, 2-12. https://doi.org/10.1016/j.plaphy.2016.07.030

Ucuncu, E., et al., 2014. Effects of laser ablated silver nanoparticles on *Lemna minor*. Chemosphere. 108, 251-7. https://doi.org/10.1016/j.chemosphere.2014.01.049

Van Koetsem, F., et al., 2016. Impact of water composition on association of Ag and CeO_2 nanoparticles with aquatic macrophyte *Elodea canadensis*. Environ Sci Pollut Res. 23, 5277-5287. https://doi.org/10.1007/s11356-015-5708-8

Vidal, T., et al., 2012. Acute and chronic toxicity of Betanal((R))Expert and its active ingredients on nontarget aquatic organisms from different trophic levels. Environ Toxicol. 27, 537-48. https://doi.org/10.1002/tox.20671

Wang, J., et al., 2013. Phytostimulation of poplars and *Arabidopsis* exposed to silver nanoparticles and Ag^+ at sublethal concentrations. Environ Sci Technol. 47, 5442-9. https://doi.org/10.1021/es4004334

Wang, S., et al., 2016. Cellular internalization and intracellular biotransformation of silver nanoparticles in *Chlamydomonas reinhardtii*. Nanotoxicology. 10, 1129-1135. https://doi.org/10.1080/17435390.2016.1179809

Weis, J. S., Weis, P., 2004. Metal uptake, transport and release by wetland plants: implications for phytoremediation and restoration. Environ Int. 30, 685-700. https://doi.org/10.1016/j.envint.2003.11.002

Zou, X., et al., 2016. The different response mechanisms of *Wolffia globosa*: Light-induced silver nanoparticle toxicity. Aquat Toxicol. 176, 97-105. https://doi.org/10.1016/j.aquatox.2016.04.019

Chapter III

COMPARISON OF TOXICITY OF SILVER NANOMATERIALS AND SILVER NITRATE ON DEVELOPING ZEBRAFISH EMBRYOS: BIOAVAILABILITY, OSMOREGULATORY AND OXIDATIVE STRESS

3   Chapter III – Comparison of toxicity of silver nanomaterials and silver nitrate on developing zebrafish embryos: bioavailability, osmoregulatory and oxidative stress

Work published in:

3.1 **Highlights**

- Silver nanomaterials (Ag ENMs) were less toxic than the $AgNO_3$.

- Hatching success endpoint was much more sensitive to $AgNO_3$ compared to Ag ENMs.

- 99.8% (Ag ENMs) and 96.3% ($AgNO_3$) of total Ag accumulated on the chorion.

- Both Na^+ and Ca^{2+} decreased, but only Na^+ had a nano-specific osmoregulatory stress.

- Total GSH was depleted in both Ag treatments, with a nano-specific oxidative stress.

3.2 **Abstract**

The mechanisms of toxicity of engineered nanomaterials (ENMs) to the early life stages of freshwater fish, and the relative hazard compared to dissolved metals, is only partially understood. In the present study, zebrafish (*Danio rerio*) embryos were exposed to lethal concentrations of silver nitrate ($AgNO_3$) or silver (Ag) ENMs (primary size 42.5 ± 10.2 nm). The 96h-LC_{50} for $AgNO_3$ was 32.8 ± 0.72 µg Ag L^{-1} (mean ± 95% CI) compared to 6.5 ± 0.4 mg L^{-1} of the whole material for Ag ENMs; with the ENMs being orders of magnitude less toxic than the metal salt. The EC_{50} for hatching success was 30.5 ± 1.4 µg Ag L^{-1} and 6.04 ± 0.4 mg L^{-1} for $AgNO_3$ and Ag ENMs, respectively. Further sub-lethal exposures were performed with the estimated LC_{10} concentrations for both $AgNO_3$ or Ag ENMs over 96 h where about 3.7% of the total Ag as $AgNO_3$ was internalised, as measured by Ag accumulation in the dechorionated embryos. However, for the ENMs exposures, nearly all (99.8%) of the total Ag was associated with chorion; indicating the chorion as an effective barrier to protect the embryo in the short term. Calcium (Ca^{2+}) and sodium (Na^+) depletion was induced in embryos by both forms of Ag, but hyponatremia was more pronounced in the nano form. Total glutathione (tGSH) levels declined in embryos exposed to both Ag forms, but a superior depletion occurred with the nano form. Nevertheless, oxidative stress was mild as superoxide dismutase (SOD) activity stayed uniform and the sodium pump (Na^+/K^+-ATPase) activity had no appreciable inhibition compared to the control. In conclusion, $AgNO_3$ was more toxic to the early life stage zebrafish than the Ag ENMs, still differences were found in the exposure and toxic mechanisms of both Ag forms.

Keywords

Danio rerio, silver toxicity, nanoparticles, hatching success, ionic regulation, glutathione

3.3 **Introduction**

Silver (Ag) engineered nanomaterials (ENMs) are widely applied in the nanotechnology sector (Calderón-Jiménez et al., 2017), with the global production estimated to be 800 tons by 2025 (Pulit-Prociak and Banach, 2016). Ag ENMs have numerous applications, including water disinfection, wastewater treatment, food preservation, medical implants and dressings, and anti-odour textile fabrication. The wide range of applications has been attributed to their antimicrobial efficiency (Zhang et al., 2016). Dissolution of Ag ions from the EMNs and/or direct contact of Ag ENMs with the surface of the bacteria is often associated with their antimicrobial activity, but this also raises a concern for silver toxicity to other wildlife when such ENMs are released to the environment (Lead et al., 2018). About 6.4% of the manufacturing and domestic wastes from Ag ENMs are expected to reach natural water bodies, with surface water concentrations in the ng L^{-1} range (Sun et al., 2014). In European rivers, concentrations of Ag ENMs can exceed 0.18 ng L^{-1} in 10% of river reaches, and with the highest concentrations in the summer months (Dumont et al., 2015). Recently,, samples from forty-six data sites across the globe were collected from different surface water sources (sea, lakes, creeks, rivers, etc.) and nanomaterials surveyed, where Ag ENMs were detected sporadically and below 1 ng L^{-1} (Azimzada et al., 2021).

The dissolution of Ag ENMs in natural waters poses concerns, as dissolved Ag is very toxic to aquatic organisms in freshwater, where acute mortality to fish occurs between 2 and 30 μg L^{-1} – depending on water chloride concentration, hardness and pH [reviews (Grosell et al., 2002b; Wood, 2011)]. A plausible mechanism of nanotoxicity in fishes might also be the release of high concentrations of dissolved metal from ENMs in the microenvironment on the surface of the organism (Shaw and Handy, 2011). Notably, Ag ENMs were found to be toxic to juvenile or adult fish, including fathead minnow [*Pimephales promelas* (Hoheisel et al., 2012)], medaka [*Oryzias latipes* (Kashiwada et al., 2012)], and zebrafish [*Danio rerio* (Böhme et al., 2017)]. Dissolved Ag in waterborne exposure of freshwater fish cause gill injury and inhibition of the branchial sodium pump (Na$^+$/K$^+$-ATPase) resulting in lethal osmoregulatory distress (Grosell et al., 2002b; Wood, 2011)]. Ag,

or Ag ENMs, can also catalyse Haber-Weiss and/or Fenton reactions that generate oxygen radicals and consequently oxidative stress is a feature of Ag toxicity to fishes (Fu et al., 2014).

The early-life stages of fishes are especially vulnerable to metal toxicity, including dissolved Ag [rainbow trout, (Brauner and Wood, 2002; Guadagnolo et al., 2001); zebrafish (Powers et al., 2010)]. Evidence is also emerging on the effects of Ag ENMs to medaka (Kashiwada et al., 2012), fathead minnow (Hoheisel et al., 2012) and zebrafish (Böhme et al., 2017; Khoshnamvand et al., 2020). The early-life stages of zebrafish are now widely used in regulatory toxicity testing, most notably the fish embryo acute toxicity test (FET) OECD TG 236 (OECD, 2013b) and fish early life-stage test OECD TG 210 (OECD, 2013a), the former has been validated for traditional chemicals (Busquet et al., 2014), but the early life-stage tests require modifications to work for ENMs (Shaw et al., 2016).

Under optimal conditions, embryos have a physical (chorion) and chemical (perivitelline fluid) protection from the surrounding environment (Eddy and Handy, 2012).The semi-permeable chorion is the first barrier and influences the sensitivity of zebrafish embryos to dissolved metals, including silver. When embryos are developed, a proteolytic enzyme (ZHE$_1$) in the perivitelline space is released to break down chorion and allow the hatching of the larvae (Ong et al., 2014). Larvae are often more vulnerable to waterborne chemicals than embryos (Mohammed, 2013), with this being also the case for some ENMs (Shaw et al., 2016). Dissolved Ag has been shown to inhibit the hatching success, thus impairing zebrafish embryos survival (Ong et al., 2014). Still, the mechanism of action of Ag ENMs in zebrafish embryos and whether the chorion is protective enough against ENMs is unclear.

This study aimed to evaluate the lethal and sub-lethal effects of Ag ENMs in zebrafish embryos compare to that of AgNO$_3$. Mortality and hatching success were used as the endpoints to assess lethal effects on zebrafish embryos. To understand if chorion has a protective effect, experiments were conducted on embryos with the chorion present (chorionated) and without it (dechorionated) and the subsequent metal accumulation in the embryos was measured. Finally, in dechorionated embryos where internal Ag exposure was confirmed, the sub-lethal effects on

osmoregulation (electrolyte concentrations and sodium pump activity) and oxidative stress parameters [superoxide dismutase (SOD) activity, total glutathione (tGSH)] were measured to help unravel the mechanisms of toxicity of Ag ENMs.

3.4 Materials and Methods

3.4.1 Silver Nanomaterials and characterisation

Silver engineered nanomaterials (Ag ENMs, PVP coated, dry powder form, > 99% purity and expected size of ≤ 100 nm) were obtained from Sigma-Aldrich. Stock suspensions of Ag ENMs (0.5 g L^{-1}) were prepared in ultrapure water (18 MΩ, ELGA DV25 Pure Lab Option-Q, Veolia Water Technologies, High Wycombe, UK) and dispersed by sonication for 1 h (160 W/L at 37 kHz; S-Series unheated ultrasonic cleaning bath, Fisherbrand, Loughborough, UK) before further dilutions in freshwater (aerated, dechlorinated and recirculating Plymouth city water). Stock solutions of 20 mg L^{-1} of Ag metal as $AgNO_3$ were prepared similarly to the Ag ENMs.

The primary particle diameter and morphology of Ag ENMs was determined using a tomography electronic microscope (TEM, JEOL 12000EXII, Tokyo, Japan). Fresh (0 h) and aged (24 h) suspensions (50 g L^{-1}) of Ag ENMs were prepared in both ultrapure water and tap water (freshwater) and measurements were made on triplicated samples. Small volumes (less than 1 mL) of the suspensions were placed on the grids (copper coated with Formvar/carbon), allowed to sit for 10 min and then placed in the instrument for analysis. The primary particle diameters were measured on the images obtained using Image J (https://imagej.nih.gov/ij/) with at least 35 particles counted from each dispersion.

The suspensions of Ag ENMs were also examined for particle aggregation and settling behaviour over 24 h. Freshly prepared suspensions of Ag ENMs (15 mg L^{-1} in freshwater) were placed in triplicates (300 mL beakers previously acid washed and deionized) at room temperature without stirring and water samples taken after 0, 0.5, 1, 2, 4, 8, 24 h. From these suspensions, particle settling was estimated based on the loss of total silver concentrations from the water column over 24 h. Total metal concentrations were measured by inductively coupled plasm mass

spectrometry (ICP-MS, X-Series II quadruple, Thermo Scientific, Paisley, UK). Particle size distribution of the Ag ENMs (hydrodynamic diameters) was also evaluated in triplicate at the start and end of the same experiment using Nanoparticle Tracking Analysis (NTA, Nanosight LM10, Amesbury, UK).

Dissolution of dissolved Ag from the Ag ENMs was determined by equilibrium dialysis following the method of Besinis et al. (2014). These experiments were conducted in triplicate at room temperature using Plymouth water. All glassware was acid washed in 5% nitric acid (HNO_3) and triple rinsed in ultrapure water before use. The cellulose dialysis tubing [12 kDa molecular weight cut off (Sigma-Aldrich, Gillingham, UK)] were cut into strips (70 × 25 mm), thoroughly cleaned, acid washed and rinsed in ultrapure water. The dialysis bags were filled with either 3 mL of 500 mg L^{-1} of Ag ENMs suspension (i.e., 1.5 mg of Ag ENMs in ultrapure water) or 3 mL of 500 Ag mg L^{-1} of $AgNO_3$ solution (i.e., 2.37 mg of Ag as $AgNO_3$ in ultrapure water) and then closed at both ends with Medi-clips to prevent leakages. The dialysis membranes were sealed, added to the beakers containing 297 mL of tap water (the same composition as used for the fish) and stirred gently with a magnetic stirrer. Samples from the beakers (i.e., from outside the dialysis bag) were collected after 0, 0.5, 1, 2, 4, 8, 24 h and acidified (68% HNO_3) prior to total Ag determination by ICP-MS.

3.4.2 Experimental fish

Stocks of adult zebrafish (*Danio rerio*), bred in house at Plymouth University (Devon, UK) were held in a facility at 26 ± 1 °C and 16 h light:8 h dark cycle. Fish were held in glass tanks (25 L) with aerated, re-circulating, filtered and dechlorinated freshwater (water chemistry in mM, means ± S.D., $n = 3$: Ca^{2+}, 1.12 ± 0.05; K^+, 0.10 ± 0.01; Mg^{2+}, 0.14 ± 0.01; Na^+, 0.93 ± 0.04; pH 7.3; conductivity 168.3 µS/cm) (Boyle et al., 2020). The background concentration of Ag in the tap water was below the detection limit (LOD= 0.31 µg L^{-1}, $n= 3$ replicates). Fish were twice day fed with flake and brine shrimp nauplii *ad libitum*. Breeding pairs of fish were allowed to spawn at first light and resulting embryos carefully collected into clean freshwater. Fertilized embryos in blastula stage (3-6 hpf) were selected for viability under a

stereo microscope (Olympus SZX7 with an Infinity 2 camera, Shinjuku-ku, Japan) and separated from unfertilized eggs. Coagulated (visually white and opaque embryos) or unhealthy embryos were discarded, and the batches of healthy embryos were kept in petri dishes prior exposure.

3.4.3 Lethal and sub-lethal exposures of zebrafish embryos

The embryo assay was based on the OECD draft guideline on Fish Embryo Toxicity Test (FET) (OECD, 2013b). Tap water used for all egg collection procedures and toxicity assays was previously filtered (0.2µm PES vacuum filter, VWR, Lutterworth, UK). Preliminary range finding experiments were performed to determine the lethal concentration of the Ag ENMs compared to $AgNO_3$, and to derive an LC_{10} for subsequent sub-lethal studies. A series of twelve concentrations (3 replicate plates, with a total of $n = 24$ replicate wells per concentration) in 48-well microplates (one embryo per well with 1 mL of exposure solution) was used for the lethality test. Endpoints were selected to assess lethality of both $AgNO_3$ and Ag ENMs, including % mortality (visually assessed by the lack of heartbeat) and % hatching success (i.e., visually assessed by the ability of embryos to hatch – break the chorion – where a ratio of hatched and live embryos is calculated). After determining the lethal concentration that killed 10% of embryos (LC_{10}) values (**see Figure 6-I** and **Table 6-IX, Appendix C**), sub-lethal exposures were performed with 25 µg Ag L^{-1} as $AgNO_3$ and 4.5 mg L^{-1} of Ag ENMs. Exposures were conducted in low density polypropylene cups (70 embryos in 100 mL of Ag suspensions) with twelve replicates per Ag treatment and quadruplicates for the unexposed controls as reference. All assays were incubated at 26 ± 1 ºC and 16 h light/8 h dark cycle for 96 h. The $AgNO_3$ solutions and Ag ENMs suspensions were renewed daily to maintain the exposures. After 96 h, pools of embryos were thoroughly washed in clean tap water (3 times) and then stored for different purposes: pools of 30 manually dechorionated embryos were snap-frozen in liquid nitrogen and stored at -80 °C for biochemical assays; pools of 3 chorionated and 15 dechorionated embryos for trace metal analysis; and pools of 15 dechorionated embryos for whole

body electrolytes (Ca^{2+}, Na^+ and Mg^{2+}), based on our previous experience (Boyle et al., 2020).

3.4.4 Metal and electrolytes analysis from the sub-lethal exposure

Embryos were separated into two categories, with chorion (chorionated) and without chorion (dechorionated). In the dechorionated embryos, chorion and perivitelline fluid (PVF) were mechanically separated with forceps from the inner embryo. The method for trace metal determination was similar to that previously used in the laboratory (Shaw et al., 2012). Dechorionated and chorionated embryos were digested at 60 °C for 1 hour in 0.5 mL of concentrated HNO_3 (68% trace element grade, Fisher Scientific, Loughborough, UK). After digestion, samples were diluted to 4 mL in ultrapure water and spiked with Indium/Iridium to a final concentration of 10 µg L^{-1} In/Ir (internal analytical standards). Triplicates were analysed for Cu (isotope ^{65}Cu) by inductively coupled plasma mass spectrometry (ICP-MS, X-Series II quadruple, Thermo Scientific, Paisley, UK) and for electrolytes (wavelengths: Ca = 397 nm, Na = 590 nm, Mg = 280 nm) by ICP-OES. Matrix matched acidified element standards were measured every 10-15 samples to check the instrument for drift and recoveries of In/Ir. Data were expressed as ng Cu, Ca, Na and Mg per embryo. The metal content of the chorion was calculated by the subtraction of Ag concentration in the dechorionated embryos from the total amount determined for the whole embryos. Also, considering that chorionated embryos represent 100% of the measured silver.

3.4.5 Biochemical analyses from the sub-lethal exposure

Biochemical analyses were performed on pools of dechorionated embryos. Embryos were homogenised on ice (3 x 10 sec) with a disposable pestle system (VWR, Lutterworth, UK) in cold isotonic buffer (300 mmol L^{-1} sucrose, 20 mmol L^{-1} 4-(2-hydroxyethyl)-1-piperazineethanesulfonic acid (HEPES), 0.1mmol L^{-1} Ethylenediaminetetraacetic acid (EDTA), pH 7.8)). Homogenates were centrifuged (13,000 rpm for 2 min) and supernatants transferred to new tubes and stored at −80°C until further analysis. Sodium pump (Na^+/K^+-ATPase) activity was measured

according to Mccormick (1993) in sextuplicate reactions with 10 µL of homogenate, 50 µL of salt reaction and 150 µL of solution with/without inhibitor (ouabain 0.5 mmol L^{-1}). Final assay concentrations were 3 U mL^{-1} of lactase dehydrogenase (LDH), 3.75 U mL^{-1} pyruvate kinase (PK), 2.1 mmol L^{-1} phosphoenolpyruvate (PEP), 0.53 mmol L^{-1} adenosine triphosphate (ATP), 0.16 mmol L^{-1} nicotinamide adenine dinucleotide (NADH), 37.25 mmol L^{-1} HEPES, 47.25 mmol L^{-1} NaCl, 2.63 mmol L^{-1} MgCl$_2$, 10.5 mmol L^{-1} KCl, at pH 7.5. Reactions were monitored by the disappearance of NADH at 340 nm every 10 sec for 10 min on Versa Max microplate reader (Molecular Device Ltd, Wokingham, UK).

Total gluthatione (tGSH) determination was adapted from Baker et al. (1990) and measured in triplicate reactions, using 20 µL of supernatant and 180 µL of master mix. Final assay concentrations were 76.5 mmol L^{-1} of phosphate buffer (pH 7.5), 3.8 mmol L^{-1} of EDTA, 0.12 U mL^{-1} of gluthatione reductase (GR), 0.5 mmol L^{-1} of 5'5'-dithiobis-2-nitrobenzoic acid (DTNB), 0.2 mmol L^{-1} of β-Nicotinamide adenine dinucleotide phosphate tetrasodium salt (NADPH). Reactions were monitored by the increase of absorbance at 412 nm every 15 sec for 10 min on the Versa max microplate reader. Superoxide dismutase (SOD) activity was measured in triplicate reactions, using 20 µL of supernatant and a SOD determination kit (product 19160, Sigma-Aldrich, Gillingham, UK). The reaction was monitored by the formation of the superoxide anion at 450 nm on a Versa Max microplate reader. Sodium pump and SOD activities were normalised to total protein in the supernatant using the Pierce™ BCA Protein Assay Kit (product 23227, Thermo Scientific, Paisley, UK).

3.4.6 Data analysis

All statistical analyses were performed using SigmaPlot *v.* 12.5. *A priori*, all data were tested for normality (Shapiro–Wilk test) and homogeneity of variance (Brown-Forsythe test). Where data were not normally distributed, data were transformed (log10). Statistically significant differences between treatment groups were determined by ANOVA followed by Dunnett's test or Holm-Sidak test. Where log-transformation failed, the Kruskal–Wallis test was applied as appropriate on untransformed data. Two significance levels ($p<0.01$ and $p<0.05$) were employed

for statistical analyses. Lethal and effect concentrations values of 10, 20 and 50% (LC_{10}, LC_{20}, LC_{50} and EC_{10}, EC_{20}, EC_{50}) and corresponding 95% confidence limits were calculated using a non-linear allosteric decay function. Lowest observed effect concentration (LOEC), no observed effect concentration (NOEC) and maximum acceptable toxicant concentration (MATC) were also calculated. All data are presented as means ± standard deviation, unless otherwise stated.

3.5 **Results**

3.5.1 **Characterization of Ag ENMs**

Images from TEM of Ag ENMs suspensions showed primary particles with a quasi-spherical shape (**Figure 3-1a**). The measured primary particle diameter in fresh suspensions of ultrapure water was 42.51 ± 10.23 nm (mean ± S.D., *n= 35*) and smaller than the information provided by the manufacturer (≤ 100nm). Freshly prepared particles in tap water were larger in diameter (76.17 ± 15.92 nm) than the ones in ultrapure water. However, aged suspensions (24 h) in freshwater had a smaller particle diameter (66.50 ± 14.94 nm) than the initial dispersion; being significantly different from 0 h (*$F_{2,69} = 6.67$, P=0.012*).

The particle size distributions and mean hydrodynamic diameters were measured, using NTA, in ultrapure water over 0.5 h and differences were found (*$F_{1,79} = 18.53$, P≤0.001*) at 25 mg L^{-1} of Ag ENMs, suggesting instability of particles. Then, the same measurements were done in freshwater over 24 h (**Figure 3-1b**), at a lower concentration, 15 mg L^{-1} of Ag ENMs, and still was observed some particle instability. At 0 h immediately after dosing, most of the agglomerates of Ag ENMs were smaller than 300 nm in freshwater (96 %, **Figure 3-1b**) and with a total particle number concentration of 425.26 x 10^6 particles mL^{-1} and a mean hydrodynamic diameter of 157.33 ± 6.13 nm. After 24 h, a dispersion of smaller agglomerates below 70 nm kept stable, but the particle number concentration in the size range of 90-300 nm increased approximately 1.7-fold (**Figure 3-1b;** *$F_{2,32} = 10.76$, P <0.001*). The mean hydrodynamic diameter of the dispersion (149 ± 17.8 nm) decreased after 24 h, but not significantly (*$F_{2,8} = 0.396$, P=0.69*).
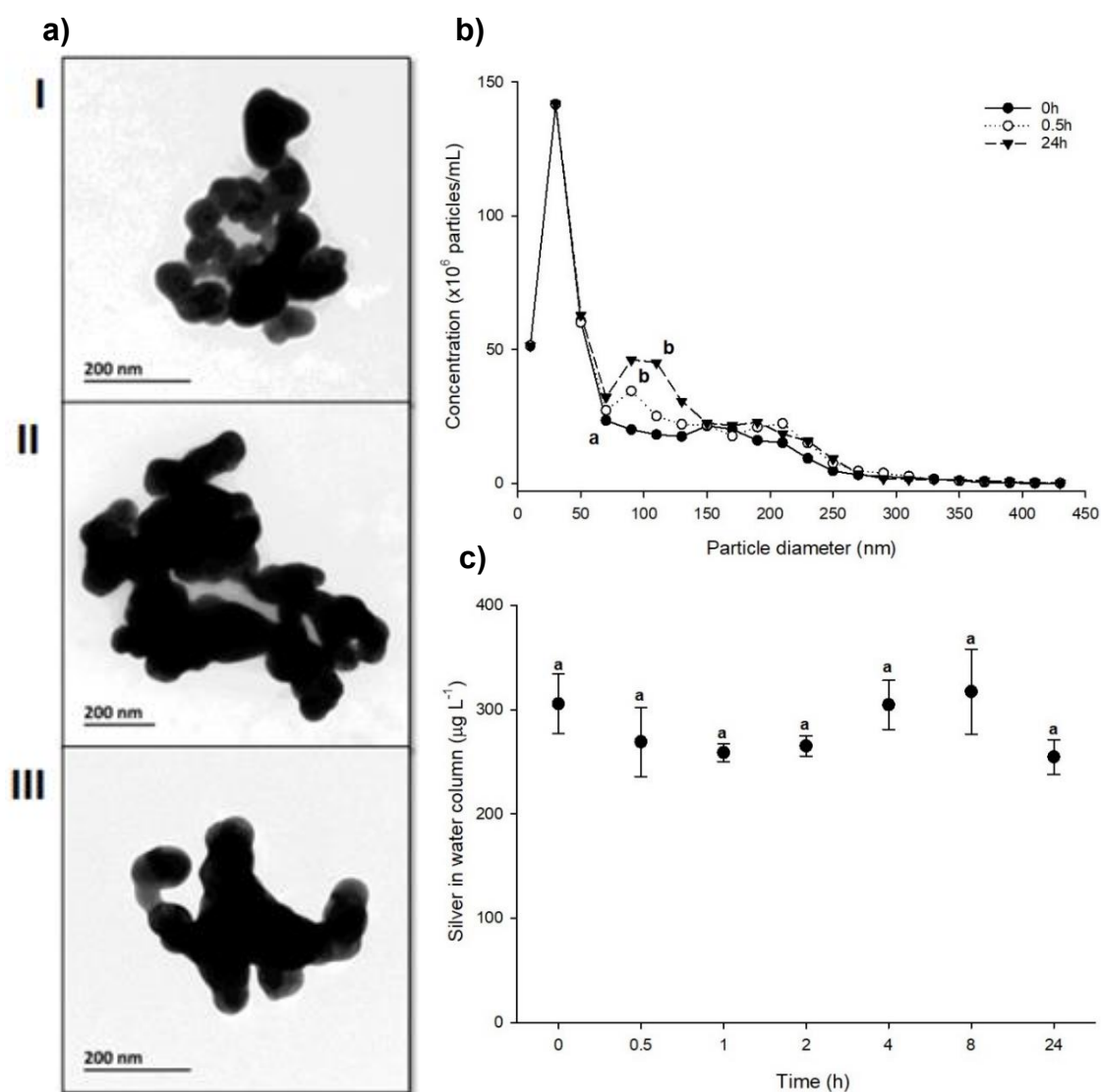
Figure 3-1 – Characterization of silver nanomaterials (Ag ENMs) in the water column of freshwater. (a) Transmission electronic microscope (TEM) images of Ag ENMs in ultrapure water (t= 0 h, I), or freshwater water (t= 0 h, II, and 24 h, III). (b) Particle size distribution measurements of Ag ENMs were obtained by Nanoparticle tracking analysis (NTA, Nanosight LM10) in freshwater. Values represent mean ± S.D. (n = 3 replicates of dispersion). Data points with different lower-case letters are significantly different (two-way ANOVA, Holm-Sidak test, $P < 0.01$). (c) Total silver concentration in the water column of freshwater for Ag ENMs (example nominal concentration 15 mg L^{-1}). Values stand for mean ± S.D. (n = 3). Data points with distinct lower-case letters are significantly different (Holm-Sidak test, $P<0.01$).

The particle settling was confirmed by measuring the total Ag concentration in the water column from the Ag ENMs suspensions over 24 h (**Figure 3-1c**). The measured total Ag concentration showed 305.6 ± 23.42 µg L^{-1} that slightly decreased to 254.6 ± 13.67 µg L^{-1} after 24 h (**Figure 3-1c;** $F_{6,20} = 3.1, P=0.038$). However, the settling in freshwater was instantaneous, and even at 0 h (within a few minutes of mixing) only than 2% of the nominal exposure concentration was retained in the water column itself, suggesting that most adhered to the surface of the exposure container or sank in the bottom (thus exposing the embryos).

A dialysis experiment was also conducted to explore the dissolution of dissolved Ag from the particles (**Figure 3-2**). The AgNO$_3$ had an increase and apparently reached an equilibrium in the beaker (from the initial 2.37 mg of Ag as AgNO$_3$ added to the dialysis bag), reaching a plateau within two h and then increasing, with an average concentration of 423.5 ± 62.4 µg Ag L^{-1} – equivalent to 3.92 ± 0.58 µmoles L^{-1} – for AgNO$_3$ treatment over 24 h (**Figure 3-2a**)**,** which represents <0.1% of the Ag remaining as a diffused phase in the water column. The release of dissolved Ag from Ag EMNs was 131.01 ± 53.69 µg L^{-1} in the beaker at 24 h (**Figure 3-2b**), suggesting the Ag ENMs are very sparingly soluble and remained in the particulate form during the experiments. This represents ~0.03% dissolution of the Ag metal in fresh water from the particles in 24 h. A maximum dissolution rate of 13.8 µg h^{-1} was attained in the first hour. Additionally, pH was measured in fresh (0 h) and aged suspensions (24 h) of both AgNO$_3$ solution and Ag ENMs suspension. No differences were found in either AgNO$_3$ (24 h = 6.07 ± 0.03), Ag ENMs (24 h = 5.95 ± 0.085) and control (freshwater = 6.07 ± 0.06), considering time and/or nature of Ag form.
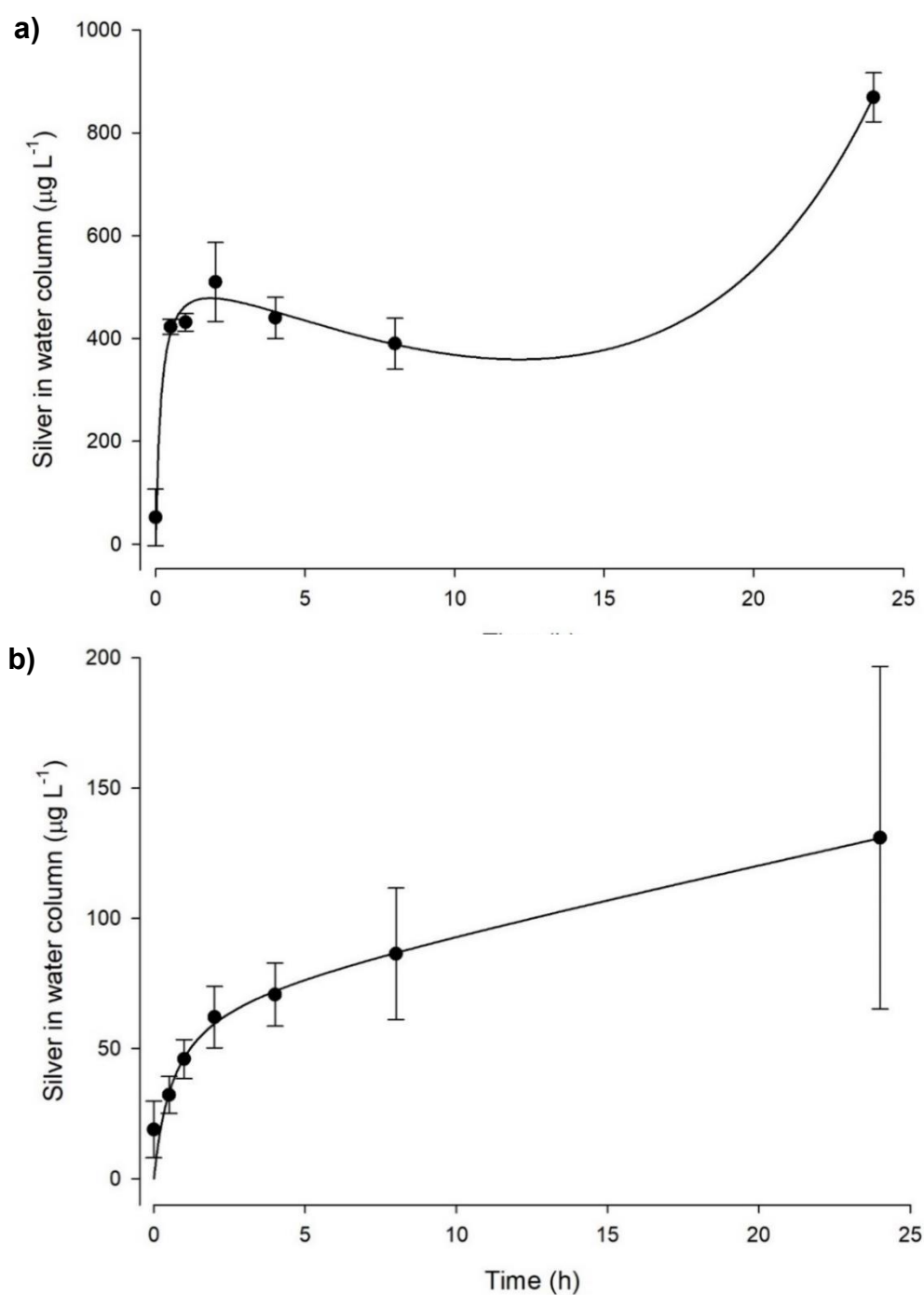
Figure 3-2 – Total silver concentration measured in the water column (freshwater) during equilibrium dialysis over 24 h; (a) AgNO$_3$ and, (b) Ag ENMs. Values represent mean ± S.D. (n = 3, independent replicates). Curves were fitted using hyperbolic functions in SigmaPlot for AgNO$_3$ (r^2= 0.956) $y = \dfrac{\left(\frac{-1002x}{(-38.8+x)+584.4x}\right)}{(-0.44+x)+19.3x}$ and Ag ENMs (r^2= 0.667) $y = \left(\dfrac{71.8x}{(0.64+x)+2.54x}\right)$.

3.5.2 **Lethal effects**

The lethal concentration range finding test identified both the 96h-LC_{50} for $AgNO_3$ [32.82 ± 0.72 μg Ag L^{-1} (± 95% CI)] and Ag ENMs (6.46 ± 0.4 mg L^{-1}), where ENMs were less toxic than the dissolved metal form. Mortality curves from both Ag forms between 48 and 96 hpf are shown in **Figure 6-I** and **Table 6 IX** (**Appendix C**). In the lethal exposure, embryos exposed to $AgNO_3$ (20 μg Ag L^{-1}) and Ag ENMs (5 mg L^{-1}) were compared with the respective control treatments in **Figure 3-3b** and **d**. Additional, sub-lethal endpoints were assessed in the lethal concentration test, but only hatching success (%) was affected (**Figure 3-3a and c**). The effect concentration (EC) values were calculated for the hatching success of embryos exposed to both Ag forms after 96h (**Figure 3-3a** and **c** and **Table 6-IX**, **Appendix C**), where the 96-EC_{50} was 30.53 ± 1.39 μg Ag L^{-1} for $AgNO_3$ and 6.04 ± 0.4 mg L^{-1} for Ag ENMs. Hatching success of embryos was significantly different between $AgNO_3$ and Ag ENMs after 72 hpf (*$F_{11,71}$ = 21.42, p≤0.001*) and 96 hpf (*$F_{11,71}$ = 9.46, p≤0.001*).
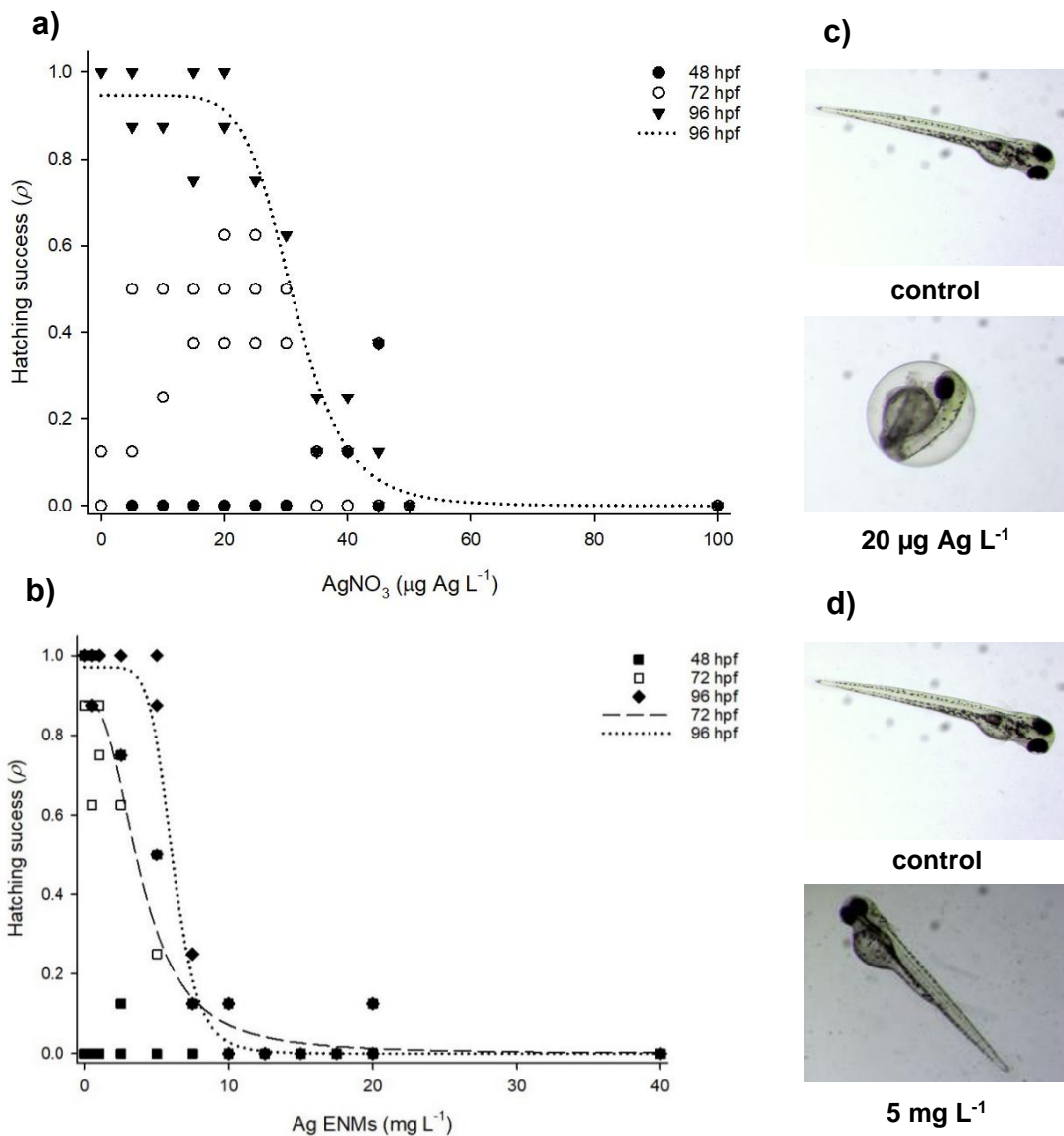
Figure 3-3 – Effects of AgNO$_3$ (a & c) or Ag ENMs (b & d) on zebrafish embryos during the lethal exposures over 96 hpf. Curves in panels (a) to (d) are embryos (n = 36) represented as independent replicates. Hatching success refers the proportion (ρ) of embryos that successfully hatched in AgNO$_3$ (filled black circles, 48 hpf; empty white circles, 72 hpf; filled black inverted triangle, 96hpf; in panel a) and Ag ENMs (filled black squares, 48 hpf; empty white squares, 72 hpf; filled black diamond-shaped, 96hpf; in panel b). Images in panels (b) and (d) show the typical morphology, from the AgNO$_3$ (20 µg Ag L^{-1}) and Ag ENMs (5 mg L^{-1}) concentrations, on 96 hpf old zebrafish embryos or larvae against the respective controls. Curves were fitted using Sigmaplot and were based on the sigmoidal functions of AgNO$_3$ after 96 hpf (r^2= 0.948), $y = \left(\frac{(0.95*31.3)^{7.4}}{(31.2^{7.4})+x^{7.4}}\right)$ and Ag ENMs after 72 hpf (r^2= 0.96), $y = \left(\frac{(0.89*3.9)^{2.6}}{(3.9^{2.6})+x^{2.6}}\right)$ and 96 hpf (r^2= 0.97) $y = \left(\frac{(0.97*6.1)^{7.1}}{(6.1^{7.1})+x^{7.1}}\right)$ data, respectively.

91

3.5.3 **Metal distribution in zebrafish embryos during sub-lethal exposures**

The sub-lethal exposure was based on the 96h-LC_{10} calculated values for $AgNO_3$ and Ag ENMs. However, the mortality in the initial sub-lethal experimental conditions of $AgNO_3$ (27 µg Ag L^{-1}) and Ag ENMs (4.5 mg L^{-1}) was higher than expected, 93% and 67%, respectively. The lethal and sub-lethal were conducted with different experimental designs, the first in isolated wells ($n = 1$ embryo per well) and the second in cups ($n = 70$ embryos per cup), where the density of embryos might have been responsible for the higher mortality rates. Thus, we repeated the sub-lethal exposures and adjusted with lower concentrations until achieving acceptable levels of mortality – 5 µg Ag L^{-1} of $AgNO_3$ (<5 %, n=5) and 1.5 mg L^{-1} of Ag ENMs (35 ± 4.7 %, n=5). It was challenging to find an Ag ENM concentration with no mortality and yet enable detection of accumulation inside the embryo, and so a compromise was struck. Regardless, all sub-lethal measurements were on the surviving embryos in each experiment. The total Ag in the embryos reflected the LC_{10} exposure concentrations to $AgNO_3$ (**Figure 3-4a**) and Ag ENMs (**Figure 3-4b**) for 96 h, respectively. For $AgNO_3$, the chorion was not a barrier to dissolved metal uptake and total Ag was measured in both chorionated and dechorionated embryos, still only 3.7 % of silver was associated to the inner embryo and perivitelline space and 96.3 % of silver was retained to the chorion (**Figure 3-4a,** 27-fold difference). Regarding the exposure to Ag ENMs, the total Ag in chorionated embryos was much higher than in the dechorionated ones (469-fold difference; $F_{2,30} = 2.59, p=0.095$), indicating that most of the total silver was associated with the chorion (99.8 %), not the inner embryo. Nonetheless, a few hundred picograms of Ag were measured inside dechorionated embryos (0.2% of the total Ag accumulated), confirming that the embryos were still exposed.
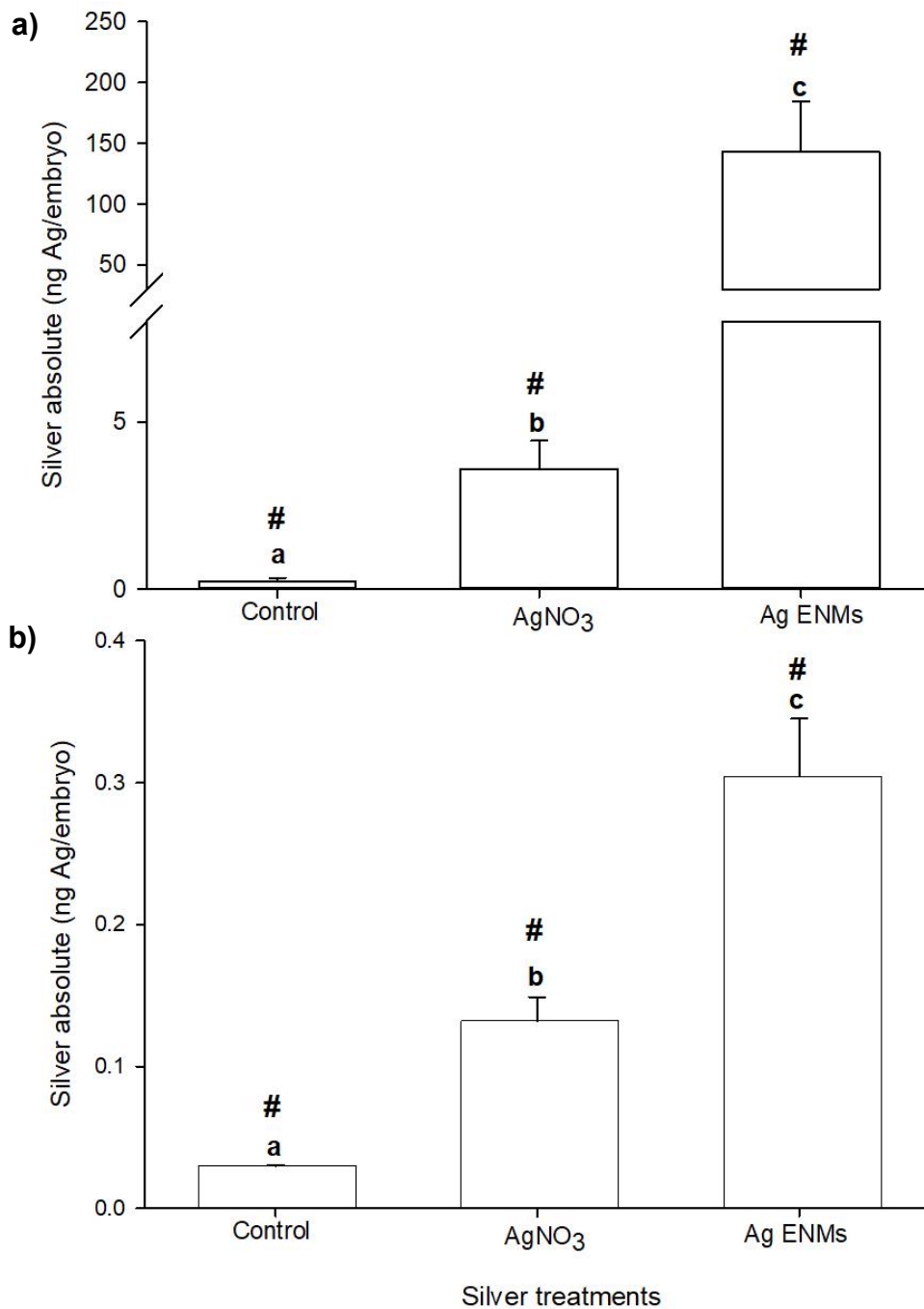
Figure 3-4 – Total absolute mass of silver (ng per embryo) in the (a) chorionated and (b) dechorionated zebrafish embryos exposed (sub-lethal) to $AgNO_3$ (5 µg Ag L^{-1}) and Ag ENMs (1.5 mg L^{-1}). Values stand for mean ± S.D. ($n = 3 - 9$ independent samples of embryos). Whereas bars with different lower-case letters are significantly different between silver treatments; bars with cardinal symbol (#) show significantly differences between chorionated and dechorionated embryos for the same silver treatment (two-way ANOVA, Holm-Sidak test, $P<0.01$).

3.5.4 **Osmoregulation and oxidative stress during sub-lethal exposures**

Silver nitrate (AgNO$_3$) is known to interfere with ion homeostasis and the dechorionated embryos showed evidence of depletion of Ca^{2+} ($F_{2,11} = 19.88$, $p<0.001$) and Na$^+$ ($F_{2,11} = 16.83$, $p<0.001$), but not Mg^{2+} ($F_{2,11} = 1.49$, $p=0.276$) compared to the control (**Table 3-1**). Exposure to Ag ENMs caused a similar level of Ca^{2+} depletion to the metal salt, and greater Na$^+$ depletion with the nano form. However, the trend was not the same for the sodium pump activity, with no statistical differences found compared to the control, and only between AgNO$_3$ and Ag ENMs with more inhibition in the latter (**Figure 3-5a**; $F_{2,15} = 5.19$, $p=0.022$). Embryos showed evidence of oxidative stress, where the total GSH was significantly depleted in embryos exposed to AgNO$_3$ and even more to Ag ENMs (**Figure 3-5b**; $F_{2,12} = 52.11$, $p<0.001$). However, this trend was not repeated in the SOD activity, which remained similar among all Ag treatments (**Figure 3-5c**; $F_{2,12} = 1.93$, $p=0.196$).

Table 3-1– Total electrolyte concentrations in dechorionated zebrafish embryos following 96 h exposure to AgNO$_3$ (5 µg Ag L^{-1}) and Ag ENMs (1.5 mg L^{-1}).

Electrolyte (ng per embryo)	Control (*n*=3)	AgNO$_3$ (*n*=6)	Ag ENMs (*n*=3)
Calcium (Ca^{2+})	210.8 ± 22.7 [a]	138.6 ± 12.1 [b]	146.9 ± 4.2 [b]
Magnesium (Mg^{2+})	133.5 ± 21.08 [a]	130.84 ± 8.5 [a]	114.6 ± 9.4 [a]
Sodium (Na$^+$)	256.02 ± 44.8 [a]	180.03 ± 19.7 [b]	110.8 ± 6.3 [c]

Values are mean ± S.D. (*n* = replicate samples of embryos). Different lower-case letters are significantly different within rows (one-way ANOVA: *Holm-Sidak test, P <0.05*).
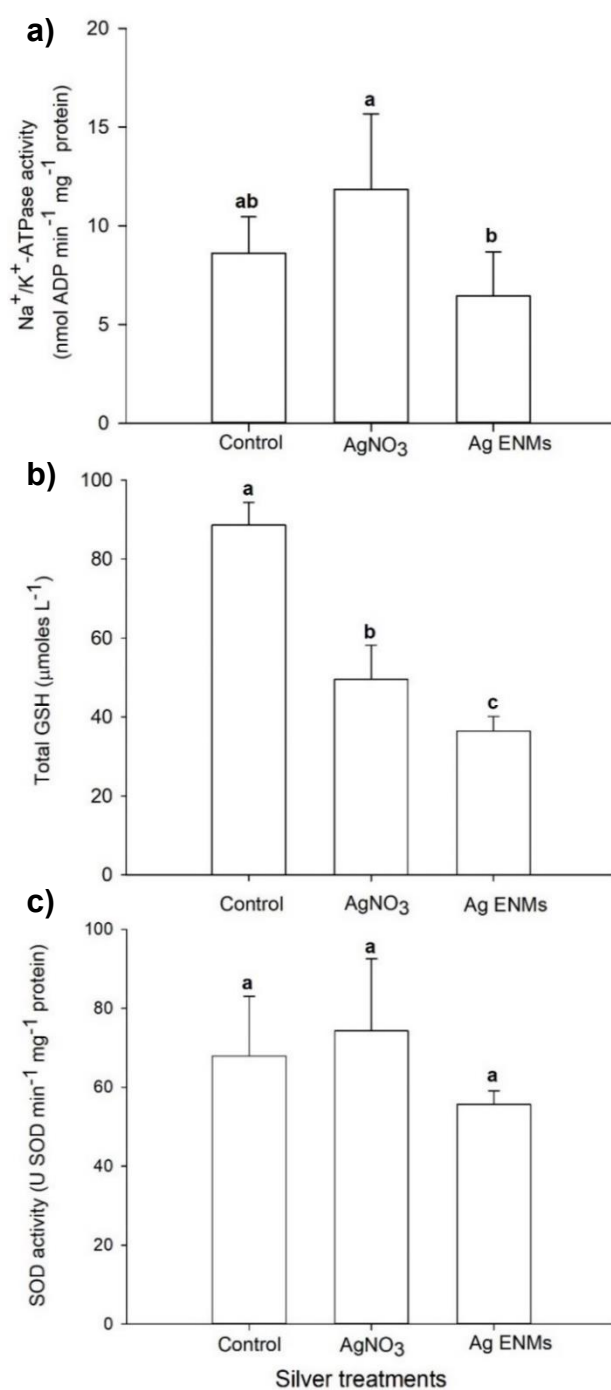
Figure 3-5 – Biochemical responses of zebrafish dechorionated embryos exposed (sub-lethal) to $AgNO_3$ (5 µg Ag L^{-1}) and Ag ENMs (1.5 mg L^{-1}). **a**) shows sodium pump (Na^+/K^+-ATPase) activity, **b**) shows for total glutathione (tGSH) and **c**) shows superoxide dismutase (SOD) activity. Values stand for mean ± S.D. ($n = 3 - 7$ independent samples of embryos). Bars with different lower-case letters are significantly different (one-way ANOVA, Holm-Sidak test, *P<0.01*).

3.6 Discussion

This study shows that the salt metal ($AgNO_3$) is more toxic to zebrafish embryos than the nano form (Ag ENMs). In the sub-lethal exposure, the accumulation of Ag from the metal salt occurred inside the embryo despite a natural barrier, the chorion. In contrast, for the nano exposure, a large fraction of the total Ag was associated with the chorion, although some total Ag (form unknown) was internalised resulting in exposure of the embryos. Regarding the mode of action, both the metal salt and Ag ENMs caused electrolyte depletion in the embryos, but without appreciable inhibition of the sodium pump activity. Both forms of Ag prompted the depletion of tGSH in the embryos, indicating some oxidative stress, but SOD activity remained unaltered.

3.6.1 Acute toxicity of $AgNO_3$ compared to Ag ENMs (Lethal exposure)

In the present study, the 96 h LC_{50} for the zebrafish early life stage with $AgNO_3$ was around 0.0328 mg L^{-1} compared to 6.4 mg L^{-1} for Ag ENMs (**Table 6-IX, Appendix C**), with the nano form being at least two orders of magnitude less toxic than the metal salt. The lethal concentration values for $AgNO_3$ (**Table 6-IX, Appendix C**) are broadly similar to previous reports on Ag salts. The 96 h-LC_{50} values of $AgNO_3$ were reported in the micromolar range from 0.0047 to 0.079 mg L^{-1} in embryos of zebrafish (Heinlaan et al., 2016; Khoshnamvand et al., 2020; Massarsky et al., 2013; Ribeiro et al., 2014; Wang et al., 2012), and from 0.0023 to 0.015 mg L^{-1} in embryos of *Pimephales promelas* (Bielmyer et al., 2008; Hoheisel et al., 2012; Laban et al., 2010). Inevitably, the ranges of these acute lethal values for $AgNO_3$ depended partly on the animal species, but mainly the diverse physicochemical characteristics of the exposure medium from those studies that range from dechlorinated tap water to standardised laboratory medium and natural water from lakes.

The Ag ENMs were much less toxic than the metal salt, and 96h LC_{50} for the former were around 6.46 mg L^{-1} for zebrafish early life stages (**Table 6-IX, Appendix C**) and consistent with previous reports where the metal salt also shown to be less toxic. Several 96 h-LC_{50} values were established in previous studies for zebrafish embryos exposed to Ag ENMs – from 0.129 to 5.9 mg L^{-1} – where the nano form

was 2 to 454 times less toxic than the metal salt control (Heinlaan et al., 2016; Massarsky et al., 2013; Ribeiro et al., 2014; Wang et al., 2012; Xin et al., 2015). Although Yen et al. (2019) did not include a metal salt control, this study had a similar 96h-LC_{50} value to the one calculated in this study for Ag ENMs of 6.1 mg L^{-1}. These ranges of nanotoxicity for these species occurred with Ag ENMs with different type of surface coatings – bare (particles without any surface coating), organic and polymeric – and with size of a nominal diameter below 80 nm.

In the present study, the cumulative mortality was not linear. Most of it occurred in the 72-96 hpf interval, which coincided with the hatching of embryos (**Figure 6-IV** and **Table 6-IX, Appendix C**). This trend suggests that the larvae were more vulnerable to lethal toxicity during the stress of hatching, and afterwards due to direct exposure of the gills (i.e., animals now without the protection of the chorion), as expected for ENMs (Shaw et al., 2016).

3.6.2 **Hatching success in the lethal exposure**

Clearly, hatched zebrafish larvae are more sensitive to ENMs that the unhatched embryos (Shaw et al., 2016). So, in order to interpret the cumulative toxicity over time, it is essential to understand when embryos hatch in any experiment and the likely mechanisms of toxicity (see below on the latter). Hatching success is often used as an endpoint in early life stage studies, and a dose-dependent adverse effects occurred on hatching (**Figure 3-3a**). In this study, the metal salt affected the hatching success of embryos (**96h-EC_{50}** = 30.53 ± 1.39 µg Ag L^{-1}; **Table 6-IX, Appendix C**). Ribeiro et al. (2014) observed that 40 ug L^{-1} of $AgNO_3$ (as dissolved Ag) only induced a 30% decrease in the hatching rate of zebrafish embryos after 96 hpf. Considering the nano form, Ag ENMs induced a delay in the hatching of embryos, since under optimal conditions, zebrafish embryos hatch in the 48-72h interval (Kimmel et al., 1995), and the EC_{50} value almost doubled from 72h to 96hpf (**96h-EC_{50}** = 6.04 ± 0.4 mg L^{-1}; **Table 6-IX, Appendix C**). Yen et al. (2019) observed a transient reduction of hatching success at 72 hpf with exposures to 0.1 and 1 mg L^{-1} of Ag ENMs (10 nm), but no effects with 3 and 5 mg L^{-1} of Ag ENMs compared to unexposed controls. Such a counterintuitive dose-response might be explained

by metal ion dissolution with better dispersions at the lower ENM concentrations, but unfortunately, Yen et al. (2019) did not measure dissolution or report metal salt control. Bar-Ilan et al. (2009) observed that 35% of embryos failed to hatch after 120 hpf when exposed to Ag ENMs of 50 nm (nominal size), but there were negligible effects on hatching at other particle sizes (3, 10 and 100 nm) and seemed not to relate to the particle size distributions in the study (also no metal salt control). Ong et al. (2014) noticed a delay in hatching and established a correlation between hatching inhibition and protease activity, where the latter decreased by 65% in the chorionic fluid of zebrafish embryos exposed to 10 mg L^{-1} of Ag ENMs (6-35 nm), suggesting Ag-dependent inhibition of the enzymes involved weakening the chorion as the cause of failure to hatch or delayed hatch. Notably, Ong et al. (2014) manually dechorionated embryos and they survived, confirming that the stress of prolonged or difficult hatching was also a cause of mortality. Regardless of the mechanisms involved, the 96h-EC_{50} hatching success in the present study indicated the animals were much more sensitive to Ag as the metal salt than the nano form.

3.6.3 Sub-lethal exposure and total Ag accumulation

Daily suspensions changes during the exposure period were done to help ensure the presence of Ag ENMs in the water column, but the exposure was mainly confirmed in the sub-lethal experiment by measuring the total Ag concentrations in the zebrafish (**Figure 3-4**). This was a pragmatic decision, partly because the sub-lethal exposure was performed with very low concentrations that would be hard to detect Ag in the water column against the instantaneous adsorption to the surfaces of the organism and test vessels. Thus, measuring the total Ag on/in the zebrafish embryos themselves was the best way to assess actual exposure. Nonetheless, the particle size distribution analysis (**Figure 3-1b**) suggests that smaller particles (≤ 70 nm) remained stable in the water column over 24h, whereas the concentration of larger particles (90–200 nm) increased. This effect supports the notion that a small fraction of the particles dwelled in the water column (**Figure 3-1c**), and most adhered to the surface of the exposure container or aggregated and settled at the bottom of the vessels to expose the unhatched embryos.

The dialysis experiment helped to examine the dissolution of dissolved Ag from Ag ENMs (**Figure 3-2**). The $AgNO_3$ did not achieve a clear steady-state equilibrium in the beaker, but the 2.4 mg of Ag as $AgNO_3$ added to the dialysis bag resulted in a total Ag concentration of 850.9 ± 38.86 µg Ag L^{-1} for $AgNO_3$ after 24 h (**Figure 3-2a**), which only represents a 0.17% of the Ag remaining as a diffused phase in the water column. This is likely explained by spontaneous insoluble AgCl particle formation (69% of the speciation in either pH 6 or 7.3) in the dialysis bag when millimolar concentrations of chloride ions are present in the freshwater [see Clark et al. (2019) for discussion]. In fact, such speciation predicts the freshwater likely contains less than 20% of Ag as dissolved ions (Ag^+). Thus, the dialysis represents only the remaining soluble species of Ag. The release of dissolved Ag from Ag ENMs was even lower than that of $AgNO_3$ with only 131.01 ± 53.69 µg L^{-1} of Ag from Ag ENMs in the beaker by 24 h (**Figure 3-2b)**. This represents 0.0003% dissolution of the Ag metal in freshwater from the particles in 24 h and confirms that the ENM stayed in the particulate form during the exposures.

The quantification of total Ag concentration in the embryos helped to confirm the exposure (**Figure 3-4**). Intact embryos (i.e., chorionated) exposed to Ag, either as the ENM or metal salt, had much higher Ag concentrations comparing to the controls. The Ag concentration on/in the intact embryos resulting from Ag ENMs exposure was higher than from the $AgNO_3$ exposure, taking into account the differences in both (LC_{10} values). Nevertheless, exposure was confirmed because total Ag (form unknown) accumulated into the embryos in both $AgNO_3$ and Ag ENMs exposures (**Figure 3-5**).

For $AgNO_3$ exposures, only 4% of the total Ag associated with the embryos was internally located as measured in de-chorionated animals (i.e., around 96% of the total Ag associated with the chorion, **Figure 3-4**). The biodistribution of metals in fish embryos is reasonably understood; in rainbow trout, about two thirds (65-85%) of dissolved silver was on/associated with the chorion (Guadagnolo et al., 2001) and the values here are broadly consistent with the notion of some metal adsorption to the protective chorion. The de-chorionated embryos from the Ag EMNs exposure had only 0.3 ng/embryo compared to 143 ng/embryo on/in the chorionated counterparts (**Figure 3-4**); indicating that most (~99.8%) of the Ag from the Ag

ENMs exposure was located on the exterior of the animals. Minimal internalization of total Ag from Ag ENM exposures is consistent with Böhme et al. (2017) where <5% of the total metal was associated with the inner embryo of zebrafish in exposures to AgNO₃ and Ag ENMs. The chorion was a reasonably effective barrier to prevent the internalisation of the nanomaterial, at least in the short term. In theory, the diameter of chorionic pores of zebrafish embryos, set around 0.8-0.9 μm (Chen et al., 2020), would not hinder the diffusion of monodispersed primary particles (76 nm) (**Figure 3-1a**); however, at the start (0h), 71% of aggregates were between 0.13 and 0.3 μm (**Figure 3-1b**). Thus, even a modest number of aggregates in this range would suffice to clog or obstruct the access to the chorionic pores. Notably, the hatching success was affected by the Ag ENMs exposure (**Figure 3-3**), and this could partly be attributed to the blocked chorion (see above).

3.6.4 **Osmoregulation and oxidative stress in sub-lethal exposure**

The electrolyte concentrations in dechorionated embryos showed a prominent depletion of both whole-body Ca^{2+} and Na^+ concentrations in embryos exposed to either form of Ag compared to the control treatment (**Table 3-1**). These results suggest that embryos were not able to maintain a healthy osmoregulatory function. Unlike the other electrolytes, Mg^{2+} concentration did not decline (**Table 3-1**), and this is expected given the typical equilibrium potential of Mg^{2+} ions in fish embryos relative to the surrounding water [see van der Velden et al. (1991)], and thus Mg^{2+} is not easily lost by diffusion. Dissolved Ag acts as an ionoregulatory toxicant that especially disrupts Na^+ homeostasis. Silver ions may compete for entry through apical Na^+ channels and cause inhibition of the basolateral sodium pump (Grosell et al., 2002b; Hogstrand and Wood, 1998). Thus some Na^+ depletion during dissolved Ag exposures may be expected and has been observed in rainbow trout embryos and larvae (Guadagnolo et al., 2000). Notably, there was greater Na^+ depletion during exposure to Ag ENMs compared to the metal salt in this study (**Table 3-1**), and with negligible dissolution of the latter (**Figure 3-2b**), suggesting that the nano form was also disrupting Na^+ homeostasis. Sodium depletion during acute mg L⁻¹ exposures to Ag ENMs has been observed in adult zebrafish (Katuli et

al., 2014), juvenile rainbow trout (Schultz et al., 2012) and zebrafish larvae (Lee et al., 2019). Interestingly, Lee et al. (2019) partly attributed the salt depletion to a decrease of ionocytes on the yolk sac membrane, which indicated the osmoregulatory capacity of the embryo had not fully developed in the Ag ENMs-exposed animals; however, no metal salt controls were included in the study design to verify any incidental dissolved Ag effect.

Regarding the whole-body Ca^{2+} depletion, both the metal salt and nano form similarly disrupted Ca^{2+} homeostasis of zebrafish embryos. Dissolved Ag tends not to have direct toxicity to the ion transporters involved in the regulation of Ca^{2+} in freshwater fish (Wood et al., 1999). Instead, the loss of Ca^{2+} might be an indirect outcome of Na^+/Ca^{2+} exchange in the gills which relies ultimately on the sodium pump for energy (Bury and Handy, 2010). Lee et al. (2019) also observed a large 97% decrease of Ca^{2+} concentrations in zebrafish larvae after 96 hpf of exposure to 3 mg L^{-1} of Ag ENMs, but the mechanisms of any nano-specific Ca^{2+} depletion needs further investigation.

In terms of biochemical mechanisms of Ag toxicity, there was no appreciable inhibition of the Na^+K^+-ATPase activity in either Ag exposure compared to controls, but there was evidence of oxidative stress via some tGSH depletion (**Figure 3-5**). Inhibition of sodium pump activity in the gills of freshwater fishes is well-known for dissolved Ag (Sathya et al., 2012; Wood et al., 1999), and with data emerging on juvenile fish for the nano form (Schultz et al., 2012). For example, in Morgan et al. (2004), gill sodium pump activity and Na^+ uptake were inhibited by 41% and 91%, respectively, after 24 h of exposure to $AgNO_3$ (4.3 µg L^{-1}). In rainbow trout early life stages, exposure to 10 µg L^{-1} Ag as $AgNO_3$ caused inhibition of whole-body Na^+K^+-ATPase activity, but only in the hatched larvae, not in the intact embryos (Brauner and Wood, 2002). Similarly, the embryos here showed little sodium pump inhibition with the metal salt (**Figure 3-5a**). There was a small inhibitory effect of Ag ENMs compared to the metal salt (**Figure 3-5a**), but this was likely not biologically important in the short-term as the effect was within scope of the normal variation of the controls. The whole-body Na^+ and Ca^{2+} depletion (**Table 3-1**) without Na^+ pump inhibition (**Figure 3-5a**) implies the ion loss was caused by passive efflux from a leaky embryo, not by a failure of active Na^+ influx. Similarly, Katuli et al. (2014)

reported minor alterations in the sodium pump activity in the gill of adult zebrafish after 96 h of exposure to Ag ENMs (16.8 mg L^{-1}) against a significant decline of Na$^+$. Of course, membrane damage can arise from oxidative stress and some loss of tGSH was observed, and this was more pronounced for the nano Ag exposure than the metal salt (**Figure 3-5b**). The depletion of tGSH has been observed in freshwater fish (embryos and adults) exposed to Ag metal salts and/or Ag ENMs (Kashiwada et al., 2012; Massarsky et al., 2013). For dissolved silver, the tGSH depletion is usually caused by increases of ROS in the tissue, with Ag$^+$ avidly binding to thiol groups including those in glutathione and/or subsequently causing peroxidation (e.g., Leung et al. (2013)). For this reason, additions of thiolsulfate can protect against AgNO$_3$ toxicity in fish (Rose-Janes and Playle, 2000). However, in the present study Ag ENMs caused more tGSH depletion than the metal salt (**Figure 3-5b**), and while Ag$^+$ dissolution was very small over 24h (**Figure 3-2a**, 0.0003%) this, in theory, would be equivalent to 45 μg L^{-1} of dissolved Ag from a 1.5 mg L^{-1} Ag ENM exposure, presumably mostly delivered by the ENMs adhering to the chorion. Thus a local release of dissolved Ag from the ENMs may explain the slightly greater tGSH depletion (**Figure 3-5b**) and the higher Ag concentration in the embryo (**Figure 3-4**) with the nano form. Glutathione-*S*-transferase (GST) activity cannot be excluded as a mechanism to remove oxidised glutathione from the cells, but was not measured here and no alterations in GST activity have been seen in rainbow trout exposed to Ag ENMs (Bruneau et al., 2016; Scown et al., 2010).

The activity of SOD was not affected by either the metal salt or Ag ENMs (**Figure 3-5c**), and with tGSH still remaining in the embryos, together this indicates that any oxidative stress was mild. Stable SOD values were also reported in embryos of medaka (Kashiwada et al., 2012), and zebrafish (Massarsky et al., 2013) exposed for up to 6 days to 1.6 mg L^{-1} of Ag ENMs. Similarly, SOD activity was unaltered in the gills and liver of rainbow trout (Bruneau et al., 2016) exposed up to 40 (Ag ENMs) or 4 μg L^{-1} (AgNO$_3$) in wastewater for 96 h.

3.7 **Conclusion**

In conclusion, this study depicts that overall AgNO$_3$ was more toxic than Ag ENMs to zebrafish embryos. Still, the exposure and mechanisms were different, where the Ag ENMs were mostly on/associated with the chorion, and internalising a negligible amount of Ag (form unknown). The Ag ENM exposure induced a superior depletion on the levels of total GSH, but had not effect on the sodium pump. From an animal welfare perspective, it is desirable to find alternatives to mortality as an endpoint, and here the EC$_{50}$ values for the hatching success were affected by both Ag forms and more sensitive than mortality. From an ecological perspective, the settling of Ag ENMs from the water column would pose a risk of exposure to any fish embryos in the river sediment. Eventually the mortality and impairment of the hatching could impact recruitment in wild populations of fishes. However, with LC$_{50}$ and EC$_{50}$ values here being much lower for the metal salt, one might argue that existing environmental risk assessments for silver would also protect for the effects of the nano form.

3.8 **Acknowledgements**

3.9 **References**

Azimzada, A., et al., 2021. Quantification and Characterization of Ti-, Ce-, and Ag-Nanoparticles in Global Surface Waters and Precipitation. Environ Sci Technol. 55, 9836-9844. https://doi.org/10.1021/acs.est.1c00488

Baker, M. A., et al., 1990. Microtiter plate assay for the measurement of glutathione and glutathione disulfide in large numbers of biological samples. Anal Biochem. 190, 360-365. https://doi.org/10.1016/0003-2697(90)90208-q

Bar-Ilan, O., et al., 2009. Toxicity assessments of multisized gold and silver nanoparticles in zebrafish embryos. Small. 5, 1897-1910. https://doi.org/10.1002/smll.200801716

Besinis, A., et al., 2014. The antibacterial effects of silver, titanium dioxide and silica dioxide nanoparticles compared to the dental disinfectant chlorhexidine on *Streptococcus mutans* using a suite of bioassays. Nanotoxicology. 8, 1-16. https://doi.org/10.3109/17435390.2012.742935

Bielmyer, G. K., et al., 2008. Is Cl⁻ protection against silver toxicity due to chemical speciation? Aquat Toxicol. 87, 81-87. https://doi.org/10.1016/j.aquatox.2008.01.004

Böhme, S., et al., 2017. Metal uptake and distribution in the zebrafish (*Danio rerio*) embryo: differences between nanoparticles and metal ions. Environ Sci: Nano. 4, 1005-1015. https://doi.org/10.1039/c6en00440g

Boyle, D., et al., 2020. Toxicities of copper oxide nanomaterial and copper sulphate in early life stage zebrafish: Effects of pH and intermittent pulse exposure. Ecotoxicol Environ Saf. 190, 109985. https://doi.org/10.1016/j.ecoenv.2019.109985

Brauner, C. J., Wood, C. M., 2002. Ionoregulatory development and the effect of chronic silver exposure on growth, survival, and sublethal indicators of toxicity in early life stages of rainbow trout (*Oncorhynchus mykiss*). J Comp Physiol B. 172, 153-162. https://doi.org/10.1007/s00360-001-0238-8

Bruneau, A., et al., 2016. Fate of silver nanoparticles in wastewater and immunotoxic effects on rainbow trout. Aquat Toxicol. 174, 70-81. https://doi.org/10.1016/j.aquatox.2016.02.013

Bury, N. C., Handy, R. D., 2010. Copper and iron uptake in teleost fish, in: N. C. Bury, R. D. Handy (Eds.), Surface Chemistry, Bioavailability and Metal Homeostasis in Aquatic Organisms: An integrated approach. Society for Experimental Biology Press, London, pp. 107-127

Busquet, F., et al., 2014. OECD validation study to assess intra- and inter-laboratory reproducibility of the zebrafish embryo toxicity test for acute aquatic toxicity testing. Regul Toxicol Pharmacol. 69, 496-511. https://doi.org/10.1016/j.yrtph.2014.05.018

Calderón-Jiménez, B., et al., 2017. Silver Nanoparticles: Technological Advances, Societal Impacts, and Metrological Challenges. Front Chem. 5, 1-26. https://doi.org/10.3389/fchem.2017.00006

Chen, Z. Y., et al., 2020. The effect of the chorion on size-dependent acute toxicity and underlying mechanisms of amine-modified silver nanoparticles in zebrafish embryos. Int J Mol Sci. 21, 2864. https://doi.org/10.3390/ijms21082864

Clark, N. J., et al., 2019. An assessment of the dietary bioavailability of silver nanomaterials in rainbow trout using an ex vivo gut sac technique. Environ Sci: Nano. 6, 646-660. https://doi.org/10.1039/c8en00981c

Dumont, E., et al., 2015. Nano silver and nano zinc-oxide in surface waters – Exposure estimation for Europe at high spatial and temporal resolution. Environ Pollut. 196, 341-349. https://doi.org/10.1016/j.envpol.2014.10.022

Eddy, F. B., Handy, R. D., 2012. Ecological and Environmental Physiology of Fishes, first ed. Oxford University Press, Oxford. https://doi.org/10.1093/acprof:oso/9780199540945.001.0001

Fu, P. P., et al., 2014. Mechanisms of nanotoxicity: generation of reactive oxygen species. J Food Drug Anal. 22, 64-75. https://doi.org/10.1016/j.jfda.2014.01.005

Grosell, M., et al., 2002. Sodium turnover rate determines sensitivity to acute copper and silver exposure in freshwater animals. Comp Biochem Physiol C Toxicol Pharmacol. 133, 287-303. https://doi.org/10.1016/S1532-0456(02)00085-6

Guadagnolo, C. M., et al., 2000. Effects of an acute silver challenge on survival, silver distribution and ionoregulation within developing rainbow trout eggs (*Oncorhynchus mykiss*). Aquat Toxicol. 51, 195-211. https://doi.org/10.1016/s0166-445x(00)00112-0

Guadagnolo, C. M., et al., 2001. Chronic effects of silver exposure on ion levels, survival, and silver distribution within developing rainbow trout (*Oncorhynchus mykiss*) embryos. Environ Toxicol Chem. 20, 553-560. https://doi.org/10.1002/etc.5620200314

Heinlaan, M., et al., 2016. Natural water as the test medium for Ag and CuO nanoparticle hazard evaluation: An interlaboratory case study. Environ Pollut. 216, 689-699. https://doi.org/10.1016/j.envpol.2016.06.033

Hogstrand, C., Wood, C. M., 1998. Toward a better understanding of the bioavailability, physiology, and toxicity of silver in fish: implications for water quality criteria. Environ Toxicol Chem. 17, 547-561. https://doi.org/10.1002/etc.5620170405

Hoheisel, S. M., et al., 2012. Comparison of nanosilver and ionic silver toxicity in *Daphnia magna* and *Pimephales promelas*. Environ Toxicol Chem. 31, 2557-2563. https://doi.org/10.1002/etc.1978

Kashiwada, S., et al., 2012. Silver nanocolloids disrupt medaka embryogenesis through vital gene expressions. Environ Sci Technol. 46, 6278-6287.

https://doi.org/10.1021/es2045647

Katuli, K. K., et al., 2014. Silver nanoparticles inhibit the gill Na$^+$/ K$^+$-ATPase and erythrocyte AChE activities and induce the stress response in adult zebrafish (*Danio rerio*). Ecotoxicol Environ Saf. 106, 173-180. https://doi.org/10.1016/j.ecoenv.2014.04.001

Khoshnamvand, M., et al., 2020. Toxicity of biosynthesized silver nanoparticles to aquatic organisms of different trophic levels. Chemosphere. 258, 127346. https://doi.org/10.1016/j.chemosphere.2020.127346

Kimmel, C. B., et al., 1995. Stages of embryonic development of the zebrafish. Dev Dyn. 203, 253-310. https://doi.org/10.1002/aja.1002030302

Laban, G., et al., 2010. The effects of silver nanoparticles on fathead minnow (*Pimephales promelas*) embryos. Ecotoxicology. 19, 185-195. https://doi.org/10.1007/s10646-009-0404-4

Lead, J. R., et al., 2018. Nanomaterials in the environment: Behavior, fate, bioavailability, and effects-An updated review. Environ Toxicol Chem. 37, 2029-2063. https://doi.org/10.1002/etc.4147

Lee, C. Y., et al., 2019. Silver nanoparticle exposure impairs ion regulation in zebrafish embryos. Aquat Toxicol. 214, 105263. https://doi.org/10.1016/j.aquatox.2019.105263

Leung, B. O., et al., 2013. Silver(I) complex formation with cysteine, penicillamine, and glutathione. Inorg Chem. 52, 4593-4602. https://doi.org/10.1021/ic400192c

Massarsky, A., et al., 2013. Assessment of nanosilver toxicity during zebrafish (*Danio rerio*) development. Chemosphere. 92, 59-66. https://doi.org/10.1016/j.chemosphere.2013.02.060

Mccormick, S. D., 1993. Methods for nonlethal gill biopsy and measurement of Na$^+$, K$^+$-ATPase activity. Can J Fish Aquat Sci. 50, 656-658. https://doi.org/10.1139/f93-075

Mohammed, A., 2013. Why are Early Life Stages of Aquatic Organisms more Sensitive to Toxicants than Adults?, in: S. J. T. Gowder (Ed.), New Insights into Toxicity and Drug Testing. IntechOpen, Rijeka, pp. 49-62. https://doi.org/10.5772/55187

Morgan, T. P., et al., 2004. Time course analysis of the mechanism by which silver inhibits active Na$^+$ and Cl$^-$ uptake in gills of rainbow trout. Am J Physiol Regul Integr Comp Physiol 287, 234-242. https://doi.org/10.1152/ajpregu.00448.2003

OECD, Test No. 210: Fish, Early-life Stage Toxicity Test. Section 2. Organization for Economic Co-Operation and Development, Paris, 2013a. pp. 24. https://doi.org/10.1787/9789264203785-en

OECD, Test No. 236: Fish Embryo Acute Toxicity (FET) Test. Section 2. Organization for Economic Co-Operation and Development, Paris, 2013b. pp. 22. https://doi.org/10.1787/9789264203709-en

Ong, K. J., et al., 2014. Mechanistic insights into the effect of nanoparticles on zebrafish hatch. Nanotoxicology. 8, 295-304. https://doi.org/10.3109/17435390.2013.778345

Powers, C. M., et al., 2010. Silver exposure in developing zebrafish (*Danio rerio*): Persistent effects on larval behavior and survival. Neurotoxicol Teratol. 32, 391-397. https://doi.org/10.1016/j.ntt.2010.01.009

Pulit-Prociak, J., Banach, M., 2016. Silver nanoparticles – a material of the future…? Open Chem. 14, 76-91. https://doi.org/10.1515/chem-2016-0005

Ribeiro, F., et al., 2014. Silver nanoparticles and silver nitrate induce high toxicity to *Pseudokirchneriella subcapitata*, *Daphnia magna* and *Danio rerio*. Sci Total Environ. 466–467, 232-241. https://doi.org/10.1016/j.scitotenv.2013.06.101

Rose-Janes, N. G., Playle, R. C., 2000. Protection by two complexing agents, thiosulphate and dissolved organic matter, against the physiological effects of silver nitrate to rainbow trout (*Oncorhynchus mykiss*) in ion-poor water. Aquat Toxicol. 51, 1-18. https://doi.org/10.1016/s0166-445x(00)00103-x

Sathya, V., et al., 2012. Acute and sublethal effects in an Indian major carp *Cirrhinus mrigala* exposed to silver nitrate: Gill Na^+/K^+-ATPase, plasma electrolytes and biochemical alterations. Fish Shellfish Immunol. 32, 862-868. https://doi.org/10.1016/j.fsi.2012.02.014

Schultz, A. G., et al., 2012. Silver nanoparticles inhibit sodium uptake in juvenile rainbow trout (*Oncorhynchus mykiss*). Environ Sci Technol. 46, 10295-10301. https://doi.org/10.1021/es3017717

Scown, T. M., et al., 2010. Assessment of cultured fish hepatocytes for studying cellular uptake and (eco)toxicity of nanoparticles. Environ Chem. 7, 36-49. https://doi.org/10.1071/EN09125

Shaw, B. J., Handy, R. D., 2011. Physiological effects of nanoparticles on fish: a comparison of nanometals versus metal ions. Environ Int. 37, 1083-1097. https://doi.org/10.1016/j.envint.2011.03.009

Shaw, B. J., et al., 2016. A critical evaluation of the fish early-life stage toxicity test for engineered nanomaterials: experimental modifications and recommendations. Arch Toxicol. 90, 2077-2107. https://doi.org/10.1007/s00204-016-1734-7

Sun, T. Y., et al., 2014. Comprehensive probabilistic modelling of environmental emissions of engineered nanomaterials. Environ Pollut. 185, 69-76. https://doi.org/10.1016/j.envpol.2013.10.004

van der Velden, J. A., et al., 1991. Early life stages of carp (*Cyprinus carpio* L.) depend on ambient magnesium for their development. J Exp Biol. 158, 431-438. https://doi.org/10.1242/jeb.158.1.431

Wang, Z., et al., 2012. Aquatic toxicity of nanosilver colloids to different trophic organisms: Contributions of particles and free silver ion. Environ Toxicol Chem. 31, 2408-2413. https://doi.org/10.1002/etc.1964

Wood, C. M., 2011. Silver, in: C. M. Wood, et al. (Eds.), Homeostasis and Toxicology of Non-Essential Metals. Academic Press, San Diego, pp. 1-65. https://doi.org/10.1016/S1546-5098(11)31023-0

Wood, C. M., et al., 1999. Physiology and modeling of mechanisms of silver uptake and toxicity in fish. Environ Toxicol Chem. 18, 71-83. https://doi.org/10.1002/etc.5620180110

Xin, Q., et al., 2015. Silver nanoparticles affect the neural development of zebrafish embryos. J Appl Toxicol. 35, 1481-1492. https://doi.org/10.1002/jat.3164

Yen, H. J., et al., 2019. Toxic effects of silver and copper nanoparticles on lateral-line hair cells of zebrafish embryos. Aquat Toxicol. 215, 105273. https://doi.org/10.1016/j.aquatox.2019.105273

Zhang, C., et al., 2016. Silver nanoparticles in aquatic environments: Physiochemical behavior and antimicrobial mechanisms. Water Res. 88, 403-427. https://doi.org/10.1016/j.watres.2015.10.025

Chapter IV

DIFFERENCES IN TOXICITY AND ACCUMULATION OF METAL FROM COPPER OXIDE NANOMATERIALS COMPARED TO COPPER SULPHATE IN ZEBRAFISH EMBRYOS: DELAYED HATCHING, THE CHORION BARRIER AND PHYSIOLOGICAL EFFECTS

4   Chapter IV – Differences in toxicity and accumulation of metal from copper oxide nanomaterials compared to copper sulphate in zebrafish embryos: Delayed hatching, the chorion barrier and physiological effects

4.1 **Highlights**

- Copper oxide nanomaterials (CuO ENMs) were less toxic than the $CuSO_4$.

- Hatching delay linked to coating of the chorion and foam in the perivitelline fluid.

- 94% (CuO ENMs) and 58% ($CuSO_4$) of total Cu accumulated on the chorion.

- Na^+ and Ca^{2+} decreased in CuO ENMs and $CuSO_4$, but Na^+ pump only declined in $CuSO_4$.

- Total GSH was depleted in both Cu treatments, with a nano-specific oxidative stress.

- 94% (CuO ENMs) and 58% ($CuSO_4$) of total Cu accumulated on the chorion.

4.2 **Abstract**

The mechanisms of toxicity of engineered nanomaterials (ENMs) to the early life stages of freshwater fish, and the relative hazard compared to dissolved metals, is only partially understood. In the present study, zebrafish embryos were exposed to lethal concentrations of copper sulphate ($CuSO_4$) or copper oxide (CuO) ENMs (primary size ~15 nm), and then the sub-lethal effects investigated at the LC_{10} concentrations over 96 h. The 96h-LC_{50} (mean ± 95% CI) for $CuSO_4$ was 303 ± 14 µg Cu L^{-1} compared to 53 ± 9.9 mg L^{-1} of the whole material for CuO ENMs; with the ENMs being orders of magnitude less toxic than the metal salt. The EC_{50} for hatching success was 76 ± 11 µg Cu L^{-1} and 0.34 ± 0.78 mg L^{-1} for $CuSO_4$ and CuO ENMs respectively. Failure to hatch was associated with bubbles and foam-looking perivitelline fluid ($CuSO_4$), or particulate material smothering the chorion (CuO ENMs). In the sub-lethal exposures, about 42% of the total Cu as $CuSO_4$ was internalised, as measured by Cu accumulation in the de-chorionated embryos, but for the ENMs exposures, nearly all (94%) of the total Cu was associated with chorion; indicating the chorion as an effective barrier to protect the embryo from the ENMs in the short term. Both forms of Cu exposure caused sodium (Na^+) and calcium (Ca^{2+}), but not magnesium (Mg^{2+}), depletion from the embryos; and $CuSO_4$ caused some inhibition of the sodium pump (Na^+/K^+-ATPase) activity. Both forms of Cu exposure caused some loss of total glutathione (tGSH) in the embryos, but without induction of superoxide dismutase (SOD) activity. In conclusion, $CuSO_4$ was much more toxic than CuO ENMs to early life stage zebrafish, but there are subtle differences in the exposure and toxic mechanisms for each substance.

Keywords

4.3 **Introduction**

Metal oxide nanomaterials are finding diverse industrial applications due to their unique physico-chemical properties at the nano scale. Copper oxide engineered nanomaterials (CuO ENMs) have applications as catalysts, in air and liquid filtration units, in wood preservatives and antifouling paints for boats, as well as in industrial sealants and coatings. CuO ENMs had a global annual production of 570 tons in 2014 and it is estimated to increase to 1600 tons by 2025 (Keller et al., 2013). About 5.5% of the manufacturing and domestic wastes from CuO ENMs are expected to reach natural water bodies (Keller et al., 2013); with some direct releases from some products (e.g., Cu ions from antifouling paints). Although the concentrations of Cu-containing ENMs in surface waters have not been determined, metal-containing ENMs are expected in the low µg L^{-1} to ng L^{-1} range (Lead et al., 2018). The fate and behaviour of CuO ENMs in freshwater ecosystems is only partially understood, but they show colloidal behaviours such as aggregation, dissolution, and flocculation (Amde et al., 2017; Ross and Knightes, 2022).

The dissolution of Cu-containing ENMs is a particular concern, as dissolved Cu is toxic to aquatic organisms in freshwater and with acutely lethal concentrations for fish around 10-150 µg L^{-1}, depending on the water sodium concentration, hardness and pH [reviews (Grosell et al., 2002a; Handy, 2003)]. There is also the possibility that metal-containing ENMs could act as a delivery vehicle to release high concentrations of metals in the gill microenvironment of fishes (Shaw and Handy, 2011) and Cu ENMs are toxic to fishes (rainbow trout Shaw et al. (2012), zebrafish Griffitt et al. (2007)). The mode of action of dissolved Cu during waterborne exposure of freshwater fish is well-known and includes gill injury with a specific interference with sodium homeostasis and inhibition of the branchial sodium pump (the Na^+/K^+ ATPase (Grosell, 2011)). Copper can also catalyse the Haber-Weiss reaction leading to oxygen radicals; and oxidative stress is also a feature of Cu toxicity to fishes (Eyckmans et al., 2011; Hoyle et al., 2007). These modes of actions also occur during exposure to Cu ENMs e.g. (Al-Bairuty et al., 2016; Malhotra et al., 2020; Shaw et al., 2012).

The early life stages of fishes are especially vulnerable to metal toxicity, including dissolved Cu in trout (McKim et al., 1978) and in zebrafish (Johnson et al., 2007). Evidence is also emerging of hazard from Cu-containing ENMs, at least to zebrafish larvae (McNeil et al., 2014). The early-life stages of zebrafish are now widely used in regulatory toxicity testing, most notably the fish embryo test (FET) OECD TG 236 (OECD, 2013b), which has been validated for traditional chemicals (Busquet et al., 2014), but requires modifications to work for ENMs (Shaw et al., 2016). The sensitivity of zebrafish embryos to dissolved metals is influenced by the presence of the semi-permeable chorion and the ion-exchange properties of the mucous perivitelline fluid which is rich in fixed anionic residues to buffer metal uptake (Peterson and Martinrobichaud, 1986; Shephard, 1987). After hatching, without the protection of the egg, the larvae are often more vulnerable to waterborne chemicals (Ganesan et al., 2016), and this is also the case with some ENMs (Shaw et al., 2016). Hatching success is often used as an endpoint in early life stage studies, and dissolved Cu has been shown to inhibit hatching with consequent impairment of embryos survival (Johnson et al., 2007; Zhang et al., 2018). Hatching occurs by the joint action of proteolytic enzymes (particularly ZHE$_1$) that are released in the perivitelline space (Muller et al., 2015) and the movements of the fish embryo to break the weakening chorion (Ong et al., 2014). Still, the mechanisms of action of CuO ENMs in zebrafish embryos, and whether the chorion is protective against ENMs remains unclear. Additionally, the differences in the internalization of ENMs and salt metal forms are not fully understood.

This study aimed to evaluate the lethal and sub-lethal effects of CuO ENMs in zebrafish embryos compare to that of CuSO$_4$. Mortality and hatching success were used as the endpoints to assess lethal effects on zebrafish embryos. To understand if chorion has a protective effect, experiments were conducted on embryos with the chorion present (chorionated) and without it (de-chorionated) and the subsequent metal accumulation and distribution in the embryos was measured. Finally, in de-chorionated embryos where internal Cu exposure was confirmed, the sub-lethal effects on osmoregulation [electrolyte concentrations and sodium pump (Na$^+$/K$^+$-ATPase activity)] and oxidative stress parameters [superoxide dismutase (SOD)

activity and total glutathione (tGSH)] were measured to help unravel the mechanisms of toxicity of CuO ENMs.

4.4 **Materials and Methods**

4.4.1 **Copper oxide nanomaterials and characterisation**

Copper oxide nanomaterials (uncoated, dry powder form, > 99% purity and expected average size of 30-50 nm) were obtained from PlasmaChem GmbH (Berlin, Germany). Stock suspensions of CuO ENMs (1 g L^{-1}) were prepared in ultrapure water (18 MΩ, ELGA DV25 Pure Lab Option-Q, Veolia Water Technologies, High Wycombe, UK) and dispersed by sonication for 1 h (160 W/L at 37kHz; S-Series unheated ultrasonic cleaning bath, Fisherbrand, Loughborough, UK) before further dilutions in freshwater (aerated, dechlorinated and recirculating Plymouth city water). Stock solutions of 20 mg L^{-1} of Cu metal as $CuSO_4$ were prepared similarly to the CuO ENMs. The primary particle diameter and morphology of CuO ENMs was determined using a tomography electronic microscope (TEM, JEOL 12000EXII, Tokyo, Japan). Fresh (0 h) and aged (24 h) suspensions (50 g L^{-1}) of the CuO ENMs were prepared in both ultrapure water and tap water (freshwater) and measurements were made on triplicated samples. Small volumes (≈ 1 mL) of the suspensions were placed on the grids (copper coated with Formvar/carbon), allowed to sit for 10 min and then placed in the instrument for analysis. The primary particle diameters were measured on the images obtained using Image J (https://imagej.nih.gov/ij/) with at least 35 particles counted from each dispersion.

The suspensions of CuO ENMs were also examined for particle aggregation and settling behaviour over 24 h. Freshly prepared suspensions of CuO ENMs (25 mg L^{-1} of CuO ENMs in freshwater) were placed in triplicates (300 mL beakers previously acid washed and deionized) at room temperature without stirring and water samples taken after 0, 0.5, 1, 2, 4, 8, 24 h. From these suspensions, particle settling was estimated based on the loss of total copper concentrations from the water column over 24 h. Total metal concentrations were measured by inductively coupled plasm optical emission spectrometry (ICP-OES, Varian 725 ES, Agilent,

Stockport, UK). Particle size distribution of the CuO ENMs (hydrodynamic diameters) was also evaluated in triplicate at the start and end of the same experiment using Nanoparticle Tracking Analysis (NTA, Nanosight LM10, Amesbury, UK).

Dissolution of dissolved Cu from the CuO ENMs was determined by equilibrium dialysis following the method of Besinis et al. (2014). These experiments were conducted in triplicate at room temperature using Plymouth water. All glassware was acid washed in 5% nitric acid and triple rinsed in ultrapure water before use (i.e., clean glassware not pre-equilibrated with the test solutions). The cellulose dialysis tubing [12 kDa molecular weight cut off (Sigma-Aldrich, Gillingham, UK)] were cut into strips (70 × 25 mm), thoroughly cleaned, acid washed and rinsed in ultrapure water. The dialysis bags were filled with either 3 mL of 2.5 g L^{-1} of CuO ENMs suspension (i.e., 7.5 mg of CuO ENMs in ultrapure water) or 3 mL of 2.5 g Cu L^{-1} of CuSO$_4$ solution (29.5 mg of CuSO$_4$ in ultrapure water) and then closed at both ends with Medi-clips to prevent leakages. The dialysis membranes were sealed, added to the beakers containing 297 mL of freshwater (the same composition as used for the fish) and stirred gently with a magnetic stirrer. Samples from the beakers (i.e. from outside the dialysis bag) were collected after 0, 0.5, 1, 2, 4, 8, 24 h and acidified (68% HNO$_3$) prior to total Cu determination by ICP-OES.

4.4.2 Experimental fish

Stocks of adult zebrafish (*Danio rerio*), bred in house at Plymouth University (Devon, UK) were held in a facility at 26 ± 1 ºC and 16 h light:8 h dark cycle. Fish were held in glass tanks (25 L) with aerated, re-circulating, filtered and dechlorinated freshwater (water chemistry in mM, means ± S.D., n = 3: Ca^{2+}, 1.12 ± 0.05; K$^+$, 0.10 ± 0.01; Mg^{2+}, 0.14 ± 0.01; Na$^+$, 0.93 ± 0.04; pH 7.3; conductivity 168.3 µS/cm) (Boyle et al., 2020). The background concentration of Cu in the tap water was below the detection limit (LOD= 1.82 µg L^{-1}, n= 3 replicates). Fish were fed twice each day with flake and brine shrimp nauplii *ad libitum*. Breeding pairs of fish were allowed to spawn at first light and resulting embryos carefully collected into clean freshwater. Fertilized embryos in blastula stage (3-6 hpf) were selected for viability under a

stereo microscope (Olympus SZX7 with an Infinity 2 camera, Tokyo, Japan) and separated from unfertilized eggs. Coagulated (white and opaque) or unhealthy embryos were discarded, and the batches of healthy embryos were kept in petri dishes prior exposure.

4.4.3 Lethal and sub-lethal exposures of zebrafish embryos

The embryo assay was based on the OECD Test Guideline no. 236 on Fish Embryo Toxicity Test (FET) (OECD, 2013b). The tap water used for all egg collection procedures and toxicity assays was previously filtered (0.2μm PES vacuum filter, VWR, Lutterworth, UK). Preliminary range finding experiments were performed to determine the lethal concentration of the CuO ENMs compared to $CuSO_4$, and to derive an LC_{10} for subsequent sub-lethal studies. A series of twelve concentrations (3 replicate plates, with a total of $n = 24$ replicate wells per concentration) in 48-well microplates (one embryo per well with 1 mL of exposure solution) was used for the lethality test. Endpoints were selected to assess acute lethality of both $CuSO_4$ and CuO ENMs, including % mortality (visually, opaque embryos were counted as dead) and % hatching success (visually, embryos able to break chorion). In addition, observations were made on 'perivitelline fluid morphology' that represents embryos with an abnormal perivitelline fluid (appearance of bubbles and foam-looking that is not present in the control), and "surface coated chorion" that represents the proportion of embryos with chorion visually coated with ENMs. After determining the lethal concentration that killed 10% of embryos (LC_{10}) values (**Table 6-X**, **Appendix D**), sub-lethal assays were performed with 20 mg L^{-1} of CuO ENMs and 190 µg L^{-1} of Cu as $CuSO_4$. Exposures were conducted in low-density polypropylene cups (100 embryos in 100 mL of Cu suspensions) with triplicates per treatment and an unexposed control for reference. All assays were incubated at 26 ± 1 ºC and 16 h light/8 h dark cycle for 96 h. Suspensions of CuO ENMs and solutions of $CuSO_4$ were renewed daily (after 24 h) to maintain the exposures. After 96 h, pools of embryos were thoroughly washed in clean tap water (3 times) and then stored for different purposes. Pools of 30 manually de-chorionated embryos were snap-frozen in liquid nitrogen and stored at -80 °C for biochemical assays, pools of 3 chorionated

and 15 de-chorionated embryos were kept for trace metal analysis, and pools of 15 de-chorionated embryos for whole body electrolytes (Ca^{2+}, Na^+ and Mg^{2+}).

4.4.4 Metal and electrolytes analysis during sub-lethal exposure

Embryos were separated into two categories, with chorion (chorionated) and without chorion (de-chorionated). In the de-chorionated embryos, chorion and perivitelline fluid (PVF) were mechanically separated with forceps from the inner embryo. The method for trace metal determination was similar to that previously used in the laboratory (Shaw et al., 2012). De-chorionated and chorionated embryos were digested at 60 °C for 1 h in 0.5 mL of concentrated HNO_3 (68% trace element grade, Fisher Scientific, Loughborough, UK). After digestion, samples were diluted to 4 mL in ultrapure water and spiked with Indium/Iridium to a final concentration of 10 µg L^{-1} In/Ir (internal analytical standards). Triplicates were analysed for Cu (isotope ^{65}Cu) by inductively coupled plasma mass spectrometry (ICP-MS, X-Series II quadruple, Thermo Scientific, Paisley, UK) and for electrolytes (wavelengths: Ca = 397 nm, Na = 590 nm, Mg = 280 nm) by ICP-OES. Matrix matched acidified element standards were measured every 10-15 samples to check the instrument for drift and recoveries of In/Ir. Data were expressed as ng Cu, Ca, Na and Mg per embryo. The metal content of the chorion was calculated by the subtraction of Cu concentration in the de-chorionated embryos from the total amount determined for the whole (chorionated) embryos.

4.4.5 Biochemical analyses from the sub-lethal exposure

Biochemical analyses were performed on pools of de-chorionated embryos. Embryos were homogenised on ice (3 x 10 sec) with a disposable pestle system (VWR, Lutterworth, UK) in cold isotonic buffer (300 mmol L^{-1} sucrose, 20 mmol L^{-1} 4-(2-hydroxyethyl)-1-piperazineethanesulfonic acid (HEPES), 0.1mmol L^{-1} Ethylenediaminetetraacetic acid (EDTA), pH 7.8)). Homogenates were centrifuged (13,000 rpm for 2 min) and supernatants transferred to new tubes and stored at −80 °C until further analysis. Sodium pump (Na^+/K^+-ATPase) activity was measured according to Mccormick (1993) in sextuplicate reactions with 10 µL of homogenate,

50 µL of salt reaction and 150 µL of solution with/without inhibitor (oubain 0.5 mmol L^{-1}). Final assay concentrations were 3 U mL^{-1} of lactate dehydrogenase (LDH), 3.75 U mL^{-1} pyruvate kinase (PK), 2.1 mmol L^{-1} phosphoenolpyruvate (PEP), 0.53 mmol L^{-1} adenosine triphosphate (ATP), 0.16 mmol L^{-1} nicotinamide adenine dinucleotide (NADH), 37.25 mmol L^{-1} HEPES, 47.25 mmol L^{-1} NaCl, 2.63 mmol L^{-1} $MgCl_2$, 10.5 mmol L^{-1} KCl, at pH 7.5. Reactions were monitored by the disappearance of NADH at 340 nm every 10 sec for 10 min on Versa Max microplate reader (Molecular Device Ltd, Wokingham, UK). Total gluthatione (tGSH) determination was adapted from Baker et al. (1990) and measured in triplicate reactions, using 20 µL of supernatant and 180 µL of mastermix. Final assay concentrations were 76.5 mmol L^{-1} of phosphate buffer (pH 7.5), 3.8 mmol L^{-1} of EDTA, 0.12 U mL^{-1} of gluthatione reductase (GR), 0.5 mmol L^{-1} of 5'5'-dithiobis-2-nitrobenzoic acid (DTNB), 0.2 mmol L^{-1} of β-Nicotinamide adenine dinucleotide phosphate tetrasodium salt (NADPH). Reactions were monitored by the increase of absorbance at 412 nm every 15 sec for 10 min on the Versa max microplate reader. Superoxide dismutase (SOD) activity was measured in triplicate reactions, using 20 µL of supernatant and a SOD determination kit (product 19160, Sigma-Aldrich). The reaction was monitored by the formation of superoxide anion at 450 nm by single read on Versa Max microplate reader. Na^+/K^+-ATPase and SOD activities were normalised to total protein in the supernatant using Pierce™ BCA Protein Assay Kit (product 23227, Thermo Scientific).

4.4.6 Data analysis

All statistical analyses were performed using SigmaPlot *v.* 12.5. A priori all data were tested for normality (Shapiro–Wilk test) and homogeneity of variance (Brown-Forsythe test). Where data were not normally distributed, data were transformed (log10). Statistically significant differences between treatment groups were determined by ANOVA followed by Dunnett's test or Holm-Sidak test. Where log-transformation failed, the Kruskal–Wallis test was applied as appropriate on untransformed data. Two significance levels (*P<0.01* and *P<0.05*) were employed for statistical analyses. Lethal and effect concentrations values of 10 and 50% (EC_{10},

EC_{50} and LC_{10}, LC_{50}) and corresponding 95% confidence limits were calculated using a non-linear allosteric decay function. Lowest Observed Effect Concentration (LOEC), no effect concentration (NOEC) and maximum acceptable toxicant concentration (MATC) were also calculated. All data are presented as means ± standard deviation, unless otherwise stated.

4.5 Results

4.5.1 Characterization of Copper Oxide Nanomaterials (CuO ENMs)

Images from TEM of CuO ENMs suspensions showed primary particles with a quasi-spherical shape (**Figure 4-1a**). The measured primary particle diameter in fresh suspensions of ultrapure water was 15.31 ± 2.76 nm (mean ± S.D., $n = 35$) and smaller than the manufacturer's information (30-50 nm). Freshly prepared particles in freshwater were similar in primary diameter (14.55 ± 2.61 nm) to the ones in ultrapure water. However, aged suspensions (24 h) in freshwater had a larger diameter (20.27 ± 4.49 nm) and this was significantly different from the initial dispersion ($F_{1,69}$ = 43.29, P <0.001). The particle size distributions and mean hydrodynamic diameters were measured using NTA in ultrapure water over 0.5 h and no differences were found ($F_{1,63}$ = 0.136, P =0.715), suggesting the fresh suspensions were sufficiently stable over short periods for dosing from the stocks. Then, the same measurements were performed in freshwater over 24 h (a), where some progressive particle settling was observed. At 0 h immediately after dosing, most of the agglomerates of CuO ENMs were smaller than 300 nm in freshwater (>97%, **Figure 4-1b**) and with a total particle number concentration of 798.58 x10^6 particles mL^{-1} and a mean hydrodynamic diameter of 157.7 ± 0.94 nm. After 24h, a relatively stable dispersion of smaller agglomerates up to 70 nm remained, but the concentration of particle number in the 90-300 nm range decreased approximately 3-fold (**Figure 4-1b;** $F_{2,32}$ = 5.84, P <0.001). The mean hydrodynamic diameter of the dispersion (196.33 ± 4.92 nm) also increased after 24h ($F_{2,8}$ = 57.75, P <0.001).
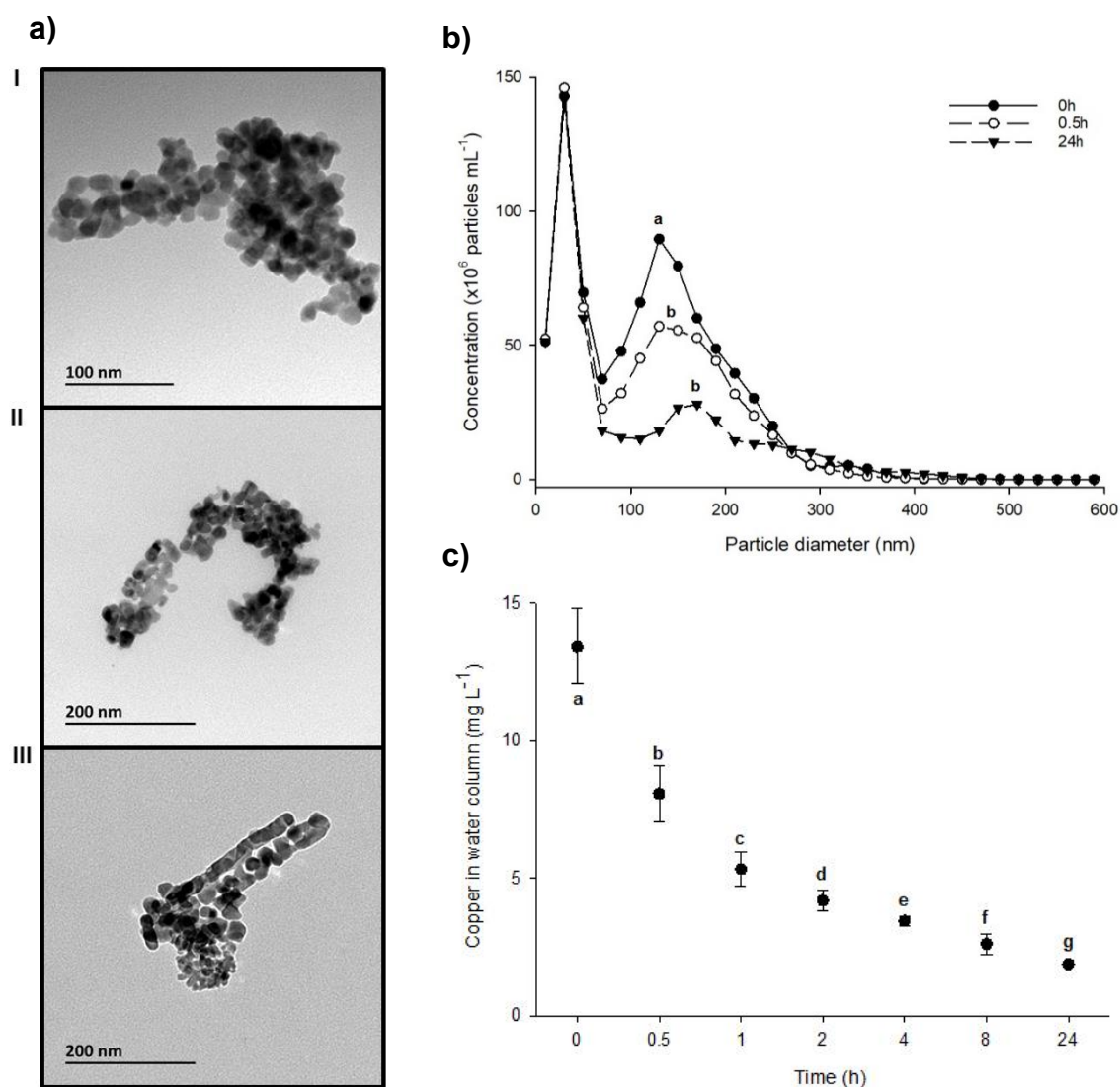
Figure 4-1 – Characterization of copper oxide nanomaterials (CuO ENMs) in the water column of freshwater; (**a**) Transmission electronic microscope (TEM) images of CuO ENMs in ultrapure water (t = 0 h, I), or freshwater water (t = 0 h, II, and 24 h, III); (**b**) Particle size distribution measurements of CuO ENMs obtained by Nanoparticle tracking analysis (NTA, Nanosight LM10) in freshwater. Values represent mean ± S.D. (n = 3 replicates of dispersion). Data points with different lower-case letters are significantly different (Holm-Sidak test, $P < 0.01$). (**c**) Total copper concentration in the water column of freshwater for CuO ENMs. Values are mean ± S.D. (n = 3). Data points with distinct lower-case letters are significantly different (Holm-Sidak test, *$P < 0.05$*).

The particle settling was confirmed by measuring the total Cu concentration in the water column from the CuO ENMs suspensions over 24h (**c**). The measured total Cu concentration showed an exponential decay, decreasing from 13.43 ± 1.12 mg L^{-1} to 1.87 ± 0.09 mg L^{-1} after 24 h (**Figure 4-1c;** $F_{2,29} = 52.53, P <0.001$). However, the settling in freshwater was instantaneous, and even at 0 h (within a few minutes of mixing) only 54% of the nominal exposure concentration was retained in the water column itself.

A dialysis experiment was also conducted to explore the dissolution of dissolved Cu from the particles (**Figure 4-2**). The CuSO$_4$ showed a hyperbolic rise to equilibrium in the beaker as expected, and the 29.5 mg of Cu as CuSO$_4$ added, reaching a plateau within two h and a steady-state concentration of 27.58 ± 1.85 mg Cu L^{-1} – equivalent to 434.02 ± 29.11 µmoles L^{-1} – for CuSO$_4$ treatment after 24 h (**Figure 4-2a**), which represents a 28% of the Cu remaining as a diffused phase in the water column. The release of dissolved Cu from CuO ENMs was even lower with only 107.15 ± 8.17 µg L^{-1} of Cu from CuO ENMs in the beaker by 24 h (**Figure 4-2**). This represents <0.01% dissolution of the Cu metal in freshwater from the particles in 24 h. A maximum dissolution rate of 57 µg h^{-1} was attained in the first 30 minutes.
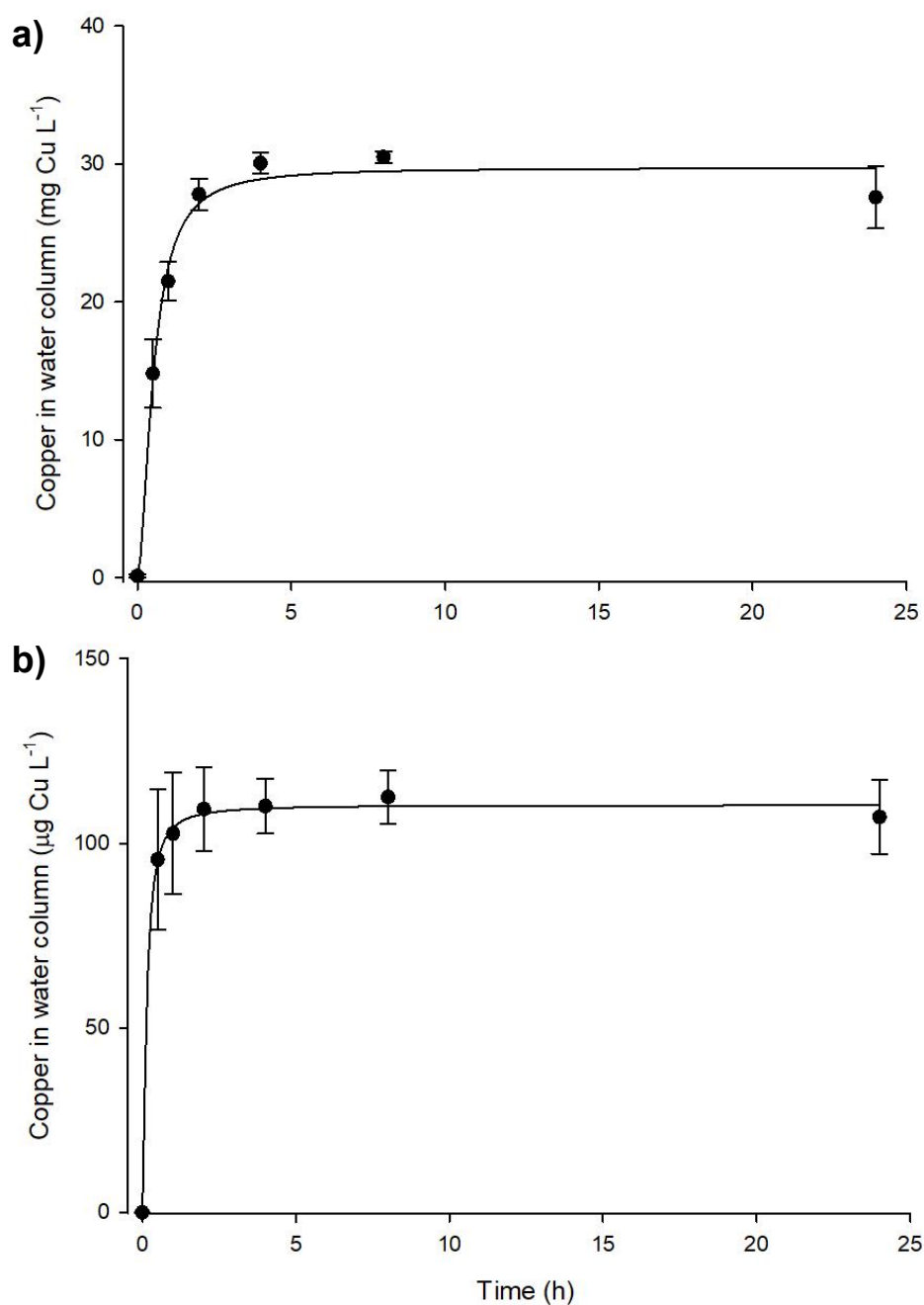
Figure 4-2 – Total copper concentration measured in the water column during equilibrium dialysis over 24 h; (**a**) CuSO₄ and, (**b**) CuO ENMs. Values are mean ± S.D. ($n = 3$ independent replicates). Curves were fitted using a rectangular hyperbola function in SigmaPlot. CuSO₄ ($r^2 = 0.974$), $y = \left(\frac{29.7x^{1.75}}{(0.52^{1.75})+x^{1.75}}\right)$ and CuO ENMs ($r^2 = 0.936$), $y = \left(\frac{110.4x^{1.4}}{(0.14^{1.4})+x^{1.4}}\right)$.

4.5.2 **Lethal effects**

The lethal concentration range finding test identified both the 96 h-LC_{50} (mean ± 95% CI) for $CuSO_4$ (303.09 ± 14.44 µg Cu L^{-1}) and CuO ENMs (53.11 ± 9.86 mg L^{-1}), where the ENMs were orders of magnitude less toxic than the metal salt (**Figure 6-III** and **Table 6-X**, **Appendix D)**. Additional, sub-lethal endpoints were measured in the lethal concentration test regarding hatching success, "perivitelline fluid morphology" and the presence of ENMs sticking to the surface of the chorion (**Figure 4-4**). The $CuSO_4$-exposed embryos exhibited a negative correlation between hatching success and "perivitelline fluid morphology" (Pearson coefficient = -0.773, *P* <0.0001) (**Figure 4-3a** and **b**); that is, embryos that did not have a clear and healthy perivitelline fluid also tended not to hatch (**Figure 4-3d**). The embryos exposed to CuO ENMs also showed a strong negative correlation between hatching success and the surface coating of chorion with particulates (Pearson coefficient = -0.804, *P* <0.0001) (i.e. embryos with chorion visually surrounded with ENMs tended not to hatch, **Figure 4-4d**). At CuO ENM concentrations ≥ 50 mg L^{-1} there was a 100% incidence of embryos with particles coating the surface, and negligible hatching success **(Figure 4-4d).** The effective concentration (EC) values were calculated for these endpoints (**Table 6-X**, **Appendix D**): the 96h-EC_{50} of the proportions of embryos showing increased "perivitelline fluid morphology" was 220.58 ± 5.23 µg Cu L^{-1} ($CuSO_4$) and the 96h-EC_{50} for the proportion of embryos with a surface coated chorion was 6.05 ± 1 mg L^{-1} (CuO ENMs). Considering hatching inhibition, for both Cu forms the 96h-EC_{50} was 68.5 ± 18.6 µg Cu L^{-1} ($CuSO_4$) and 0.92 ± 1.46 mg L^{-1} (CuO ENMs). The 96h-LC_{10} values (**Table 6-X**, **Appendix D**) for $CuSO_4$ (197.7 ± 120.03 µg Cu L^{-1}) and CuO ENMs (20.76 ± 33.51 mg L^{-1}) were also identified in the ranging lethal concentration finding test and these values were then used for the main sub-lethal exposure experiments.

a)

c)

control

b)

d)

300 µg Cu L^{-1}
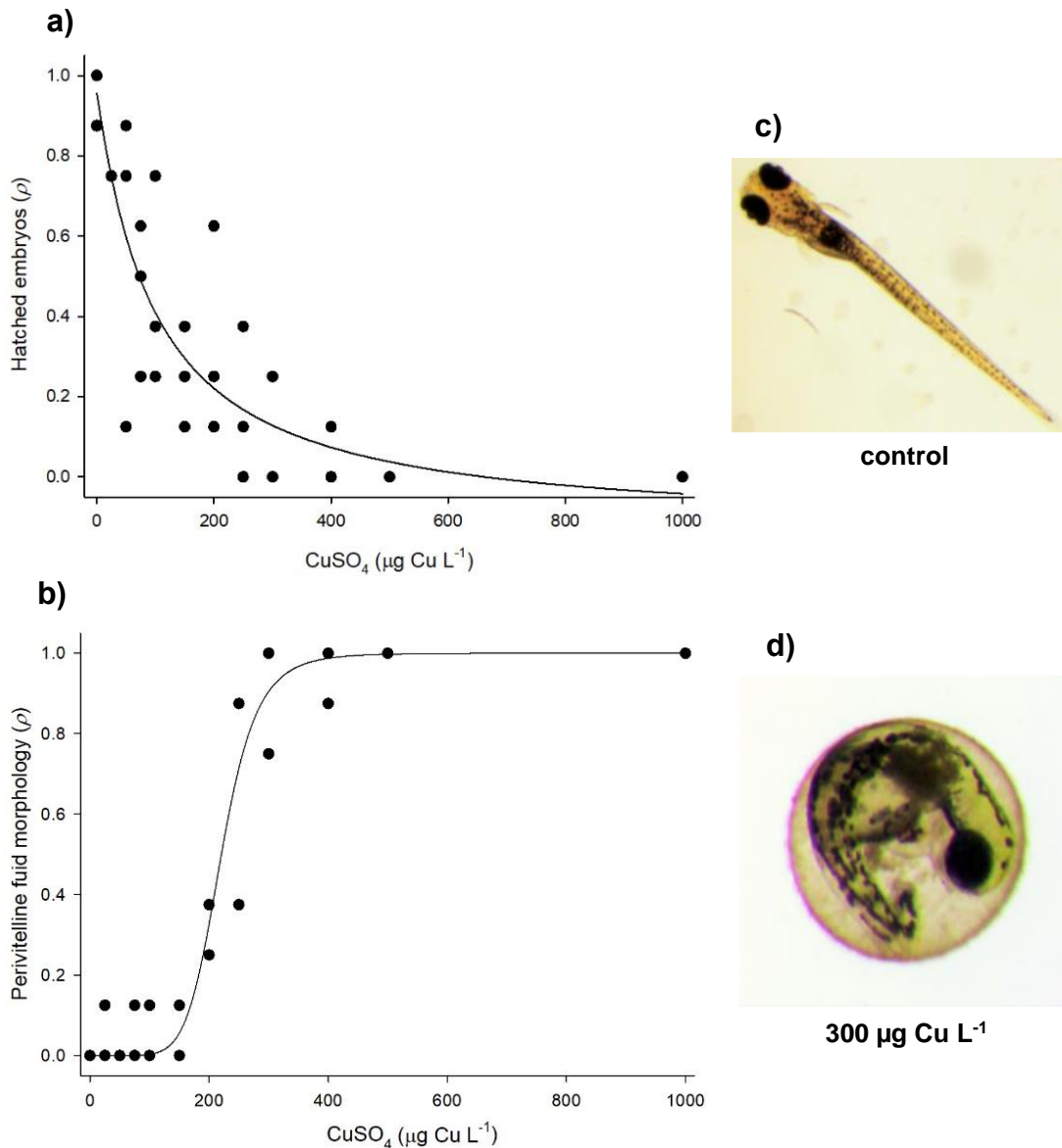
Figure 4-3 – Effects of CuSO$_4$ on zebrafish embryos resulting from lethal exposures over 96 hpf. Curves in panels (**a**) and (**b**) are embryos ($n = 24$) represented as independent replicates. Hatching success refers the proportion (ρ) of embryos that successfully hatched in CuSO$_4$ (filled circles). Curves were fitted using Sigmaplot and were based on the sigmoidal functions of CuSO$_4$ ($r^2 = 0.774$), $y = \left(\frac{(-0.13 + (0.96 + 0.13)) * (98.86^{1.05})}{(0.64^{1.05}) + x^{1.05}} \right)$. "Perivitelline fluid morphology" indicates the proportion (ρ) of embryos with a perivitelline fluid with bubbles and a foam-looking, unlike the control in the CuSO$_4$ treatment. Curves were based on sigmoidal functions of CuSO$_4$ ($r^2 = 0.956$), $y = \left(\frac{x^{7.3}}{(220.6^{7.3}) + x^{7.3}} \right)$. Images in panels (c) and (d) show the typical morphology, from the CuSO$_4$ (300 µg Cu L^{-1}) treatments, on 96hpf old zebrafish embryos or larvae against the control.

a)

b)

c)

control

d)

50 mg L⁻¹
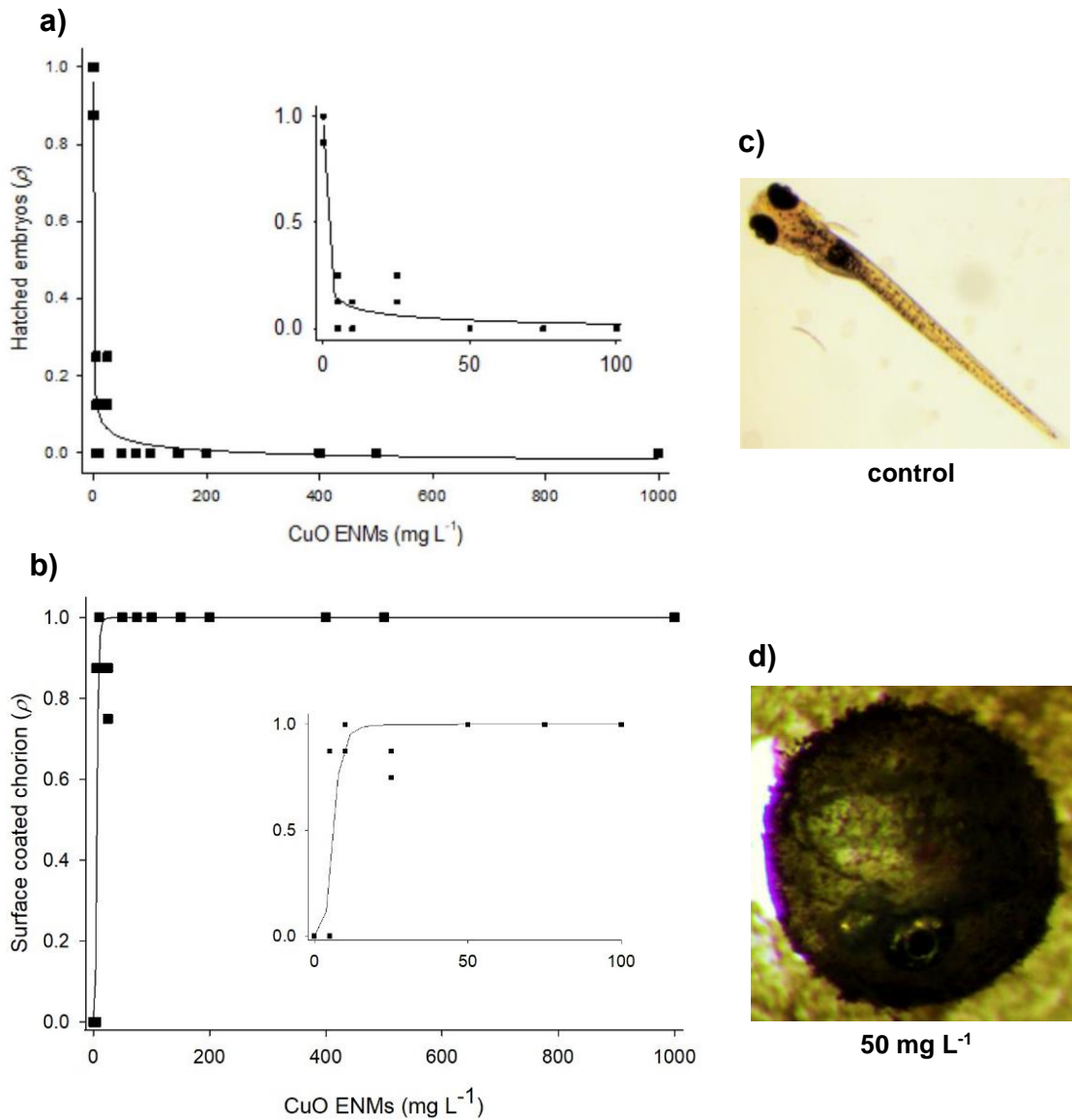
Figure 4-4 – Effects of CuO ENMs on zebrafish embryos resulting from lethal exposures over 96 hpf. Curves in panels (**a**) and (**b**) are embryos ($n = 24$) represented as independent replicates. Hatching success refers the proportion (ρ) of embryos that successfully hatched in CuO ENMs (filled squares). Curves were fitted using Sigmaplot and were based on the sigmoidal functions of CuO ENMs (r²= 0,958), $y = \left(\frac{(-0.045+(0.96+0.045))*(0.095^{0.38})}{(0.095^{0.38})+x^{0.38}} \right)$. "Surface coated chorion" indicates the proportion (ρ) of embryos with the chorion visually covered with adsorbed particulate materials (the ENMs). Curve was based on sigmoidal functions of CuO ENMs (r²= 0.853), $y = \left(\frac{x^{4.61}}{(6.05^{4.6})+x^{4.6}} \right)$. Images in panels (c) and (d) show the typical morphology, from the CuO ENMs (50 mg L⁻¹) treatments, on 96hpf old zebrafish embryos or larvae against the control.

4.5.3 **Metal distribution in zebrafish embryos during sub-lethal exposure**

The sub-lethal exposure to either $CuSO_4$ or CuO ENMs was confirmed by measuring the total Cu concentrations in the media (**Figure 4-5**) and in the embryos (**Figure 4-6**). For the exposure media, the total Cu concentration from $CuSO_4$ was reasonably close to nominal concentration ($t = -5.77$, $H=10$, $P <0.001$). The CuO ENMs suspensions (**Figure 4-5b**), as expected, showed some particle settling with the measured Cu concentration in the water column decreasing 7-fold to 1.77 mg L^{-1} by the end of the experiment ($t=44.11$, $H=10$, $P <0.001$). Nonetheless, the embryos were exposed to mg L^{-1} dose of CuO ENMs. The total Cu in the embryos reflected the exposures (**Figure 4-6**). For $CuSO_4$, the chorion was not a barrier to the dissolved metal and Cu was readily measured in both chorionated and de-chorionated embryos, where 42.2% of copper was associated to the inner embryo and perivitelline space and 57.8% of copper was associated to the chorion (**Figure 4-6a,** 2-fold difference). Regarding the exposure to CuO ENMs, the whole-body Cu mass in chorionated embryos was higher than in the de-chorionated ones (17-fold difference; $F_{2,33} = 83.37$, $P <0.001$), indicating that most of the total copper measured was retained on the chorion (94.2%, **Figure 4-6b**), not in, the embryo. Nonetheless, a few hundred ng of Cu were measured in the de-chorionated embryos (5.8% of copper), confirming that the embryos were effectively exposed.
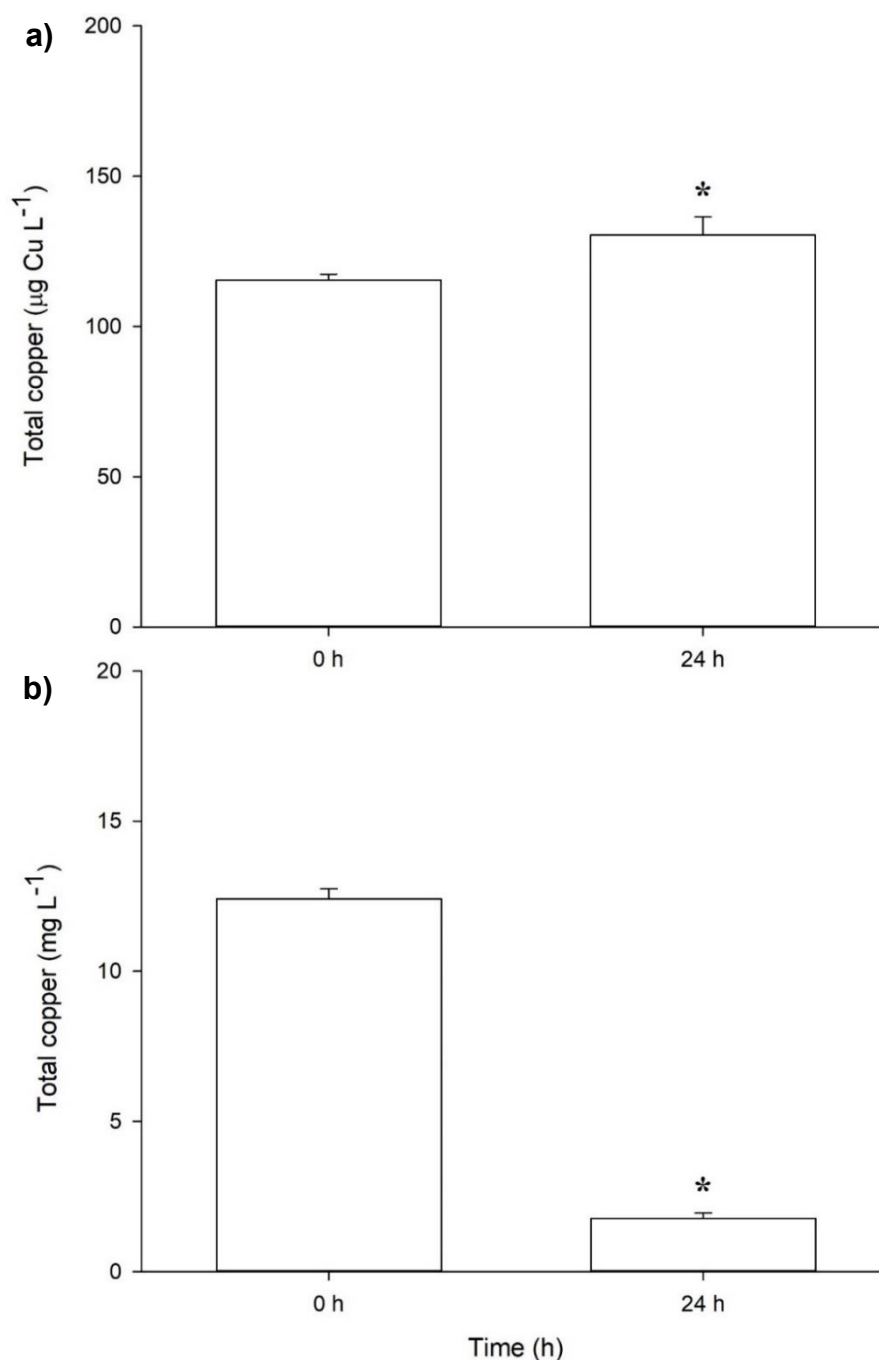
Figure 4-5 – Total copper (Cu) concentrations in the freshwater during sub-lethal exposure of zebrafish to nominal concentrations of, (a) 190 µg Cu L^{-1} presented as CuSO$_4$, or (b) as 20 mg L^{-1} of CuO ENMs. Data for the water from the controls are not shown (values all below the detection limit, < 1.82 µg L^{-1}). Values are mean ± S.D. ($n=$ 6). Bars with asterisks are significantly different (t-test, $P < 0.001$).
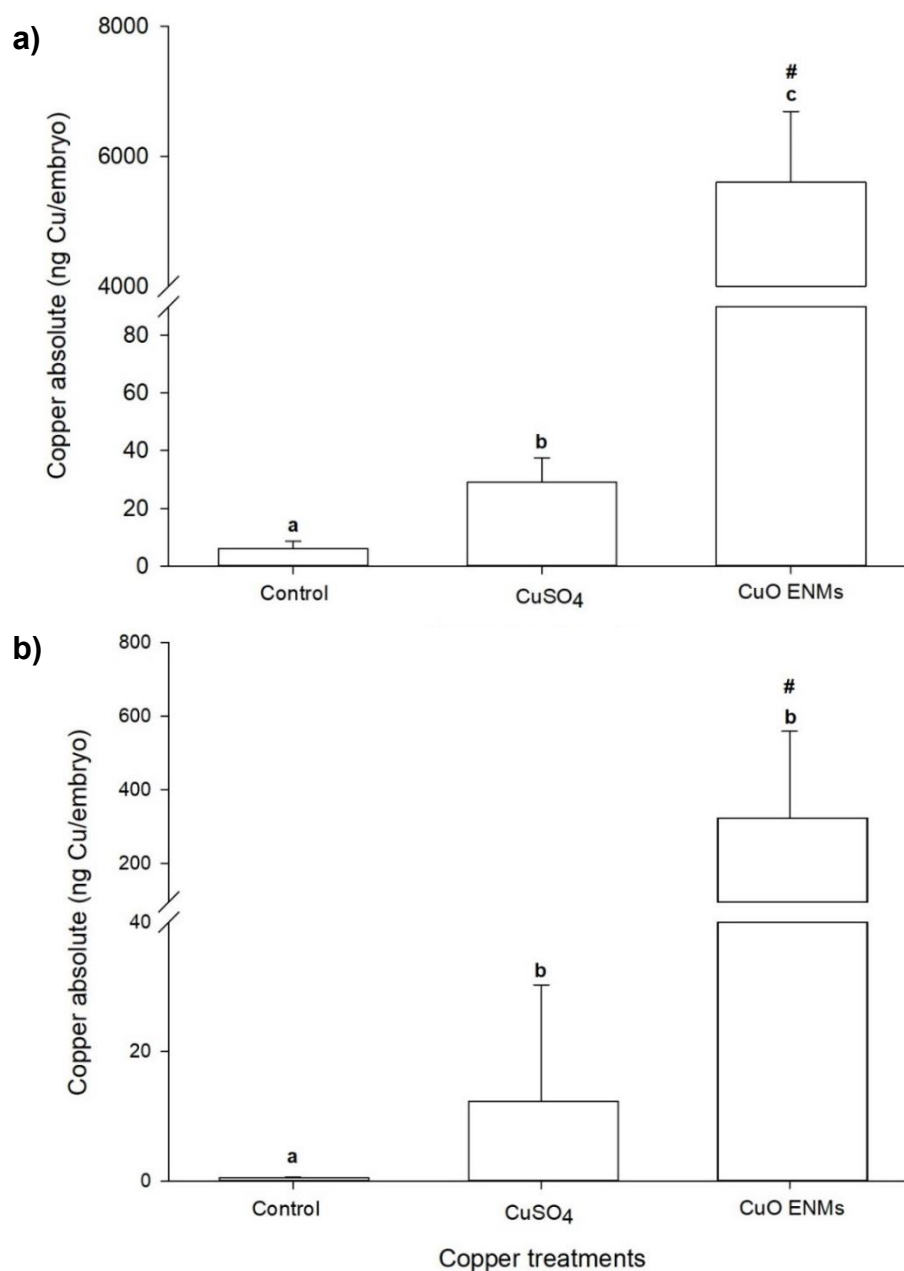
Figure 4-6 – Total absolute mass of copper (ng per embryo) in, (**a**) chorionated, and (**b**) de-chorionated zebrafish embryos exposed to the respective nominal 96 h-LC$_{10}$ (CuSO$_4$ = 190 µg Cu L^{-1} and CuO ENMs = 20 mg L^{-1}). Values are means ± S.D. (n = 3 – 9 independent samples of embryos). Bars with different lower-case letters and cardinal symbol (#) are significantly different within and/or between chorionated and de-chorionated embryos, respectively (one-way ANOVA, Holm-Sidak test, *P < 0.01*).

4.5.4 Osmoregulation and oxidative stress during sub-lethal exposures

Copper sulphate ($CuSO_4$) is known to interfere with ion homeostasis and the de-chorionated embryos showed evidence of depletion of Ca^{2+} ($F_{2,13} = 32.22, P <0.001$) and Na^+ ($F_{2,13} = 8.47, P =0.006$), but not Mg^{2+} (**Table 4-1**). This occurred with inhibition of the total Na^+/K^+-ATPase (**Figure 4-7a**; $F_{2,12} = 4.66, P =0.037$). A similar depletion of Ca^{2+} and Na^+ was observed in the CuO ENMs exposure (**Table 4-1**), but unlike $CuSO_4$, CuO ENMs did not inhibit the Na^+/K^+-ATPase (**Figure 4-7 a**). Embryos also showed evidence of oxidative stress, with depletion of tGSH in embryos exposed to either $CuSO_4$ or CuO ENMs (**Figure 4-7b**; $F_{2,16} = 38.26, P <0.001$). However, this trend was not accompanied by an increase SOD activity which remained unchanged in all treatments (**Figure 4-7c**; $F_{2,16} = 2.87, P =0.09$).

Table 4-1– Total electrolyte concentrations in de-chorionated zebrafish embryos following 96 h exposure to a sub-lethal (LC_{10}) concentration of either $CuSO_4$ or CuO ENMs.

Electrolyte (ng per embryo)	Control ($n = 3$)	$CuSO_4$ ($n = 7$)	CuO ENMs ($n = 4$)
Calcium (Ca^{2+})	210.8 ± 22.7 [a]	100.7 ± 21.8 [b]	98.7 ± 4.3 [b]
Magnesium (Mg^{2+})	133.5 ± 21.08 [a]	102.3 ± 23.6 [a]	101.08 ± 27.4 [a]
Sodium (Na^+)	256.02 ± 44.8 [a]	149.5 ± 44.4 [b]	122.7 ± 31.1 [b]

Values are means ± standard deviation (n = replicate samples of embryos). Different lower-case letters are significantly different within rows (one-way ANOVA; *Holm-Sidak test, P <0.05*).
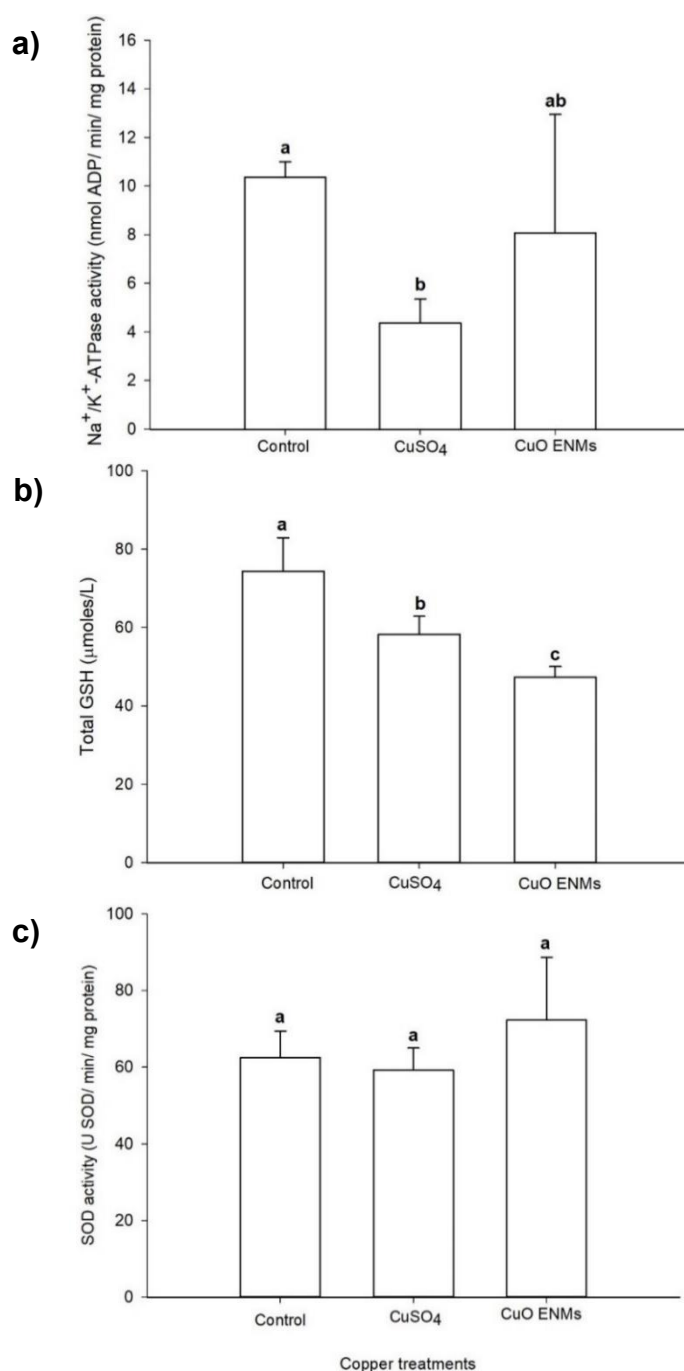
Figure 4-7 – Biochemical responses of de-chorionated zebrafish embryos exposed to the respective nominal 96 h LC_{10} of $CuSO_4$ (190 µg Cu L^{-1}) or CuO ENMs (20 mg L^{-1}); (a) sodium pump (Na^+/K^+-ATPase) activity, (b) total glutathione (Total GSH) levels, and (c) superoxide dismutase (SOD) activity. Values are mean ± S.D. ($n = 3 − 6$ independent samples of embryos). Bars with different lower-case letters are significantly different (one-way ANOVA, Holm-Sidak test, $P < 0.05$).

4.6 **Discussion**

This study shows that $CuSO_4$ is much more toxic to zebrafish embryos than CuO ENMs, and for the metal salt, the increase in the proportion of embryos with bubbles and foam-looking perivitelline fluid was associated with poor hatching success. In the case of the acute CuO ENM exposures, the chorion became smothered in particulate material, and this was associated with failure to hatch during the acute toxicity study. In the sub-lethal exposure, the chorion, as expected, was not a barrier to the accumulation of Cu from $CuSO_4$ inside the embryo. In contrast, for the CuO ENM exposure, a large proportion of the total Cu was associated with the chorion, although some total Cu (form unknown) was internalised resulting in exposure of the embryos. In terms of the mechanisms of sub-lethal toxicity, both $CuSO_4$ or CuO ENMs caused electrolyte depletion of the embryos, and $CuSO_4$ caused some inhibition of the Na^+ pump activity. Both forms of Cu exposure caused some deletion of total GSH in the embryos, but this oxidative stress was not sufficient to induce superoxide dismutase activity.

4.6.1 **Acute toxicity of $CuSO_4$ compared to CuO ENMs (Lethal exposure)**

In the present study, the 48 h LC_{50} for the zebrafish early life stage with $CuSO_4$ was around 0.3 mg L^{-1} compared to 52 mg L^{-1} for CuO ENMs (**Table 6-X**, **Appendix D**); with the nanomaterial being at least two orders of magnitude less toxic than the metal salt. The lethal concentration values report here for $CuSO_4$ (**Table 6-X**, **Appendix D**) are broadly in keeping with previous reports on Cu salts. For example, Griffitt et al. (2008) reported a 48 h LC_{50} for $CuCl_2$ of 1.78 mg L^{-1} in moderately hard water. Freiry et al. (2014) reported a 48 h LC_{50} for $CuSO_4$ of around 0.3 mg L^{-1} in 10-day old zebrafish. Studies on CuO ENMs with zebrafish early life stages have also shown that the nanomaterial form is toxic at tens of mg L^{-1} or more, and therefore, much less hazardous than the metal salt. For example, the 48 hpf LC_{50} value for zebrafish was about 64 mg L^{-1} for CuO ENMs with a primary particle diameter of about 60 nm (Ganesan et al., 2016). Similarly, Vicario-Pares et al. (2014) reported LC_{50} estimates of > 10 mg L^{-1} for early life stages of zebrafish exposed to CuO ENMs. Contrary to these reports on CuO ENMs, (Griffitt et al.,

2008) reported a 48 h LC_{50} of 0.71 mg L^{-1} for a Cu metal ENMs, which was 2.5 times more toxic than the metal salt control. So, clearly the composition of the ENM is important and the metal oxide is a less hazardous nano form. Interestingly, (Thit et al., 2017) found that zebrafish embryos exposed to equimolar concentrations of Cu as $CuCl_2$ or very small CuO ENMs (6 nm primary size) showed similar toxicities over 24 h; but the hatch larvae showed differential sensitivity with the metal salt being much more toxic at concentrations of 50 µMol L^{-1} or more. Shaw et al. (2016) reported that the hatched larvae are more sensitive to a range of ENMs that the embryos in the fish early life stage test. So, qualifying when the embryos hatch in a study will be important to the interpretation of the cumulative toxicity over time, and to understanding the Cu exposure of the fish inside the embryo (see below). Notably, in the present study, regardless of the form of Cu exposure, the LC_{50} estimates at 48, 72 and 96 hpf within each substance were very similar **(Figure 6-III** and **Table 6-X**, **Appendix D**) indicating that most of the toxicity occurred in the first 48 hpf of the exposure (i.e., before hatching).

4.6.2 Hatching success in the lethal exposure

The hatching success of fish embryos typically depends on the anatomical maturity of the fish and their ability to endure the energetic demands of hatching, as well as the integrity of the perivitelline fluid and chorion. Unfortunately, the bubbles and foam-looking nature of the perivitelline fluid ($CuSO_4$ exposures), or the particulate coating on the embryos (CuO ENM exposures), prevented any useful morphometric measurements on the fish inside the embryos. However, it was clear that failure to hatch in the $CuSO_4$ treated was partly correlated with the proportion of embryos with a dense-looking perivitelline fluid (**Figure 4-3a**). Perivitelline fluid consists of electrolytes trapped in a polyanionic matric of mucoproteins (Eddy and Handy, 2012). Mucoproteins have an affinity for Cu ions (Miller and Mackay, 1982), and it is, therefore, no surprise that some total Cu from $CuSO_4$ appeared in the embryos (**Figure 4-6**); but occurred with some denaturing of the the perivitelline fluid (observed as bubbles and foam-looking embryos, **Figure 4-3**). The latter effect on the perivitelline fluid could arise from some oxidative stress during the $CuSO_4$

exposure (**Figure 4-7**). It was not the purpose of the current study to determine the mechanism of failure to hatch with $CuSO_4$, but for example, impaired oxygen diffusion to the fish inside the embryo (Pelster and Bagatto, 2010), and/or increased viscosity of the perivitelline fluid might impede the physiological ability (i.e., exercise performance) of the fish to breach through the chorion. Another factor for hatching is the action of the proteolytic enzyme ZHE_1 that is released in the perivitelline space to weaken the chorion, but it can be inhibited by Cu^{2+} (Muller et al., 2015). Regardless of the mechanism, in the present study, $CuSO_4$ inhibited hatching (**EC$_{50}$** = 68.5 µg Cu L^{-1}) at a similar dose to that reported previously with zebrafish embryos [**EC$_{50}$** = 60 µg Cu L^{-1} Bai et al. (2010)].

Embryos exposed to CuO ENMs exhibited a particulate surface coating over the chorion and this was correlated with the failure to hatch (**Figure 4-4d** and **b**). In addition to the mechanisms above for $CuSO_4$ and any local release of Cu ions from CuO ENMs, the smothering of the chorion could impede gas exchange and/or the elimination of nitrogen waste, increasing toxicity within the perivitelline fluid. Previous studies showed hatching inhibition by mg L^{-1} amounts CuO ENMs (Ganesan et al., 2016; Kumari et al., 2017; Muller et al., 2015) or Cu ENMs (Bai et al., 2010); consistent with the present study and at much higher concentrations than $CuSO_4$. In the present study, $CuSO_4$ inhibited hatching (**EC$_{50}$** = 0.34 ± 0.781 mg L^{-1}). In zebrafish embryos exposed to ZnO ENMs, loss of the protease activity needed to weaken the chorion also explained inability to hatch, but notably, if the embryos were manually de-chorionated, the fish survived (Ong et al., 2014).

4.6.3 Sub-lethal exposure and total Cu accumulation

Exposure to Cu was confirmed in the sub-lethal experiment by measuring the total Cu concentrations in the freshwater (**Figure 4-5**) and in the zebrafish (**Figure 4-6**). In $CuSO_4$, the initial total Cu concentration measured in the test vessels was around 120 µg L^{-1} and 39% lower than the nominal concentration of 190 µg Cu L^{-1}. This to be expected as microgram amounts of Cu can be instantly adsorbed to the walls of the test containers, the surface of the organism and chelated by mucous secretions. Indeed, an OECD validation study of the zebrafish test also reported measured

concentrations of Cu as $CuSO_4$ in the media that were some 37% lower than the nominal exposure concentration (Busquet et al., 2014). Nonetheless, despite these initial losses, the concentration of Cu was stable in the exposure solution over 24h (the duration to the next water change) and the presence of Cu in the water column was confirmed (**Figure 4-5a**). The calculated Cu speciation (Visual MINTEQ version 3.1 https://vminteq.lwr.kth.se/) was: Cu^{2+}, 60.80%; $CuOH^+$, 33.93%; $Cu(OH)_2$ (aq), 1.35%; $Cu_2(OH)_2^{2+}$, 2.55%; $Cu_3(OH)_4^{2+}$, 0.11%; $CuCl^+$, 0.30%; $CuSO_4$ (aq), 0.94%. Thus, as expected about two thirds were as dissolved Cu^{2+} and the remained mostly as copper hydroxide complexes. The calculated free Cu^{2+} ion activity was 1.35 µmol L^{-1} (or 86 µg L^{-1}) and consistent with the exposure. For the CuO ENMs, the initial Cu concentration in the exposure suspension was 28% lower than the nominal concentration (20 mg L^{-1}) and then dropped by 86% over 24h, so that only a few mg L^{-1} of total Cu remained in the water column (**Figure 4-5b**). This was attributed to particle settling from the water column due to aggregation (**Figure 4-1**). Similar observations were made by Boyle et al. (2020), where particle settling of the CuO ENMs in the media removed most of the total Cu from the water column. While particle settling due to the ionic strength and composition of the media is unavoidable in semi-static exposure methods (without adding dispersing agents, mixing, etc. (Handy et al., 2012)), there was, nonetheless, a few mg L^{-1} of Cu as CuO ENMs remaining at the end of every 24 h (**Figure 4-5b**), and renewal of the test media helped to ensure the supply of CuO ENM was in excess throughout the exposure. Crucially, any CuO ENM settling from the water column would inevitably come into direct contact with the embryos in the bottom of the test vessels. Additionally, equilibrium dialysis data showed that the total Cu concentration outside the bag were as expected for $CuSO_4$, with 29.5 mg of total Cu added to the bag diffusing to the external compartment. For CuO EMNs, with 7.5 mg of material added to the dialysis bag, only µg L^{-1} concentrations of Cu were released by dissolution, suggesting the CuO ENMs are very sparingly soluble and remained in the particulate form during the experiments.

The measured total Cu concentrations in the embryos also confirmed the exposure (**Figure 4-6**). The intact (chorionated) embryos from both forms of Cu exposure showed significantly higher Cu concentrations than the unexposed controls. The Cu

concentration on/in the intact embryos was much higher from the CuO ENM exposure than the $CuSO_4$ exposure in keeping with the different exposure concentrations (LC_{10} values) of the substances (**Figure 4-6a**). Notably, total Cu (form unknown) was taken up into the embryos in both the $CuSO_4$ and CuO ENM exposures (**Figure 4-6b**). For $CuSO_4$ exposures, about 42% of the total Cu associated with the embryos was internally located as measured in de-chorionated animals (i.e., around 58% of the total Cu on/associated with the chorion). Other studies on dissolved metals show around two thirds or slightly more of metal is on/associated with the chorion, for example, cadmium (61% in zebrafish (Burnison et al., 2006)), and silver (65-85% in rainbow trout (Guadagnolo et al., 2001)).

In contrast to $CuSO_4$, the de-chorionated embryos from the CuO ENMs exposure had only some 350 ng/embryo compared to around 6000 ng/embryo on/in the chorionated counterparts (**Figure 4-6**); indicating that most (~94%) of the Cu from the CuO ENMs exposure was located on the exterior of the animals and that the chorion was a reasonably effective barrier to prevent the internalisation of the nanomaterial, at least in the short term. That is, the CuO ENMs were bioaccessible to the exterior of the chorion, but not bioavailable to the animal inside the embryo. The pore canal diameter on the zebrafish chorion is about 0.7-0.9 μm (Chen et al., 2020), indicating that it would probably not stop the diffusion of any monodispersed primary particles (~60 nm), but with aggregates of 0.15-0.3 μm in freshwater (**Figure 4-1b**), only a few aggregates at the size would be needed to block the exterior surface of the pores. Notably, particulate material coated the surface of the chorion in the CuO ENM exposures (**Figure 4-4**), in keeping with this suggestion.

4.6.4 Osmoregulation and oxidative stress in sub-lethal exposure

The electrolyte concentrations in de-chorionated embryos showed some depletion of both total Ca^{2+} and Na^+ from animals during the Cu exposures compared to unexposed controls; but with no difference between the metal salt and CuO ENMs in this effect (**Table 4-1**). This is most likely explained by passive electrolyte losses from the altered (dense-looking, presumed denatured) perivitelline fluid during the exposures, and some ion exchange with any external Cu ions. For the latter, Cu^{2+}

is well-known for its competition with Na^+ and perhaps Ca^{2+} (Handy et al., 2002). Metals have been previously reported to cause Na^+ depletion in fish embryos by such mechanisms (e.g., acid (McWilliams and Shephard, 1991)). However, the Mg concentration was not depleted (**Table 4-1**), likely because the Mg^{2+} ion activity in freshwater fish embryos is normally close to the equilibrium potential with the surrounding water (see, van der Velden et al. (1991)), therefore, not so easily lost by diffusion. Previous studies, Alsop and Wood (2011) also reported stable total Mg^{2+} concentrations in fish exposed to dissolved Cu.

The perivitelline fluid is designed to buffer the fish from changes in the external environment, and so any electrolyte depletion might add a subsequent osmotic stress to the animal. Some direct interference with ionic regulation in the fish is probable in the case of $CuSO_4$, where inhibition of the Na^+/K^+-ATPase was observed (**Figure 4-7a**). Inhibition of the sodium pump during dissolved Cu exposure is well-known in fish (Handy et al., 2002), with consequent Na^+ depletion. Calcium losses might then arise indirectly from the subsequent disruption of secondary Na^+/Ca^{2+} exchange in the gills which relies ultimately on the Na^+ pump for energy (Bury and Handy, 2010), or simply by damage to the tissue (oxidative stress via glutathione depletion, **Figure 4-7b**). Significant losses of Ca^{2+} and Na^+ (to a larger extent) were also reported in zebrafish larvae exposed to 100 µg Cu L^{-1} (Alsop and Wood, 2011). Notably, the exposure to CuO ENMs causes slightly more tGSH depletion than that of $CuSO_4$ exposure (**Figure 4-7b**), and although the Na^+ pump activity was not statistically decreased for the CuO ENM treatment, there was some considerable variation in specific activity (**Figure 4-7a**), suggesting that sodium homeostasis was approaching a threshold for inhibition. Inhibition of Na^+/K^+-ATPase activity has been reported in fish exposed to Cu ENMs and CuO ENMs (Ganesan et al., 2016; Shaw et al., 2012; Wang et al., 2014).

The Cu-dependent inhibition of the Na^+/K^+-ATPase can have an ionic basis where Cu^{2+} binds to thiols on the tertiary structure of the enzyme and/or interferes with the Mg^{2+} binding site (Handy et al., 2002; Li et al., 1996). However, there is an indirect mechanism where the general oxidative stress in the tissue from Cu exposure can inhibit the Na^+ pump, and this is possible given some depletion of tGSH (**Figure 4-7b**). However, the apparent oxidative stress was only moderate because the tGSH

loss was partial (**Figure 4-7b**) and there was no induction of SOD activity in embryos exposed to CuSO$_4$ or CuO ENMs (**Figure 4-7c**). Notably, SOD activity has been reported to increase (Gupta et al., 2016) or decrease (Ganesan et al., 2016; Sun et al., 2016; Wang et al., 2015) in fish exposed to Cu ENMs or CuO ENMs; and the activation of the Cu-dependent SOD isoforms will depend on the internal free Cu ion concentrations in the organism, as well as the overall level of oxidative stress in the different internal organs used to make the homogenates for the enzymology in each study.

4.7 **Conclusions**

In conclusion, this study shows that CuSO$_4$ is much more toxic than CuO ENMs to zebrafish embryos in terms of both acute mortality and failure to hatch. From an ecological perspective, the existing environmental risk assessment for the metal salt should be protective of fish populations for the nano form. However, environmental fate should also be considered, and it is likely the settling of CuO ENMs from the water column would put any fish embryos in the river sediment at risk of exposure. Notably, there were some subtle differences in the exposure and mechanisms, with the CuO ENMs mostly on/associated with the chorion barrier. In the sub-lethal studies, both substances caused electrolyte depletion, but despite internalising some Cu (form unknown), the CuO ENM exposure did not inhibit the Na$^+$ pump, unlike the metal salt. However, some secondary oxidative damage to the osmoregulatory machinery from the CuO ENMs could not be exclude. Finally, from an animal welfare perspective it is desirable to find alternatives to mortality as an endpoint, and here the EC$_{50}$ values for the inhibition of hatching were more sensitive than mortality. Notably, the EC$_{50}$ values for the proportions of embryos with foam-looking perivitelline fluid (CuSO$_4$) or with a particulate coated chorion (CuO ENMs) were also more sensitive than mortality; suggesting morphology as an alternative to mortality and perhaps an opportunity to shorten the fish early life stage test.

4.8 **Acknowledgements**

4.9 **References**

Al-Bairuty, G. A., et al., 2016. Sublethal effects of copper sulphate compared to copper nanoparticles in rainbow trout (*Oncorhynchus mykiss*) at low pH: physiology and metal accumulation. Aquat Toxicol. 174, 188-198. https://doi.org/10.1016/j.aquatox.2016.02.006

Alsop, D., Wood, C. M., 2011. Metal uptake and acute toxicity in zebrafish: common mechanisms across multiple metals. Aquat Toxicol. 105, 385-393. https://doi.org/10.1016/j.aquatox.2011.07.010

Amde, M., et al., 2017. Transformation and bioavailability of metal oxide nanoparticles in aquatic and terrestrial environments. A review. Environ Pollut 230, 250-267. https://doi.org/10.1016/j.envpol.2017.06.064

Bai, W., et al., 2010. Effects of copper nanoparticles on the development of zebrafish embryos. J Nanosci Nanotechnol 10, 8670-8676. https://doi.org/10.1166/jnn.2010.2686

Baker, M. A., et al., 1990. Microtiter plate assay for the measurement of glutathione and glutathione disulfide in large numbers of biological samples. Anal Biochem. 190, 360-365. https://doi.org/10.1016/0003-2697(90)90208-q

Boyle, D., et al., 2020. Toxicities of copper oxide nanomaterial and copper sulphate in early life stage zebrafish: Effects of pH and intermittent pulse exposure. Ecotoxicol Environ Saf. 190, 109985. https://doi.org/10.1016/j.ecoenv.2019.109985

Burnison, B. K., et al., 2006. Cadmium accumulation in zebrafish (*Danio rerio*) eggs is modulated by dissolved organic matter (DOM). Aquat Toxicol. 79, 185-191. https://doi.org/10.1016/j.aquatox.2006.06.010

Bury, N. C., Handy, R. D., 2010. Copper and iron uptake in teleost fish, in: N. C. Bury, R. D. Handy (Eds.), Surface Chemistry, Bioavailability and Metal Homeostasis in Aquatic Organisms: An integrated approach. Society for Experimental Biology Press, London, pp. 107-127

Busquet, F., et al., 2014. OECD validation study to assess intra- and inter-laboratory reproducibility of the zebrafish embryo toxicity test for acute aquatic toxicity testing. Regul Toxicol Pharmacol. 69, 496-511. https://doi.org/10.1016/j.yrtph.2014.05.018

Chen, Z. Y., et al., 2020. The effect of the chorion on size-dependent acute toxicity and underlying mechanisms of amine-modified silver nanoparticles in zebrafish embryos. Int J Mol Sci. 21, 2864. https://doi.org/10.3390/ijms21082864

Eddy, F. B., Handy, R. D., 2012. Ecological and Environmental Physiology of Fishes, first ed. Oxford University Press, Oxford. https://doi.org/10.1093/acprof:oso/9780199540945.001.0001

Eyckmans, M., et al., 2011. Exposure to waterborne copper reveals differences in oxidative stress response in three freshwater fish species. Aquat Toxicol. 103, 112-120. https://doi.org/10.1016/j.aquatox.2011.02.010

Freiry, R., et al., 2014. Sensitivity of *Danio rerio* (Teleostei, Cyprinidae) during two stages of development based on acute toxicity tests. Bull Environ Contam Toxicol. 93, 442-5. https://doi.org/10.1007/s00128-014-1367-6

Ganesan, S., et al., 2016. Acute and sub-lethal exposure to copper oxide nanoparticles causes oxidative stress and teratogenicity in zebrafish embryos. J Appl Toxicol. 36, 554-567. https://doi.org/10.1002/jat.3224

Griffitt, R. J., et al., 2008. Effects of particle composition and species on toxicity of metallic nanomaterials in aquatic organisms. Environ Toxicol Chem. 27, 1972-1978. https://doi.org/10.1897/08-002.1

Griffitt, R. J., et al., 2007. Exposure to copper nanoparticles causes gill injury and acute lethality in zebrafish (*Danio rerio*). Environ Sci Technol. 41, 8178-8186. https://doi.org/10.1021/es071235e

Grosell, M., 2011. Copper, in: C. M. Wood, et al. (Eds.), Homeostasis and Toxicology of Essential Metals. Academic Press, San Diego, pp. 53-133. https://doi.org/10.1016/s1546-5098(11)31002-3

Grosell, M., et al., 2002. Sodium turnover rate determines sensitivity to acute copper and silver exposure in freshwater animals. Comp Biochem Physiol C Toxicol Pharmacol. 133, 287-303. https://doi.org/10.1016/S1532-0456(02)00085-6

Guadagnolo, C. M., et al., 2001. Chronic effects of silver exposure on ion levels, survival, and silver distribution within developing rainbow trout (*Oncorhynchus mykiss*) embryos. Environ Toxicol Chem. 20, 553-560.

https://doi.org/10.1002/etc.5620200314

Gupta, Y. R., et al., 2016. Effect of copper nanoparticles exposure in the physiology of the common carp (*Cyprinus carpio*): Biochemical, histological and proteomic approaches. Aquaculture and Fisheries. 1, 15-23. https://doi.org/10.1016/j.aaf.2016.09.003

Handy, R. D., 2003. Chronic effects of copper exposure versus endocrine toxicity: two sides of the same toxicological process? Comp Biochem Physiol A 135, 25-38. https://doi.org/10.1016/s1095-6433(03)00018-7

Handy, R. D., et al., 2012. Ecotoxicity test methods for engineered nanomaterials: practical experiences and recommendations from the bench. Environ Toxicol Chem. 31, 15-31. https://doi.org/10.1002/etc.706

Handy, R. D., et al., 2002. Sodium-dependent copper uptake across epithelia: a review of rationale with experimental evidence from gill and intestine. Biochim Biophys Acta. 1566, 104-115. https://doi.org/10.1016/s0005-2736(02)00590-4

Hoyle, I., et al., 2007. Dietary copper exposure in the African walking catfish, *Clarias gariepinus*: transient osmoregulatory disturbances and oxidative stress. Aquat Toxicol. 83, 62-72. https://doi.org/10.1016/j.aquatox.2007.03.014

Johnson, A., et al., 2007. The effects of copper on the morphological and functional development of zebrafish embryos. Aquat Toxicol. 84, 431-438. https://doi.org/10.1016/j.aquatox.2007.07.003

Keller, A. A., et al., 2013. Global life cycle releases of engineered nanomaterials. J Nanopart Res. 15, 1692. https://doi.org/10.1007/s11051-013-1692-4

Kumari, P., et al., 2017. Mechanistic insight to ROS and apoptosis regulated cytotoxicity inferred by green synthesized CuO nanoparticles from *Calotropis gigantea* to embryonic zebrafish. Sci Rep. 7, 16284. https://doi.org/10.1038/s41598-017-16581-1

Lead, J. R., et al., 2018. Nanomaterials in the environment: Behavior, fate, bioavailability, and effects-An updated review. Environ Toxicol Chem. 37, 2029-2063. https://doi.org/10.1002/etc.4147

Li, J., et al., 1996. Kinetics of Cu^{2+} inhibition of Na^+/K($^+$)-ATPase. Toxicol Lett. 87, 31-38. https://doi.org/10.1016/0378-4274(96)03696-x

Malhotra, N., et al., 2020. Review of copper and copper nanoparticle toxicity in fish. Nanomaterials. 10, 1126. https://doi.org/10.3390/nano10061126

Mccormick, S. D., 1993. Methods for nonlethal gill biopsy and measurement of Na^+, K^+-ATPase activity. Can J Fish Aquat Sci. 50, 656-658. https://doi.org/10.1139/f93-075

McKim, J. M., et al., 1978. Metal toxicity to embryos and larvae of eight species of freshwater fish-II: copper. Bull Environ Contam Toxicol. 19, 608-616. https://doi.org/10.1007/BF01685847

McNeil, P. L., et al., 2014. Effects of metal nanoparticles on the lateral line system and behaviour in early life stages of zebrafish (*Danio rerio*). Aquat Toxicol. 152, 318-323. https://doi.org/10.1016/j.aquatox.2014.04.022

McWilliams, P. G., Shephard, K. L., 1991. Water quality during egg incubation influences yolk-sac fry sodium kinetics in Atlantic salmon, *Salmo salar* L.: a possible mechanism of adaptation to acid waters. Journal of Fish Biology. 39, 469-483. https://doi.org/10.1111/j.1095-8649.1991.tb04379.x

Miller, T. G., Mackay, W. C., 1982. Relationship of secreted mucus to copper and acid toxicity in rainbow trout. Bull Environ Contam Toxicol. 28, 68-74. https://doi.org/10.1007/BF01608415

Muller, E. B., et al., 2015. Quantitative adverse outcome pathway analysis of hatching in zebrafish with CuO nanoparticles. Environ Sci Technol. 49, 11817-11824. https://doi.org/10.1021/acs.est.5b01837

OECD, Test No. 236: Fish Embryo Acute Toxicity (FET) Test. Section 2. Organization for Economic Co-Operation and Development, Paris, 2013. pp. 22. https://doi.org/10.1787/9789264203709-en

Ong, K. J., et al., 2014. Mechanistic insights into the effect of nanoparticles on zebrafish hatch. Nanotoxicology. 8, 295-304. https://doi.org/10.3109/17435390.2013.778345

Pelster, B., Bagatto, B., 2010. Respiration, in: S. F. Perry, et al. (Eds.), Zebrafish. Academic Press, London, pp. 289-309. https://doi.org/10.1016/s1546-5098(10)02907-9

Peterson, R. H., Martinrobichaud, D. J., 1986. Perivitelline and vitelline potentials in teleost eggs as influenced by ambient ionic-strength, natal salinity, and electrode electrolyte; and the influence of these potentials on cadmium dynamics within the egg. Can J Fish Aquat Sci. 43, 1445-1450. https://doi.org/10.1139/f86-177

Ross, B. N., Knightes, C. D., 2022. Simulation of the Environmental Fate and Transformation of Nano Copper Oxide in a Freshwater Environment. ACS ES&T Water. 2, 1532-1543. https://doi.org/10.1021/acsestwater.2c00157

Shaw, B. J., et al., 2012. Effects of waterborne copper nanoparticles and copper sulphate on rainbow trout, (*Oncorhynchus mykiss*): physiology and accumulation. Aquat Toxicol. 116-117, 90-101. https://doi.org/10.1016/j.aquatox.2012.02.032

Shaw, B. J., Handy, R. D., 2011. Physiological effects of nanoparticles on fish: a comparison of nanometals versus metal ions. Environ Int. 37, 1083-1097.

https://doi.org/10.1016/j.envint.2011.03.009

Shaw, B. J., et al., 2016. A critical evaluation of the fish early-life stage toxicity test for engineered nanomaterials: experimental modifications and recommendations. Arch Toxicol. 90, 2077-2107. https://doi.org/10.1007/s00204-016-1734-7

Shephard, K. L., 1987. Ion-exchange phenomena regulate the environment of embryos in the eggs of freshwater fish. Comp Biochem Physiol A 88, 659-662. https://doi.org/10.1016/0300-9629(87)90679-7

Sun, Y., et al., 2016. Effects of copper oxide nanoparticles on developing zebrafish embryos and larvae. Int J Nanomedicine. 11, 905-918. https://doi.org/10.2147/IJN.S100350

Thit, A., et al., 2017. Effects of copper oxide nanoparticles and copper ions to zebrafish (*Danio rerio*) cells, embryos and fry. Toxicol In Vitro. 45, 89-100. https://doi.org/10.1016/j.tiv.2017.08.010

van der Velden, J. A., et al., 1991. Early life stages of carp (*Cyprinus carpio* L.) depend on ambient magnesium for their development. J Exp Biol. 158, 431-438. https://doi.org/10.1242/jeb.158.1.431

Vicario-Pares, U., et al., 2014. Comparative toxicity of metal oxide nanoparticles (CuO, ZnO and TiO$_2$) to developing zebrafish embryos. J Nanopart Res. 16, 2550. https://doi.org/10.1007/s11051-014-2550-8

Wang, T., et al., 2014. The potential toxicity of copper nanoparticles and copper sulphate on juvenile *Epinephelus coioides*. Aquat Toxicol. 152, 96-104. https://doi.org/10.1016/j.aquatox.2014.03.023

Wang, T., et al., 2015. Effect of copper nanoparticles and copper sulphate on oxidation stress, cell apoptosis and immune responses in the intestines of juvenile *Epinephelus coioides*. Fish Shellfish Immunol. 44, 674-682. https://doi.org/10.1016/j.fsi.2015.03.030

Zhang, Y., et al., 2018. Copper inhibits hatching of fish embryos via inducing reactive oxygen species and down-regulating Wnt signaling. Aquat Toxicol. 205, 156-164. https://doi.org/10.1016/j.aquatox.2018.10.015

Chapter
V

GENERAL DISCUSSION

5   Chapter V – General discussion

The main aims of my research project were to study how metal and metal oxide ENMs and some their characteristics can affect freshwater organisms in comparison to respective salt metal. These aims were extended to study the effect of surface coating of Ag ENMs and exposure period in *Lemna minor* (**Chapter II**). Furthermore, the bioavailability of Ag ENMs (**Chapter III**) and CuO ENMs (**Chapter IV**) was also assessed in *Danio rerio* (zebrafish) embryos. Factors as surface coating and exposure period influenced the effects of Ag ENMs in *L. minor* (**Chapter II**). In zebrafish, salt metals (AgNO$_3$ and CuSO$_4$) were more toxic than their ENMs counterparts: Ag ENMs (**Chapter III**) and CuO ENMs (**Chapter IV**). Most of ENMs remained on top of the chorion. Whereas, the osmoregulatory stress as a nano-specific effect (i.e. effect significantly different from salt metal) was only associated to Ag ENMs; the nano-specific effect oxidative stress was associated to both Ag and CuO ENMs.

Engineered NMs became very attractive to a wide range of industries in the last decade, leading to their increased production and use, documented in the literature (**Chapter I and Appendix A**). Consequently, the probability of ENMs arriving to the environmental compartments, as surface waters, progressively increases, which raises concern about their adverse ecological impacts (**Chapter I**). Freshwater is an essential resource for ecosystems and humans that endures immense pressure by diverse factors, as climate change, overexploitation (industrial, agricultural or domestic purposes) or water pollution (Brack et al., 2017; Reyjol et al., 2014). Furthermore, freshwater systems (ponds, streams, etc.) support 10% of all described species and around one-third of vertebrate species (Strayer and Dudgeon, 2010). Freshwater systems seem to be more threatened than other ecosystems, as 83% of its species population declined since 1970, which represents a biodiversity decline two-to-three times faster than other ecosystems (marine or terrestrial) (WWF, 2018).

Aquatic plant, as macrophytes, provide diverse services to these freshwater ecosystems (**Chapter I**), including the indirect protection from environmental contaminants through bioremediation (Couto et al., 2022; Rezania et al., 2016; Srivastava et al., 2008). In the last five years, several reviews and book chapters compiled the available evidence concerning the fate and effects of Ag ENMs to aquatic plants (Ahmad et al., 2021; Biba et al., 2021a; Biba et al., 2021b; Ceschin et al., 2021; Dasari et al., 2021; Dhiman et al., 2021; Dykman and Shchyogolev, 2018; Feregrino-Pérez et al., 2023; Hamadache et al., 2021; Kang et al., 2023; Kralova et al., 2019; Krishnappa et al., 2022; Kumar et al., 2023; Marimuthu et al., 2020; Mathur et al., 2023; Musee et al., 2020; Rezvani et al., 2019; Sharma and Sharma, 2022; Singh et al., 2022; Soares et al., 2018; Urík et al., 2021; Wang et al., 2022; Yan and Chen, 2019). Among the source of evidence was Pereira et al. (2018) that compared of the effects of citrate-Ag ENMs and PVP-Ag ENMs to *Lemna minor*. Glavas Ljubimir et al. (2023) validated some of the *L. minor* outcomes (**Chapter II**), also observing growth inhibition, decreased photosynthetic pigments, increased GPox activity leading to negative morphological effects (leaf necrosis), under similar or higher PVP-Ag ENMs concentrations (0.5-5 mg L^{-1}). Tran et al. (2023) found no effects on the frond number on *L. minor* exposed to citrate-Ag ENMs despite its initial number, in consistence to this thesis (**Chapter II**). Another study comparing citrate/cysteine-Ag ENMs effects on two *Lemna species* reported that the chlorosis phenomena were dose- and time-dependent (Iannelli et al., 2022), as observed in this study (**Chapter II**).

Freshwater fish play a pivotal role in nutrients cycling (phosphorus and nitrogen) that is essential for primary producers (e.g. algae, aquatic plants) and ultimately, crucial to achieve balanced ecosystems (Lapointe et al., 2014; McIntyre et al., 2008). Zebrafish embryos were affected by both ENMs: Ag ENMs (**Chapter III**) and CuO ENMs (**Chapter IV**). The behaviour of Ag and CuO ENMs was considerably different, CuO ENMs tended to agglomerate more and dissolve faster than Ag ENMs. This is a probable result of the fact that unlike CuO ENMs, Ag ENMs were coated with an amphiphilic non-charged polymer (PVP), resulting in the steric repulsion of the particles (Huynh and Chen, 2011), and thus, more stability. For

zebrafish, salt metals (AgNO$_3$ and CuSO$_4$) were more toxicity than both Ag ENMs and CuO ENMs. Whereas, larvae were more susceptible to Ag ENMs during stress of hatching, for CuO ENMs most of toxicity in embryos occurred before hatching. The chorion was a reasonably effective barrier to prevent the internalisation both Ag and CuO ENMs, most of both ENMs remained on top of the chorion, agreeing with Böhme et al. (2017). Additionally, CuO ENMs exhibited a specific behaviour smothering the chorion of embryos which was inversely correlated with the inability to hatch; still, Ag ENMs also affected the hatching. Embryos exposed to both Ag and CuO ENMs were not able to maintain a healthy osmoregulatory function, but only embryos exposed to Ag ENMs had harsher effects than the salt metal. Considering oxidative stress, total glutathione was more depleted both ENMs than respective salt metals, and Ag ENMs effects were more intense than CuO ENMs. These results suggest differences in the toxic mechanisms of both forms of both metals, Ag and CuO.

Single-species toxicity tests alone are useful tools to assess the effects of environmental contaminants, but are not predictive of the effects at population or community levels. Nonetheless, those lethal or sub-lethal values are advantageous when applied in a holistic approach as Ecological Risk Assessment (ERA). Risk assessment of chemicals is a tool applied by regulators to minimize the damage of these substance when enough evidence indicates a risk to the human or environment health. This tool allows to establish acceptable environmental concentrations of chemicals, defined as predicted no effect concentrations (PNEC) (Sorgog and Kamo, 2019). Species Sensitive Distribution (SSD) is a method to obtain the PNEC values in ERA. In SSD analysis, different assessment factors (AF) are applied to lethal and sub-lethal values from different taxonomic groups (in the EU 8 is the minimum advisable number of Taxa) (ECB, 2003). Ecotoxicity for these taxa are gathered to achieve a hazardous concentration for 5% of species (HC$_5$) values (Materials and Methods for data search, selection, triage and manipulation are described in **Appendix E**).
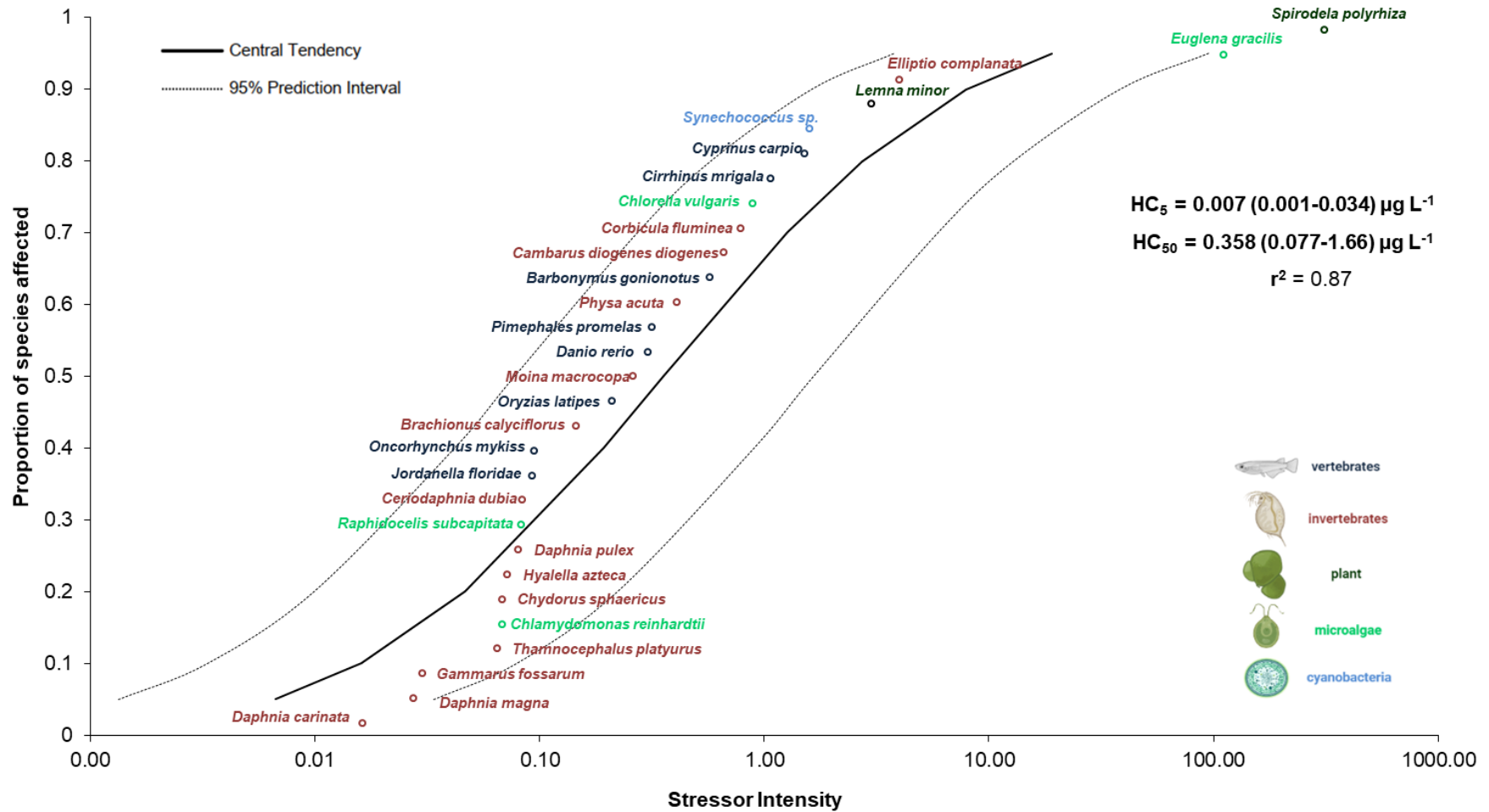
Figure 5-1 – Sensitive species distribution (SSD) of normalized lethal and sub-lethal values of freshwater species (*n*= 29) exposed to AgNO$_3$ (*n*= 142, Appendix E).
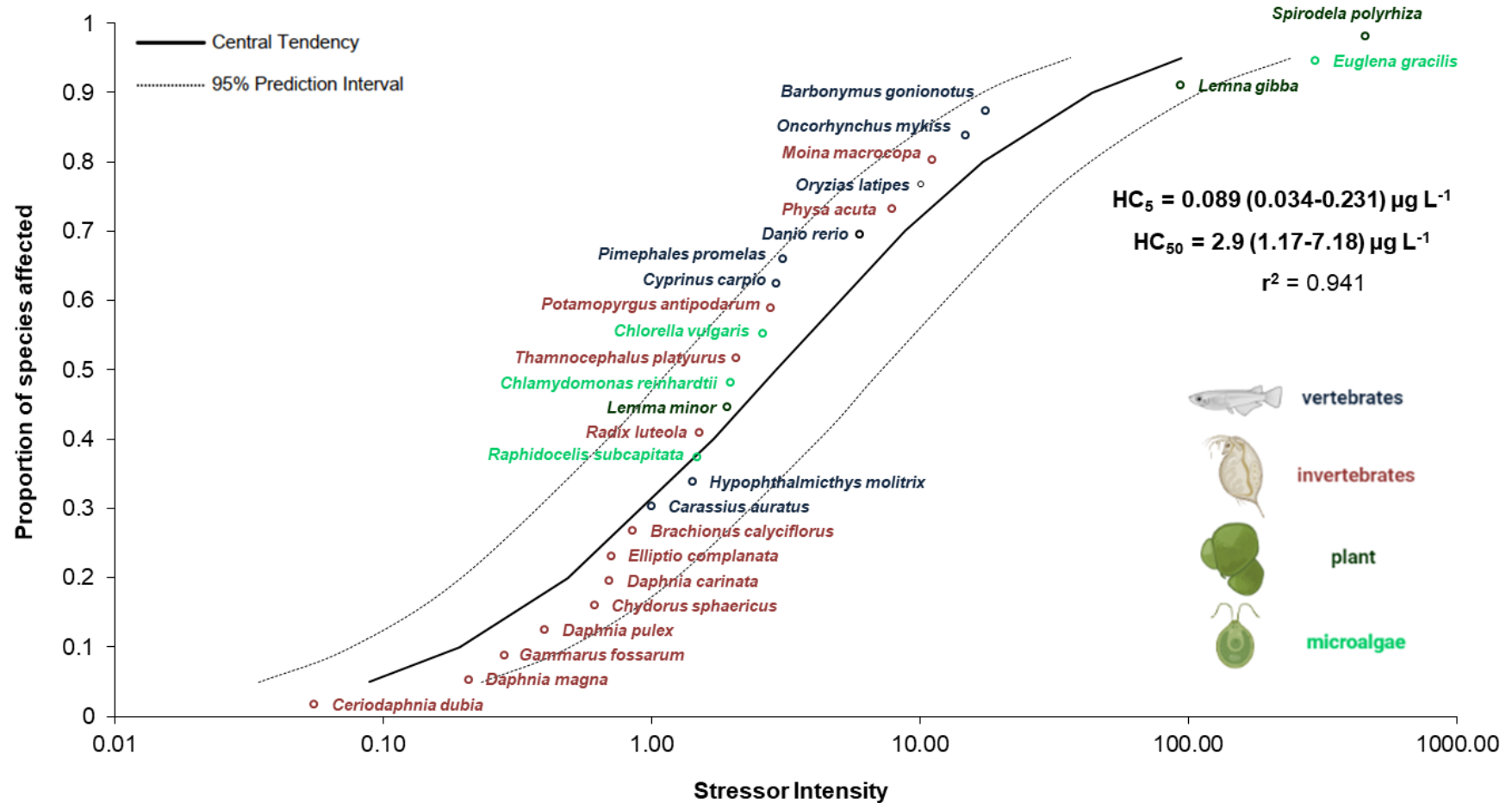
Figure 5-2 – SSD of normalized lethal and sub-lethal values of freshwater species (*n*= 28) exposed to Ag ENMs (*n*= 277 data entries, Appendix E).

Considering the extensive literature regarding Ag ENMs in freshwater organisms and the higher toxicity of Ag ENMs relative to CuO ENMs, SSDs analysis was performed to both forms of Ag. High variability of species from different taxonomic groups was displayed in both forms of Ag, AgNO$_3$ (**Figure 5-1**) and Ag ENMs (**Figure 5-2**). The HC$_5$ values was 0.007 µg L^{-1} (0.001-0.034, prediction interval (PI)) for AgNO$_3$ and 0.089 µg L^{-1} (0.034-0.231 PI) for Ag ENMs; the variability trend occurred in both Ag forms, with a 13-fold difference. The least sensitive species was *Spirodela polyrhiza* (*n*= 1) for both Ag forms, an aquatic plant as *Lemna minor* (**Chapter II**). This group of organisms can be described as the least sensitive despite their low number of data entries (AgNO$_3$ *n*= 2; Ag ENMs *n*= 4; **Table 6 XIII and Table 6 XIV**, **Appendix E**), which is a hint of their remediation potential for ENMs (Santos et al., 2022). On the other side, the most sensitive species was *Daphnia carinata* for AgNO$_3$ (*n*= 4) and *Ceriodaphnia dubia* for Ag ENMs (*n*= 11), both from the Daphniidae family. In fact, in the Ag ENMs SSD, the majority of the most sensitive species are invertebrates. Their sensitivity might be related to the characteristic locomotion behaviours that also modulate the feeding habits.

Invertebrates comprise an immense diversity of organisms from different Phylum (e.g. Arthropoda, Mollusca). Zooplakton, as some rotifers, as *Brachionus calyciflorus* (**Figure 5-1** and **Figure 5-2**), move in the water column through rotary motion with their ciliated corona, allowing them to eat particles with 10 µm (e.g. organic detritus, dead bacteria, algae or protozoans) (Thackeray, 2022). Cladocerans, as *Daphnia magna* or *Moina macrocopa* (**Figure 5-1** and **Figure 5-2**), use their antennae to create a motion that allows them to swim in the water column and twitch the food into their mouths, being filter feeders mostly on algae (Thackeray, 2022). Some amphipods, as *Gammarus fossarum* or *Hyalella azteca* (**Figure 5-1** and **Figure 5-2**), are detritivorous (not exclusively), shredding leaf litter detritus in the stream beds (Glazier, 2014). Fairy shrimps, as *Thamnocephalus platyurus* (**Figure 5-1** and **Figure 5-2**), swim "upside-down" and are filter feeders of organic particles from the water or by scraping algae from surfaces (Los Huertos, 2020). Gastropods, as *Physa acuta* or *Radix luteola* (**Figure 5-1** and **Figure 5-2**), are that grazer-scrapers that feed either on plant and animal detritus (Pyron and

Brown, 2015). Most of bivalves, as *Corbicula fluminea* and *Elliptio complanata* (**Figure 5-1** and **Figure 5-2**), are sessile benthic organisms and active suspension filters on algae or detritus (Cummings and Graf, 2015). Therefore, due to their small size and feeding behaviours, some of these invertebrates are more sensitive to both AgNO$_3$ and Ag ENMs since, as previously demonstrated (Pereira et al., 2023), ENMs tend to settle and accumulate in the bottom of the test vessels (**Chapter III** and **Chapter IV**). Engineered NMs have high potential to aggregate to natural organic matter (NOM) resulting, for example, from the decomposition of bacteria, plants or animals, which is known as NOM-coronas (Baalousha et al., 2018), or even biomolecules that can form exogenously by invertebrates (e.g. proteins release by neonates, eco-corona) or endogenously in invertebrates (e.g. haemolymph, bio-corona) (Liu et al., 2022). Therefore, the ecological implications of the fate of these ENMs could put some of these invertebrates (e.g. detritivorous or filter feeders) at higher risk, as confirmed by Nasser and Lynch (2016) that showed daphnids with impaired feeding intake after the ingestion of eco-coronas.

Ecotoxicity data for the freshwater fish of used in both SSDs for AgNO$_3$ (**Figure 5-1**) and Ag ENMs (**Figure 5-2**), are mostly from the Cyprinidae family (*Barbonymus gonionotus*, *Carassius auratus*, *Cirrhinus mrigala*, *Cyprinus carpio*, *D. rerio* (**Chapters III** and **IV**), *Hypophthalmichthys molitrix*, *Pimephales promelas*). Most of this species are above the hazardous concentration for 60% of species, revealing less sensitivity for this group of organisms.

Considering the risk assessment of Ag ENMs, PNEC values are obtained dividing the HC$_5$ by a suitable AF, that in the case of SSD method is advisable to be between 1 and 5 (ECB, 2003). The use of 4 to 8 taxonomic groups is recommended to calculate the HC5 by SSD (ECB, 2003). However, in Ag ENMs SSD the dataset had only 7 taxonomic groups (**Appendix E**) whereas the dataset for dissolved Ag had more than 8 taxonomic groups. Thus, a AF of 1 was applied to AgNO$_3$ and a AF of 2 was applied to Ag ENMs. The obtained PNEC values was 0.007 µg L^{-1} for AgNO$_3$ and 0.045 µg L^{-1} for Ag ENMs. Arijs et al. (2021) established a PNEC value of 0.039 µg L^{-1} for Ag, that is also the value used under EU REACH. The difference of one

order of magnitude might be caused by variations in the diversity of taxonomic groups.

Risk quotients (RQ) are calculated by dividing the Predicted effect concentration (PEC) by the PNEC (Amiard and Amiard-Triquet, 2015). Arijs et al. (2022) established a value of 0.044 µg L^{-1} of Ag for the PEC, based on the 95th percentile value from a Waterbase monitoring (2010-2019). Using this value, the calculated RQ using is 6.3, a risk quite above 1. However, when substituting for Arijs et al. (2021) PNEC (0.039 µg L^{-1}), the RQ falls to 1.1. In the case of Ag ENMs, a value of 1.5 ng L^{-1} was predicted to accumulate in the EU surface waters (Sun et al., 2016), when calculating the RQ a value of 0.03 was established. When using values measure in Dutch rivers, the worst case scenario displays a value of 2.5 ng L^{-1} (Peters et al., 2018), doubling the RQ to 0.06. Still, both values of RQ for Ag ENMs are far below 1.

Furthermore, the diversity of ENMs characteristics (e.g. surface coating) requires further toxicological studies aiming to improve the knowledge on ENMs toxicity and risk assessment and, accordingly establish guidelines for the safety and sustainable use of ENMs.

5.1 References

Ahmad, S. S., et al., 2021. Silver nanoparticles as an active packaging ingredient and its toxicity. Packag Technol Sci. 34, 653-663. https://doi.org/10.1002/pts.2603

Amiard, J.-C., Amiard-Triquet, C., 2015. Chapter 2 - Conventional Risk Assessment of Environmental Contaminants, in: C. Amiard-Triquet, et al. (Eds.), Aquatic Ecotoxicology. Academic Press, pp. 25-49. https://doi.org/10.1016/B978-0-12-800949-9.00002-4

Arijs, K., et al., 2021. Setting a Protective Threshold Value for Silver Toward Freshwater Organisms. Environ Toxicol Chem. 40, 1678-1693. https://doi.org/10.1002/etc.5026

Arijs, K., et al., 2022. European freshwater silver monitoring data do not suggest a potential European-wide risk. Integr Environ Assess Manag. 0, 1-10. https://doi.org/10.1002/ieam.4729

Baalousha, M., et al., 2018. Natural organic matter composition determines the molecular nature of silver nanomaterial-NOM corona. Environ. Sci. Nano. 5, 868-881. https://doi.org/10.1039/C8EN00018B

Biba, R., et al., 2021a. Surface Coating-Modulated Phytotoxic Responses of Silver Nanoparticles in Plants and Freshwater Green Algae. Nanomaterials. 12, 24. https://doi.org/10.3390/nano12010024

Biba, R., et al., 2021b. Silver nanoparticles phytotoxicity mechanisms, in: K. A. Abd-Elsalam (Ed.), Silver Nanomaterials for Agri-Food Applications. Elsevier, Amsterdam, pp. 317-356. https://doi.org/10.1016/B978-0-12-823528-7.00026-3

Böhme, S., et al., 2017. Metal uptake and distribution in the zebrafish (*Danio rerio*) embryo: differences between nanoparticles and metal ions. Environ Sci: Nano. 4, 1005-1015. https://doi.org/10.1039/c6en00440g

Brack, W., et al., 2017. Towards the review of the European Union Water Framework Directive: Recommendations for more efficient assessment and management of chemical contamination in European surface water resources. Sci Total Environ. 576, 720-737. https://doi.org/10.1016/j.scitotenv.2016.10.104

Ceschin, S., et al., 2021. Aquatic plants and ecotoxicological assessment in freshwater ecosystems: a review. Environ Sci Pollut Res Int. 28, 4975-4988. https://doi.org/10.1007/s11356-020-11496-3

Couto, E., et al., 2022. The potential of algae and aquatic macrophytes in the pharmaceutical and personal care products (PPCPs) environmental removal: a review. Chemosphere. 302, 134808.
https://doi.org/10.1016/j.chemosphere.2022.134808

Cummings, K. S., Graf, D. L., 2015. Class Bivalvia, in: J. H. Thorp, D. C. Rogers (Eds.), Thorp and Covich's Freshwater Invertebrates (Fourth Edition). Academic Press, Boston, pp. 423-506. https://doi.org/10.1016/B978-0-12-385026-3.00019-X

Dasari, T., et al., 2021. Nanomaterials in the Environment, in: M. Barakat, R. Kumar (Eds.), Nanomaterials for Environmental Applications. CRC Press, Boca Raton, pp. 317-341. https://doi.org/10.1201/9781003129042

Dhiman, S., et al., 2021. Nanoparticle-Induced Oxidative Stress in Plant, in: V. P. Singh, et al. (Eds.), Plant Responses to Nanomaterials: Recent Interventions, and Physiological and Biochemical Responses. Springer, Cham, pp. 269-313. https://doi.org/10.1007/978-3-030-36740-4_12

Dykman, L., Shchyogolev, S., 2018. The effect of gold and silver nanoparticles on plant growth and development, in: Y. Saylor, V. Irby (Eds.), Metal Nanoparticles: Properties, Synthesis and Applications. Nova Science, Hauppauge, pp. 263-300

ECB, 2003. Technical Guidance Document on risk assessment in support of Commission Directive 93/67/EEC on risk assessment for new notified substances, Commission Regulation (EC) No 1488/94 on risk assessment for existing substances, Directive 98/8/EC of the European Parliament and of the Council concerning the placing of biocidal products on the market. Part II. European Commission, Dublin. pp. 337

Feregrino-Pérez, A., et al., 2023. Toxic Effects of Nanomaterials on Plant Cellular Mechanisms, in: J. M. Al-Khayri, et al. (Eds.), Nanomaterial Interactions with Plant Cellular Mechanisms and Macromolecules and Agricultural Implications. Springer, Cham, pp. 171-209. https://doi.org/10.1007/978-3-031-20878-2_7

Glavas Ljubimir, K., et al., 2023. Phytotoxic Action of Silver Nanoparticles on *Lemna minor*: Multi-Parameter Analysis of Different Physiological Processes. Plants. 12, 343. https://doi.org/10.3390/plants12020343

Glazier, D. S., 2014. Amphipoda, Reference Module in Earth Systems and Environmental Sciences. Elsevier, pp. 1-49. https://doi.org/10.1016/B978-0-12-409548-9.09437-9

Hamadache, M., et al., 2021. Contribution of Chemometric Modeling to Chemical Risks Assessment for Aquatic Plants, in: K. Roy (Ed.), Chemometrics and Cheminformatics in Aquatic Toxicology. Wiley, Hoboken, pp. 391-416. https://doi.org/10.1002/9781119681397.ch20

Huynh, K. A., Chen, K. L., 2011. Aggregation kinetics of citrate and polyvinylpyrrolidone coated silver nanoparticles in monovalent and divalent electrolyte solutions. Environ Sci Technol. 45, 5564-71. https://doi.org/10.1021/es200157h

Iannelli, M. A., et al., 2022. Differential phytotoxic effect of silver nitrate ($AgNO_3$) and bifunctionalized silver nanoparticles (AgNPs-Cit-L-Cys) on *Lemna* plants (duckweeds). Aquat Toxicol. 250, 106260. https://doi.org/10.1016/j.aquatox.2022.106260

Kang, M., et al., 2023. A Review on the Toxicity Mechanisms and Potential Risks of Engineered Nanoparticles to Plants. Rev Environ Contam Toxicol. 261, 5. https://doi.org/10.1007/s44169-023-00029-x

Kralova, K., et al., 2019. Plant responses to stress induced by toxic metals and their nanoforms, in: M. Pessarakli (Ed.), Handbook of Plant and Crop Stress. CRC Press, Boca Raton, pp. 479-522. https://doi.org/10.1201/9781351104609

Krishnappa, S., et al., 2022. A brief review of the impact of silver nanoparticles on agriculture and certain biological properties: A case study. J Health Allied Sci NU. 11, 62-69. https://doi.org/10.55691/2278-344x.1010

Kumar, S., et al., 2023. A review on phytotoxicity and defense mechanism of silver nanoparticles (AgNPs) on plants. J Nanopart Res. 25, 54. https://doi.org/10.1007/s11051-023-05708-3

Lapointe, N. W. R., et al., 2014. Principles for ensuring healthy and productive freshwater ecosystems that support sustainable fisheries. Environ Rev. 22, 110-134. https://doi.org/10.1139/er-2013-0038

Liu, W., et al., 2022. Aquatic organisms modulate the bioreactivity of engineered nanoparticles: focus on biomolecular corona. Front Toxicol. 4, 933186. https://doi.org/10.3389/ftox.2022.933186

Los Huertos, M., 2020. The Players: Evolving Aquatic Species, in: M. Los Huertos (Ed.), Ecology and Management of Inland Waters. Elsevier, Oxford, pp. 67-130. https://doi.org/10.1016/B978-0-12-814266-0.00016-7

Marimuthu, S., et al., 2020. Silver nanoparticles in dye effluent treatment: A review on synthesis, treatment methods, mechanisms, photocatalytic degradation, toxic effects and mitigation of toxicity. J Photochem Photobiol B. 205, 111823. https://doi.org/10.1016/j.jphotobiol.2020.111823

Mathur, P., et al., 2023. Engineered nanoparticles in plant growth: Phytotoxicity concerns and the strategies for their attenuation. Plant Physiol Biochem. 199, 107721. https://doi.org/10.1016/j.plaphy.2023.107721

McIntyre, P. B., et al., 2008. Fish distributions and nutrient cycling in streams: can fish create biogeochemical hotspots? Ecology. 89, 2335-2346. https://doi.org/10.1890/07-1552.1

Musee, N., et al., 2020. Implications of surface coatings on engineered nanomaterials for environmental systems: status quo, challenges, and perspectives, in: C. M. Hussain (Ed.), Handbook of Functionalized Nanomaterials for Industrial Applications. Elsevier, Amsterdam, pp. 399-416. https://doi.org/10.1016/C2018-0-00341-2

Nasser, F., Lynch, I., 2016. Secreted protein eco-corona mediates uptake and impacts of polystyrene nanoparticles on Daphnia magna. J Proteomics. 137, 45-51. https://doi.org/10.1016/j.jprot.2015.09.005

Pereira, S. P. P., et al., 2023. Differences in toxicity and accumulation of metal from copper oxide nanomaterials compared to copper sulphate in zebrafish embryos: Delayed hatching, the chorion barrier and physiological effects. Ecotoxicol Environ Saf. 253, 114613. https://doi.org/10.1016/j.ecoenv.2023.114613

Pereira, S. P. P., et al., 2018. Phytotoxicity of silver nanoparticles to *Lemna minor*: Surface coating and exposure period-related effects. Sci Total Environ. 618, 1389-1399. https://doi.org/10.1016/j.scitotenv.2017.09.275

Peters, R. J. B., et al., 2018. Detection of nanoparticles in Dutch surface waters. Sci Total Environ. 621, 210-218. https://doi.org/10.1016/j.scitotenv.2017.11.238

Pyron, M., Brown, K. M., 2015. Introduction to Mollusca and the Class Gastropoda, in: J. H. Thorp, D. C. Rogers (Eds.), Thorp and Covich's Freshwater Invertebrates. Academic Press, Boston, pp. 383-421. https://doi.org/10.1016/B978-0-12-385026-3.00018-8

Reyjol, Y., et al., 2014. Assessing the ecological status in the context of the European Water Framework Directive: where do we go now? Sci Total Environ. 497-498, 332-344. https://doi.org/10.1016/j.scitotenv.2014.07.119

Rezania, S., et al., 2016. Comprehensive review on phytotechnology: Heavy metals removal by diverse aquatic plants species from wastewater. J Hazard Mater. 318, 587-599. https://doi.org/10.1016/j.jhazmat.2016.07.053

Rezvani, E., et al., 2019. Adverse effects of nanosilver on human health and the environment. Acta Biomater. 94, 145-159. https://doi.org/10.1016/j.actbio.2019.05.042

Santos, J. S., et al., 2022. Ecological aspects of aquatic macrophytes for environmental pollution control: An eco-remedial approach, in: V. Kumar, et al. (Eds.), Phytoremediation Technology for the Removal of Heavy Metals and Other Contaminants from Soil and Water. Elsevier, Amsterdam, pp. 497-523. https://doi.org/10.1016/B978-0-323-85763-5.00030-1

Sharma, T., Sharma, N., 2022. Nanoparticles: Uptake, Translocation, Physiological, Biochemical Effects in Plants and their Molecular Aspects, in: V. Rajput, et al. (Eds.), The Role of Nanoparticles in Plant Nutrition under Soil Pollution: Nanoscience in Nutrient Use Efficiency. Springer, Cham, pp. 103-116. https://doi.org/10.1007/978-3-030-97389-6_5

Singh, S., et al., 2022. Fate and toxicity of nanoparticles in aquatic systems. Acta Geochimica. 42, 63-76. https://doi.org/10.1007/s11631-022-00572-9

Soares, C., et al., 2018. Metal-Based Nanomaterials and Oxidative Stress in Plants: Current Aspects and Overview, in: M. Faisal, et al. (Eds.), Phytotoxicity of Nanoparticles. Springer, Cham, pp. 197-227. https://doi.org/10.1007/978-3-319-76708-6_8

Sorgog, K., Kamo, M., 2019. Quantifying the precision of ecological risk: Conventional assessment factor method vs. species sensitivity distribution method. Ecotoxicol Environ Saf. 183, 109494. https://doi.org/10.1016/j.ecoenv.2019.109494

Srivastava, J., et al., 2008. Managing water quality with aquatic macrophytes. Rev Environ Sci Biotechnol. 7, 255-266. https://doi.org/10.1007/s11157-008-9135-x

Strayer, D. L., Dudgeon, D., 2010. Freshwater biodiversity conservation: recent progress and future challenges. J North Am Benthol Soc. 29, 344-358. https://doi.org/10.1899/08-171.1

Sun, T. Y., et al., 2016. Dynamic Probabilistic Modeling of Environmental Emissions of Engineered Nanomaterials. Environ Sci Technol. 50, 4701-11. https://doi.org/10.1021/acs.est.5b05828

Thackeray, S. J., 2022. Zooplankton Diversity and Variation Among Lakes, in: T. Mehner, K. Tockner (Eds.), Encyclopedia of Inland Waters. Elsevier, Oxford, pp. 52-66. https://doi.org/10.1016/B978-0-12-819166-8.00013-X

Tran, I. T., et al., 2023. Silver Inhibits *Lemna minor* Growth at High Initial Frond Densities. Plants. 12, 1104. https://doi.org/10.3390/plants12051104

Urík, M., et al., 2021. Effects of Natural Organic Matter on Bioavailability of Elements from Inorganic Nanomaterial, in: A. P. Ingle (Ed.), Nanotechnology in Plant Growth Promotion and Protection, pp. 113-128. https://doi.org/10.1002/9781119745884.ch7

Wang, L., et al., 2022. Recent advances in responses of arbuscular mycorrhizal fungi - Plant symbiosis to engineered nanoparticles. Chemosphere. 286, 131644. https://doi.org/10.1016/j.chemosphere.2021.131644

WWF, 2018. Living Planet Report - 2018: Aiming Higher. M. Grooten, R. E. A. Almond (Eds.). WWF, Gland, Switzerland. pp. 75

Yan, A., Chen, Z., 2019. Impacts of Silver Nanoparticles on Plants: A Focus on the Phytotoxicity and Underlying Mechanism. Int J Mol Sci. 20, 1003. https://doi.org/10.3390/ijms20051003

APPENDICES

6 Appendices

6.1 Appendix A: Supplementary Information for Chapter I

General Introduction

Table 6-I – Applications of the most used metal engineered nanomaterials (Me ENMs) in different industries and respective characteristics/functions.

Metal	Industries	Characteristic/ Function/ Application	Reference
Copper (Cu)	Biomedical	anticancer therapy	Al-Hakkani (2020)
	Antifouling paints	biocide	Adeleye et al. (2016)
	Antimicrobial treatment	biocide	Din and Rehan (2016)
	Biosensors or biolabels	fluorescence quenching and enhancement	Mandal and De (2015)
	Environmental remediation	high adsorption	Al-Hakkani (2020)
	Inkjet printing	high conductivity	
	Heat transfer systems	high conductivity	
	Metallurgy	electrical conductivity	Varol and Canakci (2015)
	Nanofluids	electrocatalysis, photocatalysis and gas-phase catalysis	Gawande et al. (2016)
Gold (Au)	Cellular imaging	light-scattering	Murphy et al. (2008)
	Photodynamic therapy	light absorption	Paszko et al. (2011)
Manganese (Mn)	Biomedical	antimicrobial agent	Hoseinpour and Ghaemi (2018)
		cancer therapy (photodynamic and photothermal)	Sobanska et al. (2021)
		drug delivery	

Metal	Industries	Characteristic/ Function/ Application	Reference
Nickel (Ni)	Dyes absorption	high surface area	Jaji et al. (2020)
	Battery manufacture	high conductivity	
	Biomedical	drug and gene delivery	
		magnetic resonance imaging	
	Optoelectronics	catalysis	
	Superconductors	high conductivity	
Silver (Ag)	Air and water purification	antimicrobial/ disinfectant	Deshmukh et al. (2019)
	Animal husbandry	antimicrobial	
	Antimicrobial coatings/materials	antimicrobial	Vasilev (2019)
	Biomedical	anti-tumoral	Caruso et al. (2014)
		wound healing	Deshmukh et al. (2019)
		wound dressings, tissue scaffolds, protective coatings and drug delivery	Burdusel et al. (2018)
	Cosmetics	antimicrobial	Fytianos et al. (2020)
	Food packaging	antimicrobial	Deshmukh et al. (2019)
	Printing inks	electro conductivity	Fernandes et al. (2020)
	Textiles	antimicrobial	Xu et al. (2017)

Table 6-II – Applications of the most used metal oxide engineered nanomaterials (MeO ENMs) in different industries and respective characteristics/functions

Metal Oxide	Industries	Characteristic/ Function/ Application	Reference
Aluminium oxide (Al_2O_3)	Biosensors	imaging	Hassanpour et al. (2018)
	Biomedical	drug delivery	
	Textiles	flame retardant, abrasion resistance	Korkmaz and Alay Aksoy (2015)
Cerium oxide (CeO_2)	Biomedical	drug delivery	Singh et al. (2020)
	Biosensors	oxygen ion conductivity	
	Fuel additive	catalyst for fuel oxidation	
	Micro- and nanoelectronics	corrosion protection	Ivanov et al. (2009)
	Polishing formulas		
	Solar cells	thermal stability	Singh et al. (2020)
Cobalt (II) oxide (CoO)	Biomedical	drug and gene delivery	Chattopadhyay et al. (2012)
Cobalt (II,III) oxide (Co_3O_4)	Batteries	electrical properties	Li et al. (2005)
	Biomedical	antimicrobial activity	Hafeez et al. (2020)
		cancer therapy	Iravani and Varma (2020)
	Capacitors	electrical properties	
	Catalysts	catalysis	
	Gas sensors	high sensivity to hydrogen and alcohol	Li et al. (2005)

Metal Oxide	Industries	Characteristic/ Function/ Application	Reference
Copper oxide (CuO)	Nanofluids	electrocatalysis, photocatalysis and gas-phase catalysis	Gawande et al. (2016)
	Chemical sensor	semi-conductor	Steinhauer (2021)
	Microelectronics, Transportation, Manufacturing, Heating and cooling systems	thermal conductivity	Zhu et al. (2018)
	Water cleaning	nanoremediation	McDonald et al. (2015)
Iron (II,III) oxide (Fe_3O_4)	Biomedical	biosensors	Ganapathe et al. (2020)
		cancer diagnosis (magnetic resonance imaging)	Ju-Nam and Lead (2016)
		drug delivery	Ganapathe et al. (2020)
		photoablation therapy	
	Water cleaning	nanoremediation (weak magnetic fields)	Yavuz et al. (2006)
Manganese (II) Oxide (MnO)	Chemical sensors	electrochemical detection	Hoseinpour and Ghaemi (2018)
	Water cleaning	nanoremediation	
	Batteries	supercapacitor electrodes	
Manganese (IV) oxide (MnO_2)	Cancer treatment	photodynamic and photothermal therapy	Sobanska et al. (2021)
	Environmental remediation	dye degradation activity	Hoseinpour and Ghaemi (2018)
Manganese (II,III) oxide (Mn_3O_4)	Aquaculture	dietary supplements	Hoseinpour and Ghaemi (2018)
	Biomedical	magnetic resonance imaging (contrasting agent)	Sobanska et al. (2021)

Metal Oxide	Industries	Characteristic/ Function/ Application	Reference
Silica dioxide (SiO$_2$)	Agriculture	gene delivery	Jeelani et al. (2019)
	Biomedical	drug and gene delivery	Jeelani et al. (2019)
	Building, Industry	electrical and thermal insulators	Zhuo et al. (2021)
	Cosmetics	anti-caking agent	Fytianos et al. (2020)
	Food packaging	increased shelf-life	Jeelani et al. (2019)
	Plastic, Rubber	filler material	Jeelani et al. (2019)
	Textiles	water repellence, dirt repellence, abrasion resistance	Oguz and Remzi (2017)
	Water cleaning	nanoremediation	Jeelani et al. (2019)
Titanium dioxide (TiO$_2$)	Biomedical	cancer therapy (photocatalyst)	Haider et al. (2019)
	Cosmetics; Textiles, Sunscreens	UV absorption and filter	Fytianos et al. (2020)
	Disinfection	antibacterial activity (photocatalysis)	Haider et al. (2019)
	Paints	anti-fouling	
	Self-cleaning materials (semiconductor)	photocatalyst	Barakat and Kumar (2016)
	Textiles	dyes self-cleaning	Abbas et al. (2018)
	Water cleaning	arsenic removal	Ashraf et al. (2019)
Zinc oxide (ZnO)	Biomedical	antidiabetic, antimicrobial, larvicidal activity	Rajeshkumar and Sandhiya (2020)
		cancer therapy	
		drug and gene delivery	Lakshmipriya and Gopinath (2021)
	Chemical sensors, Solar cells	photocatalysis	
	Cosmetics, Textiles	UV absorption and filter	Fytianos et al. (2020)
	Textiles	antimicrobial, abrasion resistance	Verbič et al. (2019)

6.1.1 **References**

Adeleye, A. S., et al., 2016. Release and detection of nanosized copper from a commercial antifouling paint. Water Res. 102, 374-382. https://doi.org/10.1016/j.watres.2016.06.056

Al-Hakkani, M. F., 2020. Biogenic copper nanoparticles and their applications: A review. SN Appl Sci. 2, 505. https://doi.org/10.1007/s42452-020-2279-1

Burdusel, A. C., et al., 2018. Biomedical Applications of Silver Nanoparticles: An Up-to-Date Overview. Nanomaterials. 8, 681. https://doi.org/10.3390/Nano8090681

Caruso, G., et al., 2014. Nanoparticles potential: types, mechanisms of action, actual in vitro and animal studies, recent patents, in: G. Caruso, et al. (Eds.), Innovative Brain Tumor Therapy. Woodhead Publishing, Sawston, pp. 53-150. https://doi.org/10.1533/9781908818744.53

Chattopadhyay, S., et al., 2012. Surface-modified cobalt oxide nanoparticles: new opportunities for anti-cancer drug development. Cancer Nanotechnol. 3, 13-23. https://doi.org/10.1007/s12645-012-0026-z

Deshmukh, S. P., et al., 2019. Silver nanoparticles as an effective disinfectant: A review. Mater Sci Eng C. 97, 954-965. https://doi.org/10.1016/j.msec.2018.12.102

Din, M. I., Rehan, R., 2016. Synthesis, Characterization, and Applications of Copper Nanoparticles. Anal Lett. 50, 50-62. https://doi.org/10.1080/00032719.2016.1172081

Fernandes, I. J., et al., 2020. Silver nanoparticle conductive inks: synthesis, characterization, and fabrication of inkjet-printed flexible electrodes. Sci Rep. 10, 8878. https://doi.org/10.1038/s41598-020-65698-3

Fytianos, G., et al., 2020. Nanomaterials in Cosmetics: Recent Updates. Nanomaterials. 10, 979. https://doi.org/10.3390/nano10050979

Ganapathe, L. S., et al., 2020. Magnetite (Fe_3O_4) Nanoparticles in Biomedical Application: From Synthesis to Surface Functionalisation. Magnetochemistry. 6, 68. https://doi.org/10.3390/magnetochemistry6040068

Gawande, M. B., et al., 2016. Cu and Cu-Based Nanoparticles: Synthesis and Applications in Catalysis. Chem Rev. 116, 3722-811. https://doi.org/10.1021/acs.chemrev.5b00482

Hafeez, M., et al., 2020. Green synthesis of cobalt oxide nanoparticles for potential biological applications. Mater Res Express. 7, 025019. https://doi.org/10.1088/2053-1591/ab70dd

Hassanpour, P., et al., 2018. Biomedical applications of aluminium oxide nanoparticles. Micro Nano Lett. 13, 1227-1231. https://doi.org/10.1049/mnl.2018.5070

Hoseinpour, V., Ghaemi, N., 2018. Green synthesis of manganese nanoparticles: Applications and future perspective-A review. J Photochem Photobiol B. 189, 234-243. https://doi.org/10.1016/j.jphotobiol.2018.10.022

Iravani, S., Varma, R. S., 2020. Sustainable synthesis of cobalt and cobalt oxide nanoparticles and their catalytic and biomedical applications. Green Chem. 22, 2643-2661. https://doi.org/10.1039/d0gc00885k

Ivanov, V. K., et al., 2009. Structure-sensitive properties and biomedical applications of nanodispersed cerium dioxide. Russ Chem Rev. 78, 855-871. https://doi.org/10.1070/rc2009v078n09abeh004058

Jaji, N.-D., et al., 2020. Advanced nickel nanoparticles technology: From synthesis to applications Nanotechnol Rev. 9, 1456-1480. https://doi.org/10.1515/ntrev-2020-0109

Ju-Nam, Y., Lead, J., 2016. Properties, Sources, Pathways, and Fate of Nanoparticles in the Environment, in: B. Xing, et al. (Eds.), Engineered Nanoparticles and the Environment: Biophysicochemical Processes and Toxicity. Wiley, Hoboken, pp. 93-117. https://doi.org/10.1002/9781119275855.ch6

Korkmaz, N., Alay Aksoy, S., 2015. Enhancing the performance properties of ester-cross-linked cotton fabrics using Al_2O_3-NPs. Text Res J. 86, 636-648. https://doi.org/10.1177/0040517515592806

Li, W. Y., et al., 2005. Co_3O_4 Nanomaterials in Lithium-Ion Batteries and Gas Sensors. Adv Funct Mater. 15, 851-857. https://doi.org/10.1002/adfm.200400429

Mandal, S., De, S., 2015. Catalytic and fluorescence studies with copper nanoparticles synthesized in polysorbates of varying hydrophobicity. Colloids Surf A Physicochem Eng Asp. 467, 233-250. https://doi.org/10.1016/j.colsurfa.2014.11.026

McDonald, K. J., et al., 2015. Intrinsic properties of cupric oxide nanoparticles enable effective filtration of arsenic from water. Sci Rep. 5, 11110. https://doi.org/10.1038/srep11110

Murphy, C. J., et al., 2008. Gold Nanoparticles in Biology: Beyond Toxicity to Cellular Imaging. Acc Chem Res. 41, 1721-1730. https://doi.org/10.1021/ar800035u

Paszko, E., et al., 2011. Nanodrug applications in photodynamic therapy. Photodiagnosis Photodyn Ther. 8, 14-29. https://doi.org/10.1016/j.pdpdt.2010.12.001

Singh, K. R. B., et al., 2020. Cerium oxide nanoparticles: properties, biosynthesis and biomedical application. RSC Adv. 10, 27194-27214. https://doi.org/10.1039/D0RA04736H

Sobanska, Z., et al., 2021. Applications and Biological Activity of Nanoparticles of Manganese and Manganese Oxides in In Vitro and In Vivo Models. Nanomaterials. 11, 1084. https://doi.org/10.3390/nano11051084

Steinhauer, S., 2021. Gas Sensors Based on Copper Oxide Nanomaterials: A Review. Chemosensors. 9, 51. https://doi.org/10.3390/chemosensors9030051

Varol, T., Canakci, A., 2015. Microstructure, electrical conductivity and hardness of multilayer graphene/Copper nanocomposites synthesized by flake powder metallurgy. Met Mater Int. 21, 704-712. https://doi.org/10.1007/s12540-015-5058-6

Vasilev, K., 2019. Nanoengineered Antibacterial Coatings and Materials: A Perspective. Coatings. 9, 654. https://doi.org/10.3390/coatings9100654

Xu, Q., et al., 2017. Antibacterial cotton fabric with enhanced durability prepared using silver nanoparticles and carboxymethyl chitosan. Carbohydr Polym. 177, 187-193. https://doi.org/10.1016/j.carbpol.2017.08.129

Yavuz, C. T., et al., 2006. Low-field magnetic separation of monodisperse Fe_3O_4 nanocrystals. Science. 314, 964-967. https://doi.org/10.1126/science.1131475

Zhu, D., et al., 2018. Intriguingly high thermal conductivity increment for CuO nanowires contained nanofluids with low viscosity. Sci Rep. 8, 5282. https://doi.org/10.1038/s41598-018-23174-z

6.2 **Appendix B: Supplementary Information for Chapter II**

Phytotoxicity of silver nanoparticles to *Lemna minor*: surface coating and exposure period-related effects

Table 6-III – ANOVA analysis for zeta potential of citrate and PVP-Ag ENMs suspensions in Steinberg medium at day 0 and day 7. For one-way ANOVA, the independent variable was concentration, whereas for two-way ANOVA the independent variables were both concentration and surface coating.

Variables		citrate-Ag ENMs	PVP-Ag ENMs
Exposure (day)	Concentration (mg L^{-1})	*t and p values*	
0	0.05 vs. 2	*t = 5.4*, ***p<0.001***	*t = 3.36*, *p=0.01*
		t = 4.83, ***p<0.001***	
7	0.05 vs. 2	*t = 4.22*, ***p=0.003***	*t = 1.3*, *p=0.229*
		t = 0.536, *p=0.607*	
0 vs. 7		*t = 22.96*, ***p<0.001***	*t = 1.63*, *p=0.142*

Table 6-IV – Conductivity (mS/cm) of citrate and PVP-Ag ENMs suspensions in Steinberg medium at day 0 and day 7 for the lowest and highest test (nominal) concentrations (mean ± standard deviation, *n*=3).

Surface coating	Concentration (mg L^{-1})	Conductivity (mS cm^{-1})	
		Day 0	Day 7
citrate	0.05	0.96 ± 0.02	1.06± 0.05
	2	0.9 ± 0.009	0.93 ± 0.001
PVP	0.05	0.95± 0.016	0.99 ± 0.02
	2	0.9 ± 0.025	0.92 ± 0.001

Table 6-V – ANOVA analysis for the specific growth rate (SGR) of *Lemna minor* exposed to citrate and PVP-Ag ENMs and $AgNO_3$ (as salt metal) along 7 and 14 days. For one-way ANOVA, the independent variable was concentration, whereas in two-way ANOVA the independent variables were both concentration and surface coating.

Exposure (days)	ANOVA	citrate-Ag ENMs	PVP-Ag ENMs	AgNO₃
			F and p values	
7	one-way	$F_{5,17}$ =5.6, *p=0.007*	$F_{5,17}$ =6.7, *p=0.003*	$F_{5,17}$ =34.9, *p<0.001*
	two-way	$F_{5,35}$ =4.9, *p=0.003*		–
14	one-way	$F_{5,17}$ =7.3, *p=0.002*	$F_{5,17}$ =16.8, *p<0.001*	$F_{5,17}$ =125, *p<0.001*
	two-way	$F_{5,35}$ =4.89, *p=0.003*		–
7 vs 14	two-way	$F_{5,35}$ =0.59, p=0.71	$F_{5,35}$ =1.6, p=0.19	$F_{5,35}$ =0.65, p=0.67

Table 6-VI – ANOVA analysis for the percentage of chlorosis of *Lemna minor* exposed to citrate and PVP-Ag ENMs and $AgNO_3$ (as salt metal) along 7 and 14 days. For the one-way ANOVA, the independent variable was the concentration, whereas the two-way ANOVA the independent variables were both the concentration and the surface coating.

Exposure (days)	ANOVA	citrate-Ag ENMs	PVP-Ag ENMs	AgNO₃
			F and p values	
7	one-way	H = 16.8, *p=0.005*	H= 16.8, *p=0.005*	H= 19.8, *p=0.003*
	two-way	$F_{5,35}$= 17.70, *p<0.001*		–
14	one-way	H= 16.7, *p=0.005*	H= 16.8, *p=0.005*	H= 16.8, *p=0.005*
	two-way	$F_{5,35}$=22.08, *p<0.001*		–
7 vs 14	two-way	$F_{5,35}$= 23, *p<0.001*	$F_{5,35}$= 3.5, *p=0.017*	$F_{5,35}$= 4.8, *p=0.004*

Table 6-VII – ANOVA analysis for the number of colonies of *Lemna minor* exposed to citrate and PVP-Ag ENMs and AgNO$_3$ (as salt metal) along 7 and 14 days. For the one-way ANOVA, the independent variable was the concentration, whereas the two-way ANOVA the independent variables were both the concentration and the surface coating.

Exposure (days)	ANOVA	citrate-Ag ENMs	PVP-Ag ENMs	AgNO$_3$
			F and p values	
7	one-way	$F_{5,17}= 0.88$, $p=0.52$	$F_{5,17}= 3.6$, **$p=0.032$**	$H= 18.2$, **$p=0.006$**
	two-way	$F_{5,35}= 2.78$, **$p=0.041$**		–
14	one-way	$F_{5,17}= 2.35$, $p=0.1$	$F_{5,17}= 7.7$, **$p=0.002$**	$F_{5,17}= 43.6$, **$p<0.001$**
	two-way	$F_{5,35}= 4.45$, **$p=0.005$**		–
7 vs 14	two-way	$F_{5,35}= 1.33$, $p=0.29$	$F_{5,35}= 5.4$, **$p=0.002$**	$F_{6,41}= 2.05$, $p=0.093$

Table 6-VIII – ANOVA analysis for the enzymatic activities of guaiacol-peroxidase (GPox), glutathione-S-transferase (GST) and catalase (CAT) of *Lemna minor* exposed to citrate and PVP-Ag ENMs along 14 days. For the one-way ANOVA, the independent variable was the concentration, whereas the two-way ANOVA the independent variables were both the concentration and the surface coating.

Enzymes	ANOVA	citrate-Ag ENMs	PVP-Ag ENMs
		F and p values	
GPox	one-way	$F_{4,35} = 59.23$, **$p<0.001$**	$F_{3,26} = 9.58$, **$p<0.001$**
	two-way	$F_{3,56} = 8.83$, **$p<0.001$**	
GST	one-way	$F_{5,41} = 3.64$, **$p=0.009$**	$F_{3,26} = 1.02$, $p=0.403$
	two-way	$F_{3,56} = 0.437$, $p=0.728$	
CAT	one-way	$F_{4,32} = 0.759$, $p=0.561$	$H = 0.83$, $p=0.842$
	two-way	$F_{3,53} = 0.299$, $p=0.826$	

6.3 Appendix C: Supplementary Information for Chapter III

Comparison of toxicity of silver nanomaterials and silver nitrate on developing zebrafish embryos: bioavailability, osmoregulatory and oxidative stress
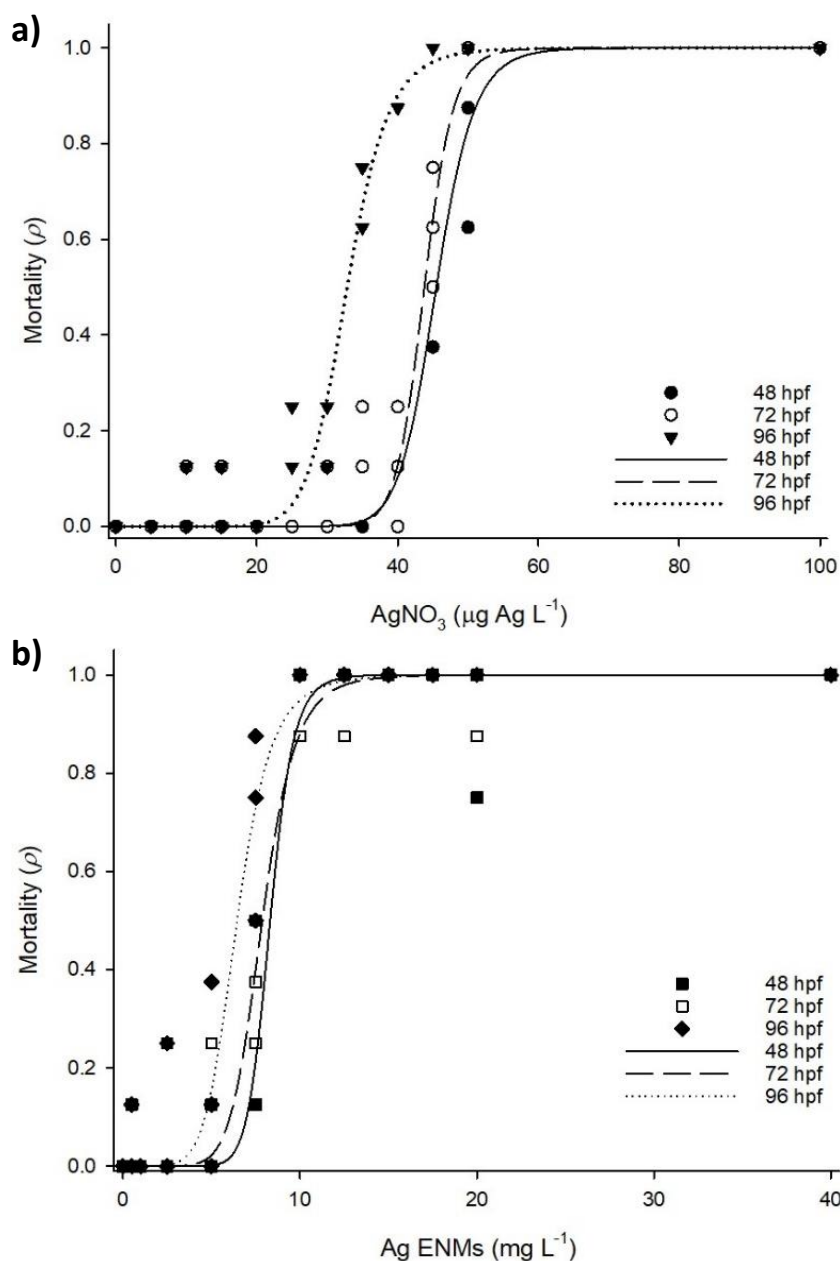
Figure 6-I – Mortality of zebrafish embryos from lethal exposure to AgNO₃ (filled black circles, 48 hours post fertilization (hpf); empty white circles, 72hpf; filled black inverted triangle, 96hpf; in panel a) and Ag ENMs (filled black squares, 48hpf; empty white squares, 72hpf; filled black diamond-shaped, 96hpf; in panel b). Curves based on sigmoidal functions of AgNO₃ after 48 hpf (r^2= 0.949), $y = \left(\frac{x^{16.9}}{(45.5^{16.9})+x^{16.9}}\right)$, 72 hpf (r^2= 0.956), $y = \left(\frac{x^{21.3}}{(43.8^{21.3})+x^{21.3}}\right)$ and 96 hpf (r^2= 0.979), $y = \left(\frac{x^{11.1}}{(32.8^{11.1})+x^{11.1}}\right)$; and of Ag ENMs after 48 hpf (r^2= 0.972), $y = \left(\frac{x^{12.6}}{(8.3^{12.6})+x^{12.6}}\right)$;72 hpf ($r^2$= 0.97), $y = \left(\frac{x^{8.3}}{(7.9^{8.3})+x^{8.3}}\right)$;and 96 hpf ($r^2$= 0.969), $y = \left(\frac{x^{6.7}}{(6.5^{6.7})+x^{6.7}}\right)$.
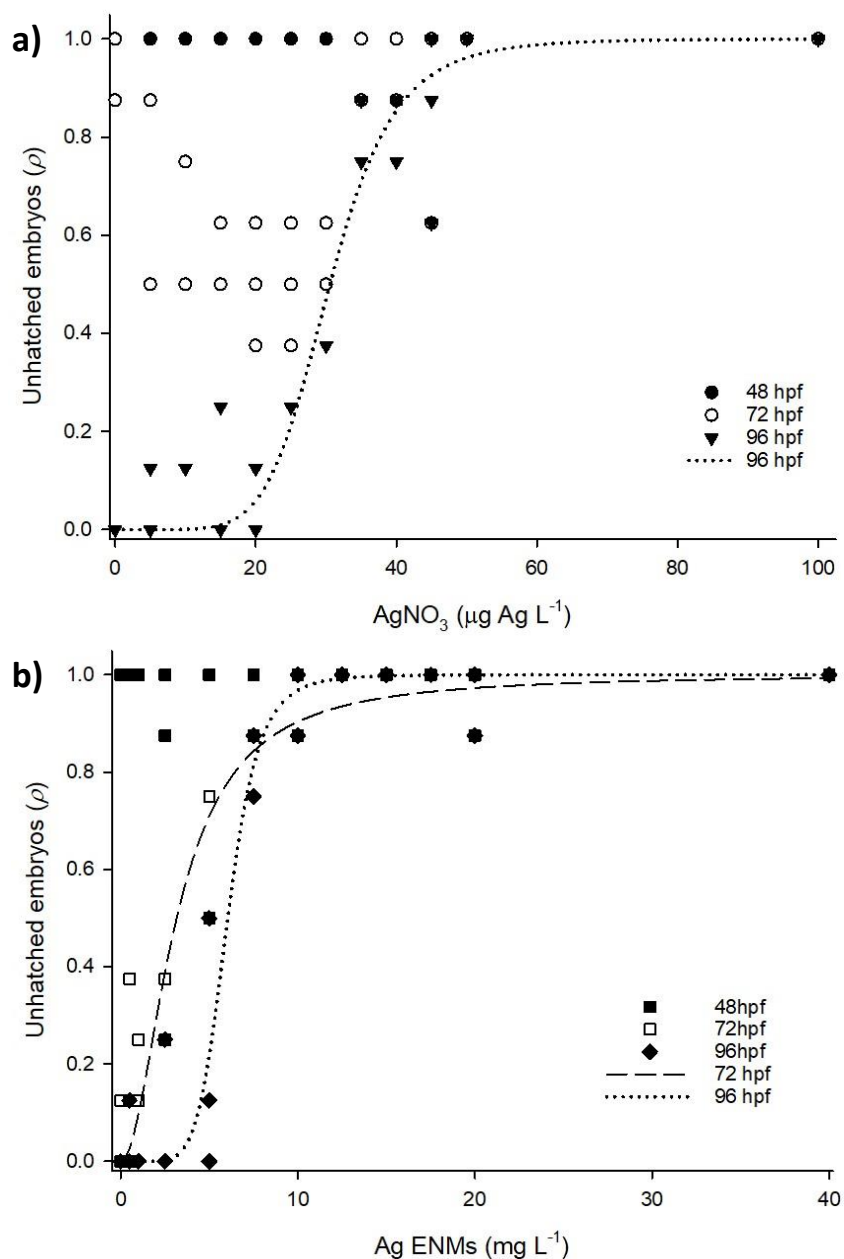
Figure 6-II – The proportion (ρ) of unhatched zebrafish embryos from lethal exposure to AgNO$_3$ (filled black circles, 48hpf; empty white circles, 72hpf; filled black inverted triangle, 96hpf; in panel a) and Ag ENMs (filled black squares, 48hpf; empty white squares, 72hpf; filled black diamond-shaped, 96hpf; in panel b). Same data as in Figure 3. Curves were fitted using Sigmaplot and were based on sigmoidal functions of AgNO$_3$ after 96hpf (r^2= 0.942), $y = \left(\frac{x^{6.6}}{(30.5^{6.6})+x^{6.6}}\right)$ and Ag ENMs after 72 hpf (r^2= 0.944), $y = \left(\frac{x^{1.95}}{(3.2^{1.95})+x^{1.95}}\right)$ and 96 hpf (r^2= 0.965), $y = \left(\frac{x^{6.8}}{(6.04^{6.8})+x^{6.8}}\right)$, respectively. Values equal or close to 1 after 48 and 72 hpf do not allow curve fitting for both AgNO$_3$ and Ag ENMs data.

Table 6-IX – *Lethal concentrations* (LC$_{10}$, LC$_{20}$, LC$_{50}$) expressed as mortality, *effect concentrations* (EC$_{10}$, EC$_{20}$, EC$_{50}$) expressed as hatching success, *low effect concentration* (LOEC), *no effect concentration* (NOEC) and *maximum acceptable toxicant concentration* (MATC) in lethal exposure of zebrafish embryos to AgNO$_3$ and Ag ENMs after 48, 72 and 96 hpf. Effect concentration only describes hatching success in both AgNO$_3$ and Ag ENMs at 72 and 96 hpf.

Mortality	LC$_{10}$ ± 95% CI	LC$_{20}$ ± 95% CI	LC$_{50}$ ± 95% CI	[a]LOEC ([b]NOEC)	[c]MATC	slope	r^2 (*n*)
AgNO$_3$ 48 hpf (µg Ag L^{-1})	39.9 ± 8.01	41.9 ± 3.7	45.5 ± 0.84	50 (45)	47.4	16.9	0.949 (36)
AgNO$_3$ 72 hpf (µg Ag L^{-1})	39.5 ± 7	41.03 ± 2.6	43.8 ± 0.76	50 (45)	47.4	21.3	0.956 (36)
AgNO$_3$ 96 hpf (µg Ag L^{-1})	26.9 ± 7.1	29 ± 4	32.8 ± 0.72	45 (40)	42.4	11.1	0.979 (36)
Ag ENMs 48 hpf (mg L^{-1}) *	7 ± 3.02	7.5 ± 0.88	8.3 ± 0.35	15 (12.5)	13.7	12.6	0.972 (36)
Ag ENMs 72 hpf (mg L^{-1}) *	6.05 ± 4.9	6.7 ± 1.5	7.88 ± 0.34	17.5 (15)	16.2	8.3	0.97 (36)
Ag ENMs 96 hpf (mg L^{-1}) *	4.6 ± 3.1	5.24 ± 1.1	6.46 ± 0.4	**ND**	**ND**	6.7	0.969 (36)

Hatching success	EC$_{10}$ ± 95% CI	EC$_{20}$ ± 95% CI	EC$_{50}$ ± 95% CI	[a]LOEC ([b]NOEC)	[c]MATC	slope	r^2 (*n*)
AgNO$_3$ 72 hpf (µg Ag L^{-1})	NC	NC	NC	ND	ND	NC	NC
AgNO$_3$ 96 hpf (µg Ag L^{-1})	21.8 ± 11.6	24.7 ± 5.9	30.5 ± 1.4	50 (45)	47.4	6.6	0.942 (36)
Ag ENMs 72 hpf (mg L^{-1}) *	1.3 ± 2.2	1.8 ± 1.3	3.5 ± 0.48	12.5 (10)	11.2	2	0.953 (36)
Ag 96 hpf (mg L^{-1}) *	4.4 ± 3.6	4.9 ± 1.1	6.04 ± 0.4	ND	ND	6.8	0.965 (36)

[a] LOEC – Lowest Observed Effect Concentration corresponds to the lowest concentration with statistical significant difference (*P<0.05*, Dunnet test) against the control group.

[b] NOEC – No Observed Effect Concentration stands as the highest tested concentration without statistical significant difference (*P<0.05*, Dunnet test) against the control group.

[c] MATC – Maximal acceptable toxicant concentration is calculated as the geometric mean of NOEC and LOEC.

NC – not calculated. It was not possible to reliably calculate the EC$_{10}$, EC$_{20}$ and EC$_{50}$ because 96% of the controls failed to hatch after 72 hpf.

ND – not defined. No significant differences were found against respective controls, thus LOEC and NOEC values were unfeasible and MATC value was also not calculated.

P<0.001 for all endpoints.

6.4 Appendix D: Supplementary Information for Chapter IV

Differences in toxicity and accumulation of metal from copper oxide nanomaterials compared to copper sulphate in zebrafish embryos: Delayed hatching, the chorion barrier and physiological effects
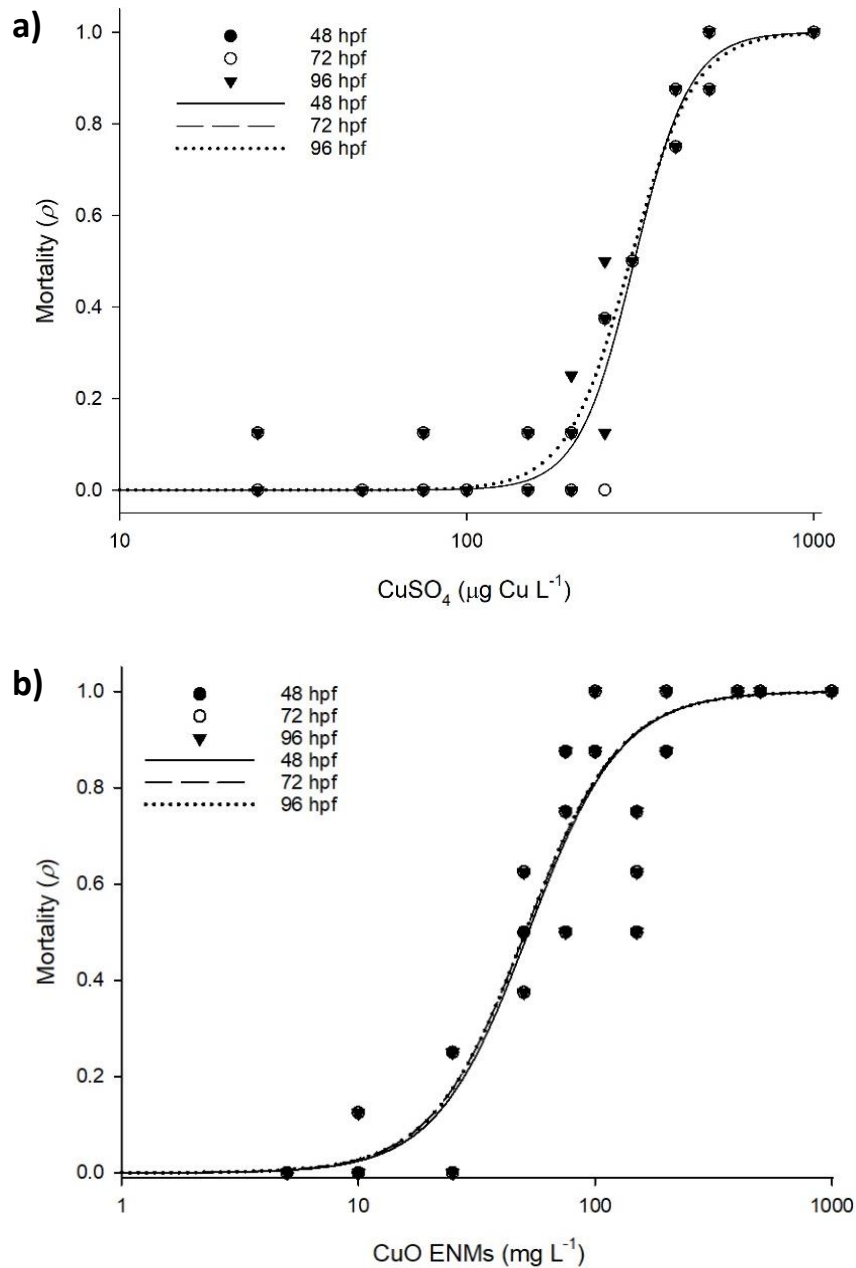
Figure 6-III – Mortality ($\hat{\rho}$) of zebrafish embryos exposed to; (a) CuSO$_4$, or (b) CuO ENMs. Curves were based on the sigmoidal functions of CuSO$_4$ after 48 hpf (r^2 = 0.964), $y = \left(\frac{x^{5.4}}{(303.9^{5.4})+x^{5.4}}\right)$; 72 hpf ($r^2$ = 0.964), $y = \left(\frac{x^{5.4}}{(303.9^{5.4})+x^{5.4}}\right)$; and 96hpf ($r^2$ = 0.964), $y = \left(\frac{x^{4.8}}{(295.9^{4.8})+x^{4.8}}\right)$; and CuO ENMs after 48 hpf (r^2 = 0.911), $y = \left(\frac{x^{2.2}}{(295.9^{2.2})+x^{2.2}}\right)$; 72 hpf ($r^2$ = 0.911), $y = \left(\frac{x^{2.2}}{(50.7^{2.2})+x^{2.2}}\right)$; and 96 hpf ($r^2$ = 0.907), $y = \left(\frac{x^{2.2}}{(50.7^{2.2})+x^{2.2}}\right)$.
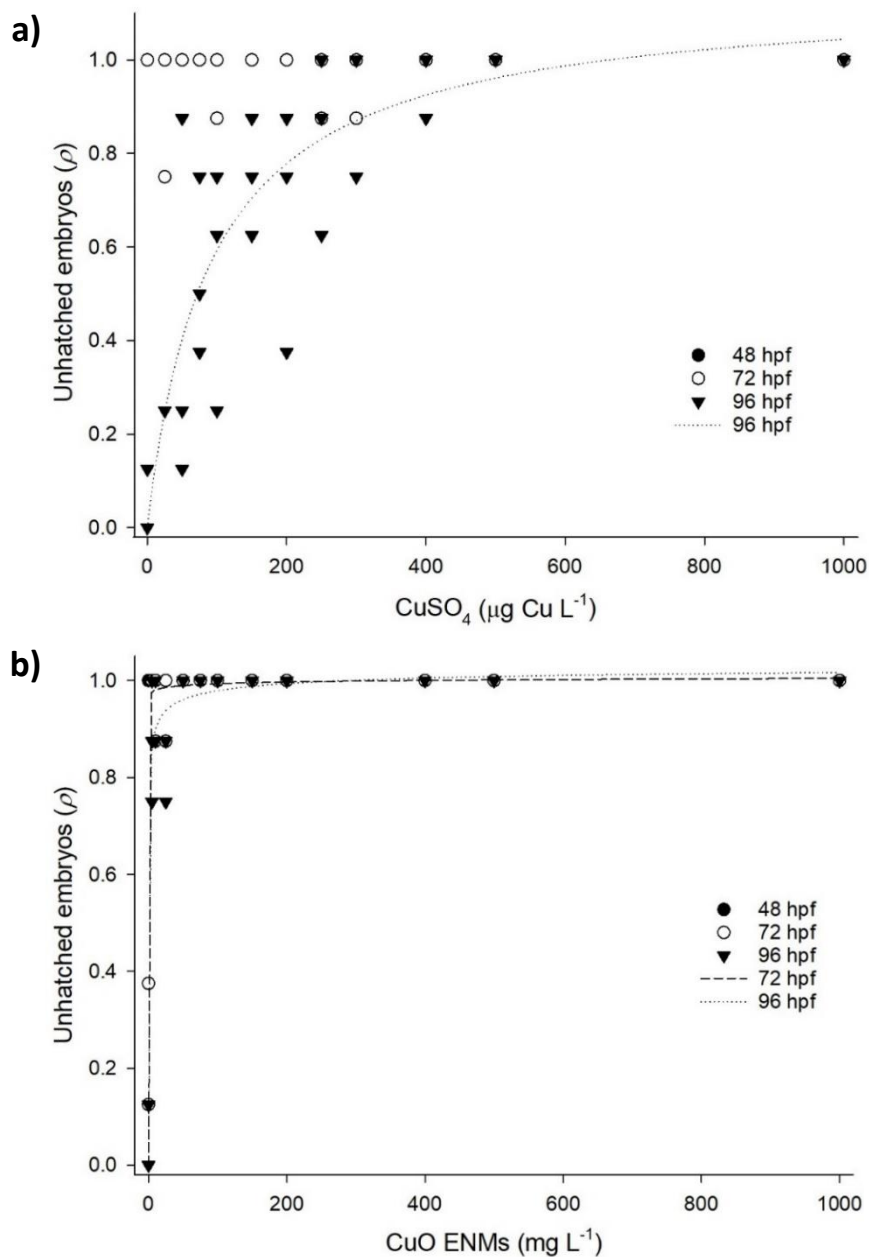
Figure 6-IV – The proportion ($\hat{p}$) of unhatched embryos of zebrafish exposed to; (a) CuSO$_4$, or (b) CuO ENMs for 96 hpf. Data are from the same experiment as in Figure 3. Curves were fitted using Sigmaplot and were based on sigmoidal functions of CuSO$_4$ after 96hpf (r^2= 0.773), $y = \left(\frac{1.15*(x^{0.98})}{(92.9^{0.98})+x^{0.98}}\right)$; and CuO ENMs after 72 hpf (r^2 = 0.833), $y = \left(\frac{1.06*(x^{0.085})}{(0.00000000000108^{0.085})+x^{0.085}}\right)$;and 96 hpf ($r^2$ = 0.956), $y = \left(\frac{1.05*(x^{0.38})}{(0.08^{0.38})+x^{0.38}}\right)$ (all with the same equation), respectively. Values equal or close to 1 after 48 and 72 hpf do not allow curve fitting for both CuSO$_4$ and CuO ENMs data.

Table 6-X – *Lethal concentrations* (LC_{10}, LC_{20}, LC_{50}), *effect concentrations* (EC_{10}, EC_{20}, EC_{50}), *lowest effect concentration* (LOEC), *no effect concentration* (NOEC) and *maximum acceptable toxicant concentration* (MATC) of $CuSO_4$ and CuO ENMs in zebrafish embryos at 48, 72 and 96 hours post fertilization (hpf). Effect concentration only describes hatching inhibition in both $CuSO_4$ and CuO ENMs at 96 hpf.

Mortality	LC_{10} ± 95% CI	LC_{20} ± 95% CI	LC_{50} ± 95% CI	[a] LOEC ([b] NOEC)	[c] MATC	slope	r^2 (*n*)
$CuSO_4$ 48 hpf (µg Cu L^{-1})	213.15 ± 119.42	244.83 ± 62.9	310.26 ± 13.93	ND	ND	5.4	0.965 (36)
$CuSO_4$ 72 hpf (µg Cu L^{-1})	213.15 ± 119.42	244.83 ± 62.9	310.26 ± 13.93	ND	ND	5.4	0.965 (36)
$CuSO_4$ 96 hpf (µg Cu L^{-1})	197.70 ± 120.03	231.47 ± 67.74	303.09 ± 14.44	ND	ND	4.75	0.964 (36)
CuO ENMs 48 hpf (mg L^{-1})	19.43 ± 32.39	27.99 ± 21.52	52.24 ± 9.2	400 (200)	282.8	2.22	0.914 (36)
CuO ENMs 72 hpf (mg L^{-1})	18.59 ± 31.88	26.92 ± 21.31	50.71 ± 9.26	400 (200)	282.8	2.19	0.911 (36)
CuO ENMs 96 hpf (mg L^{-1})	20.76 ± 33.51	29.36 ± 21.85	53.11 ± 9.86	50 (25)	35.4	2.19	0.904 (36)

Hatching inhibition	$EC_{10} \pm$ 95% CI	$EC_{20} \pm$ 95% CI	$EC_{50} \pm$ 95% CI	[a] LOEC ([b] NOEC)	[c] MATC	slope	r^2 (*n*)
$CuSO_4$ 96 hpf (µg Cu L^{-1})	14.25 ± 190.29	26.37± 46.57	75.53 ± 22.34	75 (50)	61.24	1.049	0.767 (36)
CuO ENMs 96 hpf (mg L^{-1})	0.012 ± ND	0.0412 ± 2.8	0.34 ± 0.78	ND	ND	0.382	0.956 (36)

Morphological Effects	$EC_{10} \pm$ 95% CI	$EC_{20} \pm$ 95% CI	$EC_{50} \pm$ 95% CI	[a] LOEC ([b] NOEC)	[c] MATC	slope	r^2 (*n*)
[d] **"Perivitelline fluid morphology"** $CuSO_4$ 96 hpf (µg Cu L^{-1})	163.41 ± 70.11	182.54 ± 42.16	220.58 ± 10.62	500 (400)	447.21	7.32	0.956 (34)
[e] **"Surface coated chorion"** [d] CuO ENMs 96 hpf (mg L^{-1})	3.76 ± 79.73	4.48 ± 6.97	6.05 ± 1	ND	ND	4.61	0.853 (34)

[a] LOEC – Lowest Observed Effect Concentration corresponds to the lowest concentration with statistical significant difference (*P<0.05*, Dunnet test) against the control group.
[b] NOEC – No Observed Effect Concentration stands as the highest tested concentration without statistical significant difference (*P<0.05*, Dunnet test) against the control group.
[c] MATC – Maximal acceptable toxicant concentration is calculated as the geometric mean of NOEC and LOEC.
[d] "Perivitelline fluid morphology" stands for the proportion of embryos with a perivitelline fluid with a foam-looking.
[e] "Surface coated chorion" stands for the proportion of embryos with particulate material smothering the chorion.
ND – not defined. It was not possible to reliably define LOEC and NOEC due to lack of significant differences against the controls. Consequently, the MATC due the lack of LOEC and NOEC for those rows in the table.
P<0.001 for all endpoints.

6.5 **Appendix E: Supplementary Information for Chapter V**

General Discussion

6.5.1 **Methodology for selection of studies for Sensitive Species Distribution (SSD) analysis**

For the Sensitive Species Distribution (SSD) analysis, a search for Ag ENMs was conducted in August 2021 in Scopus with the following description: (TITLE-ABS-KEY ("SILVER" AND "NANO*" AND "FRESH WATER" AND "TOXIC*") AND ALL ("PARTICLE*" OR "MATERIAL*") AND ALL ("MACROPHYTE*" OR "FISH*" OR "INVERTEBRATE*" OR "MICROALG*" OR "CRUSTACEAN*" OR "MOLLUSC*" OR "*PLAKTON*") AND NOT TITLE-ABS-KEY ("MARINE*" AND "VITRO*" AND "BACTERIA*" AND "CYTOTOX*" AND "GOLD*" AND "CELL*" AND "NANOWIRE*" AND "SEDIMENT*" AND "SOIL*") AND ALL ("LC50" OR "EC50" OR "EC10" OR "EC10" OR "LOEC" OR "NOEC" OR "toxic*")) AND PUBYEAR > 2006).

This search filtered 77 publications, and after a systematic examination, only a fraction of these studies fulfilled all the search parameters, but most decisively, included any lethal (LC$_{50}$, EC$_{50}$) or sub-lethal (LC$_{10}$, LC$_{20}$, EC$_{10}$, EC$_{20}$, LOEC, NOEC, MATC) endpoints. Thus, the publications included in the SSD analysis were the following ones (Ali, 2014; Angel et al., 2013; Asghari et al., 2012; Burchardt et al., 2012; Cho et al., 2013; Coll et al., 2016; Gagné et al., 2013; Georgantzopoulou et al., 2018; Gonçalves et al., 2017; Heinlaan et al., 2016; Kennedy et al., 2012; Khoshnamvand et al., 2020; Książyk et al., 2015; Lekamge et al., 2019; Martins et al., 2020; McLaughlin and Bonzongo, 2012; Mehennaoui et al., 2016; Sohn et al., 2015; Völker et al., 2014; Wang et al., 2012; Zhang et al., 2020).

Additionally, a search in Google Scholar resulted in more publications included manually in the SSD analysis (Allen et al., 2010; Asghari et al., 2012; Bar-Ilan et al., 2009; Blinova et al., 2013; Choi et al., 2010; Das et al., 2013; Gao et al., 2009; George et al., 2012; Griffitt et al., 2008; Gubbins et al., 2011; Hedayati A. et al., 2012; Hoheisel et al., 2012; Jo et al., 2012; Johari et al., 2013; Kennedy et al., 2010; Kim et al., 2011b; Kim et al., 2013; Laban et al., 2010; Lee et al., 2012a; Lee et al., 2012b; Li et al., 2010; Massarsky et al., 2013; McLaughlin and Bonzongo, 2012; Navarro et al., 2008b; Oukarroum et al., 2013; Pereira et al., 2018; Poynton et al., 2012; Shaluei et al., 2013). Data from Chapter III (submitted) were also added to the SSD analysis.

6.5.2 **Methodology for data selection for SSD analysis**

The selection of endpoints to include in the SSD analysis from each study followed an adapted method described by Coll et al. (2016) (**Table 6-XI**). The first assessment factor (AF) normalized all effect values (e.g. LC_{50}, LOEC) to no effect values (NOEC). The second AF aimed to normalise both acute and chronic studies, based on the parameters evaluated in the study. Whereas, parameters as mortality, hatching or abnormalities are usually representative of acute studies; parameters as growth, ingestion or biomarkers are representative of chronic studies (EPA, 2022).

Table 6-XI – Summary of Assessment factors (AF) for the two-level normalization (effect-to-no-effect) and (acute vs chronic studies).

Endpoint	1st AF (effect-to-no-effect)	Type of study	Parameters	2nd AF (acute-to-chronic)
LC_{50}, EC_{50}, LC_{25}, EC_{25}	10	**acute**	Mortality Hatching Abnormalities (e.g. heart rate)	10
LC_{20}, EC_{20}, LC_{10}, EC_{10}, LOEC	2	**chronic**	Growth Ingestion Biomarkers	1
MATC, NOEC	1			

However, the growth parameter raises an issue. Whereas in algae (unicellular organisms) growth refers to cellular duplication, in other organisms (e.g. fish) growth refers to the increase of size or weight. Thus, to avoid confusion, a flow chart developed by Brill et al. (2021) was followed to identify the nature of the algal studies, needed to select a suitable AF (acute-to-chronic) for each study (**Figure 6-V**).
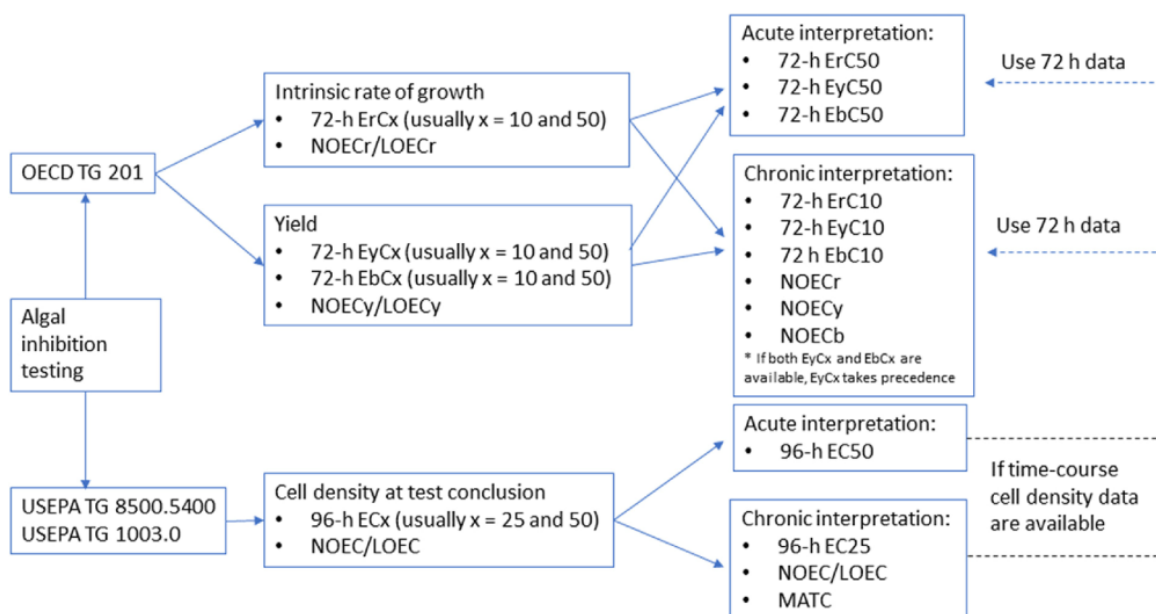
Figure 6-V – Flow-chart for determining if an algal toxicity endpoint is defined as acute or chronic. Effects may be based on inhibition of growth rate (ECr), biomass area under the curve (ECb), or cell yield (ECy) (from Brill et al., 2021).

6.5.3 **Selected Data**

Table 6-XII – Summary of the studies and data type for SSD analysis

Number of:	Salt metal (AgNO$_3$)	Ag ENMs
Publications	61	77
Total entries	142	277
Biological species	29	28
Taxonomic classes (number / description)	8	7
	Cyanobacteria, Chlorophyta, Tracheophytes, Rotifera, Crustacea, Mollusca, Chordata (Cyprinidae and Salmonidae)	Chlorophyta, Tracheophytes, Rotifera, Crustacea, Mollusca, Chordata (Cyprinidae and Adrianichthyidae)
Parameters	17	22
MATC values	4	8
NOEC values	6	18
LOEC values	0	4
EC$_{10}$ or EC$_{20}$ values	7	18
EC$_{50}$ or LC$_{50}$ values	125	229

Table 6-XIII – Data used in the SSD analysis for $AgNO_3$

Organism			Exposure					Assessment Factor (AF)					Reference
Type	Species	Life stage	Medium	Type	Length (h)	End-point	Value (mg L^{-1})	1st AF	Parameter	Study	2nd AF	Final value	
C	*Synechococcus sp.*	EGP	Blue green 11	S	72	EC_{50}	0.16	10	GRI (cell density)	A	10	0.002	Burchardt et al. (2012)
M	*Chlamydomonas reinhardtii*	EGP	SGM	S	1	EC_{50}	0.031	10	PY (PII)	A	10	0.0003	Navarro et al. (2015)
M	*Chlamydomonas reinhardtii*	EGP	MHSM	CR	24	EC_{50}	0.0015	10	cell (amol $cell^{-1}$)	A	10	0.00002	Hiriart-Baer et al. (2006)
M	*Chlorella vulgaris*	EGP	OECD 201	S	48	EC_{50}	0.39	10	biomass (cells mL^{-1})	A	10	0.004	Yoo-iam et al. (2015)
M	*Chlorella vulgaris*	EGP	OECD 201	S	72	EC_{50}	0.02	10	biomass (cells mL^{-1})	A	10	0.0002	Khoshnamvand et al. (2020)
M	*Euglena gracilis*	EGP	Sinfo	S	72	EC_{50}	0.16	10	cell (n)	A	10	0.002	Zhang and Wang (2019)
M	*Euglena gracilis*	EGP	Talaquil (pH 7.5)	S	1	EC_{10}	15.1	2	PY	A	10	0.8	Yue et al. (2017)
M	*Raphidocelis subcapitata*	EGP	MBL	S	72	EC_{50}	0.034	10	GRI (cell density)	A	10	0.0003	Ribeiro et al. (2014)
M	*Raphidocelis subcapitata*	EGP	SFM	S	72	IC_{50}	0.001	10	GRI (cell density)	A	10	0.00001	Angel et al. (2013)
M	*Raphidocelis subcapitata*	EGP	RTM(DSW)	S	4.5	EC_{50}	0.05	10	PhEI	A	10	0.0005	Wang et al. (2012)
M	*Raphidocelis subcapitata*	EGP	BBM	S	96	EC_{50}	0.001	10	cell (n)	A	10	0.0001	Kennedy et al. (2010)
M	*Raphidocelis subcapitata*	EGP	Algal Toxkit F	S	72	EC_{50}	0.007	10	GRI (cell density)	A	10	0.00007	Jemec et al. (2016)
M	*Raphidocelis subcapitata*	EGP	MHSM	CR	24	EC_{50}	0.0024	10	GRI (influent free Ag)	A	10	0.00002	Hiriart-Baer et al. (2006)
P	*Lemna minor*	EGP	Steinberg	S	168	EC_{50}	0.03	10	GRI (wet wt)	A	10	0.003	Pereira et al. (2018)
P	*Spirodela polyrhiza*	EGP	10% Hoagland	S	72	EC_{50}	3.1	10	NN	A	10	0.3	Jiang et al. (2012)
I	*Brachionus calyciflorus*	juveniles	SFM	S	24	EC_{10}	0.0029	2	mortality	A	10	0.0002	Martins et al. (2020)
I	*Cambarus diogenes diogenes*	adults	DTW	CR	96	LC_{50}	0.066	10	mortality	A	10	0.0007	Bianchini et al. (2002)

Organism			Exposure					Assessment Factor (AF)					Reference
Type	Species	Life stage	Medium	Type	Length (h)	End-point	Value (mg L^{-1})	1st AF	Parameter	Study	2nd AF	Final value	
I	*Ceriodaphnia dubia*	neonates	MHRW	S	48	LC$_{50}$	0.0007	10	immobilisation	A	10	0.000007	Kennedy et al. (2012)
I	*Ceriodaphnia dubia*	neonates	MHRW + DOC (4 mg L^{-1})	S	48	LC$_{50}$	0.0019	10	immobilisation	A	10	0.00002	Kennedy et al. (2012)
I	*Ceriodaphnia dubia*	neonates	MHRW + DOC (10 mg L^{-1})	S	48	LC$_{50}$	0.0022	10	immobilisation	A	10	0.00002	Kennedy et al. (2012)
I	*Ceriodaphnia dubia*	neonates	SFW	S	48	LC$_{50}$	0.0001	10	mortality	A	10	0.000001	Angel et al. (2013)
I	*Ceriodaphnia dubia*	neonates	DeioW + WCL-1	S	48	LC$_{50}$	0.027	10	mortality	A	10	0.0003	Hook and Fisher (2001)
I	*Ceriodaphnia dubia*	adults	FDTW	SR	48	LC$_{50}$	0.16	10	mortality	A	10	0.002	Griffitt et al. (2008)
I	*Ceriodaphnia dubia*	neonates	MHW	SR	168	NOEC	0.02	1	reproduction	C	1	0.02	Naddy et al. (2007a)
I	*Chydorus sphaericus*	neonates	RTM(DSW)	S	48	EC$_{50}$	0.0068	10	immobilisation	A	10	0.00007	Wang et al. (2012)
I	*Corbicula fluminea*	juveniles	New River	SR	480	NOEC	0.0078	1	mortality	A	10	0.0008	Diamond et al. (1990)
I	*Daphnia carinata*	neonates	ASTM	SR	48	LC$_{50}$	0.0006	10	mortality	A	10	0.000006	Lekamge et al. (2018)
I	*Daphnia carinata*	neonates	ASTM	SR24	48	EC$_{10}$	0.0009	2	immobilisation	A	10	0.00004	Lekamge et al. (2019)
I	*Daphnia magna*	neonates	Elendt SM7	S	48	LC$_{50}$	0.0025	2	mortality	A	10	0.00003	Zhao and Wang (2011)
I	*Daphnia magna*	neonates	Elendt M4	SR	48	EC$_{10}$	0.0017	2	immobilisation	A	10	0.00009	Asghari et al. (2012)
I	*Daphnia magna*	neonates	ASTM (+) food	S	24	EC$_{50}$	0.002	10	feeding	C	1	0.0002	Ribeiro et al. (2014)
I	*Daphnia magna*	neonates	ASTM (-) no food	SR24	504	EC$_{50}$	0.0004	10	reproduction	C	1	0.00004	Ribeiro et al. (2014)
I	*Daphnia magna*	neonates	ASTM pH 6.5 (-) DOM	S	48	EC$_{50}$	0.0017	10	immobilisation	A	10	0.00002	Seitz et al. (2015)
I	*Daphnia magna*	neonates	ASTM pH 6.5 (+) DOM	S	48	EC$_{50}$	0.0017	10	immobilisation	A	10	0.00002	Seitz et al. (2015)
I	*Daphnia magna*	neonates	ASTM pH 8 (-) DOM	S	48	EC$_{50}$	0.0019	10	immobilisation	A	10	0.00002	Seitz et al. (2015)

Organism			Exposure					Assessment Factor (AF)					Reference
Type	Species	Life stage	Medium	Type	Length (h)	End-point	Value (mg L^{-1})	1st AF	Parameter	Study	2nd AF	Final value	
I	*Daphnia magna*	neonates	ASTM pH 8 (+) DOM	S	48	EC$_{50}$	0.003	10	immobilisation	A	10	0.00003	Seitz et al. (2015)
I	*Daphnia magna*	neonates	Elendt SM4	S	8	LC$_{50}$	0.0008	10	mortality	A	10	0.000008	Shen et al. (2015)
I	*Daphnia magna*	neonates	Elendt M7	S	48	EC$_{50}$	0.0008	10	mortality	A	10	0.000008	Mackevica et al. (2015)
I	*Daphnia magna*	neonates	OECD 202	S	48	EC$_{50}$	0.001	10	immobilisation	A	10	0.00001	Heinlaan et al. (2016)
I	*Daphnia magna*	neonates	Lake Greifen	S	48	EC$_{50}$	0.002	10	immobilisation	A	10	0.00002	Heinlaan et al. (2016)
I	*Daphnia magna*	neonates	Lake Lucerne	S	48	EC$_{50}$	0.0007	10	immobilisation	A	10	0.000007	Heinlaan et al. (2016)
I	*Daphnia magna*	neonates	ADaM	S	48	EC$_{50}$	0.002	10	immobilisation	A	10	0.00002	Heinlaan et al. (2016)
I	*Daphnia magna*	neonates	Lake Greifen 2014	S	48	EC$_{50}$	0.001	10	immobilisation	A	10	0.00001	Heinlaan et al. (2016)
I	*Daphnia magna*	neonates	Lake Greifen 2015	S	48	EC$_{50}$	0.0007	10	immobilisation	A	10	0.000007	Heinlaan et al. (2016)
I	*Daphnia magna*	neonates	Lake Lucerne 2014	S	48	EC$_{50}$	0.0006	10	immobilisation	A	10	0.000006	Heinlaan et al. (2016)
I	*Daphnia magna*	neonates	Lake Lucerne 2015	S	48	EC$_{50}$	0.0008	10	immobilisation	A	10	0.000008	Heinlaan et al. (2016)
I	*Daphnia magna*	neonates	Elendt M7	S	48	EC$_{50}$	0.004	10	immobilisation	A	10	0.00004	Sørensen et al. (2016)
I	*Daphnia magna*	neonates	Elendt M7	3h pulse	48	EC$_{50}$	0.004	10	immobilisation	A	10	0.00004	Sørensen et al. (2016)
I	*Daphnia magna*	neonates	Elendt M4	S	48	EC$_{50}$	0.002	10	mortality	A	10	0.00002	Hu et al. (2018)
I	*Daphnia magna*	neonates	OECD 202	S	48	LC$_{50}$	0.001	10	immobilisation	A	10	0.00001	Khoshnamvand et al. (2020)
I	*Daphnia magna*	neonates	LTW	S	48	LC$_{50}$	0.0006	10	mortality	A	10	0.000006	Erickson et al. (1998)
I	*Daphnia magna*	neonates	St. Louis river	S	48	LC$_{50}$	0.035	10	mortality	A	10	0.0004	Erickson et al. (1998)
I	*Daphnia magna*	neonates	tap water	SR24	48	LC$_{50}$	0.0003	10	mortality	A	10	0.000003	Bianchini et al. (2002)

Organism			Exposure					Assessment Factor (AF)					Reference
Type	Species	Life stage	Medium	Type	Length (h)	End-point	Value (mg L^{-1})	1st AF	Parameter	Study	2nd AF	Final value	
I	*Daphnia magna*	neonates	Hard water	SR	504	NOEC	0.002	1	dry wt	C	1	0.002	Naddy et al. (2007a)
I	*Daphnia magna*	neonates	MHW	SR24	48	LC$_{50}$	0.007	10	mortality	A	10	0.00007	Bianchini and Wood (2008)
I	*Daphnia magna*	adults	MHW	SR24	504	LC$_{20}$	0.002	2	mortality	A	10	0.0001	Bianchini and Wood (2008)
I	*Daphnia magna*	neonates	MHRW	SR	48	LC$_{50}$	0.0011	10	mortality	A	10	0.00001	Allen et al. (2010)
I	*Daphnia magna*	neonates	MHRW	S	48	LC$_{50}$	0.0007	10	mortality	A	10	0.000007	Kennedy et al. (2010)
I	*Daphnia magna*	neonates	SSF	S	48	LC$_{50}$	0.002	10	mortality	A	10	0.00002	Li et al. (2010)
I	*Daphnia magna*	neonates	Elendt M4	S	48	EC$_{50}$	0.0005	10	mortality	A	10	0.000005	Kim et al. (2011)
I	*Daphnia magna*	neonates	Elendt M4	SR24	48	EC$_{10}$	0.0017	2	mortality	A	10	0.00009	Asghari et al. (2012)
I	*Daphnia magna*	adults	Lake Superior (UV treated)	SR24	48	LC$_{50}$	0.001	10	mortality	A	10	0.00001	Hoheisel et al. (2012)
I	*Daphnia magna*	adults	MHRW	S	24	LC$_{50}$	0.0004	10	mortality	A	10	0.000004	Poynton et al. (2012)
I	*Daphnia magna*	neonates	AFW	S	48	EC$_{50}$	0.0022	10	mortality	A	10	0.00002	Blinova et al. (2013)
I	*Daphnia magna*	neonates	River 1	S	48	EC$_{50}$	0.012	10	mortality	A	10	0.0001	Blinova et al. (2013)
I	*Daphnia magna*	neonates	River 2	S	48	EC$_{50}$	0.016	10	mortality	A	10	0.0002	Blinova et al. (2013)
I	*Daphnia magna*	neonates	Lake 1	S	48	EC$_{50}$	0.008	10	mortality	A	10	0.00008	Blinova et al. (2013)
I	*Daphnia magna*	neonates	Lake 2	S	48	EC$_{50}$	0.013	10	mortality	A	10	0.0001	Blinova et al. (2013)
I	*Daphnia magna*	neonates	Lake 3	S	48	EC$_{50}$	0.007	10	mortality	A	10	0.00007	Blinova et al. (2013)
I	*Daphnia magna*	neonates	ADaM	S	48	EC$_{50}$	0.0014	10	immobilisation	A	10	0.00001	Jemec et al. (2016)
I	*Daphnia magna*	neonates	OECD 202	S	48	EC$_{50}$	0.001	10	immobilisation	A	10	0.00001	Jemec et al. (2016)

Organism			Exposure					Assessment Factor (AF)					Reference
Type	Species	Life stage	Medium	Type	Length (h)	End-point	Value (mg L^{-1})	1st AF	Parameter	Study	2nd AF	Final value	
I	*Daphnia magna*	neonates	Elendt M7	S	48	EC$_{10}$	0.04	2	immobilisation	A	10	0.002	Cupi et al. (2016)
I	*Daphnia pulex*	adult	FDTW	SR	48	LC$_{50}$	0.008	10	mortality	A	10	0.00008	Griffitt et al. (2008)
I	*Elliptio complanata*	adults	tap water	S	48	MATC	0.004	1	LPO (gills)	C	1	0.004	Gagné et al. (2013)
I	*Gammarus fossarum*	*G.f1*	Volvic®	SR24	72	LC$_{50}$	0.004	10	mortality	A	10	0.00004	Mehennaoui et al. (2016)
I	*Gammarus fossarum*	*G.f2*	Volvic®	SR24	72	LC$_{50}$	0.002	10	mortality	A	10	0.00002	Mehennaoui et al. (2016)
I	*Hyalella azteca*	juveniles	Soft water	CR	240	LC$_{50}$	0.005	10	mortality	A	10	0.00005	Call et al. (2006)
I	*Hyalella azteca*	juveniles	New River	SR	480	NOEC	0.001	1	mortality	A	10	0.0001	Diamond et al. (1990)
I	*Moina macrocopa*	neonates	OECD	S	48	EC$_{50}$	0.026	10	immobilisation	A	10	0.0003	Hiriart-Baer et al. (2006)
I	*Physa acuta*	embryos (2–4 d)	APW	SR	312	EC$_{50}$	0.001	10	hatching	A	10	0.00001	Goncalves et al. (2017)
I	*Physa acuta*	juveniles	APW	SR	96	LC$_{50}$	0.046	10	mortality	A	10	0.0005	Goncalves et al. (2017)
I	*Physa acuta*	juveniles	MAPW	SR	96	LC$_{50}$	0.0274	10	mortality	A	10	0.0003	Goncalves et al. (2017)
I	*Physa acuta*	adults	APW	SR	96	LC$_{50}$	0.74	10	mortality	A	10	0.007	Goncalves et al. (2017)
I	*Physa acuta*	adults	MAPW	SR	96	LC$_{50}$	0.116	10	mortality	A	10	0.0012	Goncalves et al. (2017)
I	*Thamnocephalus platyurus*	larvae	AFW	S	24	LC$_{50}$	0.0057	10	mortality	A	10	0.00006	Blinova et al. (2013)
I	*Thamnocephalus platyurus*	larvae	River 1	S	24	LC$_{50}$	0.001	10	mortality	A	10	0.00001	Blinova et al. (2013)
I	*Thamnocephalus platyurus*	larvae	Lake 1	S	24	LC$_{50}$	0.012	10	mortality	A	10	0.0001	Blinova et al. (2013)
I	*Thamnocephalus platyurus*	larvae	Lake 2	S	24	LC$_{50}$	0.024	10	mortality	A	10	0.0002	Blinova et al. (2013)
V	*Barbonymus gonionotus*	juveniles	OECD 203	S	48	LC$_{50}$	0.057	10	mortality	A	10	0.0006	Yoo-iam et al. (2015)

Organism			Exposure					Assessment Factor (AF)					Reference
Type	Species	Life stage	Medium	Type	Length (h)	End-point	Value (mg L^{-1})	1st AF	Parameter	Study	2nd AF	Final value	
V	*Cirrhinus mrigala*	fingerlings	DTW	S	96	LC$_{50}$	0.11	10	mortality	A	10	0.001	Sathya et al. (2012)
V	*Cyprinus carpio*	juveniles	tap water	S	96	LC$_{50}$	0.15	10	mortality	A	10	0.002	Khosravi-Katuli et al. (2018)
V	*Danio rerio*	embryos	CFW+IOSSS	S	96	LC$_{50}$	0.078	10	mortality	A	10	0.0008	Ribeiro et al. (2014)
V	*Danio rerio*	embryos	RTM(DSW)	S	96	EC$_{50}$	0.079	10	mortality	A	10	0.0008	Wang et al. (2012)
V	*Danio rerio*	embryos	ISO medium 2015	SR24	96	LC$_{50}$	0.032	10	mortality	A	10	0.0003	Heinlaan et al. (2016)
V	*Danio rerio*	embryos	Lake Greifen 2015	SR24	96	LC$_{50}$	0.015	10	mortality	A	10	0.0002	Heinlaan et al. (2016)
V	*Danio rerio*	embryos	Lake Lucerne 2015	SR24	96	LC$_{50}$	0.016	10	mortality	A	10	0.0002	Heinlaan et al. (2016)
V	*Danio rerio*	embryos	OECD 202	S	96	LC$_{50}$	0.0047	10	mortality	A	10	0.00005	Khoshnamvand et al. (2020)
V	*Danio rerio*	adults	FDTW	SR	48	LC$_{50}$	0.022	10	mortality	A	10	0.0002	Griffitt et al. (2008)
V	*Danio rerio*	adults	DDW+ NaCl	SR	48	LC$_{50}$	0.025	10	mortality	A	10	0.0003	Bilberg et al. (2012)
V	*Danio rerio*	embryos	DTW	S	96	LC$_{50}$	0.07	10	mortality	A	10	0.0007	Massarsky et al. (2013)
V	*Danio rerio*	adults	Soft water (10 μM Cl^{-})	SR48	96	LC$_{50}$	0.01	10	mortality	A	10	0.0001	Bielmyer et al. (2008)
V	*Danio rerio*	adults	Soft water (1 mM KCl)	SR48	96	LC$_{50}$	0.011	10	mortality	A	10	0.0001	Bielmyer et al. (2008)
V	*Danio rerio*	embryos	ISO medium	SR	48	EC$_{50}$	0.07	10	mortality	A	10	0.0007	Muth-Kohne et al. (2013)
V	*Danio rerio*	embryos	ROW	SR	72	EC$_{50}$	0.14	10	hatching	A	10	0.001	Gao et al. (2015)
V	*Danio rerio*	embryos	ISO medium	S	48	LC$_{50}$	0.032	10	mortality	A	10	0.0003	Jemec et al. (2016)
V	*Danio rerio*	embryos	tap water	S	120	LC$_{50}$	0.047	10	mortality	A	10	0.0005	Lacave et al. (2016)
V	*Danio rerio*	ELS	DTW	S	120	LC$_{50}$	0.06	10	mortality	A	10	0.0006	Boyle and Goss (2018)

190

Organism			Exposure					Assessment Factor (AF)					Reference
Type	Species	Life stage	Medium	Type	Length (h)	End-point	Value (mg L^{-1})	1st AF	Parameter	Study	2nd AF	Final value	
V	*Danio rerio*	embryos	tap water	SR24	96	EC$_{50}$	0.0013	10	mortality	A	10	0.00001	Xin et al. (2015)
V	*Danio rerio*	embryos	DTW	SR24	96	NOEC	0.04	1	mortality	A	10	0.004	Pereira et al. (2023) unpublished
V	*Jordanella floridae*	juveniles	Lake superior	S	96	LC$_{50}$	0.009	10	mortality	A	10	0.00009	Lima et al. (1982)
V	*Oncorhynchus mykiss*	juveniles	DTW	SR24	168	LC$_{50}$	0.009	10	mortality	A	10	0.00009	Hogstrand et al. (1996)
V	*Oncorhynchus mykiss*	juveniles	50 Cl$^-$ + 50 Ca^{2+}+ 0.3 DOC	SR	96	LC$_{50}$	0.007	10	mortality	A	10	0.00007	Bury et al. (1999)
V	*Oncorhynchus mykiss*	juveniles	250 Cl$^-$ + 50 Ca^{2+}+ 0.3 DOC	SR	96	LC$_{50}$	0.008	10	mortality	A	10	0.00008	Bury et al. (1999)
V	*Oncorhynchus mykiss*	juveniles	800 Cl$^-$ + 50 Ca^{2+}+ 0.3 DOC	SR	96	LC$_{50}$	0.008	10	mortality	A	10	0.00008	Bury et al. (1999)
V	*Oncorhynchus mykiss*	juveniles	1500 Cl$^-$ + 50 Ca^{2+}+ 0.3 DOC	SR	96	LC$_{50}$	0.009	10	mortality	A	10	0.00009	Bury et al. (1999)
V	*Oncorhynchus mykiss*	juveniles	50 Cl$^-$ + 500 Ca^{2+} + 0.3 DOC	SR	96	LC$_{50}$	0.008	10	mortality	A	10	0.00008	Bury et al. (1999)
V	*Oncorhynchus mykiss*	juveniles	50 Cl$^-$ + 2000 Ca^{2+} + 0.3 DOC	SR	96	LC$_{50}$	0.01	10	mortality	A	10	0.0001	Bury et al. (1999)
V	*Oncorhynchus mykiss*	juveniles	50 Cl$^-$ + 50 Ca^{2+}+ 1.6 DOC	SR	96	LC$_{50}$	0.013	10	mortality	A	10	0.0001	Bury et al. (1999)
V	*Oncorhynchus mykiss*	juveniles	50 Cl$^-$ + 50 Ca^{2+}+ 5.8 DOC	SR	96	LC$_{50}$	0.018	10	mortality	A	10	0.0002	Bury et al. (1999)
V	*Oncorhynchus mykiss*	adults	MHW	FT	168	LC$_{50}$	0.01	10	mortality	A	10	0.0001	Wood et al. (1996)
V	*Oryzias latipes*	adults	FCW	S	96	LC$_{50}$	0.021	10	mortality	A	10	0.0002	Kim et al. (2011)
V	*Pimephales promelas*	juveniles	Lake Superior	S	96	LC$_{50}$	0.011	10	mortality	A	10	0.0001	Lima et al. (1982)
V	*Pimephales promelas*	juveniles	50 Cl$^-$ + 50 Ca^{2+}+ 0.3 DOC	SR	96	LC$_{50}$	0.0075	10	mortality	A	10	0.00008	Bury et al. (1999)
V	*Pimephales promelas*	juveniles	250 Cl$^-$ + 50 Ca^{2+}+ 0.3 DOC	SR	96	LC$_{50}$	0.009	10	mortality	A	10	0.00009	Bury et al. (1999)
V	*Pimephales promelas*	juveniles	800 Cl$^-$ + 50 Ca^{2+}+ 0.3 DOC	SR	96	LC$_{50}$	0.019	10	mortality	A	10	0.0002	Bury et al. (1999)

Organism			Exposure					Assessment Factor (AF)					Reference
Type	Species	Life stage	Medium	Type	Length (h)	End-point	Value (mg L^{-1})	1st AF	Parameter	Study	2nd AF	Final value	
V	*Pimephales promelas*	juveniles	1500 Cl$^-$ + 50 Ca^{2+}+ 0.3 DOC	SR	96	LC$_{50}$	0.026	10	mortality	A	10	0.0003	Bury et al. (1999)
V	*Pimephales promelas*	juveniles	50 Cl$^-$ + 500 Ca^{2+}+ 0.3 DOC	SR	96	LC$_{50}$	0.0099	10	mortality	A	10	0.0001	Bury et al. (1999)
V	*Pimephales promelas*	juveniles	50 Cl$^-$ + 2000 Ca^{2+}+ 0.3 DOC	SR	96	LC$_{50}$	0.0105	10	mortality	A	10	0.0001	Bury et al. (1999)
V	*Pimephales promelas*	juveniles	50 Cl$^-$ + 50 Ca^{2+}+ 1.6 DOC	SR	96	LC$_{50}$	0.018	10	mortality	A	10	0.0002	Bury et al. (1999)
V	*Pimephales promelas*	juveniles	50 Cl$^-$ + 50 Ca^{2+}+ 5.8 DOC	SR	96	LC$_{50}$	0.028	10	mortality	A	10	0.0003	Bury et al. (1999)
V	*Pimephales promelas*	juveniles	LTW	SR48	96	LC$_{50}$	0.01	10	mortality	A	10	0.0001	Erickson et al. (1998)
V	*Pimephales promelas*	juveniles	St. Louis River	SR48	96	LC$_{50}$	0.11	10	mortality	A	10	0.001	Erickson et al. (1998)
V	*Pimephales promelas*	embryos	Soft water (10 µM Cl$^-$)	SR48	96	LC$_{50}$	0.0023	10	mortality	A	10	0.00002	Bielmyer et al. (2008)
V	*Pimephales promelas*	embryos	Soft water (1 mM KCl)	SR48	96	LC$_{50}$	0.0027	10	mortality	A	10	0.00003	Bielmyer et al. (2008)
V	*Pimephales promelas*	embryos	VHW	S	96	LC$_{50}$	0.015	10	mortality	A	10	0.0002	Laban et al. (2010)
V	*Pimephales promelas*	embryos	Lake Superior (UV treated)	SR24	96	LC$_{50}$	0.0047	10	mortality	A	10	0.00005	Hoheisel et al. (2012)
V	*Pimephales promelas*	embryos	MHRW	S	96	LC$_{50}$	0.0057	10	mortality	A	10	0.00006	Kennedy et al. (2010)
V	*Pimephales promelas*	ELS	HR (NF)	FT	870	EC$_{20}$	0.00045	2	mortality	A	10	0.13	Naddy et al. (2007b)
V	*Pimephales promelas*	ELS	HR (HF)	FT	870	EC$_{20}$	0.0003	2	mortality	A	10	0.06	Naddy et al. (2007b)
V	*Pimephales promelas*	ELS	HR (NF)	FT	168	EC$_{20}$	0.0003	2	mortality	A	10	0.12	Naddy et al. (2007b)
V	*Pimephales promelas*	embryos	Lake superior	FT	168	NOEC	0.0007	1	growth	A	10	0.00073	Norberg-King (1989)
V	*Pimephales promelas*	embryos	Lake superior	SR	96	LC$_{50}$	0.008	10	mortality	A	10	0.000082	Norberg-King (1989)

Type of organism: C=Cyanobacteria; M = Microalgae; P = Plant; I = Invertebrates; V = Vertebrates

Life-stage: EGP**=** exponential growth phase; ELS= early-life stages; embryos = embryos (< 24 hpf); neonates = neonates (<24h old)

MEDIUM: 50 Cl^- + 50 Ca^{2+} + 0.3 DOC =50 µM (Cl) + 50 µM (Ca) + 0.3 mg/L (DOC); 250 Cl^- + 50 Ca^{2+} + 0.3 DOC =250 µM (Cl) + 50 µM (Ca) + 0.3 mg/L (DOC); 800 Cl^- + 50 Ca^{2+} + 0.3 DOC = 800 µM (Cl) + 50 µM (Ca) +0.3 mg/L (DOC); 1500 Cl^- + 50 Ca^{2+} + 0.3 DOC = 1500 µM (Cl) + 50 µM (Ca) +0.3 mg/L (DOC); 50 Cl^- + 500 Ca^{2+} + 0.3 DOC = 50 µM (Cl) : 500 µM (Ca): 0.3 mg/L (DOC); 50 Cl^- + 2000 Ca^{2+} + 0.3 DOC= 50 µM (Cl) : 2000 µM (Ca): 0.3 mg/L (DOC); 50 Cl^- + 50 Ca^{2+} + 1.6 DOC = 50 µM (Cl) : 50 µM (Ca): 1.6 mg/L (DOC); 50 Cl^- + 50 Ca^{2+} + 5.8 DOC = 50 µM (Cl) : 50 µM (Ca): 5.8 mg/L (DOC); ADaM = Aachener Daphnienmedium; AFW = Artificial Fresh water; APW = Artificial Pond Water; BBM = Bold's Basal medium; CFW+IOSSS =Carbon-filtered water + salt "Instant Ocean Synthetic Sea Salt"; DeioW + WCL-1 = Deionized water with WCL-1 salts (pH = 7); DOC = dissolved organic carbon; DTW = Dechlorinated tap water; FCW = Fish culture water; DDW+ NaCl = Demineralised and dechlorinated water (16:1) plus NaCl (132 mg/L); FDTW = Filtered (0.45 µm) DTW; HR(NF) = Horsetooth reservoir (normal flow); HR(HF) Horsetooth reservoir (high flow); LTW = Laboratory test water; MAPW = Modified APW; MBL medium = Woods Hole; MHW = Moderately hard water; MHRW = Moderately hard reconstituted water; MHSM= Modified high salt medium; ROW = Reverse Osmosis water; RTM(DSW) = Reconstituted test medium (Dutch standard water); SFW = Synthetic fresh water; SGM = Standard growth medium; SM7 = Simplified M7 medium; SSF = Standard synthetic freshwater; VHW = Very hard water

EXPOSURE: CR= continuous renewal; FT= flow-through; SR= static renewal; SR24= static-renewal (24h); SR48= static-renewal (48h)

PARAMETERS: GRI= Growth rate inhibition; NN = nitrate-nitrogen; LPO = lipid peroxidation; PEI= Photosynthetic efficiency inhibition; PII= photosystem II; PY= Photosynthetic yield; wt = weight

Study: A = Acute; C = Chronic

Table 6-XIV – Data used in the SSD analysis for spherical particles of Ag ENMs

Species			ENMs				Exposure					Assessment Factor (AF)					Reference
Type	Name	Stage	Size	Surface coating	Origin	State	Medium	Type	Time (h)	End-point	Value (mgL^{-1})	1st AF	Parameter	Stu-dy	2nd AF	Final value	
M	*Chlamydomo-nas reinhardtii*	EGP	25 ± 13	carbo-nate	NanoSys	S	MOPS (pH 7.5)	S	5	EC_{50}	0.089	10	PY (PII)	A	10	0.0009	Navarro et al. (2008)
M	*Chlamydomo-nas reinhardtii*	EGP	84 ± 40	PVP	NanoSys	S	SGM	S	1	EC_{50}	0.085	10	PY (PII)	A	10	0.0009	Navarro et al. (2015)
M	*Chlamydomo-nas reinhardtii*	EGP	70 ± 8	PEG	NanoSys	S	SGM	S	1	EC_{50}	0.13	10	PY (PII)	A	10	0.0013	Navarro et al. (2015)
M	*Chlamydomo-nas reinhardtii*	EGP	45 ± 3	SDBS	NanoSys	S	SGM	S	1	EC_{50}	0.41	10	PY (PII)	A	10	0.0041	Navarro et al. (2015)
M	*Chlamydomo-nas reinhardtii*	EGP	35 ± 15	lactate	NanoSys	S	SGM	S	1	EC_{50}	0.22	10	PY (PII)	A	10	0.0022	Navarro et al. (2015)
M	*Chlamydomo-nas reinhardtii*	EGP	52 ± 3	gelatin	NanoSys	S	SGM	S	1	EC_{50}	0.51	10	PY (PII)	A	10	0.005	Navarro et al. (2015)
M	*Chlamydomo-nas reinhardtii*	EGP	456 ± 200	dexpan-thenol	NanoSys	S	SGM	S	1	EC_{50}	0.030	10	PY (PII)	A	10	0.0003	Navarro et al. (2015)
M	*Chlamydomo-nas reinhardtii*	EGP	17 ± 1	citrate	NanoSys	S	SGM	S	1	EC_{50}	0.566	10	PY (PII)	A	10	0.0057	Navarro et al. (2015)
M	*Chlamydomo-nas reinhardtii*	EGP	25 ± 2	chitosan	NanoSys	S	SGM	S	1	EC_{50}	0.35	10	PY (PII)	A	10	0.0035	Navarro et al. (2015)
M	*Chlamydomo-nas reinhardtii*	EGP	40 ± 1	carbo-nate	NanoSys	S	SGM	S	1	EC_{50}	0.32	10	PY (PII)	A	10	0.0032	Navarro et al. (2015)
M	*Chlorella vulgaris*	EGP	85 ± 14 (TEM)	bare	Dongyang	P	OECD 201	S	48	EC_{50}	0.89	10	biomass (cells mL^{-1})	A	10	0.009	Yoo-iam et al. (2015)
M	*Chlorella vulgaris*	EGP	49 ± 25 (TEM)	plant extract	synthe-sis	S	OECD 201	S	72	EC_{50}	0.034	10	biomass (cells mL^{-1})	A	10	0.0003	Khoshnamv and et al. (2020)
M	*Chlorella vulgaris*	EGP	20	citric acid	DeKe Nanotech	S	Blue Green 11	S	72	EC_{10}	0.012	2	GRI (cell density)	C	1	0.006	Zhang et al. (2020)
M	*Chlorella vulgaris*	EGP	20	PEI	DeKe Nanotech	S	Blue Green 11	S	72	EC_{10}	0.005	2	GRI (cell density)	C	1	0.0025	Zhang et al. (2020)
M	*Euglena gracilis*	EGP	20	citrate	synthesis	S	Sinfo	S	72	EC_{50}	2.74	10	cell (n)	A	10	0.027	Zhang et al. (2019)
M	*Euglena gracilis*	EGP	60	citrate	synthesis	S	Sinfo	S	72	EC_{50}	5.03	10	cell (n)	A	10	0.05	Zhang et al. (2019)
M	*Euglena gracilis*	EGP	19	citrate	NanoSys	S	Talaquil (pH 7.5)	S	1	EC_{10}	38.3	2	PY	C	1	19.2	Yue et al. (2017)
M	*Raphidocelis subcapitata*	EGP	3-8	alkane	AMEPOX	S	MBL	S	72	EC_{50}	0.0032	10	GRI (cell density)	A	10	0.00003	Ribeiro et al. (2014)
M	*Raphidocelis subcapitata*	EGP	5-25	citrate	ABC Nanotech	S	MM7	S	72	EC_{50}	0.14	10	Yield (cell density)	A	10	0.0014	Sohn et al. (2015)
M	*Raphidocelis subcapitata*	EGP	14	citrate	ABC Nanotech	NA	SFW	S	72	IC_{50}	0.003	10	GRI (cell density)	A	10	0.00003	Angel et al. (2013)
M	*Raphidocelis subcapitata*	EGP	14	PVP	Mercator	NA	SFW	S	72	IC_{50}	0.0195	10	GRI (cell density)	A	10	0.0002	Angel et al. (2013)

Species			ENMs				Exposure					Assessment Factor (AF)					Reference
Type	Name	Stage	Size	Surface coating	Origin	State	Medium	Type	Time (h)	End-point	Value (mgL^{-1})	1st AF	Parameter	Stu-dy	2nd AF	Final value	
M	*Raphidocelis subcapitata*	EGP	<100	bare	Sigma-Aldrich	P	OECD 201	S	72	NOEC	0.85	1	GRI (cell density)	C	1	0.85	Książyk et al. (2015)
M	*Raphidocelis subcapitata*	EGP	25	bare	Quantum Sphere	P	ACTWW	S	96	IC$_{50}$	1.6	10	GRI (chl a)	A	10	0.016	McLaughlin et al. (2012)
M	*Raphidocelis subcapitata*	EGP	25	bare	Quantum Sphere	P	AGCM	S	96	IC$_{50}$	0.0046	10	GRI (chl a)	A	10	0.0001	McLaughlin et al. (2012)
M	*Raphidocelis subcapitata*	EGP	25	bare	Quantum Sphere	P	SFIR	S	96	IC$_{50}$	0.023	10	GRI (chl a)	A	10	0.0002	McLaughlin et al. (2012)
M	*Raphidocelis subcapitata*	EGP	35	bare	NanoAmor	P	RTM (DSW)	S	4.5	EC$_{50}$	120	10	PhEI	A	10	1.2	Wang et al. (2012)
M	*Raphidocelis subcapitata*	EGP	15	Tween 20 + 65	JRC EU	S	RTM (DSW)	S	4.5	EC$_{50}$	0.929	10	PhEI	A	10	0.009	Wang et al. (2012)
M	*Raphidocelis subcapitata*	EGP	80	PVP	NanoAmor	P	RTM (DSW)	S	4.5	EC$_{50}$	4.34	10	PhEI	A	10	0.043	Wang et al. (2012)
M	*Raphidocelis subcapitata*	EGP	20-30	bare	Quantum Sphere	P	FDTW	S	96	LC$_{50}$	0.19	10	GR (chl a)	A	10	0.002	Griffitt et al. (2008)
M	*Raphidocelis subcapitata*	EGP	20 ± 7 (TEM)	PVP	Colorobbia	S	Algal Toxkit F	S	72	EC$_{50}$	0.0086	10	GR (cell density)	A	10	0.0001	Jemec et al. (2016)
M	*Raphidocelis subcapitata*	EGP	15 (SEM)	bare	synthesis	S	OECD 201	S	72	EC$_{50}$	0.015	10	GR (chl)	A	10	0.0002	Hund-Rinke et al. (2018)
M	*Raphidocelis subcapitata*	EGP	15 (SEM)	bare	synthesis	S	OECD 201	S	72	EC$_{50}$	0.081	10	GR (chl)	A	10	0.0008	Hund-Rinke et al. (2018)
P	*Lemna gibba*	EGP	50	bare	MTI	P	MSM	SR 24	168	EC$_{50}$	9.36	10	Frond (n)	A	10	0.094	Oukarroum et al. (2013)
P	*Lemma minor*	EGP	29 ± 11 (TEM)	citrate	synthesis	S	MSM	S	336	EC$_{50}$	0.019	10	GR (dry wt)	C	1	0.002	Gubbins et al. (2011)
P	*Lemma minor*	EGP	94 ± 49 (TEM)	citrate	synthesis	S	MSM	S	336	EC$_{50}$	0.019	10	GR (dry wt)	C	1	0.002	Gubbins et al. (2011)
P	*Spirodela polyrhiza*	EGP	6 ± 2	gum arabic	synthesis	S	10% Hoagland	S	72	EC$_{50}$	4.54	10	NN	C	1	0.45	Jiang et al. (2012
I	*Brachionus calyciflorus*	juveniles	20-30	citrate	NanoSys	S	SFM	S	24	EC$_{10}$	0.0017	2	GR (population)	A	10	0.0009	Martins et al. (2020)
I	*Ceriodaphnia dubia*	neonates	20	citrate	nano Composix	S	FM (MHRW)	S	48	LC$_{50}$	0.0048	10	immobi-lisation	A	10	0.0001	Kennedy et al. (2012)
I	*Ceriodaphnia dubia*	neonates	20	citrate	nano Composix	S	OM (30d NPs)	S	48	LC$_{50}$	0.003	10	immobi-lisation	A	10	0.00003	Kennedy et al. (2012)
I	*Ceriodaphnia dubia*	neonates	100	citrate	nano Composix	S	FM (MHRW)	S	48	LC$_{50}$	0.027	10	immobi-lisation	A	10	0.0003	Kennedy et al. (2012)
I	*Ceriodaphnia dubia*	neonates	100	citrate	nano Composix	S	OM (30d NPs)	S	48	LC$_{50}$	0.0088	10	immobi-lisation	A	10	0.0001	Kennedy et al. (2012)
I	*Ceriodaphnia dubia*	neonates	25	bare	Quantum Sphere	P	ACTWW	S	48	LC$_{50}$	0.22	10	mortality	A	10	0.002	McLaughlin et al. (2012)
I	*Ceriodaphnia dubia*	neonates	25	bare	Quantum Sphere	P	MHW	S	48	LC$_{50}$	0.0005	10	mortality	A	10	0.00001	McLaughlin et al. (2012)
I	*Ceriodaphnia dubia*	neonates	25	bare	Quantum Sphere	P	SFIR	S	48	LC$_{50}$	0.0004	10	mortality	A	10	0.000004	McLaughlin et al. (2012)

	Species			ENMs				Exposure					Assessment Factor (AF)					
Type	Name	Stage	Size	Surface coating	Origin	State	Medium	Type	Time (h)	End-point	Value (mgL⁻¹)	1st AF	Parameter	Study	2nd AF	Final value	Reference
I	*Ceriodaphnia dubia*	neonates	14	citrate	ABC Nanotech	NA	SFW	S	48	LC_{50}	0.00015	10	mortality	A	10	0.000002	Angel et al. (2013)
I	*Ceriodaphnia dubia*	neonates	15	PVP	Mercator	NA	SFW	S	48	LC_{50}	0.002	10	mortality	A	10	0.00002	Angel et al. (2013)
I	*Ceriodaphnia dubia*	neonates	20-30	bare	Quantum Sphere	P	FDTW	SR	48	LC_{50}	0.067	10	immobi-lisation	A	10	0.0007	Griffitt et al. (2008)
I	*Ceriodaphnia dubia*	neonates	20-30	metal oxide	synthesis	S	MHW	S	48	LC_{50}	0.046	10	immobi-lisation	A	10	0.0005	(Gao et al., 2009)
I	*Chydorus sphaericus*	neonates	35	bare	NanoAmor	P	RTM (DSW)	S	48	EC_{50}	0.13	10	immobi-lisation	A	10	0.001	Wang et al. (2012)
I	*Chydorus sphaericus*	neonates	15	Tween 20 + 65	JRC EU	S	RTM (DSW)	S	48	EC_{50}	0.049	10	immobi-lisation	A	10	0.0005	Wang et al. (2012)
I	*Chydorus sphaericus*	neonates	80	PVP	NanoAmor	P	RTM (DSW)	S	48	EC_{50}	0.037	10	immobi-lisation	A	10	0.0004	Wang et al. (2012)
I	*Daphnia carinata*	neonates	30 (TEM)	tyrosine	synthesis	S	ASTM	SR	48	LC_{50}	0.035	10	mortality	A	10	0.0004	Lekamge et al. (2018)
I	*Daphnia carinata*	neonates	14 ± 1 (TEM)	curcumin	synthesis	S	ASTM	SR 24	48	EC_{10}	0.015	2	immobi-lisation	A	10	0.0008	Lekamge et al. (2019)
I	*Daphnia carinata*	neonates	9± 1 (TEM)	EGCG	synthesis	S	ASTM	SR 24	48	EC_{10}	0.0105	2	immobi-lisation	A	10	0.0005	Lekamge et al. (2019)
I	*Daphnia carinata*	neonates	11 ± 2 (TEM)	tyrosine	synthesis	S	ASTM	SR 24	48	EC_{10}	0.034	2	immobi-lisation	A	10	0.002	Lekamge et al. (2019)
I	*Daphnia magna*	neonates	35	bare	NanoAmor	P	RHW	SR	96	NOEC	0.01	1	mortality	A	10	0.001	Gaiser et al. (2011)
I	*Daphnia magna*	neonates	220	carbonate	NanoSys	S	SM7	S	504	NOEC	0.005	1	NLP	C	1	0.005	Zhao et al. (2011)
I	*Daphnia magna*	neonates	5-25	citrate	ABC Nanotech	S	Elendt M4	SR	48	EC_{10}	0.003	2	immobi-lisation	A	10	0.0002	Asghari et al. (2012)
I	*Daphnia magna*	neonates	17	bare	Nanocid	S	Elendt M4	SR	48	EC_{10}	0.0015	2	immobi-lisation	A	10	0.0001	Asghari et al. (2012)
I	*Daphnia magna*	neonates	20	bare	Hongwu Nanometer	P	Elendt M4	SR	48	EC_{10}	0.014	2	immobi-lisation	A	10	0.0007	Asghari et al. (2012)
I	*Daphnia magna*	neonates	3-8	alkane	AMEPOX	P	ASTM (-) no food	S	48	EC_{50}	0.011	10	immobi-lisation	A	10	0.0001	Ribeiro et al. (2014)
I	*Daphnia magna*	neonates	3-8	alkane	AMEPOX	P	ASTM (+) food	S	48	EC_{50}	0.0034	10	immobi-lisation	A	10	0.00003	Ribeiro et al. (2014)
I	*Daphnia magna*	neonates	3-8	alkane	AMEPOX	P	ASTM (-) no food	SR 24	504	EC_{50}	0.001	10	immobi-lisation	C	1	0.0001	Ribeiro et al. (2014)
I	*Daphnia magna*	neonates	5-25	citrate	ABC Nanotech	S	Elendt M7	S	48	EC_{10}	0.007	2	immobi-lisation	A	10	0.0004	Sohn et al. (2015)
I	*Daphnia magna*	neonates	140	bare	Io.Li.Tec	P	ASTM pH 6.5 (-) DOM	S	48	EC_{50}	0.0039	10	immobi-lisation	A	10	0.00004	Seitz et al. (2015)
I	*Daphnia magna*	neonates	20	citrate	Sigma-Aldrich	S	ASTM pH 6.5 (-) DOM	S	48	EC_{50}	0.029	10	immobi-lisation	A	10	0.0003	Seitz et al. (2015)

196

Species			ENMs				Exposure					Assessment Factor (AF)					Reference
Type	Name	Stage	Size	Surface coating	Origin	State	Medium	Type	Time (h)	End-point	Value (mgL^{-1})	1st AF	Parameter	Study	2nd AF	Final value	
I	*Daphnia magna*	neonates	30	citrate	synthesis	S	ASTM pH 6.5 (-) DOM	S	48	EC$_{50}$	0.126	10	immobi-lisation	A	10	0.001	Seitz et al. (2015)
I	*Daphnia magna*	neonates	60	citrate	Sigma-Aldrich	S	ASTM pH 6.5 (-) DOM	S	48	EC$_{50}$	0.078	10	immobi-lisation	A	10	0.0008	Seitz et al. (2015)
I	*Daphnia magna*	neonates	100	citrate	Sigma-Aldrich	S	ASTM pH 6.5 (-) DOM	S	48	EC$_{50}$	0.216	10	immobi-lisation	A	10	0.002	Seitz et al. (2015)
I	*Daphnia magna*	neonates	140	bare	Io.Li.Tec	P	ASTM pH 6.5 (+) DOM	S	48	EC$_{50}$	0.033	10	immobi-lisation	A	10	0.0003	Seitz et al. (2015)
I	*Daphnia magna*	neonates	20	citrate	Sigma-Aldrich	S	ASTM pH 6.5 (+) DOM	S	48	EC$_{50}$	0.35	10	immobi-lisation	A	10	0.004	Seitz et al. (2015)
I	*Daphnia magna*	neonates	30	citrate	synthesis	S	ASTM pH 6.5 (+) DOM	S	48	EC$_{50}$	0.11	10	immobi-lisation	A	10	0.001	Seitz et al. (2015)
I	*Daphnia magna*	neonates	140	bare	Io.Li.Tec	P	ASTM pH 8 (-) DOM	S	48	EC$_{50}$	0.0081	10	immobi-lisation	A	10	0.0001	Seitz et al. (2015)
I	*Daphnia magna*	neonates	20	citrate	Sigma-Aldrich	S	ASTM pH 8 (-) DOM	S	48	EC$_{50}$	0.081	10	immobi-lisation	A	10	0.0008	Seitz et al. (2015)
I	*Daphnia magna*	neonates	30	citrate	synthesis	S	ASTM pH 8 (-) DOM	S	48	EC$_{50}$	0.374	10	immobi-lisation	A	10	0.004	Seitz et al. (2015)
I	*Daphnia magna*	neonates	60	citrate	Sigma-Aldrich	S	ASTM pH 8 (-) DOM	S	48	EC$_{50}$	0.0916	10	immobi-lisation	A	10	0.0009	Seitz et al. (2015)
I	*Daphnia magna*	neonates	100	citrate	Sigma-Aldrich	S	ASTM pH 8 (-) DOM	S	48	EC$_{50}$	0.186	10	immobi-lisation	A	10	0.002	Seitz et al. (2015)
I	*Daphnia magna*	neonates	140	bare	Io.Li.Tec	P	ASTM pH 8 (+) DOM	S	48	EC$_{50}$	0.019	10	immobi-lisation	A	10	0.0002	Seitz et al. (2015)
I	*Daphnia magna*	neonates	10	citrate	Sigma-Aldrich	S	SM4	S	8	LC$_{50}$	0.005	10	mortality	A	10	0.0001	Shen et al. (2015)
I	*Daphnia magna*	neonates	20	citrate	Sigma-Aldrich	S	SM4	S	8	LC$_{50}$	0.0164	10	mortality	A	10	0.0002	Shen et al. (2015)
I	*Daphnia magna*	neonates	40	citrate	Sigma-Aldrich	S	SM4	S	8	LC$_{50}$	0.0063	10	mortality	A	10	0.0001	Shen et al. (2015)
I	*Daphnia magna*	neonates	60	citrate	Sigma-Aldrich	S	SM4	S	8	LC$_{50}$	0.039	10	mortality	A	10	0.0004	Shen et al. (2015)
I	*Daphnia magna*	neonates	100	citrate	Sigma-Aldrich	S	SM4	S	8	LC$_{50}$	0.103	10	mortality	A	10	0.001	Shen et al. (2015)

Species			ENMs				Exposure					Assessment Factor (AF)					Reference
Type	Name	Stage	Size	Surface coating	Origin	State	Medium	Type	Time (h)	End-point	Value (mgL⁻¹)	1st AF	Parameter	Stu-dy	2nd AF	Final value	
I	*Daphnia magna*	neonates	10	PVP	synthesis	S	SM4	S	8	LC₅₀	0.117	10	mortality	A	10	0.001	Shen et al. (2015)
I	*Daphnia magna*	neonates	28	PVP	synthesis	S	SM4	S	8	LC₅₀	0.14	10	mortality	A	10	0.001	Shen et al. (2015)
I	*Daphnia magna*	neonates	30	citric acid	Cline Scientific	S	Elendt M7 no food	S	48	EC₅₀	0.048	10	mortality	A	10	0.0005	Mackevica et al. (2015)
I	*Daphnia magna*	neonates	30	citric acid	Cline Scientific	S	Elendt M7 low food	S	48	EC₅₀	0.18	10	mortality	A	10	0.002	Mackevica et al. (2015)
I	*Daphnia magna*	neonates	30	citric acid	Cline Scientific	S	Elendt M7 high food	S	48	EC₅₀	0.3	10	mortality	A	10	0.003	Mackevica et al. (2015)
I	*Daphnia magna*	neonates	20-30	citrate	Cline Scientific	S	Elendt M7	SR 72	504	NOEC	0.0096	1	broods (n)	C	1	0.01	Sakka et al. (2016)
I	*Daphnia magna*	neonates	21	PVP	Colorobbia	S	OECD 202	S	48	EC₅₀	0.003	10	immobi-lisation	A	10	0.00003	Heinlaan et al. (2016)
I	*Daphnia magna*	neonates	21	PVP	Colorobbia	S	Lake Greifen	S	48	EC₅₀	0.0022	10	immobi-lisation	A	10	0.00002	Heinlaan et al. (2016)
I	*Daphnia magna*	neonates	21	PVP	Colorobbia	S	Lake Lucerne	S	48	EC₅₀	0.001	10	immobi-lisation	A	10	0.00001	Heinlaan et al. (2016)
I	*Daphnia magna*	neonates	21	PVP	Colorobbia	S	ADaM	S	48	EC₅₀	0.0034	10	immobi-lisation	A	10	0.00003	Heinlaan et al. (2016)
I	*Daphnia magna*	neonates	21	PVP	Colorobbia	S	Lake Greifen 2014	S	48	EC₅₀	0.0055	10	immobi-lisation	A	10	0.0001	Heinlaan et al. (2016)
I	*Daphnia magna*	neonates	21	PVP	Colorobbia	S	Lake Greifen 2015	S	48	EC₅₀	0.0011	10	immobi-lisation	A	10	0.00001	Heinlaan et al. (2016)
I	*Daphnia magna*	neonates	21	PVP	Colorobbia	S	Lake Lucerne 2014	S	48	EC₅₀	0.0021	10	immobi-lisation	A	10	0.00002	Heinlaan et al. (2016)
I	*Daphnia magna*	neonates	21	PVP	Colorobbia	S	Lake Lucerne 2015	S	48	EC₅₀	0.0019	10	immobi-lisation	A	10	0.00002	Heinlaan et al. (2016)
I	*Daphnia magna*	neonates	30 ± 5 (TEM)	citrate	Cline Scientific	S	Elendt M7	3h pulse	48	EC₅₀	0.11	10	immobi-lisation	A	10	0.001	Sørensen et al. (2016)
I	*Daphnia magna*	neonates	30-50	PVP	NanoAmor	S	Boreal Lake 1	S	24	LC₅₀	0.034	10	mortality	A	10	0.0003	(Conine et al., 2017)
I	*Daphnia magna*	neonates	30-50	PVP	NanoAmor	S	Boreal Lake 2	S	24	LC₅₀	0.29	10	mortality	A	10	0.003	(Conine et al., 2017)
I	*Daphnia magna*	neonates	9 ± 3 (TEM)	citrate	synthesis	S	Elendt M4	S	48	EC₅₀	0.11	10	mortality	A	10	0.001	Hu et al. (2018)
I	*Daphnia magna*	neonates	9 ± 3 (TEM)	citrate	synthesis	S	Surface water	S	48	EC₅₀	0.27	10	mortality	A	10	0.003	Hu et al. (2018)
I	*Daphnia magna*	neonates	25	PVP	nano Composix	S	Elendt M7	S	48	NOEC	0.005	1	immobi-lisation	A	10	0.0005	(Georgantz opoulou et al., 2018)

Species			ENMs				Exposure					Assessment Factor (AF)					Reference
Type	Name	Stage	Size	Surface coating	Origin	State	Medium	Type	Time (h)	End-point	Value (mgL^{-1})	1st AF	Parameter	Study	2nd AF	Final value	
I	*Daphnia magna*	neonates	49 ± 25 (TEM)	plant extract	synthesis	S	OECD 202	S	48	LC$_{50}$	0.0019	10	immobi-lisation	A	10	0.00002	Khoshnamv and et al. (2020)
I	*Daphnia magna*	neonates	6 (DLS)	citrate	synthesis	S	MHRW	SR	48	LC$_{50}$	0.0011	10	mortality	A	10	0.00001	Allen et al. (2010)
I	*Daphnia magna*	neonates	<150 (DLS)	coffee	synthesis	S	MHRW	SR	48	LC$_{50}$	0.001	10	mortality	A	10	0.00001	Allen et al. (2010)
I	*Daphnia magna*	neonates	<100	PVP	Sigma-Aldrich	P	MHRW	SR	48	LC$_{50}$	0.032	10	mortality	A	10	0.0003	Allen et al. (2010)
I	*Daphnia magna*	neonates	<150	bare	Sigma-Aldrich	P	MHRW	SR	48	LC$_{50}$	0.017	10	mortality	A	10	0.0002	Allen et al. (2010)
I	*Daphnia magna*	neonates	29	citrate	synthesis	S	MHRW	S	48	LC$_{50}$	0.011	10	mortality	A	10	0.0001	Kennedy et al. (2010)
I	*Daphnia magna*	neonates	10	bare	nano Composix	S	MHRW	S	48	LC$_{50}$	0.0054	10	mortality	A	10	0.0001	Kennedy et al. (2010)
I	*Daphnia magna*	neonates	20	bare	nano Composix	S	MHRW	S	48	LC$_{50}$	0.0053	10	mortality	A	10	0.0001	Kennedy et al. (2010)
I	*Daphnia magna*	neonates	50	bare	nano Composix	S	MHRW	S	48	LC$_{50}$	0.0054	10	mortality	A	10	0.0001	Kennedy et al. (2010)
I	*Daphnia magna*	neonates	80	bare	nano Composix	S	MHRW	S	48	LC$_{50}$	0.018	10	mortality	A	10	0.0002	Kennedy et al. (2010)
I	*Daphnia magna*	neonates	41	PVP	Luna Innovations	S	MHRW	S	48	LC$_{50}$	0.097	10	mortality	A	10	0.001	Kennedy et al. (2010)
I	*Daphnia magna*	neonates	36	EDTA	Virginia Tech	S	MHRW	S	48	LC$_{50}$	0.015	10	mortality	A	10	0.0002	Kennedy et al. (2010)
I	*Daphnia magna*	neonates	36	citrate	synthesis	S	SSF	S	48	LC$_{50}$	0.003	10	mortality	A	10	0.00003	Li et al. (2010)
I	*Daphnia magna*	neonates	52	citrate	synthesis	S	SSF	S	48	LC$_{50}$	0.004	10	mortality	A	10	0.00004	Li et al. (2010)
I	*Daphnia magna*	neonates	66	citrate	synthesis	S	SSF	S	48	LC$_{50}$	0.004	10	mortality	A	10	0.00004	Li et al. (2010)
I	*Daphnia magna*	neonates	60	bare	Namatech	P	Elendt M4	S	48	EC$_{50}$	0.001	10	mortality	A	10	0.00001	Kim et al. (2011)
I	*Daphnia magna*	neonates	300	bare	Ferro	P	Elendt M4	S	48	EC$_{50}$	0.0014	10	mortality	A	10	0.00001	Kim et al. (2011)
I	*Daphnia magna*	neonates	5-25	citrate	ABC Nanotech	S	Elendt M4	SR 24	48	EC$_{10}$	0.003	2	mortality	A	10	0.0002	Asghari et al. (2012)
I	*Daphnia magna*	neonates	17	bare	Nanocid	S	Elendt M4	SR 24	48	EC$_{10}$	0.0015	2	mortality	A	10	0.0001	Asghari et al. (2012)
I	*Daphnia magna*	neonates	20	bare	Hongwu Nanometer	P	Elendt M4	SR 24	48	EC$_{10}$	0.14	2	mortality	A	10	0.007	Asghari et al. (2012)
I	*Daphnia magna*	neonates	<100	bare	Sigma-Aldrich	P	MHRW	S	24	EC$_{50}$	0.53	10	mortality	A	10	0.005	Jo et al. (2012)
I	*Daphnia magna*	neonates	<150	bare	Sigma-Aldrich	P	MHRW	S	24	EC$_{50}$	1.4	10	mortality	A	10	0.014	Jo et al. (2012)

Species			ENMs				Exposure					Assessment Factor (AF)					Reference
Type	Name	Stage	Size	Surface coating	Origin	State	Medium	Type	Time (h)	End-point	Value (mgL⁻¹)	1st AF	Parameter	Study	2nd AF	Final value	
I	*Daphnia magna*	adults	10	bare	nano Composix	S	Lake Superior (UV DM1)	SR 24	48	LC_{50}	0.0043	10	mortality	A	10	0.00004	Hoheisel et al. (2012)
I	*Daphnia magna*	adults	20	bare	nano Composix	S	Lake Superior (UV DM1)	SR 24	48	LC_{50}	0.008	10	mortality	A	10	0.0001	Hoheisel et al. (2012)
I	*Daphnia magna*	adults	30	bare	nano Composix	S	Lake Superior (UV DM1)	SR 24	48	LC_{50}	0.018	10	mortality	A	10	0.0002	Hoheisel et al. (2012)
I	*Daphnia magna*	adults	50	bare	nano Composix	S	Lake Superior (UV DM1)	SR 24	48	LC_{50}	0.024	10	mortality	A	10	0.0002	Hoheisel et al. (2012)
I	*Daphnia magna*	adults	10	bare	nano Composix	S	Lake Superior (UV DM2)	SR 24	48	LC_{50}	0.0096	10	mortality	A	10	0.0001	Hoheisel et al. (2012)
I	*Daphnia magna*	adults	20	bare	nano Composix	S	Lake Superior (UV DM2)	SR 24	48	LC_{50}	0.014	10	mortality	A	10	0.0001	Hoheisel et al. (2012)
I	*Daphnia magna*	adults	30	bare	nano Composix	S	Lake Superior (UV DM2)	SR 24	48	LC_{50}	0.018	10	mortality	A	10	0.0002	Hoheisel et al. (2012)
I	*Daphnia magna*	adults	50	bare	nano Composix	S	Lake Superior (UV DM2)	SR 24	48	LC_{50}	0.03	10	mortality	A	10	0.0003	Hoheisel et al. (2012)
I	*Daphnia magna*	neonates	60-100	bare	ABC Nanotech	P	Elendt M4	S	48	EC_{50}	0.00075	10	mortality	A	10	0.00001	Lee et al. (2012b)
I	*Daphnia magna*	neonates	13	citrate	ABC Nanotech	S	Elendt M4	S	48	EC_{50}	0.008	10	mortality	A	10	0.0001	Lee et al. (2012b)
I	*Daphnia magna*	adults	35-50	PVP	NanoAmor	S	MHRW	S	24	LC_{50}	0.011	10	mortality	A	10	0.0001	Poynton et al. (2012)
I	*Daphnia magna*	adults	40	citrate	synthesis	S	MHRW	S	24	LC_{50}	0.0018	10	mortality	A	10	0.00002	Poynton et al. (2012)
I	*Daphnia magna*	neonates	8 ± 3 (TEM)	PVP	synthesis	P	AFW	S	48	EC_{50}	0.054	10	mortality	A	10	0.0005	Blinova et al. (2013)
I	*Daphnia magna*	neonates	8 ± 3 (TEM)	PVP	synthesis	P	River 1	S	48	EC_{50}	0.19	10	mortality	A	10	0.002	Blinova et al. (2013)
I	*Daphnia magna*	neonates	8 ± 3 (TEM)	PVP	synthesis	P	River 2	S	48	EC_{50}	0.099	10	mortality	A	10	0.001	Blinova et al. (2013)
I	*Daphnia magna*	neonates	8 ± 3 (TEM)	PVP	synthesis	P	Lake 1	S	48	EC_{50}	0.18	10	mortality	A	10	0.002	Blinova et al. (2013)
I	*Daphnia magna*	neonates	8 ± 3 (TEM)	PVP	synthesis	P	Lake 2	S	48	EC_{50}	0.24	10	mortality	A	10	0.002	Blinova et al. (2013)
I	*Daphnia magna*	neonates	8 ± 3 (TEM)	PVP	synthesis	P	Lake 3	S	48	EC_{50}	0.16	10	mortality	A	10	0.0016	Blinova et al. (2013)
I	*Daphnia magna*	neonates	13 ± 4 (TEM)	protein	ED	S	AFW	S	48	EC_{50}	0.049	10	mortality	A	10	0.0005	Blinova et al. (2013)

Species			ENMs				Exposure					Assessment Factor (AF)					Reference
Type	Name	Stage	Size	Surface coating	Origin	State	Medium	Type	Time (h)	End-point	Value (mgL⁻¹)	1st AF	Parameter	Study	2nd AF	Final value	Reference
I	*Daphnia magna*	neonates	13 ± 4 (TEM)	protein	ED	S	River 1	S	48	EC_{50}	0.059	10	mortality	A	10	0.0006	Blinova et al. (2013)
I	*Daphnia magna*	neonates	13 ± 4 (TEM)	protein	ED	S	River 2	S	48	EC_{50}	0.04	10	mortality	A	10	0.0004	Blinova et al. (2013)
I	*Daphnia magna*	neonates	13 ± 4 (TEM)	protein	ED	S	Lake 1	S	48	EC_{50}	0.075	10	mortality	A	10	0.0008	Blinova et al. (2013)
I	*Daphnia magna*	neonates	13 ± 4 (TEM)	protein	ED	S	Lake 2	S	48	EC_{50}	0.051	10	mortality	A	10	0.0005	Blinova et al. (2013)
I	*Daphnia magna*	neonates	13 ± 4 (TEM)	protein	ED	S	Lake 3	S	48	EC_{50}	0.066	10	mortality	A	10	0.0007	Blinova et al. (2013)
I	*Daphnia magna*	neonates	1–10	CFP	ViveNano	S	COMBO	S	48	NOEC	0.00075	1	mortality	A	10	0.0001	Das et al. (2013)
I	*Daphnia magna*	neonates	20	citrate	nano Composix	S	VSRW	S	48	EC_{50}	0.012	10	immobi-lisation	A	10	0.0001	Harmon et al. (2014)
I	*Daphnia magna*	neonates	50	citrate	nano Composix	S	VSRW	S	48	EC_{50}	0.0098	10	immobi-lisation	A	10	0.0001	Harmon et al. (2014)
I	*Daphnia magna*	neonates	80	citrate	nano Composix	S	VSRW	S	48	EC_{50}	0.0094	10	immobi-lisation	A	10	0.0001	Harmon et al. (2014)
I	*Daphnia magna*	neonates	20	citrate	nano Composix	S	SRW	S	48	EC_{50}	0.011	10	immobi-lisation	A	10	0.0001	Harmon et al. (2014)
I	*Daphnia magna*	neonates	50	citrate	nano Composix	S	SRW	S	48	EC_{50}	0.011	10	immobi-lisation	A	10	0.0001	Harmon et al. (2014)
I	*Daphnia magna*	neonates	80	citrate	nano Composix	S	SRW	S	48	EC_{50}	0.014	10	immobi-lisation	A	10	0.0001	Harmon et al. (2014)
I	*Daphnia magna*	neonates	20 ± 7 (TEM)	PVP	Colorobbia	S	ADaM	S	48	EC_{50}	0.0034	10	immobi-lisation	A	10	0.00003	Jemec et al. (2016)
I	*Daphnia magna*	neonates	20 ± 7 (TEM)	PVP	Colorobbia	S	OECD	S	48	EC_{50}	0.0025	10	immobi-lisation	A	10	0.00003	Jemec et al. (2016)
I	*Daphnia magna*	neonates	8-47 (TEM)	POE Triolein + Tween 20	JRC EU	S	EPA	S	48	EC_{10}	0.032	2	immobi-lisation	A	10	0.002	Cupi et al. (2016)
I	*Daphnia magna*	neonates	10	CFP	ViveNano	S	COMBO (fed)	S	48	LC_{50}	0.0039	10	mortality	A	10	0.00004	Conine and Frost (2017)
I	*Daphnia magna*	neonates	10	CFP	ViveNano	S	COMBO (not fed)	S	48	LC_{50}	0.0045	10	mortality	A	10	0.0001	Conine and Frost (2017)
I	*Daphnia magna*	neonates	10	CFP	ViveNano	S	COMBO (no algae)	S	48	LC_{50}	0.017	10	mortality	A	10	0.0002	Conine and Frost (2017)
I	*Daphnia magna*	neonates	10	CFP	ViveNano	S	COMBO (algae)	S	48	LC_{50}	0.0052	10	mortality	A	10	0.0001	Conine and Frost (2017)
I	*Daphnia magna*	neonates	10	CFP	ViveNano	S	COMBO (filtrate)	S	48	LC_{50}	0.023	10	mortality	A	10	0.0002	Conine and Frost (2017)
I	*Daphnia magna*	neonates	10	CFP	ViveNano	S	COMBO (high P)	SR	144	LC_{50}	0.012	10	mortality	A	10	0.0001	Conine and Frost (2017)
I	*Daphnia magna*	neonates	10	CFP	ViveNano	S	COMBO (low P)	SR	144	LC_{50}	0.015	10	mortality	A	10	0.0002	Conine and Frost (2017)

Species			ENMs				Exposure					Assessment Factor (AF)					Reference
Type	Name	Stage	Size	Surface coating	Origin	State	Medium	Type	Time (h)	End-point	Value (mgL⁻¹)	1st AF	Parameter	Stu-dy	2nd AF	Final value	
I	*Daphnia magna*	neonates	10	CFP	ViveNano	S	COMBO (high P + food)	SR	144	LC$_{50}$	0.0054	10	mortality	A	10	0.0001	Conine and Frost (2017)
I	*Daphnia magna*	neonates	10	CFP	ViveNano	S	COMBO (low P+ food)	SR	144	LC$_{50}$	0.0067	10	mortality	A	10	0.0001	Harmon et al. (2014)
I	*Daphnia magna*	neonates	10	CFP	ViveNano	S	COMBO (high P exposure)	SR	144	LC$_{50}$	0.0074	10	mortality	A	10	0.0001	Conine and Frost (2017)
I	*Daphnia magna*	neonates	15 (SEM)	bare	synthesis	S	ADaM	S	48	EC$_{50}$	0.031	10	mortality	A	10	0.0003	Conine and Frost (2017)
I	*Daphnia pulex*	adults	20-30	bare	Quantum Sphere	P	FDTW	SR	48	LC$_{50}$	0.04	10	immobi-lisation	A	10	0.0004	Hund-Rinke et al. (2018)
I	*Elliptio complanata*	adults	20	bare	Ted Pella	S	tap water	S	48	MATC	0.002	1	MTs	C	1	0.002	Griffitt et al. (2008)
I	*Elliptio complanata*	adults	20	bare	Ted Pella	S	tap water	S	48	MATC	0.0004	1	LPO (dg)	C	1	0.0004	Gagné et al. (2013)
I	*Elliptio complanata*	adults	20	bare	Ted Pella	S	tap water	S	48	MATC	0.0008	1	LPO (g)	C	1	0.0008	Gagné et al. (2013)
I	*Elliptio complanata*	adults	20	bare	Ted Pella	S	tap water	S	48	MATC	0.0008	1	LPO (go)	C	1	0.0008	Gagné et al. (2013)
I	*Elliptio complanata*	adults	80	bare	Ted Pella	S	tap water	S	48	MATC	0.0004	1	MTs	C	1	0.0004	Gagné et al. (2013)
I	*Elliptio complanata*	adults	80	bare	Ted Pella	S	tap water	S	48	MATC	0.0004	1	LPO (dg)	C	1	0.0004	Gagné et al. (2013)
I	*Elliptio complanata*	adults	80	bare	Ted Pella	S	tap water	S	48	MATC	0.0008	1	LPO (g)	C	1	0.0008	Gagné et al. (2013)
I	*Elliptio complanata*	adults	80	bare	Ted Pella	S	tap water	S	48	MATC	0.0008	1	LPO (go)	C	1	0.0008	Gagné et al. (2013)
I	*Gammarus fossarum*	*G.f1*	20	bare	Plasma Chem	P	Volvic®	SR 24	72	LC$_{50}$	0.84	10	mortality	A	10	0.008	Gagné et al. (2013)
I	*Gammarus fossarum*	*G.f2*	23	plant extract	synthesis	S	Volvic®	SR 24	72	LC$_{50}$	0.0049	10	mortality	A	10	0.0001	Mehennaoui et al. (2016)
I	*Gammarus fossarum*	*G.f2*	27	plant extract	synthesis	S	Volvic®	SR 24	72	LC$_{50}$	0.0055	10	mortality	A	10	0.0001	Mehennaoui et al. (2016)
I	*Moina macrocopa*	neonates	85 ± 14 (TEM)	bare	Dongyang	P	OECD	S	48	EC$_{50}$	1.11	10	immobi-lisation	A	10	0.01	Mehennaoui et al. (2016)
I	*Radix luteola*	adults	≤50	TGME	Sigma-Aldrich	S	tap water	SR	96	LC$_{50}$	0.048	10	mortality	A	10	0.0005	Yoo-iam et al. (2015)
I	*Radix luteola*	adults	≤50	TGME	Sigma-Aldrich	S	tap water	SR	96	LOEC	0.004	2	LDH	C	1	0.002	Ali (2014)
I	*Radix luteola*	adults	≤50	TGME	Sigma-Aldrich	S	tap water	SR	96	LOEC	0.004	2	GST	C	1	0.002	Ali (2014)
I	*Radix luteola*	adults	≤50	TGME	Sigma-Aldrich	S	tap water	SR	96	LOEC	0.004	2	GSH	C	1	0.002	Ali (2014)

Species			ENMs				Exposure					Assessment Factor (AF)					Reference
Type	Name	Stage	Size	Surface coating	Origin	State	Medium	Type	Time (h)	End-point	Value (mgL⁻¹)	1st AF	Parameter	Stu-dy	2nd AF	Final value	
I	*Radix luteola*	adults	≤50	TGME	Sigma-Aldrich	S	tap water	SR	96	LOEC	0.004	2	CAT	C	1	0.002	Ali (2014)
I	*Physa acuta*	embryos (2–4 d)	3-8	alkane	AMEPOX	P	APW	SR	312	LC$_{50}$	0.082	10	mortality	C	1	0.008	Goncalves et al. (2017)
I	*Physa acuta*	juveniles	3-8	alkane	AMEPOX	P	APW	SR	96	LC$_{50}$	0.26	10	mortality	A	10	0.003	Goncalves et al. (2017)
I	*Physa acuta*	juveniles	3-8	alkane	AMEPOX	P	MAPW	SR	96	LC$_{50}$	0.049	10	mortality	A	10	0.0005	Goncalves et al. (2017)
I	*Physa acuta*	adults	3-8	alkane	AMEPOX	P	APW	SR	96	LC$_{50}$	7.1	10	mortality	A	10	0.071	Goncalves et al. (2017)
I	*Physa acuta*	adults	3-8	alkane	AMEPOX	P	MAPW	SR	96	LC$_{50}$	4.1	10	mortality	A	10	0.041	Goncalves et al. (2017)
I	*Potamopyrgus antipodarum*	adults	15 (TEM)	PVP	RAS	S	RW	SR 72	756	EC$_{10}$	0.0056	2	reprodu-ction	C	1	0.003	(Völker et al., 2014)
I	*Thamnocepha-lus platyurus*	larvae	8 ± 3 (TEM)	PVP	synthesis	P	AFW	S	24	LC$_{50}$	0.069	10	mortality	A	10	0.0007	Blinova et al. (2013)
I	*Thamnocepha-lus platyurus*	larvae	8 ± 3 (TEM)	PVP	synthesis	P	River 1	S	24	LC$_{50}$	0.19	10	mortality	A	10	0.002	Blinova et al. (2013)
I	*Thamnocepha-lus platyurus*	larvae	8 ± 3 (TEM)	PVP	synthesis	P	Lake 1	S	24	LC$_{50}$	0.25	10	mortality	A	10	0.003	Blinova et al. (2013)
I	*Thamnocepha-lus platyurus*	larvae	8 ± 3 (TEM)	PVP	synthesis	P	Lake 2	S	24	LC$_{50}$	0.61	10	mortality	A	10	0.006	Blinova et al. (2013)
I	*Thamnocepha-lus platyurus*	larvae	13 ± 4 (TEM)	protein	ED	P	AFW	S	24	LC$_{50}$	0.26	10	mortality	A	10	0.003	Blinova et al. (2013)
I	*Thamnocepha-lus platyurus*	larvae	13 ± 4 (TEM)	protein	ED	P	River 1	S	24	LC$_{50}$	0.18	10	mortality	A	10	0.002	Blinova et al. (2013)
I	*Thamnocepha-lus platyurus*	larvae	13 ± 4 (TEM)	protein	ED	P	River 2	S	24	LC$_{50}$	0.15	10	mortality	A	10	0.002	Blinova et al. (2013)
I	*Thamnocepha-lus platyurus*	larvae	13 ± 4 (TEM)	protein	ED	P	Lake 2	S	24	LC$_{50}$	0.25	10	mortality	A	10	0.0025	Blinova et al. (2013)
V	*Barbonymus gonionotus*	juveniles	85 ± 14 (TEM)	bare	Dongyang	P	OECD 203	S	48	LC$_{50}$	1.76	10	mortality	A	10	0.018	Yoo-iam et al. (2015)
V	*Carassius auratus*	juveniles	18	bare	Nanocid	P	tap water	S	96	NOEC	0.01	1	mortality	A	10	0.001	Hedayati A. et al. (2012)
V	*Cyprinus carpio*	juveniles	18	bare	Nanocid	P	tap water	S	96	LC$_{50}$	0.29	10	mortality	A	10	0.003	Khosravi-Katuli et al. (2018)
V	*Danio rerio*	embryos	3-8	alkane	AMEPOX	P	CFW+IOSSS	S	96	LC$_{50}$	0.13	10	mortality	A	10	0.0013	Ribeiro et al. (2014)
V	*Danio rerio*	embryos	35	bare	NanoAmor	P	RTM (DSW)	S	96	EC$_{50}$	0.21	10	mortality	acute	10	0.002	Wang et al. (2012)
V	*Danio rerio*	embryos	15	Tween (20+ 65)	JRC EU	S	RTM (DSW)	S	96	EC$_{50}$	0.089	10	mortality	acute	10	0.0009	Wang et al. (2012)
V	*Danio rerio*	embryos	80	PVP	NanoAmor	P	RTM (DSW)	S	96	EC$_{50}$	0.16	10	mortality	acute	10	0.002	Wang et al. (2012)

Species			ENMs				Exposure					Assessment Factor (AF)					Reference
Type	Name	Stage	Size	Surface coating	Origin	State	Medium	Type	Time (h)	End-point	Value (mgL⁻¹)	1st AF	Parameter	Stu-dy	2nd AF	Final value	
V	*Danio rerio*	embryos	21	PVP	Colorobbia	S	ISO 2014	SR 24	96	LC$_{50}$	0.0088	10	mortality	acute	10	0.0001	Heinlaan et al. (2016)
V	*Danio rerio*	embryos	21	PVP	Colorobbia	S	ISO 2015	SR 24	96	LC$_{50}$	0.02	10	mortality	acute	10	0.0002	Heinlaan et al. (2016)
V	*Danio rerio*	embryos	21	PVP	Colorobbia	S	Lake Greifen 2014	SR 24	96	LC$_{50}$	0.02	10	mortality	acute	10	0.0002	Heinlaan et al. (2016)
V	*Danio rerio*	embryos	21	PVP	Colorobbia	S	Lake Greifen 2015	SR 24	96	LC$_{50}$	0.03	10	mortality	acute	10	0.0003	Heinlaan et al. (2016)
V	*Danio rerio*	embryos	21	PVP	Colorobbia	S	Lake Lucerne 2014	SR 24	96	LC$_{50}$	0.011	10	mortality	acute	10	0.00011	Heinlaan et al. (2016)
V	*Danio rerio*	embryos	21	PVP	Colorobbia	S	Lake Lucerne 2015	SR 24	96	LC$_{50}$	0.02	10	mortality	acute	10	0.0002	Heinlaan et al. (2016)
V	*Danio rerio*	embryos	49 ± 25 (TEM)	plant extract	synthesis	S	OECD 202	S	96	LC$_{50}$	0.01	10	immobi-lisation	acute	10	0.0001	Khoshnamv and et al. (2020)
V	*Danio rerio*	embryos	5-20	starch	synthesis	S	EW	S	72	LC$_{50}$	25	10	mortality	acute	10	0.25	Asharani et al. (2008)
V	*Danio rerio*	embryos	5-20	albumin	synthesis	pellet	EW	S	72	LC$_{50}$	25	10	mortality	acute	10	0.25	Asharani et al. (2008)
V	*Danio rerio*	juveniles	20-30	citrate	Quantum Sphere	P	FDTW	SR	48	LC$_{50}$	7.2	10	mortality	acute	10	0.072	Griffitt et al. (2008)
V	*Danio rerio*	adults	20-30	citrate	Quantum Sphere	P	FDTW	SR	48	LC$_{50}$	7.1	10	mortality	acute	10	0.071	Griffitt et al. (2008)
V	*Danio rerio*	embryos	3	citrate	synthesis	S	IO60	SR	120	LC$_{50}$	10.1	10	mortality	A	10	0.1	Bar-Ilan et al. (2009)
V	*Danio rerio*	embryos	10	citrate	synthesis	S	IO60	SR	120	LC$_{50}$	13. 6	10	mortality	A	10	0.14	Bar-Ilan et al. (2009)
V	*Danio rerio*	embryos	50	citrate	synthesis	S	IO60	SR	120	LC$_{50}$	13.7	10	mortality	A	10	0.14	Bar-Ilan et al. (2009)
V	*Danio rerio*	embryos	100	citrate	synthesis	S	IO60	SR	120	LC$_{50}$	14.8	10	mortality	A	10	0.15	Bar-Ilan et al. (2009)
V	*Danio rerio*	adults	5-20 (TEM)	bare	Nanopoly	S	bottled water	SR	24	LC$_{50}$	250	10	mortality	A	10	2.5	Choi et al. (2010)
V	*Danio rerio*	adults	30–40	PVP	NanoAmor	S	DDW+NaCl	SR	48	LC$_{50}$	0.084	10	mortality	A	10	0.0008	Bilberg et al. (2012)
V	*Danio rerio*	embryos	10	PVP	nano Composix	S	HM	S	120	NOEC	1.3	1	mortality	A	10	0.13	George et al. (2012)
V	*Danio rerio*	embryos	20	PVP	nano Composix	S	HM	S	120	NOEC	1.3	1	mortality	A	10	0.13	George et al. (2012)
V	*Danio rerio*	embryos	40	PVP	nano Composix	S	HM	S	120	NOEC	1.3	1	mortality	A	10	0.13	George et al. (2012)

Species			ENMs				Exposure					Assessment Factor (AF)					Reference
Type	Name	Stage	Size	Surface coating	Origin	State	Medium	Type	Time (h)	End-point	Value (mgL^{-1})	1st AF	Parameter	Stu-dy	2nd AF	Final value	
V	*Danio rerio*	embryos	41.6 (TEM)	citrate	nano Composix	S	Egg water	S	120	NOEC	2.2 E^{-06}	1	mortality	A	10	2.2 E^{-07}	Lee et al. (2012a)
V	*Danio rerio*	embryos	10-20 (TEM)	polyacrylate	ViveNano	S	DTW	S	96	LC$_{50}$	1.2	10	mortality	A	10	0.012	Massarsky et al. (2013)
V	*Danio rerio*	adults	16.6	bare	Nanocid	S	tap water	SR	96	LC$_{50}$	16.8	10	mortality	A	10	0.17	Katuli et al. (2014)
V	*Danio rerio*	embryos	15	POE Triolein + Tween 20	JRC EU	S	ISO	SR	48	EC$_{50}$	1.09	10	mortality	A	10	0.011	Muth-Kohne et al. (2013)
V	*Danio rerio*	embryos	ø	bare	Odor Zero Crew Socks	ø	ROW (OS 24h)	SR	72	EC$_{50}$	0.05	10	hatching	A	10	0.0005	Gao et al. (2015)
V	*Danio rerio*	embryos	ø	bare	Odor Zero Crew Socks	ø	ROW (OS 24h + cent 1h)	SR	72	EC$_{50}$	0.04	10	hatching	A	10	0.0004	Gao et al. (2015)
V	*Danio rerio*	embryos	20 ± 7 (TEM)	PVP	Colorobbia	S	ISO	S	48	LC$_{50}$	0.061	10	mortality	A	10	0.0006	Jemec et al. (2016)
V	*Danio rerio*	dech embryos (28 hpf)	20 ± 7 (TEM)	PVP	Colorobbia	S	ISO	S	48	LC$_{50}$	0.033	10	mortality	A	10	0.0003	Jemec et al. (2016)
V	*Danio rerio*	dech embryos (72 hpf)	20 ± 7 (TEM)	PVP	Colorobbia	S	ISO	S	48	LC$_{50}$	0.014	10	mortality	A	10	0.0001	Jemec et al. (2016)
V	*Danio rerio*	embryos	20	maltose	JRC EU	S	tap water	S	120	LC$_{50}$	0.53	10	mortality	A	10	0.005	Lacave et al. (2016)
V	*Danio rerio*	embryos	40	maltose	JRC EU	S	tap water	S	120	LC$_{50}$	3.9	10	mortality	A	10	0.039	Lacave et al. (2016)
V	*Danio rerio*	embryos	100	maltose	JRC EU	S	tap water	S	120	LC$_{50}$	1.98	10	mortality	A	10	0.02	Lacave et al. (2016)
V	*Danio rerio*	adults	5-50 (SEM)	plant extract	synthesis	S	tap water	S	96	LC$_{50}$	0.14	10	mortality	A	10	0.0014	Krishnaraj et al. (2016)
V	*Danio rerio*	ELS	< 100	PVP	Sigma-Aldrich	P	DTW	S	120	LC$_{50}$	17	10	mortality	A	10	0.17	Boyle and Goss (2018)
V	*Danio rerio*	embryos	15 (SEM)	bare	synthesis	S	ISSO	S	72	EC$_{50}$	1.1	10	mortality	A	10	0.011	Hund-Rinke et al. (2018)
V	*Danio rerio*	embryos	4	oleic acid	ColdStones Tech	P	tap water	SR 24	96	EC$_{50}$	4.1	10	mortality	A	10	0.041	Xin et al. (2015)
V	*Danio rerio*	embryos	10	oleic acid	ColdStones Tech	P	tap water	SR 24	96	EC$_{50}$	5.9	10	mortality	A	10	0.059	Xin et al. (2015)
V	*Danio rerio*	embryos	< 100	PVP	Sigma-Aldrich	S	DTW	SR 24	96	EC$_{10}$	4.4	2	hatching	A	10	0.22	Pereira et al. (submitted)
V	*Hypophthalmi-cthys molitrix*	adults	61	bare	Nanocid	S	DTW	S	96	LC$_{50}$	0.2	10	mortality	A	10	0.002	(Shaluei et al., 2013)
V	*Hypophthalmi-cthys molitrix*	adults	18	bare	Nanocid	P	DTW	S	96	NOEC	0.01	1	mortality	A	10	0.001	Hedayati A. et al. (2012)

Species			ENMs				Exposure					Assessment Factor (AF)					Reference
Type	Name	Stage	Size	Surface coating	Origin	State	Medium	Type	Time (h)	End-point	Value (mgL⁻¹)	1st AF	Parameter	Study	2nd AF	Final value	
V	*Oncorhyn-chus mykiss*	EE	6.5 (TEM)	bare	Nanocid	P	DTW	SR	96	NOEC	0.01	1	mortality	A	10	0.001	Johari et al. (2013)
V	*Oncorhyn-chus mykiss*	larvae	6.5 (TEM)	bare	Nanocid	P	DTW	SR	96	NOEC	0.3	1	mortality	A	10	0.03	Johari et al. (2013)
V	*Oncorhyn-chus mykiss*	juveniles	6.5 (TEM)	bare	Nanocid	P	DTW	SR	96	NOEC	1	1	mortality	A	10	0.1	Johari et al. (2013)
V	*Oryzias latipes*	adults	28.3	PVP	synthesis	S	DTW	SR 24	120	NOEC	0.2	1	heart rate	A	10	0.02	Wu et al. (2010)
V	*Oryzias latipes*	adults	60	bare	Namatech	P	FCW	S	96	LC$_{50}$	0.028	10	mortality	A	10	0.0003	Kim et al. (2011)
V	*Oryzias latipes*	adults	300	bare	Ferro	P	FCW	S	96	LC$_{50}$	0.067	10	mortality	A	10	0.0007	Kim et al. (2011)
V	*Oryzias latipes*	adults	30 (TEM)	PVP	synthesis	P	DTW	SR 24	336	NOEC	0.1	1	mortality	A	10	0.01	Wu and Zhou (2013)
V	*Oryzias latipes*	embryos	< 100	bare	Sigma-Aldrich	P	ERM	S	96	LC$_{50}$	3.5	10	mortality	A	10	0.035	Kim et al. (2013)
V	*Oryzias latipes*	embryos	< 100	bare	Sigma-Aldrich	S (10d)	ERM	S	96	LC$_{50}$	1.4	10	mortality	A	10	0.014	Kim et al. (2013)
V	*Oryzias latipes*	embryos	514 ± 83	bare	Sigma-Aldrich	P	ERM	S	96	NOEC	1.9	1	hatching	A	10	0.19	Kim et al. (2013)
V	*Oryzias latipes*	embryos (S 11)	3.6	bare	Synerge-nesis	S	ERM	SR 24	96	LC$_{50}$	1.4	10	mortality	A	10	0.014	Kashiwada et al. (2012)
V	*Oryzias latipes*	embryos (S 21)	4.6	bare	Synerge-nesis	S	ERM	SR 24	96	LC$_{50}$	1.4	10	mortality	A	10	0.014	Kashiwada et al. (2012)
V	*Oryzias latipes*	embryos (S 30)	5.6	bare	Synerge-nesis	S	ERM	SR 24	96	LC$_{50}$	1.4	10	mortality	A	10	0.014	Kashiwada et al. (2012)
V	*Oryzias latipes*	juveniles	5-25	citrate	ABC Nanotech	S	DTW	S	96	EC$_{50}$	1.8	10	mortality	A	10	0.018	Sohn et al. (2015)
V	*Oryzias latipes*	embryos	8 ± 4 (TEM)	citrate	ABC NanoTech	S	OECD	SR 48	96	LC$_{50}$	0.84	10	mortality	A	10	0.008	Cho et al. (2013)
V	*Oryzias latipes*	adults	8 ± 4 (TEM)	citrate	ABC NanoTech	S	OECD	S	96	LC$_{50}$	0.8	10	mortality	A	10	0.008	Cho et al. (2013)
V	*Pimephales promelas*	embryos	31-50	bare	NanoAmor	P (St)	VHW	S	96	LC$_{50}$	9.4	10	mortality	A	10	0.09	Laban et al. (2010)
V	*Pimephales promelas*	embryos	21-280	bare	Sigma-Aldrich	P (St)	VHW	S	96	LC$_{50}$	10.6	10	mortality	A	10	0.11	Laban et al. (2010)
V	*Pimephales promelas*	embryos	31-50	bare	NanoAmor	P (So)	VHW	S	96	LC$_{50}$	1.3	10	mortality	A	10	0.013	Laban et al. (2010)
V	*Pimephales promelas*	embryos	21-280	bare	Sigma-Aldrich	P (So)	VHW	S	96	LC$_{50}$	1.4	10	mortality	A	10	0.014	Laban et al. (2010)
V	*Pimephales promelas*	embryos	10	bare	nano Composix	S	Lake Superior (UV)	SR 24	96	LC$_{50}$	0.089	10	mortality	A	10	0.0009	Hoheisel et al. (2012)
V	*Pimephales promelas*	larvae	10	bare	nano Composix	S	Lake Superior (UV)	SR 24	168	EC$_{20}$	0.046	2	growth	C	1	0.023	Hoheisel et al. (2012)

Species			ENMs				Exposure					Assessment Factor (AF)					Reference
Type	Name	Stage	Size	Surface coating	Origin	State	Medium	Type	Time (h)	End-point	Value (mgL^{-1})	1st AF	Parameter	Stu-dy	2nd AF	Final value	
V	*Pimephales promelas*	embryos	29	citrate	synthesis	S	MHRW	S	96	LC$_{50}$	0.019	10	mortality	A	10	0.0002	Kennedy et al. (2010)
V	*Pimephales promelas*	embryos	10	bare	nano Composix	S	MHRW	S	96	LC$_{50}$	0.041	10	mortality	A	10	0.0004	Kennedy et al. (2010)
V	*Pimephales promelas*	embryos	20	bare	nano Composix	S	MHRW	S	96	LC$_{50}$	0.064	10	mortality	A	10	0.0006	Kennedy et al. (2010)
V	*Pimephales promelas*	embryos	50	bare	nano Composix	S	MHRW	S	96	LC$_{50}$	0.061	10	mortality	A	10	0.0006	Kennedy et al. (2010)
V	*Pimephales promelas*	embryos	80	bare	nano Composix	S	MHRW	S	96	LC$_{50}$	0.126	10	mortality	A	10	0.001	Kennedy et al. (2010)
V	*Pimephales promelas*	embryos	36	EDTA	Virginia Tech	S	MHRW	S	96	LC$_{50}$	0.055	10	mortality	A	10	0.0006	Kennedy et al. (2010)

Type: I = Invertebrates; M = Microalgae; P = Plant; V = Vertebrates

Surface coating: albumin = bovine serum albumin; citrate = sodium citrate; CFP = carboxy-functionalized polyacrylate; EDTA = Ethylenediamine tetraacetic acid; EGCG = epigallocatechin gallate; oleic acid = Oleic acid (10-13%); PEI = Polyethylenimine; PEG = polyethylene glycol; POE Triolein + Tween 20 = polyoxyethylene (POE) Glycerol Trioleate and POE Sorbitan mono-Laurate (Tween 20); PVP = poly(vinylpyrrolidone); SDBS = sodium dodecylbenzenesulfonate; polyacrylate = sodium polyacrylate; Tween20 = Polyoxyethylene (20) sorbitan monolaurate; Tween 65 = Polyoxyethylene Sorbitan Tristearate Polysorbate; TGME = triethylene glycol monomethyl ether

Company: ED = Estonian drugstore

State: P = Powder; S = suspension; So =Sonicated; St =Stirred;

Life-stage: dech = dechorionated; EE= eleutheroembryos; EGP= exponential growth phase; ELS= early-life stages; neonates = neonates (<24h old); S = Stage; d= days

MEDIUM: ADaM = Aachener Daphnienmedium; ACTWW = Alachua Conservation Trust wetland water; AGCM = algal growth culture medium; AFW = Artificial Fresh water; APW = artificial pond water; BBM = Bold's Basal medium; Cent =centrifuged; CFW+IOSSS =Carbon-filtered water + salt "Instant Ocean Synthetic Sea Salt"; DDW+ NaCl = Demineralised and dechlorinated water (16:1) plus NaCl (132 mg/L); DOC = dissolved organic carbon; DTW = Dechlorinated tap water; Egg water = 1 mM NaCl; ERM = Embryos rearing medium; EW = Embryos water (60 mg of sea salt/L ultrapure water); FCW = Fish culture water; FDTW = Filtered (0.45 µm) DTW; FM = Fresh medium; HM = Holtfreter medium; HR(NF) = Horsetooth reservoir (normal flow); HR(HF) Horsetooth reservoir (high flow); IO60 =60 mg Instant Ocean/L; LTW = Laboratory test water; MAPW = modified APW; MBL = Woods Hole medium; MHSM= Modified high salt medium; MHW = Moderately hard water; MHRW = Moderately hard reconstituted water; MM7 = modified M7 medium pH 7.5; MSM = Modified Steinberg medium; MOPS = (3-(N-morpholino)propanesulfonic acid) buffer; OS = orbital shaker; OM = Old medium; ROW = Reverse Osmosis water; RTM(DSW) = Reconstituted test medium (Dutch standard water); RW = Reconstituted water; SFIR = Spring-fed Ichetucknee River; SFM = Standard freshwater medium; SFW = Synthetic fresh water; SGM = Standard growth medium; SM7 = Simplified M7 medium; SRW = Soft reconstituted water (150 µS/cm); SSF = Standard synthetic freshwater; VHW = Very hard water; VSRW = very soft reconstituted water (30 µS/cm)

EXPOSURE: CR= continuous renewal; FT= flow-through; S= static; SR= static renewal; SR24= S-renewal (24h); SR48= S-renewal (48h); SR72 = S-renewal (72h)

PARAMETERS: CAT = catalase (haemolymph); Chl a = chlorophyll a; GR = growth rate; GRI= Growth rate inhibition; GSH = reduced glutathione (haemolymph); GST = glutathione-S-transferase (haemolymph); LDH = lactate dehydrogenase (haemolymph); LPO (dg) = Lipid peroxidation (digestive gland); LPO (g) = Lipid peroxidation (gills); LPO (go) = Lipid peroxidation (gonads); MTs = Metallothioneins (digestive gland); NN = nitrate-nitrogen; NLP = average neonate per living parent; PhEI= Photosynthetic efficiency inhibition; PII= photosystem II; PY= Photosynthetic yield; wt= weight

Study: A = Acute**; C =** Chronic

6.5.4 **References**

Allen, H. J., et al., 2010. Effects from filtration, capping agents, and presence/absence of food on the toxicity of silver nanoparticles to *Daphnia magna*. Environ Toxicol Chem. 29, 2742-2750. https://doi.org/10.1002/etc.329

Ali, D., 2014. Oxidative Stress-Mediated Apoptosis and Genotoxicity Induced by Silver Nanoparticles in Freshwater Snail *Lymnea luteola* L. Biol Trace Elem Res. 162, 333-341. https://doi.org/10.1007/s12011-014-0158-6

Angel, B. M., et al., 2013. The impact of size on the fate and toxicity of nanoparticulate silver in aquatic systems. Chemosphere. 93, 359-365. https://doi.org/10.1016/j.chemosphere.2013.04.096

Asghari, S., et al., 2012. Toxicity of various silver nanoparticles compared to silver ions in *Daphnia magna*. J Nanobiotechnology. 10, 14. https://doi.org/10.1186/1477-3155-10-14

Asharani, P. V., et al., 2008. Toxicity of silver nanoparticles in zebrafish models. Nanotechnology. 19, 255102. https://doi.org/10.1088/0957-4484/19/25/255102

Bar-Ilan, O., et al., 2009. Toxicity assessments of multisized gold and silver nanoparticles in zebrafish embryos. Small. 5, 1897-1910. https://doi.org/10.1002/smll.200801716

Bianchini, A., et al., 2002. Acute silver toxicity in aquatic animals is a function of sodium uptake rate. Environ Sci Technol. 36, 1763-1766. https://doi.org/10.1021/es011028t

Bianchini, A., Wood, C. M., 2008. Does sulfide or water hardness protect against chronic silver toxicity in *Daphnia magna*? A critical assessment of the acute-to-chronic toxicity ratio for silver. Ecotoxicol Environ Saf. 71, 32-40. https://doi.org/10.1016/j.ecoenv.2008.03.006

Bielmyer, G. K., et al., 2008. Is Cl$^-$ protection against silver toxicity due to chemical speciation? Aquat Toxicol. 87, 81-87. https://doi.org/10.1016/j.aquatox.2008.01.004

Bilberg, K., et al., 2012. In Vivo Toxicity of Silver Nanoparticles and Silver Ions in Zebrafish (*Danio rerio*). J Toxicol. 2012, 293784. https://doi.org/10.1155/2012/293784

Blinova, I., et al., 2013. Toxicity of two types of silver nanoparticles to aquatic crustaceans *Daphnia magna* and *Thamnocephalus platyurus*. Environ Sci Pollut Res. 20, 3456-3463. https://doi.org/10.1007/s11356-012-1290-5

Boyle, D., Goss, G. G., 2018. Effects of silver nanoparticles in early life-stage zebrafish are associated with particle dissolution and the toxicity of soluble silver. NanoImpact. 12, 1-8. https://doi.org/10.1016/j.impact.2018.08.006

Brill, J. L., et al., 2021. Derivation of algal acute to chronic ratios for use in chemical toxicity extrapolations. Chemosphere. 263, 127804. https://doi.org/10.1016/j.chemosphere.2020.127804

Burchardt, A. D., et al., 2012. Effects of silver nanoparticles in diatom *Thalassiosira pseudonana* and cyanobacterium *Synechococcus sp.* Environ Sci Technol. 46, 11336-11344. https://doi.org/10.1021/es300989e

Bury, N. R., et al., 1999. Effects of chloride, calcium, and dissolved organic carbon on silver toxicity: Comparison between rainbow trout and fathead minnows. Environ Toxicol Chem. 18, 56-62. https://doi.org/10.1002/etc.5620180108

Call, D. J., et al., 2006. Toxicity of silver in water and sediment to the freshwater amphipod *Hyalella azteca*. Environ Toxicol Chem. 25, 1802-1808. https://doi.org/10.1897/05-319R.1

Coll, C., et al., 2016. Probabilistic environmental risk assessment of five nanomaterials (nano-TiO_2, nano-Ag, nano-ZnO, CNT, and fullerenes). Nanotoxicology. 10, 436-444. https://doi.org/10.3109/17435390.2015.1073812

Cho, J. G., et al., 2013. Stepwise embryonic toxicity of silver nanoparticles on *Oryzias latipes*. Biomed Res Int. 2013, 494671. https://doi.org/10.1155/2013/494671

Choi, J. E., et al., 2010. Induction of oxidative stress and apoptosis by silver nanoparticles in the liver of adult zebrafish. Aquat Toxicol. 100, 151-159. https://doi.org/10.1016/j.aquatox.2009.12.012

Conine, A. L., Frost, P. C., 2017. Variable toxicity of silver nanoparticles to Daphnia magna: effects of algal particles and animal nutrition. Ecotoxicology. 26, 118-126. https://doi.org/10.1007/s10646-016-1747-2

Conine, A. L., et al., 2017. Variable silver nanoparticle toxicity to *Daphnia* in boreal lakes. Aquat Toxicol. 192, 1-6. https://doi.org/10.1016/j.aquatox.2017.09.004

Cupi, D., et al., 2016. Influence of pH and media composition on suspension stability of silver, zinc oxide, and titanium dioxide nanoparticles and immobilization of *Daphnia magna* under guideline testing conditions. Ecotoxicol Environ Saf. 127, 144-152. https://doi.org/10.1016/j.ecoenv.2015.12.028

Das, P., et al., 2013. Toxicity of silver and titanium dioxide nanoparticle suspensions to the aquatic invertebrate, *Daphnia magna*. Bull Environ Contam Toxicol. 91, 76-82. https://doi.org/10.1007/s00128-013-1015-6

Diamond, J. M., et al., 1990. Derivation of a freshwater silver criteria for the New River, Virginia, using representative species. Environ Toxicol Chem. 9, 1425-1434. https://doi.org/10.1002/etc.5620091112

Erickson, R. J., et al., 1998. Effects of laboratory test conditions on the toxicity of silver to aquatic organisms. Environ Toxicol Chem. 17, 572-578. https://doi.org/10.1002/etc.5620170407

EPA, 2022. Technical Overview of Ecological Risk Assessment - Analysis Phase: Ecological Effects Characterization. Retrieved on 06/05/2023 from: https://www.epa.gov/pesticide-science-and-assessing-pesticide-risks/technical-overview-ecological-risk-assessment-0

Gagné, F., et al., 2013. Bioavailability and Immunotoxicity of Silver Nanoparticles to the Freshwater Mussel *Elliptio complanata*. J Toxicol Environ Health Part A. 76, 767-777. https://doi.org/10.1080/15287394.2013.818602

Gaiser, B. K., et al., 2011. Effects of silver and cerium dioxide micro- and nano-sized particles on *Daphnia magna*. J Environ Monit. 13, 1227-1235. https://doi.org/10.1039/c1em10060b

Gao, J., et al., 2009. Dispersion and toxicity of selected manufactured nanomaterials in natural river water samples: effects of water chemical composition. Environ Sci Technol. 43, 3322-3328. https://doi.org/10.1021/es803315v

Gao, J., et al., 2015. Nanosilver-coated socks and their toxicity to zebrafish (*Danio rerio*) embryos. Chemosphere. 119, 948-952. https://doi.org/10.1016/j.chemosphere.2014.08.031

Georgantzopoulou, A., et al., 2018. Ecotoxicological Effects of Transformed Silver and Titanium Dioxide Nanoparticles in the Effluent from a Lab-Scale Wastewater Treatment System. Environ Sci Technol. 52, 9431-9441. https://doi.org/10.1021/acs.est.8b01663

George, S., et al., 2012. Surface Defects on Plate-Shaped Silver Nanoparticles Contribute to Its Hazard Potential in a Fish Gill Cell Line and Zebrafish Embryos. ACS Nano. 6, 3745-3759. https://doi.org/10.1021/nn204671v

Goncalves, S. F., et al., 2017. Effects of silver nanoparticles on the freshwater snail *Physa acuta*: The role of test media and snails' life cycle stage. Environ Toxicol Chem. 36, 243-253. https://doi.org/10.1002/etc.3532

Griffitt, R. J., et al., 2008. Effects of particle composition and species on toxicity of metallic nanomaterials in aquatic organisms. Environ Toxicol Chem. 27, 1972-1978. https://doi.org/10.1897/08-002.1

Gubbins, E. J., et al., 2011. Phytotoxicity of silver nanoparticles to *Lemna minor* L. Environ Pollut. 159, 1551-1559. https://doi.org/10.1016/j.envpol.2011.03.002

Harmon, A. R., et al., 2014. Determination of nanosilver dissolution kinetics and toxicity in an environmentally relevant aqueous medium. Environ Toxicol Chem. 33, 1783-1791. https://doi.org/10.1002/etc.2616

Hedayati A., et al., 2012. Evaluation of silver nanoparticles ecotoxicity in Silver Carp (*Hypophthalmicthys molitrix*) and Goldfish (*Carassius auratus*). Bulg J Vet Med. 15, 172–177.

Heinlaan, M., et al., 2016. Natural water as the test medium for Ag and CuO nanoparticle hazard evaluation: An interlaboratory case study. Environ Pollut. 216, 689-699. https://doi.org/10.1016/j.envpol.2016.06.033

Hiriart-Baer, V. P., et al., 2006. Toxicity of silver to two freshwater algae, *Chlamydomonas reinhardtii* and *Pseudokirchneriella subcapitata*, grown under continuous culture conditions: influence of thiosulphate. Aquat Toxicol. 78, 136-148. https://doi.org/10.1016/j.aquatox.2006.02.027

Hogstrand, C., et al., 1996. Toxicity, silver accumulation and metallothionein induction in freshwater rainbow trout during exposure to different silver salts. Environ Toxicol Chem. 15, 1102-1108. https://doi.org/10.1002/etc.5620150713

Hoheisel, S. M., et al., 2012. Comparison of nanosilver and ionic silver toxicity in *Daphnia magna* and *Pimephales promelas*. Environ Toxicol Chem. 31, 2557-2563. https://doi.org/10.1002/etc.1978

Hook, S. E., Fisher, N. S., 2001. Sublethal effects of silver in zooplankton: importance of exposure pathways and implications for toxicity testing. Environ Toxicol Chem. 20, 568-574. https://doi.org/10.1002/etc.5620200316

Hu, Y., et al., 2018. Distinct toxicity of silver nanoparticles and silver nitrate to *Daphnia magna* in M4 medium and surface water. Sci Total Environ. 618, 838-846. https://doi.org/10.1016/j.scitotenv.2017.08.222

Hund-Rinke, K., et al., 2018. Grouping concept for metal and metal oxide nanomaterials with regard to their ecotoxicological effects on algae, daphnids and fish embryos. NanoImpact. 9, 52-60. https://doi.org/10.1016/j.impact.2017.10.003

Jemec, A., et al., 2016. An interlaboratory comparison of nanosilver characterisation and hazard identification: Harmonising techniques for high quality data. Environ Int. 87, 20-32. https://doi.org/10.1016/j.envint.2015.10.014

Jiang, H.-S., et al., 2012. Physiological analysis of silver nanoparticles and $AgNO_3$ toxicity to *Spirodela polyrhiza*. Environ Toxicol Chem. 31, 1880-1886. https://doi.org/10.1002/etc.1899

Jo, H. J., et al., 2012. Acute toxicity of Ag and CuO nanoparticle suspensions against *Daphnia magna*: the importance of their dissolved fraction varying with preparation methods. J Hazard Mater. 227-228, 301-308.

https://doi.org/10.1016/j.jhazmat.2012.05.066

Johari, S. A., et al., 2013. Toxicity comparison of colloidal silver nanoparticles in various life stages of rainbow trout (*Oncorhynchus mykiss*). Iran J Fish Sci. 12, 76-95.

Kashiwada, S., et al., 2012. Silver nanocolloids disrupt medaka embryogenesis through vital gene expressions. Environ Sci Technol. 46, 6278-6287. https://doi.org/10.1021/es2045647

Katuli, K. K., et al., 2014. Silver nanoparticles inhibit the gill Na^+/ K^+-ATPase and erythrocyte AChE activities and induce the stress response in adult zebrafish (*Danio rerio*). Ecotox Environ Saf. 106, 173-180. https://doi.org/10.1016/j.ecoenv.2014.04.001

Kennedy, A. J., et al., 2012. Impact of organic carbon on the stability and toxicity of fresh and stored silver nanoparticles. Environ Sci Technol. 46, 10772-10780. https://doi.org/10.1021/es302322y

Kennedy, A. J., et al., 2010. Fractionating Nanosilver: Importance for Determining Toxicity to Aquatic Test Organisms. Environ Sci Technol. 44, 9571-9577. https://doi.org/10.1021/es1025382

Khoshnamvand, M., et al., 2020. Toxicity of biosynthesized silver nanoparticles to aquatic organisms of different trophic levels. Chemosphere. 258, 127346. https://doi.org/10.1016/j.chemosphere.2020.127346

Khosravi-Katuli, K., et al., 2018. Comparative toxicity of silver nanoparticle and ionic silver in juvenile common carp (*Cyprinus carpio*): Accumulation, physiology and histopathology. J Hazard Mater. 359, 373-381. https://doi.org/10.1016/j.jhazmat.2018.07.064

Kim, J., et al., 2011. Differentiation of the toxicities of silver nanoparticles and silver ions to the Japanese medaka (*Oryzias latipes*) and the cladoceran *Daphnia magna*. Nanotoxicology. 5, 208-214. https://doi.org/10.3109/17435390.2010.508137

Kim, J. Y., et al., 2013. Developmental toxicity of Japanese medaka embryos by silver nanoparticles and released ions in the presence of humic acid. Ecotoxicol Environ Saf. 92, 57-63. https://doi.org/10.1016/j.ecoenv.2013.02.004

Krishnaraj, C., et al., 2016. In Vivo toxicological assessment of biologically synthesized silver nanoparticles in adult Zebrafish (*Danio rerio*). J Hazard Mater. 301, 480-491. https://doi.org/10.1016/j.jhazmat.2015.09.022

Książk, M., et al., 2015. Toxic effect of silver and platinum nanoparticles toward the freshwater microalga *Pseudokirchneriella subcapitata*. Bull Environ Contam Toxicol. 94, 554-558. https://doi.org/10.1007/s00128-015-1505-9

Laban, G., et al., 2010. The effects of silver nanoparticles on fathead minnow (*Pimephales promelas*) embryos. Ecotoxicology. 19, 185-195. https://doi.org/10.1007/s10646-009-0404-4

Lacave, J. M., et al., 2016. Effects of metal-bearing nanoparticles (Ag, Au, CdS, ZnO, SiO_2) on developing zebrafish embryos. Nanotechnology. 27, 325102. https://doi.org/10.1088/0957-4484/27/32/325102

Lee, K. J., et al., 2012a. In vivo quantitative study of sized-dependent transport and toxicity of single silver nanoparticles using zebrafish embryos. Chem Res Toxicol. 25, 1029-1046. https://doi.org/10.1021/tx300021u

Lee, Y. J., et al., 2012b. Ion-release kinetics and ecotoxicity effects of silver nanoparticles. Environ Toxicol Chem. 31, 155-159. https://doi.org/10.1002/etc.717

Lekamge, S., et al., 2018. The Toxicity of Silver Nanoparticles (AgNPs) to Three Freshwater Invertebrates With Different Life Strategies: *Hydra vulgaris*, *Daphnia carinata*, and *Paratya australiensis*. Front Environ Sci. 6, 152. https://doi.org/10.3389/fenvs.2018.00152

Lekamge, S., et al., 2019. The toxicity of coated silver nanoparticles to *Daphnia carinata* and trophic transfer from alga *Raphidocelis subcapitata*. PLoS One. 14, e0214398. https://doi.org/10.1371/journal.pone.0214398

Li, T., et al., 2010. Comparative toxicity study of Ag, Au, and Ag-Au bimetallic nanoparticles on *Daphnia magna*. Anal Bioanal Chem. 398, 689-700. https://doi.org/10.1007/s00216-010-3915-1

Lima, A. R., et al., 1982. Acute toxicity of silver to selected fish and invertebrates. Bull Environ Contam Toxicol. 29, 184-189. https://doi.org/10.1007/BF01606148

Mackevica, A., et al., 2015. Chronic toxicity of silver nanoparticles to *Daphnia magna* under different feeding conditions. Aquat Toxicol. 161, 10-6.

https://doi.org/10.1016/j.aquatox.2015.01.023

Martins, N., et al., 2020. Effects of metal nanoparticles on freshwater rotifers may persist across generations. Aquat Toxicol. 229, 105652. https://doi.org/10.1016/j.aquatox.2020.105652

Massarsky, A., et al., 2013. Assessment of nanosilver toxicity during zebrafish (*Danio rerio*) development. Chemosphere. 92, 59-66. https://doi.org/10.1016/j.chemosphere.2013.02.060

McLaughlin, J., Bonzongo, J. C., 2012. Effects of natural water chemistry on nanosilver behavior and toxicity to *Ceriodaphnia dubia* and *Pseudokirchneriella subcapitata*. Environ Toxicol Chem. 31, 168-175. https://doi.org/10.1002/etc.720

Mehennaoui, K., et al., 2016. *Gammarus fossarum* (Crustacea, Amphipoda) as a model organism to study the effects of silver nanoparticles. Sci Total Environ. 566-567, 1649-1659. https://doi.org/10.1016/j.scitotenv.2016.06.068

Muth-Kohne, E., et al., 2013. The toxicity of silver nanoparticles to zebrafish embryos increases through sewage treatment processes. Ecotoxicology. 22, 1264-1277. https://doi.org/10.1007/s10646-013-1114-5

Naddy, R. B., et al., 2007a. Chronic toxicity of silver nitrate to *Ceriodaphnia dubia* and *Daphnia magna*, and potential mitigating factors. Aquat Toxicol. 84, 1-10. https://doi.org/10.1016/j.aquatox.2007.03.022

Naddy, R. B., et al., 2007b. Comparison of short-term chronic and chronic silver toxicity to fathead minnows in unamended and sodium chloride-amended waters. Environ Toxicol Chem. 26, 1922-1930. https://doi.org/10.1897/06-638R.1

Navarro, E., et al., 2008. Toxicity of Silver Nanoparticles to *Chlamydomonas reinhardtii*. Environ Sci Technol. 42, 8959-8964. https://doi.org/10.1021/es801785m

Navarro, E., et al., 2015. Effects of Differently Coated Silver Nanoparticles on the Photosynthesis of *Chlamydomonas reinhardtii*. Environ Sci Technol. 49, 8041-8047. https://doi.org/10.1021/acs.est.5b01089

Norberg-King, T. J., 1989. An evaluation of the fathead minnow seven-day subchronic test for estimating chronic toxicity. Environ Toxicol Chem. 8, 1075-1089. https://doi.org/10.1002/etc.5620081113

Oukarroum, A., et al., 2013. Silver nanoparticle toxicity effect on growth and cellular viability of the aquatic plant *Lemna gibba*. Environ Toxicol Chem. 32, 902-907. https://doi.org/10.1002/etc.2131

Pereira, S. P. P., et al., 2018. Phytotoxicity of silver nanoparticles to *Lemna minor*: Surface coating and exposure period-related effects. Sci Total Environ. 618, 1389-1399. https://doi.org/10.1016/j.scitotenv.2017.09.275

Poynton, H. C., et al., 2012. Toxicogenomic responses of nanotoxicity in *Daphnia magna* exposed to silver nitrate and coated silver nanoparticles. Environ Sci Technol. 46, 6288-6296. https://doi.org/10.1021/es3001618

Ribeiro, F., et al., 2014. Silver nanoparticles and silver nitrate induce high toxicity to *Pseudokirchneriella subcapitata*, *Daphnia magna* and *Danio rerio*. Sci Total Environ. 466–467, 232-241. https://doi.org/10.1016/j.scitotenv.2013.06.101

Sakka, Y., et al., 2016. Behavior and chronic toxicity of two differently stabilized silver nanoparticles to Daphnia magna. Aquatic Toxicol. 177, 526-535. https://doi.org/10.1016/j.aquatox.2016.06.025

Sathya, V., et al., 2012. Acute and sublethal effects in an Indian major carp *Cirrhinus mrigala* exposed to silver nitrate: Gill Na$^+$/K$^+$-ATPase, plasma electrolytes and biochemical alterations. Fish Shellfish Immunol. 32, 862-868. https://doi.org/10.1016/j.fsi.2012.02.014

Seitz, F., et al., 2015. Effects of silver nanoparticle properties, media pH and dissolved organic matter on toxicity to *Daphnia magna*. Ecotoxicol Environ Saf. 111, 263-270. https://doi.org/10.1016/j.ecoenv.2014.09.031

Shaluei, F., et al., 2013. Effect of subacute exposure to silver nanoparticle on some hematological and plasma biochemical indices in silver carp (*Hypophthalmichthys molitrix*). Hum Exp Toxicol. 32, 1270-1277. https://doi.org/10.1177/0960327113485258

Shen, M.-H., et al., 2015. Exposure Medium: Key in Identifying Free Ag$^+$ as the Exclusive Species of Silver Nanoparticles with Acute Toxicity to *Daphnia magna*. Sci Rep. 5, 9674. https://doi.org/10.1038/srep09674

Sohn, E. K., et al., 2015. Aquatic toxicity comparison of silver nanoparticles and silver nanowires. BioMed Res Int. 2015, 1-12. https://doi.org/10.1155/2015/893049

Sørensen, S. N., et al., 2016. Acute and chronic effects from pulse exposure of *D. magna* to silver and copper oxide nanoparticles. Aquatic Toxicol. 180, 209-217. https://doi.org/10.1016/j.aquatox.2016.10.004

Völker, C., et al., 2014. Combined effects of silver nanoparticles and 17α-ethinylestradiol on the freshwater mudsnail *Potamopyrgus antipodarum*. Environ Sci Pollut Res. 21, 10661-10670. https://doi.org/10.1007/s11356-014-3067-5

Wang, Z., et al., 2012. Aquatic toxicity of nanosilver colloids to different trophic organisms: Contributions of particles and free silver ion. Environ Toxicol Chem. 31, 2408-2413. https://doi.org/10.1002/etc.1964

Wood, C. M., et al., 1996. The physiology of waterborne silver toxicity in freshwater rainbow trout (*Oncorhynchus mykiss*) 1. The effects of ionic Ag$^+$. Aquatic Toxicology. 35, 93-109. https://doi.org/10.1016/0166-445X(96)00003-3

Wu, Y., Zhou, Q., 2013. Silver nanoparticles cause oxidative damage and histological changes in medaka (*Oryzias latipes*) after 14 days of exposure. Environ Toxicol Chem. 32, 165-173. https://doi.org/10.1002/etc.2038

Wu, Y., et al., 2010. Effects of silver nanoparticles on the development and histopathology biomarkers of Japanese medaka (*Oryzias latipes*) using the partial-life test. Aquat Toxicol. 100, 160-167. https://doi.org/10.1016/j.aquatox.2009.11.014

Xin, Q., et al., 2015. Silver nanoparticles affect the neural development of zebrafish embryos. J Appl Toxicol. 35, 1481-1492. https://doi.org/10.1002/jat.3164

Yoo-iam, M., et al., 2015. Toxicity, bioaccumulation and biomagnification of silver nanoparticles in green algae (*Chlorella sp.*), water flea (*Moina macrocopa*), blood worm (*Chironomus spp.*) and silver barb (*Barbonymus gonionotus*). Chem Speciat Bioavailab. 26**,** 257-265. https://doi.org/10.3184/095422914x14144332205573

Yue, Y., et al., 2017. Interaction of silver nanoparticles with algae and fish cells: a side by side comparison. J Nanobiotechnology. 15**,** 16. https://doi.org/10.1186/s12951-017-0254-9

Zhang, L., Wang, W. X., 2019. Dominant Role of Silver Ions in Silver Nanoparticle Toxicity to a Unicellular Alga: Evidence from Luminogen Imaging. Environ Sci Technol. 53**,** 494-502. https://doi.org/10.1021/acs.est.8b04918

Zhang, J., et al., 2020. Surface charge-dependent bioaccumulation dynamics of silver nanoparticles in freshwater algae. Chemosphere. 247**,** 125936. https://doi.org/10.1016/j.chemosphere.2020.125936

Zhao, C. M., Wang, W. X., 2011. Comparison of acute and chronic toxicity of silver nanoparticles and silver nitrate to *Daphnia magna*. Environ Toxicol Chem. 30**,** 885-892. https://doi.org/10.1002/etc.45